CFD Modelling of Pathogen Transport due to Human Activity

Elizabeth Abigail Hathway

Submitted in accordance with the requirements for the degree of

Doctor of Philosophy

The University of Leeds
School of Civil Engineering

June, 2008

The candidate confirms that the work submitted is her own, except where work which has formed part of jointly-authored publications has been included. The contribution of the candidate and the other authors to this work has been explicitly indicated overleaf. The candidate confirms that appropriate credit has been given within the thesis where reference has been made to the work of others

PAGINATED BLANK PAGES ARE SCANNED AS FOUND IN ORIGINAL THESIS

NO INFORMATION IS MISSING

PAGE NUMBERING AS ORIGINAL

Work Formed from Jointly Authored Publications

The following details the work in this thesis that has been previously published or submitted for publication. The relevant papers are reproduced in Appendix 2. Chapter 4 of this thesis "Observational and Sampling Study on a Respiratory Ward" presents work from two studies. Study 1 is based on work carried out for a joint publication as combined lead author with Katherine Roberts (Roberts K., *et al.,* (2006). "Bioaerosol production on a respiratory ward." *Indoor and Built Environment* **15**(1): 35-40). The observational and sampling work in the hospital ward was carried out as a pair, including the following laboratory work. The initial analysis presented in the publication was carried out jointly with supervision from other authors. Subsequent analysis of the results, including the statistical work (except the correlations between fluctuations of different particle sizes) presented in Chapter 4 was independently undertaken for this thesis.

Part of Study 2 in Chapter 4 has been reproduced and accepted for publication as a short paper in the proceedings of Indoor Air 2008 (Hathway E.A., *et al.*, (2008). "Bioaerosol production from routine activities within a hospital ward." *Proceeding of Indoor Air 2008*, Copenhagen). The published work forms the beginning of section 4.4.3 in which correlations are drawn between people in the hospital bay and levels of particles and bioaerosol total viable count sampled in Study 2. Contributions from the other authors were as supervision to the study.

Chapters 5 and 6 draw on work that was published in Hathway *et al* (2007) (Hathway E.A. *et al* "CFD Modelling of Transient Pathogen Release in Indoor Environments due to Human Activity". *Proceedings of Roomvent*. Helsinki. Finland). The publication includes the experimental validation using a linear source (section 5.5.2) and aspects of numerical validation of the passive scalar transport model (Chapter 6). Results from the hospital side room model presented in Chapter 7, which studies the sensitivity of the point source location and the effect of changing the size definition of a zonal source, form a second paper accepted for publication at Indoor Air 2008 (Hathway E.A. *et al.,* (2008) "CFD Modelling of a Hospital Ward: Assessing risk from bacteria produced from respiratory and activity sources." *Proceeding of Indoor Air 2008*, Copenhagen). As above the other authors on these two publications are there in a supervisory capacity.

Acknowledgements

None of this could have been achieved without the help of my supervisors who I would like to thank for their guidance and support, specifically Catherine Noakes for her constant motivation, support and endless stream of ideas and approaches; and Andy Sleigh for his programming patience and attention to detail. Furthermore I wish to thank Louise Fletcher for her essential support in the micro-biological aspects of this thesis, both concerning my experimental work and observational study. I would also like to acknowledge my first supervisor Clive Beggs for securing funding for me to carry out this PhD and his input into the initial observational study.

I also extend my thanks to Dr Mark Elliot, Dr Daniel Peckham and Dr Ian Clifton for enabling the opportunity to observe and sample within the respiratory support unit at St. James University Hospital, Leeds, and the nursing staff on the ward who not only allowed me to sample around their daily activities but made me welcome in the process. As well as making the study possible Mark Elliot's input has helped me to understand the relevance of my work to the clinical environment.

A six week period of my PhD was spent working with the Environmental Physics group as part of Arup, London. This was invaluable in terms of understanding properly the relevance of the work presented in this thesis to those using modelling tools to design hospitals and devices, as well as the differences between academic and industrial approaches to using these tools. I would like to thank Darren Woolf for giving me this opportunity and the rest of the team for taking the time to support my work.

Finally I wish to thank all my colleagues and friends in the department of Civil Engineering at The University of Leeds who have been supportive and made the time spent working on this thesis enjoyable. Namely Katherine Roberts for her advice on my lab work and joint authorship of the publication mentioned previously, all the members of the office G13; Miller Carmargo, Elly Van de Linde, Daxu Zhang, Shan Palaniyandi and others; Kiran Bhagate and Rae Taylor.

Abstract

Health-care Associated Infection is a major concern with 1 in 11 patients affected each year. There is evidence that some pathogens may be transported by an airborne route, and hence fluid modelling tools, such as Computational Fluid Dynamics (CFD), are increasingly used to aid understanding of the transport mechanisms of infection. These models tend to only consider respiratory infections that are released from a single *point*, such as a person coughing. However there is substantial evidence that certain pathogens, such as MRSA, may be released from the skin during regular routine activities (e.g. undressing, walking).

An observational and air sampling study carried out on a respiratory ward found that certain activities correlated to greatly increased numbers of large particles (> 5μm), and bioaerosols. The increased concentrations of bioaerosols also corresponded to sampling of potentially pathogenic *Staphylococcus aureus*. It is therefore necessary to be able to represent these releases of bioaerosols within CFD models used in design and risk assessment.

Bioaerosol transport is modelled in CFD simulations using passive scalar transport and Lagrangian particle tracking models with the DRW model to simulate turbulent diffusion. These are validated for the first time using spatial variation of airborne and deposited bioaerosols generated under controlled conditions. Simpler multi-zone models are compared to CFD and found to perform well at simulating the bioaerosol decay within large spaces that can be assumed to be well mixed, however they are not refined enough to simulate the detail required to study the transfer of infection between individual patients.

A zonal source model is introduced and validated with the aim of representing the time average dispersion from a transient source in a steady state model. This enables the dispersion of bioaerosols from activities occurring in hospital wards to be represented within CFD models. The zonal source model is shown to give a good representation of the average dispersion and total deposition of a transient source, whereas a point source is not. Point sources produce different dispersion patterns to zonal sources and so it is recommended that both are used to simulate bioaerosols produced due to activities or respiratory diseases. Point sources are found to be highly sensitive to the injection position, whereas the zonal source is found to produce relatively similar patterns of dispersion for varying size definitions.

CFD is a useful tool for studying pathogen transport in indoor spaces, and when doing so it is recommended that the potential bioaerosol release from the skin is considered which can be taken into account within a steady state model using a zonal source model.

Contents

List of Tables

List of Figures

Abbreviations and Symbols.

A	Area
ASHRAE	American Society for Heating, Refrigerating and Air-Conditioning Engineers
C_c	Cunningham Slip Correction Factor
C_t	Concentration at time t
CIBSE	Chartered Institute of Building Services Engineers
CFD	Computational Fluid Dynamics
CV	Control Volume
d	Diameter
div(**u**)	Vector notation for $\frac{\partial(u)}{\partial x}+\frac{\partial(v)}{\partial y}+\frac{\partial(w)}{\partial z}$
DRW	Discrete Random Walk
HAI	Health-care Associated Infection
HCW	Healthcare Worker
HD	High Dependency
HEPA	High Efficiency Particulate Air
i	internal energy
I	Infectious person
k- ϵ	Turbulent kinetic energy and dissipation model
-k grad T	Vector notation for $-k\frac{\partial T}{\partial x}-k\frac{\partial T}{\partial y}-k\frac{\partial T}{\partial z}$
LES	Large Eddy Simulation (turbulence model)
N	Population size
NHS	National Health Service
NIV	Non Invasive Ventilation
p	Pressure
q	Quanta of infective material produced
Q	Volume flow rate of air.
Q_{EAS}	Equiangle Skew
r	Dilution of infectious particles
R	Removed person (no longer capable of acquiring infection)
RANS	Reynold Average Navier-Stokes equations (turbulence model)

RNG	Renormalised Group (turbulence model)
S	Susceptible (capable of acquiring infection)
S_m	Momentum source term
S_E	Energy source term
$S\phi$	Transported property source term
SIMPLE	Semi Implicit Method for Pressure-Linked Equations
SIS	Epidemiological model considering persons progressing from Susceptible to Infective to Susceptible
SIR	Epidemiological model considering persons progressing from Susceptible to Infective to Removed.
TVC	Total Viable Count
t	Time
T	Temperature
u	Velocity Vector *(u,v,w)*
u'	Instantaneous velocity fluctuation
UDF	User Defined Function
UV	Ultra Violet
V	Volume
Γ	Diffusivity
$\partial x, \partial y, \partial z$	Differential change in distance
∂t	Differential change in time
ζ	Randomly generated number
η	Viscosity of air
μ	Dynamic viscosity
Θ	Angle
ρ	Density
τ_{ii}	Normal stress acting on surface i
τ_{ij}	Shear Stress acting across surface ij
ϕ	Transported property
Φ	Dissipation Function
$\int_{CV} dV$	Integral over a control volume
$\int_{A} dA$	Integral over a bounding surface of a control volume

Chapter 1
Introduction

This research has arisen from a need to use computer modelling techniques in order to understand the airborne pathway of disease in indoor environments and assess the efficacy of various engineering interventions. Of particular interest is the spread of disease within health care facilities. Although direct contact transmission is thought to be the most significant route of infection within these environments (Pratt *et al.*, 2007), spread through the air is also important (Beggs, 2003). Coughing is an obvious method for the airborne dispersal of bacteria and viruses, however, as detailed more extensively in Chapter 2, the release of bacteria laden skin particles during activity also adds to the airborne micro-flora within a space. Although this increases the risk of transmission it is rarely considered when evaluating infection outbreaks.

The use of modelling techniques to simulate infection risk in hospital situations has been increasing in recent years and Computational Fluid Dynamics (CFD) is one technique that is receiving much attention. However the CFD modelling work to date has focused on transmission of respiratory infections, and the risks due to the movement of bacteria laden skin particles through the air has received little attention. This research seeks to develop a method of realistically modelling this type of spread through introducing the concept of zonal sources based on the location and type of activity within a hospital ward. In this chapter a brief overview of the problem of health-care associated infections (HAI) and the routes of transmission of disease is presented, along with current application of CFD modelling in hospital settings and its future potential. This provides an introduction to a more detailed overview of these topics presented in Chapters 2 and 3. The main aims and objectives of the thesis are presented here along

with an overview of the research methodology. The layout of the thesis is described, indicating how each chapter relates to the main objectives.

1.1 Background

1.1.1 Health-care Associated Infection

Despite their intention of curing disease, hospitals provide an ideal situation for the dissemination and acquisition of disease due to the close confinement of immuno-compromised people and those suffering from infectious disease (Parker, 1972, Weinstein, 1998). In England there are at least 100,000 HAIs each year which relates to 1 in 11 people acquiring an infection from their stay in hospital (National Audit Office, 2000). The same problem is evident across the world with the rates of infection varying across USA, Australasia and Europe of between 4 and 10% of the patients using the health care facility (Chief Medical Officer, 2003). In England and Wales these infections cost the NHS in the order of £1000 million a year (National Audit Office, 2000). As well as the increased cost to the NHS (a patient with an HAI costs the NHS 2.9 times more than a non-infected patient in England (Plowman *et al.*, 1999)), HAI's result in longer stays in hospital for the patient, added distress, and sometimes permanent disabilities or even death. As multi-drug resistant bacteria are continually emerging, the potential severity and costs from HAI increase. In particular the Chief Medical Officer has highlighted the risk from Methicillin Resistant *Staphylococcus aureus* (MRSA), Vancomycin resistant *enterococci* and penicillin resistant *Streptococcus pneumonia* (Chief Medical Officer, 2003). Since the advent of compulsory reporting in 2001 there were large increases in MRSA infections up to 2004. In 2004 the government pledged to halve MRSA infections by 2008 and steady decreases in this time indicate this target may be met (Department of Health, 2008). However despite this there is still a large variation in infection rates between different health care trusts (Health Protection Agency, 2007b) and in 2006 MRSA was still responsible for a third of surgical site infections (Health Protection Agency, 2006). Due to the scale of the problem HAI's are receiving considerable attention in the media and from the government. In 'Getting Ahead of the Curve' the Chief Medical Officer (2002) highlighted the problem as being among the key priorities in dealing with infectious diseases. In order to help combat the problem mandatory surveillance systems have been introduced for some major pathogens such as MRSA and *Clostridium difficile* as

well as specifically those infections occurring at surgical sites (Health Protection Agency, 2006). Various guidelines have been written and in 2003 a performance indicator in respect to HAIs was introduced (Chief Medical Officer, 2003). Recently in 2006 a code of practice was introduced that aims to provide a framework for hospitals to keep the risk of infection as low as possible (Department of Health, 2006). This is a case of reducing the risk; health care related infections will not be eliminated, but it has been estimated that at least 20% of these infections could be avoided (Harbarth *et al.*, 2003).

In order to succeed in reducing the occurrence of hospital infections it is essential that transmission mechanisms need to be properly understood. For instance, one purpose of the surveillance systems mentioned above is to provide evidence for the efficacy of any interventions introduced. The transmission of infection can occur in a number of ways but these can be separated into three main groups:

- Contact
- Pure Airborne
- Droplet
- Airborne Component

Contact spread refers to those infections that are transmitted through physical contact. An important aspect in breaking chains of infections is a high degree of hand cleanliness when dealing with patients (Fendler *et al.*, 2002, Larson, 1988). As well as the hands of the health-care workers (HCWs), infection by contact may occur due to the use of medical devices such as catheters, intravenous feeding lines, and respiratory aids (Pratt *et al.*, 2007). These infections may originate from the patient's own skin, with bacteria being transferred to the blood stream as insertions are made. These bacteria may be a part of the natural flora of the patient's skin, or may have been acquired during their stay in hospital. Surgical procedures may also lead to the transfer of infection due to unsterilised equipment, contaminated HCWs skin and clothes, and again from the patients own skin (Chief Medical Officer, 2003).

It is well known that airborne transmission is the route of infection for certain diseases. The airborne route is the primary transmission mechanism for Tuberculosis, and if a

patient is suspected of having multi drug resistant TB they should be isolated in a negative pressure ventilated room to reduce the transmission risk (Joint Tuberculosis Committee of the British Thoracic Society, 2000). Measles is another disease that is well known for being airborne (Riley *et al.*, 1978). These two diseases are generally spread through respiratory aerosols. When an infected individual coughs or sneezes hundreds of droplets are ejected from the mouth. These droplets will contain moisture and bacteria and on dispersal into the air will evaporate rapidly to become droplet nuclei, smaller than 1μm in diameter, that remain suspended in the air for many hours (Wells, 1955). These can then be inhaled by a susceptible host and the infection is transferred.

Not all particles released into the air evaporate to such a small size. These larger particles will have a greater mass, and hence the gravitational pull acting upon them will overcome that from the air current, resulting in their deposition onto surfaces. These particles may be inhaled by a susceptible host in the short period they are airborne and this is known as droplet transmission. Alternatively once they have deposited on surfaces it is possible for the infectious particles to be picked up on the hands of HCWs, or patients, and the infection may be passed on through the contact route. In this situation the transmission has an airborne component. Some bacteria are very hardy and may survive for long periods in the environment providing reservoirs of contamination (Hota, 2004). These particles may be large droplets emitted in a cough that do not evaporate so quickly and fall to surface. Vomiting and diarrhoea are also responsible for aerosolising particles that may then deposit out of the air stream onto surfaces. Another source of airborne bacteria is the skin, which constantly releases bacteria into the environment through the natural skin shedding process (Noble, 1975). As detailed in Chapter 2, a number of researchers have published evidence that certain routine activities that may occur in hospital wards, including walking, dressing and bedmaking, can cause large numbers of particles (mostly skin) to be dispersed into the environment, which may carry with them bacteria potentially capable of spreading disease. (Speers *et al.*, 1965, Noble, 1975, Duguid and Wallace, 1948, May and Pomeroy, 1973, Hare and Thomas, 1956). The majority of these studies into the effect of activity on dispersal occurred in the 1950s and 1960s, more recently increases in the level of MRSA in the air was found during periods of bedmaking (Shiomori *et al.*, 2002).

Within a busy hospital ward the level, type and location of activity varies significantly through the day with the result that any dispersion of bacteria related to the activities may vary significantly in time and space. Chapter 4 details hospital based observation and sampling studies carried out on a respiratory ward which provides strong evidence of this. It was found that activity may be responsible for the release of a large number of particles (Roberts *et al.*, 2006), with the particle size distribution and bioaerosol concentration dependant on the type and level of activity. The majority of these are likely to be skin particles and may be larger than the respiratory aerosols expelled during coughing, with approximate sizes between 5 and 20μm diameter (Chapter 2). As such they are more likely to drop out of air streams onto surfaces and so knowledge of the behaviour of these particles; if they do land, how far they travel and is there a preferential landing place, may affect the design of the space and the appropriateness of interventions. Developing reliable tools to properly evaluate design implications is major driver for this thesis, with the majority of the work focusing on computational fluid dynamics (CFD) modelling techniques; a method capable of modelling transported particles dispersed from activity, and as such, could be highly informative about these transport mechanisms.

1.1.2 Application of Computational Fluid Dynamics in Hospital Situations

Computational Fluid Dynamics (CFD) is an increasingly popular tool for detailed modelling of the movement of air in indoor environments. The technique, described in detail in Chapter 5, involves the numerical solution of the continuity, momentum and energy equations that govern fluid flow by dividing the domain of interest into discrete volumes using a mesh or grid. With a well chosen mesh and numerical schemes, the method is capable of accurately predicting flow characteristics, such as velocity, pressure and temperature, without excessive computational requirements. The basic technique can be extended to analyse the spread of contaminants transported by an air flow using either simple passive scalar transport, or by including a second discrete phase using a Lagrangian approach.

In operating theatres it has long been recognised that clean air is essential for maintaining a sterile operation site. As such CFD has been used extensively to study the effects of different ventilation regimes (Tinker and Roberts, 1998, Chow and Yang, 2004, Colquhoun and Partridge, 2003), in particular the local flow around and over the

operating table with the aim of keeping airborne contamination away from open wound sites. Isolation room design can also be optimised by the use of CFD (Kao and Yang, 2006) and to study the effect of local exhaust systems for a single bed within a ward (Chau *et al.*, 2006). As outlined in more detail in Chapter 3, there has recently been a move to use CFD to model whole wards and to study how the bulk air flow, as well as detailed local patterns, affect the airborne transport of infectious material. Respiratory infections including Severe Acute Respiratory Syndrome (SARS) (Wong *et al.*, 2004, Li *et al.*, 2005, Chau *et al.*, 2006) and Tuberculosis (Noakes *et al.*, 2006b) have been the primary focus of these studies. In these models, because the infectious agents are accepted as respiratory pathogens being transported by a direct airborne route, the dispersal considered is primarily from the mouth of bed bound patients. For this reason the source of bioaerosols is assumed to be from a directed point source; a suitable approximation as the mouth is relatively very small in comparison to the room. Most attempts at simulating a hospital ward do not account for the many transient influences, preferring to consider a steady state or 'freeze frame', representative situation. Since it is futile to attempt to model the infinite number of possible events that may occur it is an average situation that is usually simulated. Combining this with the increase in complexity and time to simulate a transient model, the use of a steady state model is understandable. Despite this there is an interest in the effect of movement on airflow patterns and the dispersal of bioaerosols (Mattsson and Sandberg, 1996, Matsumoto and Ohba, 2004, Bjorn and Nielsen, 2002). Recently, the idea of expressing the effects of movement on the airflow within a steady state model was broached by Brohus (2006). This incorporated a turbulent kinetic energy source to simulate the influence of movement on the air flow, enabling some of the influences from movement to be approximated within a steady state model.

Despite the potential for pathogens to be released from the skin into the air through general ward activity, the use of CFD to model the spread of particles in this manner has not previously been considered. CFD modelling is increasingly being used to evaluate wider hospital environments than just the fixed local flow around an operating table. As the results from these studies are starting to influence the design of the environment and even the infection control procedures, a method of easily incorporating the time and spatial variation of airborne dispersal of infectious material due to activity is necessary. The ability to accurately include such an activity related source term of infection in a

CFD model would lead to better representation of the real situation, a greater understanding of the potential spread of disease within the ward environment and better assessment of risk and control strategies.

1.2 Aims and Objectives

This thesis aims to overcome some of the limitations of current CFD models of ward spaces by developing and validating a new method to better represent the dispersion of infectious particles generated by different types, levels and locations of activity in a hospital environment. It is proposed that typical bioaerosol generating activities within hospital wards occur in specific *zones*, rather than in exact locations. These zones can then be defined in CFD models as sources of bioaerosols that represent the release that occurs due to the activity within that zone. This method will enable a good representation of bioaerosol production due to activity within the ward to be easily included into a steady state model by distributing a contamination source over the likely volume in which it may be generated. It is intended that the resulting environmental contamination will yield a time averaged representation of the actual transient contamination due to the movement of a real source within the defined zone.

With the increase in computational power it is now possible to model this as a transient situation. However this is still a very time consuming process to set up the model, incorporate all the transient sources required, and then to obtain the solution. More importantly although this may yield realistic results for the defined inputs, the result will only be correct for that one situation. Transient modelling of a hospital ward involves unnecessary effort to obtain what is likely to be a falsely, and misleadingly accurate solution, that is actually only correct for one situation and not for real life. Since it would be impossible to model all the possible combinations of activities occurring throughout space and time for a hospital ward that changes continuously throughout a day, and from day to day, creating transient simulations is impractical as a method to obtain information about general ward situations for design or risk assessment purposes. However by creating a zone defined by the level and spatial footprint of an activity, dispersal related to that activity can be approximated for a typical day, or a high risk situation within a steady-state model. The creation and

solution of this model will involve significantly less time and effort, and the simple results from a frozen point in time convey the average behaviour of the scenario.

1.2.1 Concept of the Zonal Source

As stated the zonal source aims to represent the time averaged dispersal that would occur when bioaerosols are generated during activities. This methodology of source definition may then be used in a steady state model in order to represent the release of bioaerosols whose source position varies spatially over time. An example of a zonal based activity source is given in Figure 1-1, where a ward is shown with a possible zonal source to represent release of bioaerosols during bedmaking. This encompasses the zone around the bed where potentially pathogenic micro-organisms are ejected into the air due to movement of the sheets. The right hand picture shows an equivalent point source that may be used to simulate a cough. This is positioned where the mouth is assumed to be, and bioaerosols are released from a single position, usually with a single direction into space.

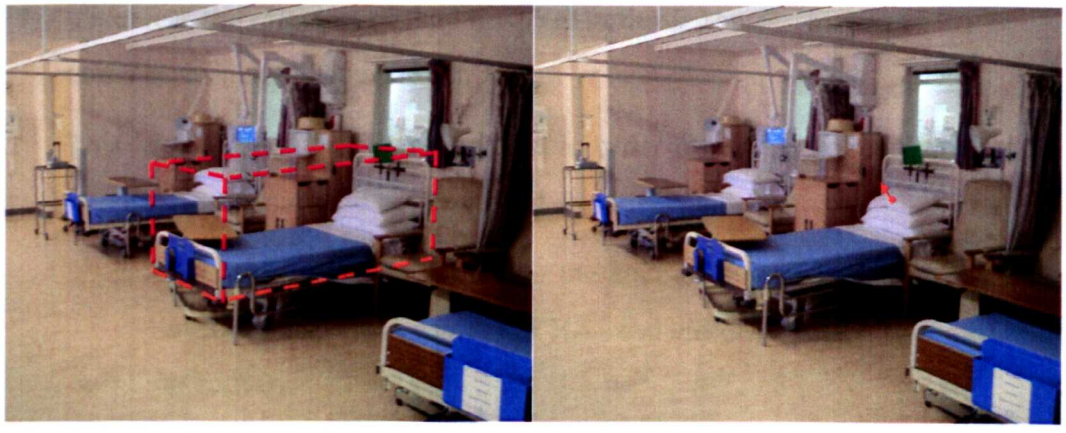

Figure 1-1: Views of a hospital ward showing (left) a zonal source for bedmaking and (right) a point source to represent a cough.

The development of this zonal source requires types of activity that can be represented in this way to be identified. This is carried out in detail through the literature review in Chapter 2 as well as through an observational and sampling study on a hospital ward described in Chapter 4, with potential activities including bedmaking or undressing/cleaning of the patient. In all these situations a static point source is clearly not representative of the whole contaminant dispersal and the zoning method should provide the ability to represent more realistic behaviour.

Once the zonal source is defined it is expected that it can be used in models of hospital wards or side rooms, possibly that incorporate various engineering infection control interventions, in order to assess the level of risk to the patients and HCWs. This may also be used in conjunction with a point source in order that both respiratory and activity sources of bioaerosols are considered when studying the risk of infection transfer within the space.

The overall aim of this thesis is therefore to develop and validate this zonal source model, establish the limitations of the model and identify when and where it should be used.

1.2.2 Objectives

In order to achieve this aim of developing and validating a zonal source model the following four major objectives were identified as being crucial to the successful development and completion of the research:

1. **To assess the effect of typical hospital activities on the airborne concentrations of bioaerosols.**

   This background study is carried out in order to assess the requirements of the modelling technique to be developed and involves:

   - Literature review to evaluate the state-of-the art in modelling airborne contaminants and problem of HAI and airborne dispersal of bacteria due to activity.
   - Observations and air sampling studies on a hospital ward to assess bioaerosol concentrations within the air due to different activities.

2. **To validate the use of CFD modelling techniques as a method for simulating the airborne dispersal and deposition of bioaerosols**

   - Literature review assessing the current status of techniques to model the transport of bioaerosols within CFD and their limitations.
   - Validation of the modelling techniques chosen through comparison with bioaerosol experiments for both airborne dispersal patterns and deposition.

3. **To develop and validate the zonal source model**

    - Numerical validation comparing the dispersal in a transient simulation from a moving source to steady state simulations with fixed point and zonal sources. Carried out using both passive scalar transport and discrete phase models to include size and mass of particles.

4. **To assess the sensitivity of the model and demonstrate the application and limitations within hospital environments**

    The use of a zonal model will be demonstrated by assessing risk in several situations

    - A hypothetical side room will be set up and risk to a HCW will be analysed considering both respiratory (point) and activity (zonal) sources. This model will be used to assess the sensitivity of both the zonal and point source to size and location respectively.
    - Both sources will also be used in a four bed ward environment. This will assess the risk an infected patient would have on fellow patients and HCWs. Also the risk a colonised HCW would have on the patients.
    - The zonal source is applied within a simple pressure driven zonal model for a ward environment and compared to equivalent CFD simulations.

1.3 Research Methodology.

The main emphasis of this thesis is on developing and evaluating numerical modelling techniques, with a particular focus on computational fluid dynamics (CFD). As outlined in Chapter 3, CFD is a useful tool for studying the transport of contaminants in fluids as such it is capable of simulating the movement of particles which could be biologically active throughout a room space. Instead of having to sample at discrete locations, as in experimental studies, entire particle paths, contours of contamination levels and flow patterns can be visualised and values at any point extracted. Whereas in an experimental study the number of sampling points is limited by equipment, and in a hospital ward the disruption to staff and patients, CFD is only limited by the computational requirements of the model and the availability of problem definition data for input. CFD also enables the user to study dispersal of potentially harmful pathogens without the health risks. For

this study it is useful to compare different types of bioaerosol source with exactly the same air flow pattern, by using the same solution of air flow for each. In order to simulate the dispersal of bioaerosols the position, size and velocity of the source needs to be realistically represented. If particles are being modelled then the mass flow rate, size and number of particles also needs to be considered. The purpose of the zonal model is to define these boundaries for a bioaerosol source due to activities.

The validation aspects of this study will not aim to produce a representation of reality, but to provide a framework to validate a zonal source against a time dependant simulation of a moving source. As such the main validation uses numerical methods comparing steady state and transient simulations and carrying out sensitivity analysis on the bioaerosol source definitions. The zonal source is also demonstrated within a pressure driven zonal model. This is a much simpler method of solving contaminant transport within indoor airflow but gives much coarser results. However this is particularly useful tool for evaluating a large series of interconnected zones, and so the use of the zonal source within this model is compared to CFD to assess its applicability.

Experimental sampling in a hospital environment is used in order to assess the importance of different activities on the airborne microbial content. This study is useful to highlight the various activities that have the greatest influence on the airborne micro-flora levels within a ward. Hence, the study will directly influence the activities that the zonal model will be used to represent, and the areas over which they occur. By recording activities within the space whilst collecting air samples, activity may be related to increases in airborne micro-flora through statistical correlation techniques. Since only a single sampling location is used, due to equipment requirements and the necessity to avoid obstruction to staff, this is purely a study on the overall effect of activity rather than detailed dispersion patterns.

Controlled experiments in a bioaerosol test chamber environment are also used in order to validate the CFD models for studying bioaerosol dispersion. By studying bioaerosol dispersal characteristics within a controlled test environment, the source type and location is known and the number of external influences on the dispersal reduced. This study uses several sampling points within the space to evaluate patterns of airborne dispersal and spatial variation in deposition of bioaerosols, within the space. One

advantage of controlled testing for this study is that a steady state air flow could be set up, enabling several successive samples to be taken from a space in which the contaminant distribution should remain steady throughout the experiment.

1.4 Layout of thesis

Following the introduction, this thesis begins by providing a more in depth explanation into the background of the study in Chapter 2. This chapter presents the literature review outlined in Objective 1. Initially the problem of airborne disease, particularly in hospitals is highlighted, concentrating on *Staphylococcus aureus* and MRSA. The various mechanisms for the spread of disease, either by contact, air, or a combination is discussed. Particular attention is paid to work discussing the dispersal of bacteria, mainly *Staphylococcus aureus* from activities. Chapter 3 consists of the second part of the literature review concentrating on the methods of modelling the spread of disease. This considers the use of epidemiological models, analytical ventilation models and multi-zone models to assess the efficacy of a ventilation system to remove airborne contaminants. Computational Fluid Dynamics is the main tool used for modelling disease in this thesis, therefore a large section of this chapter is dedicated to the application of CFD in modelling airflows and the spread of contaminants in rooms.

Chapter 4 concludes Objective 1, presenting the observational and sampling study on a hospital ward. A detailed description of the bioaerosol sampling methods is presented followed by the study methodology. The resulting data are analysed by correlating fluctuations of sampled bioaerosols and particles to specific observed activities.

Chapter 5 presents the governing equations of fluid flow and an overview of the CFD modelling technique. Initially generic aspects of CFD modelling are discussed, followed by model specific description focussing on the test chamber model used to validate the zonal source method in Chapter 6. Experimental validation of the bioaerosol transport models is presented. The bioaerosol test facility and experimental methods are described and results compared to those from CFD simulations to achieve Objective 2.

Objective 3 is carried out in Chapter 6. The zonal source method is introduced and validated numerically. The dispersion patterns from the steady state zonal source

models are compared to that from a transient simulation with a bioaerosol source that moves through the space.

Chapter 7 uses a model of a single-occupancy side room to assess the sensitivity of the zonal source to the zone size definition and contrasts this to the sensitivity of a point source to the specified location. A pressure driven zonal model is compared to a CFD model of a four-bed hospital bay, to evaluate the relative benefits and draw backs of each model for simulating bioaerosol transport. This CFD model is then used with point and zonal sources to assess relative risks to both patients and HCWs from respiratory and activity based sources.

The final chapter, Chapter 8, presents the general conclusions from the study and potential areas for further work.

Chapter 2

The Release of Bioaerosols in Health Care Settings

The following chapter introduces the problem of health-care associated infection (HAI) and the specific issues, and micro-organisms related to this thesis. After a discussion of different mechanisms for the transfer of infection the chapter focuses on the release of bioaerosols from the skin and discusses particle transport considering the size range of interest for HAI's. This chapter forms the background to determine the types of activities to be observed in the sampling study presented in Chapter 4. The data presented here also informed the definition of injection properties for the bioaerosols in the CFD models described in the later chapters.

2.1 Health-care Associated Infection

Health-care associated infection (HAI) is a major problem with 2-3 million people in Europe affected annually (Pittet *et al.*, 2005). The problem is a complicated one with many factors contributing including high bed occupancy, high patient to staff ratio, increased numbers of vulnerable patients, invasive techniques, dirty environments, poor hygiene practices, and excessive use of antibiotics (Chief Medical Officer, 2003). Not all of these infections are preventable but it is estimated that 15-30% may be. Even reducing infections by 15% would free up 546,000 bed-days annually in England and Wales and save the NHS £140 million. The cost of infection is not just on the NHS, but also the individual. It is estimated that the personal cost to the patient is 3.2 times more if they acquire an infection, not to mention the added distress to both themselves and their family (Plowman *et al.*, 2001). This cost will vary between patients, for example the acquisition of an infection may result in a longer stay on a general ward, or in intensive care, the costs of which will widely differ (Nettleman, 2003).

The emergence of multi-drug resistance micro-organisms adds further complexities to identifying and treating the infection, and as large numbers of pathogens become resistant to drugs there are fewer therapeutic treatments available (Hartstein *et al.*, 2004). The increase in *Clostridium difficile* associated disease, has recently led to policies being put in place to prevent the over prescription of antimicrobials. This is now a requirement in law, as part of The Health Act 2006: Code of Practice for the Prevention and Control of Nosocomial Infections (Department of Health, 2006, Department of Health, 2007a). The development of multi-drug resistance is not just of concern in the acquisition of disease within healthcare settings; the resistant micro-organisms may then be transferred out into the community. This has been seen with the Methicillin Resistant *Staphylococcus aureus* (MSRA) bacteria, that has been found to cause infections in those that have not frequented a hospital, and in some cases is becoming part of a persons natural skin flora (Baba *et al.*, 2002).

Although there are many micro-organisms that are responsible for HAI infection, and have the potential to be disseminated through the air, of particular interest in this thesis is the bacterium *S. aureus*. This is known to colonise the skin, from which it can contaminate the environment due to natural skin shedding, including airborne dispersion

associated with bedmaking (Shiomori *et al.*, 2002) and other nursing activities (Hambraeus, 1973). This bacterium when it develops resistance to the drug Methicillin, becomes the pathogen well known in the media as MRSA.

Methicillin is a form of penicillin that is resistant to Penicillinase, an enzyme created by bacteria to destroy penicillin (Prescott *et al.*, 2005). The introduction of Methicillin, in 1961, was a hopeful advancement, as resistance to penicillin had been increasing since Penicillinase was discovered to be synthesised by *Staphylococcus aureus* in 1944 (Kirkby, 1944). Unfortunately within a year an infection of *S. aureus* was found to be resistant to this drug, resulting in the emergence of Methicillin Resistant *S. aureus* (MRSA). Another antibiotic, Vancomycin, was introduced previous to Methicillin, yet resistance was slower to occur, taking 40 years until the first case was reported (Chambers, 2001). Resistance has since been reported on a number of occasions and there are now increasing concerns about the increase in Vancomycin resistant strains of MRSA (Tenover, 2006).

Mandatory reporting of MRSA associated bacteraemia has been in place in the UK since 2001, since surveillance of diseases is necessary in order to understand the effectiveness of control measures. Data from this reporting is shown in Figure 2-1. In 2006 the initial decrease was not deemed sufficient to tell if this was a permanent trend (Health Protection Agency, 2006). More recently the Department of Health (2008) are more positive and consider the results a promising sign that the targets of a 50% decrease on 2004 infections may be met. However there are significant variations in infection rates between different healthcare trusts indicating there is still potential for further reduction (Department of Health, 2007b). Control of MRSA in the Netherlands has been much more successful. By a method of 'Search and Destroy' infected patients are quickly identified and removed from shared wards, preventing the spread of infection to others. This method has proved successful due to the ability to isolate patients in single rooms, and the employment of a high number of health-care workers (HCWs) to enable this strategy (Chief Medical Officer, 2003). In the UK there are a large number of ongoing building projects in the health care sector, and although it is recognised now that infection control needs to be considered at the design stage (Stockley *et al.*, 2005) most guidelines still concentrate on operating theatres and isolation rooms (Beggs *et al.*, 2007). These spaces are high risk so it is understandable

to have specific guidance for them. However infection control is important throughout the entire hospital and should be considered at the design stage for all areas. Research into the effect of the environment within hospitals is vital to ensure appropriate decisions are taken at this early stage, and modelling techniques such as those discussed in Chapter 3 provide useful tools for research in this area. First evidence for airborne transmission of *Staphylococci* and MRSA through the air is presented along with detail of different sources of bacteria and *Staphylococci* within hospitals, and the dynamics of the particles released.

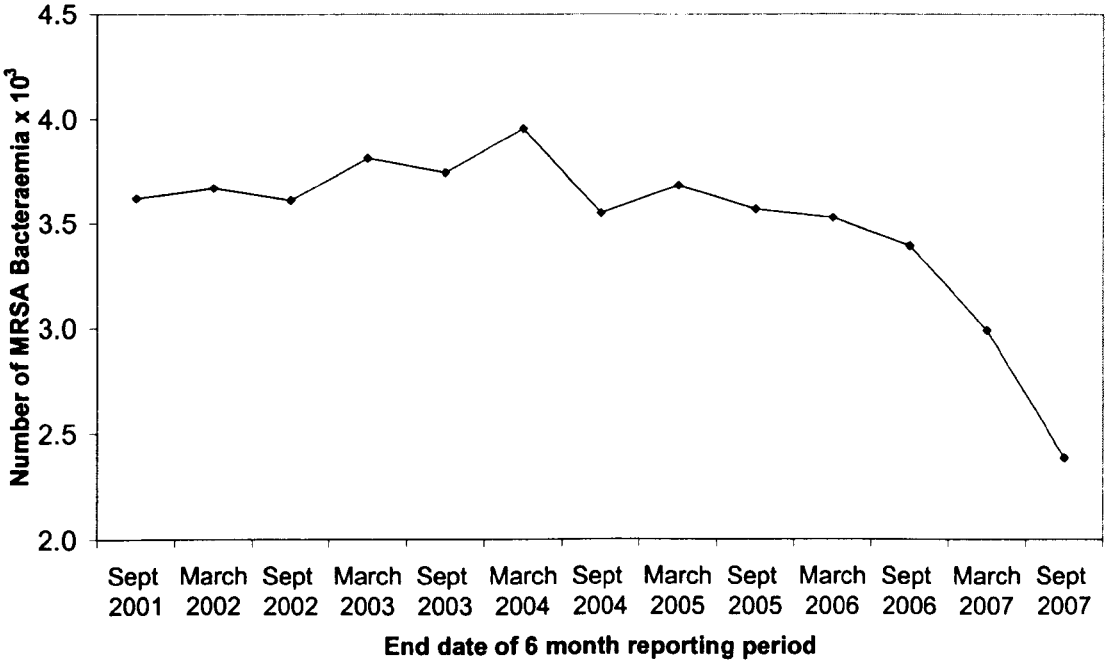

Figure 2-1: Numbers of MRSA Bacteraemias reported in England per 6 months (Health Protection Agency, 2008).

2.1.1 Airborne Transmission

There is much debate about the importance of airborne transmission for HAIs. This is partially because the level of importance of the spread of airborne infection is difficult to derive as the bacterial population in the air is never stable (Walter and Kundsin, 1973) and is difficult to sample. With gram negative bacteria it has been shown that a large number of viable micro-organisms are non-culturable and so air sampling may only produce colonies from 0.1-1% of that present (Heidelberg *et al.*, 1997). In addition where transmission is only assisted by an airborne route (section 2.2.4), the additional factor of an intermediate object makes the distinction between contact and airborne

more difficult to ascertain. It has been estimated that the airborne route of infection is responsible for between 10 and 20% of HAIs (Brachman, 1970) and although it is difficult to substantiate this figure, there is clear evidence of airborne related transmission for numerous hospital outbreaks. In terms of *S. aureus* the airborne route of infection has been implicated in several situations including: within a nursery ward (Mortimer *et al.*, 1966), in an intensive therapy unit due to extracted particles from a side room returning in through the ventilation system (Cotterill *et al.*, 1996) and in a burns unit (Farrington *et al.*, 1990). The ventilation system has twice been reported to sustain outbreaks of MRSA. Kumari *et al* (1998) found that when a supply system shut down, once a day, the negative pressure sucked air, and pathogenic material into the grilles, only to be redistributed when the system was restarted. The opposite has also been shown, when an extract system was shut down once a week and particles harbouring MRSA in the ducts were deposited on patients beneath (Wagenvoort *et al.*, 1993).

For infection to spread a source reservoir is necessary from which bacteria can be released. This reservoir can be in the environment or it can be a human host. *S. aureus* has the ability to colonise healthy individuals, and indeed it is thought that around 60% of the population will be carriers of *S. aureus* at some time in their life (Kluytmans *et al.*, 1997) and 10 to 20% of individuals are constantly colonised (Lowy, 1998). It has been shown that those who are not colonised can become rapidly so on admission to hospital (Shooter *et al.*, 1958, Williams *et al.*, 1959). Although colonisation may occur without causing harm it has been shown that those who are colonised are more likely to self-infect, and to suffer from wound infections (Williams *et al.*, 1962). Once colonised, the bacteria may penetrate deep into the skin, where sterilisation cannot occur, risking endogenous infection if the skin needs to be punctured for a medical intervention (Kluytmans *et al.*, 1997). This colonisation may occur due to an airborne source (Williams, 1966). Colonisation of a person with *S. aureus* usually occurs initially in the nasal passages, this then may spread to the skin, from which airborne dissemination may occur due to the natural shedding of skin particles (White, 1961). Skin is also shed into a patients bedding from which it may be released into the air due to the process of bedmaking, essential in the cleaning regime (Noble, 1962, Shooter *et al.*, 1958).

Under normal conditions *Staphylococci* is released into the surroundings from the skin, and not from the nose, despite high nasal colonisation (Duguid and Wallace, 1948). However it seems that when a colonised person is also infected with a upper respiratory tract infection there can be a large increase in the amount of dispersion, with this person being referred to as a 'Cloud Adult'. Since many healthcare workers are shown to be colonised with *S. aureus* they have the potential to become 'Cloud Adults' and disperse large amounts of pathogens if also infected with Rhinovirus (Sheretz *et al.*, 1996, Voss, 2004). This term originates from Eichenwald (1960) who advocated considering airborne dissemination in the design of nurseries due to the potential of 'Cloud babies' to cause outbreaks of *Staphylococci* disease.

Except for the phenomenon of 'cloud adults', the main source of *Staphylococci* dissemination into the environment is from the skin. The dispersion of skin, and thereby *S. aureus* and MRSA is discussed in further detail in section 2.3.2, following a review of the main methods of disease transfer in healthcare environments.

2.2 Mechanisms of Spread

In order to understand how the airborne transport of pathogenic particles affects the spread of infection an understanding of each distinct route of infection transmission is necessary. For this reason the following sections detail the different types of spread, using the terminology of the Centers for Disease Control and Prevention (CDC) (Siegel *et al.*, 2007) for clarity. These are:

- Contact
- Droplet
- Airborne
- Airborne Assisted

2.2.1 Contact

Contact spread, is considered to be the main route of spread for most HAIs. Contact spread can occur when a HCW attends to a second patient and, due to clothing contamination or failure to disinfect the hands, passes on a micro-organism from a previous patient. This spread of infection may also occur due to contamination of

equipment. It is also possible for the HCW to be colonised with a bacteria that they pass directly to the patient (Archibald and Hierholzer, 2004).

The role of hand washing in the reduction of infection has long been accepted. In several studies over the last century it has been shown to reduce the transfer of infection (Larson, 1988). Although most studies, and media attention, focuses on the hand hygiene of healthcare workers, it may also be the case that contamination of patients own hands through touching HCW hands, uniforms or the general environment are responsible for their own infection (Banfield and Kerr, 2005).

Contact Spread may also occur due to an intermediate reservoir of infection. For example hand washing may take place correctly but as a HCW closes the curtains around a patient's bed they pick up micro-organisms from the curtains, which may then be transferred to the patient. As discussed later in this thesis this existence of a reservoir may be due to the airborne transport of bioaerosols.

2.2.2 Droplet

According to the CDC, droplet transmission is a type of *contact* transmission although it does involve the transport of infectious particles through the air, albeit over a short distance. The CDC guidelines (Siegel *et al.*, 2007) state that "droplet transmission occurs when infectious material is ejected into the air from the respiratory tract to be deposited *into the respiratory tract* of another person within a short distance". This short distance is generally thought to be less than three feet, but following the 2002-03 SARS outbreak it is now acknowledged to depend on a variety of factors including the droplet release velocity and the environmental conditions. As such the three foot distance is now referred to as a 'typical' distance. The CDC guidelines are set in place in order to define different pathogens as having droplet or airborne spreading characteristics. By assigning these definitions to different infections suitable precautions can be defined to protect HCWs and other patients. For example infections known to be transmitted by the droplet route can be protected against by using facial protection when close to the patient but use of negative pressure rooms, or local extract is not considered necessary. Droplets are generally thought to consist of particles >5μm diameter, whereas airborne spread is in the range from 1-5μm (Siegel *et al.*, 2007).

The boundaries between *Droplet* and *Airborne* can become blurred. Infections that are spread by droplets may become airborne under certain influences. For example SARS is usually spread through droplet transmission and the use of nebulisers thought to aggravate this (Lee *et al.*, 2003). However a CFD study of one outbreak where nebulisers were used suggested airborne transmission and so the use of nebulisers may have resulted in the airborne dissemination throughout the ward (Li *et al.*, 2005). In fact the potential for nebulisers to increase the chance of spreading infection led to their use being banned on SARS patients within Hong Kong Hospitals. Airborne dissemination was also implicated in the Amoy gardens outbreak where faulty seals on the drains meant bioaerosols generated within the soil stacks were sucked back into the bathroom and out through the ventilation extract, to then return into other apartments in that building, and adjacent ones, spreading the infection (Yu *et al.*, 2004). In this instance, and possibly in the previous one, airborne spread was enabled through the presence of mechanical intervention, either through nebulisers or flushing, and a pathogen that is not naturally airborne becomes so. These examples highlight the dangers of considering diseases spread by the droplet route never to spread beyond the designated 3 foot droplet boundary.

2.2.3 Airborne

According to the CDC (Siegel *et al.*, 2007) *Airborne* diseases are described as those that result in the transport of small particles in the air over long distances, usually meaning the ability to pass through separate rooms. The particles should then be inhaled by another individual and infection will occur. *Mycobacterium tuberculosis* (TB) is one pathogen that that has long been acknowledged to be spread by the airborne route (Riley *et al.*, 1962). TB is a major health risk with a third of the world population infected (DeAngelis and Flanagin, 2005), and is becoming an increasing concern with anti-tuberculosis drug resistance found to be a world wide problem (Pablos-Medez *et al.*, 1994-1998). Measles (*rubeola virus)* is another disease known to be spread through the air, and one index case within a densely occupied environment such as a school can lead to a large outbreak (Riley *et al.*, 1978). In order to contain airborne diseases the use of local air extract systems is needed to control the transport of the pathogen and remove it from the space, the CDC recommends an air change rate of 6-12 $ac.h^{-1}$ for TB wards

(CDC, 2005). This has a greater cost than the use of face masks to control droplet spread, hence the desire to have separate definitions (Siegel *et al.*, 2007).

2.2.4 Airborne Assisted

From an engineer's, and flow modeller's point of view, and for the purpose of this thesis, if a pathogen is transported through the air, however short the distance, it can be considered to be affected by the air flow. For this reason in this thesis the term *airborne assisted* is used to refer to both droplet and airborne particles, the transport of which will be affected by the environment. Airborne assisted spread may lead to the deposition of infective material into the respiratory tract, or onto a surface where it may be picked up on hands, leading to contact transmission.

2.2.5 Environmental Reservoirs of Infection

In order for a pathogen that has dropped from the air stream onto a surface to subsequently cause infection it needs to have the ability to survive in those conditions. *Staphylococci* and MRSA have been shown to survive from just a few days to several months on typical hospital surfaces (Dietze *et al.*, 2001, Neely and Maley, 2000). Even after standard cleaning (French *et al.*, 2004, Rutala *et al.*, 1983) and supposed decontamination (Blythe *et al.*, 1998) MRSA has been found in the environment. Even if cleaning is successful, floors have been shown to rapidly re-acquire bacteria after cleaning (Ayliffe *et al.*, 1967). Curtains have been shown to harbour bacteria (Das *et al.*, 2002) including MRSA during an outbreak (Palmer, 1999). The presence of pathogens on surfaces may occur from hand contact but surface contamination has been shown to be reduced by the use of portable air cleaning devices (portable unit with HEPA filters) within side rooms (Boswell and Fox, 2006), indicating that transport through the air is an important factor.

Whether pathogens surviving in the environment, and subsequent hand contamination is responsible for further infections is hard to prove, as in any study of hospital outbreaks the possibility of contact is always present (Hota, 2004). The need for a clean environment is however intuitive, and well documented (Pratt *et al.*, 2007) and cleaning protocols and monitoring is advised (Chief Medical Officer, 2003). Micro-organisms in the environment have been shown to lead to the contamination of HCWs hands or

gloves (Ayliffe *et al.*, 1967, Bhalla *et al.*, 2004, Boyce *et al.*, 1997). Although there is a lack of direct proof, indirect evidence points towards secondary infections occurring due to environmental contamination (Talon, 1999) and completely removing MRSA from the environment has been shown to control an outbreak (Rampling *et al.*, 2001).

2.3 Bioaerosol Sources

An aerosol is defined as particles dispersed in a gas (for example air) and as such a bioaerosol is one where the particles are of a biological origin, and could therefore contain pathogenic material. It is commonly stated that the aerodynamic diameters of these particles will range from 0.5 to >100μm (Hinds, 1982).

Different sources of bioaerosols will generate particles in different ways, and this will lead to different sizes and shapes of the particles. Bacteria can be between 1-10μm in size but will be released into the air within droplets, or on a flake of skin squame or cloth fibres, the size of which may be larger. In turn these differences will affect the transport of the bioaerosols through the air and their deposition, or extraction from the space (Morawska, 2006). Within a hospital the production of bioaerosols can be caused by natural activities – coughing, sneezing, vomiting, diarrhoea or friction from physical activities; or induced from the use of medical equipment. Tang *et al* (2006) conducted a review and found that tracheostomies and bronchoscopies, and the use of oxygen masks or nebulisers can generate infectious aerosols. Faeces may also become aerosolised from flushing toilets (Morawska, 2006).

Bioaerosols responsible for HAIs may also originate from non-human sources, for example *Aspergillus fumigatus,* a fungi that is common in the outdoor environment, can be introduced via air ducts and during building work (Morris *et al.*, 2000) and *Legionella pheumophila* may be aerosolised from air conditioning systems that incorporate water cooled condensers or from shower heads (Prescott *et al.*, 2005). Kumari *et al* (1998) found the presence of *Staphylococci sp.* on ventilation grilles during an outbreak. Other non-human sources of bacteria within hospitals may originate from taps or showers, flushing toilets and wet cleaning of indoor surfaces (Cole and Cook, 1998, Morawska, 2006).

In order to use CFD models of the environment to study the transport of infectious particles, the properties and method of particle release needs to be defined. In the following section studies documenting the production of bioaerosols from humans due to respiratory and physical activity are reviewed. This will be used directly to inform the inputs for bioaerosol sources within the CFD models developed in later chapters of this thesis.

2.3.1 Respiratory Droplets

Respiratory droplets may be created in the respiratory tract due to the passage of high speed air, up to $50m.s^{-1}$, during talking, coughing and sneezing. Secretions that are present in the mucous surface are entrained into the air flow, they become detached and coil up to form a droplet that is then expelled through either the mouth or the nose (Clark and Cox, 1973). As well as the respiratory tract, the creation of bioaerosols can occur at the front of the mouth, due to obstruction by teeth, tongue and tonsils, and in the nasal passages (Morawska, 2006). Due to the difference in speed of the air flow created by talking, coughing and sneezing, different sizes and quantities of droplets may be produced by the different actions. They may also produce the droplets from different parts of the respiratory tract that expel disparate bacteria (Hamburger and Robertson, 1948).

Table 2-1: Falling distance and time before evaporation of a range of droplet diameters (water droplets in unsaturated, still air at 22°c (Wells 1955)).

Diameter of Droplets (μm)	Evaporation time (seconds)	Distance droplet will fall before evaporation (m)
200	5.2	6.61
100	1.3	0.43
50	0.31	0.026
25	0.08	0.0016
12	0.02	0.000085

These micro-organism containing droplets are small with a high surface to volume ratio, and as such evaporate quickly to become what is known as droplet nuclei. The evaporation time for water droplets was quantified by Wells (1955), along with the

distance the droplet would fall before it evaporated. Wells' data is reproduced in Table 2-1. It can be seen that even for a droplet as large as 100μm evaporation to a much smaller droplet nuclei only takes 1.3 seconds, a very short period of time.

A few authors have attempted to quantify the size, mass and speed of bioaerosols generated from coughing. However due to different methodologies the results vary, sometimes quite widely. Even using the same methodology the results differ from person to person, as individual physiology and health will affect droplet production. Since under most common conditions droplets evaporate very quickly once released into the air, it follows that the time period between release and measurement will also directly impact the size determined. Due to the rapid decrease in diameter, ranges in diameters of droplets have been found to be between 0.6μm to over 1400μm with the most common diameters below 200μm (Nicas *et al.*, 2005) depending on the measurement technique employed. At the lower end Xie *et al* (2007b) found the majority of bioaerosols were 25μm to 300μm, by calculating diameters from droplets that impacted on the sides of a chamber that a subject coughed into. However experiments using an optical particle detector found 80-90% of particles produced from breathing or coughing were smaller than 1μm (Papinieni and Rosenthal, 1997). This difference is unsurprising since in the latter any large droplets are likely to have deposited or evaporated (Table 2-1) before the measurements were taken and only those small enough to remain suspended in the air are counted.

Due to the large range of droplet sizes it is useful to consider them in different ranges, rather than individual sizes. Tang *et al* (2006) recommended classifying bioaerosols into three size ranges: <10μm as droplet nuclei, <60μm as small droplets and >60μm as large droplets. With these definitions the droplet nuclei and the small droplets (which would evaporate quickly to form droplet nuclei) are responsible for the long range transmission through the air, whereas the large droplets are more likely to deposit out of the air streams, or become inhaled by a person situated nearby before they evaporate completely, and so are only capable of short range transmission. This 'short range' may be up to 2m (Xie *et al.*, 2007a), which concurs with the CDC's definition of droplet transmission (Siegel *et al,*. 2007). The mass of particles measured also depends on the experimental methods although there does appear to be a gender difference, with

average masses typically between 4.05-6.7mg for males, and 2.4-3.4mg for females (Xie *et al.*, 2007b, Zhu *et al.*, 2006).

The speed that particles are released during coughing usually varies between 6 and 22m.s^{-1}, most commonly 10m.s^{-1}(Zhu *et al.*, 2006). Sneezing releases more saliva than coughing, as the process of sneezing expels saliva from the mouth instead of the back of the throat as in coughing and at a speed of up to 100m.s^{-1} (Wells, 1955). Although talking produces much less bioaerosols than either coughing or sneezing, extensive talking can still double the amount of bacteria dispersed (Sheretz *et al.*, 1996).

2.3.2 Bioaerosol production from physical activity

Physical characteristics of Skin Particles

Release of bacteria due to physical activity generally occurs on skin squame, although it may also occur on clothes fibres. The human body replaces a layer of skin, on average, every four days. Skin diseases may result in increased shedding, and although this promotes the shedding of very large particles, there is evidence it also increases the dispersal of smaller particles (Noble and Davies, 1965). Davies and Noble (1962) studied surface dust within hospital wards microscopically, and took air samples. They found that the majority of both were composed of similar flake like particles that resembled skin squame. The particles were compared with known skin squame by staining, confirming this similarity further. The size range of the airborne particles were found by sampling with a cascade impactor. The size of particles carrying bacteria has been measured by Noble (1963) using an air sampler that separated samples into different size ranges in different environments. Controlled experiments within chambers have been used to assess the size distribution of particles released from people during dressing (Noble and Davies, 1965) and exercising (Mackintosh *et al.*, 1978). The results from these studies are given in Table 2-2. The first three studies determined particle sizes using impactor samplers (described in section 4.1.1) to segregate the particles into different size groups. The diameters are therefore determined from their behaviour in air rather than measurements of dimensions and so should be considered as aerodynamically equivalent diameters (see section 4.1.1). However in the study by Mackintosh *et al* (1978) the particles were measured using photomicrographs and so these results can be considered actual dimensions.

Other authors have also studied the size distribution of particles during activity. Friberg *et al* (1996) showed, using a laser particle counter, that there was an increase in particles greater than 0.3μm during a mock-up[1] of a surgery. The particles were measured in five increments up to particles sized >10μm diameter, and although there was an increase in all particles the increase was greater for the largest size range. Shiomori *et al* (2002) found that 80% of particles released during bedmaking were greater than 5μm. Outside of the hospital environment higher particle counts have also been found in office staff rooms during periods of activity in the breaks and during cleaning compared to quiet parts of the day (Micallef *et al.*, 1998). A mock up of an office found that the fluctuation of airborne bacteria during the sampling period correlated well with the production of particles greater than 7.5μm (Tham and Zuraimi, 2005).

Table 2-2: Equivalent Aerodynamic Diameters of Skin Squame from literature.

Reference	**Place**	**Range (μm)**	**Average (μm)**
(Noble, 1962)	Hospital Ward		8
(Noble *et al.*, 1963)†	Offices	4 - 22	11.1
	Hospitals wards	4 – 20	13.9
(Noble and Davies, 1965)	Chamber Normal people	12-22	16
	Chamber Skin diseases	10-20	13
(Mackintosh *et al.*, 1978)*	During exercise	5 – 50	Surface 34x44 Between 3-5μm thick
*Actual dimensions (Range is smallest minimum dimension to largest maximum) † Range = interquartile range, not full range			

[1] The mock up consisted of 30minutes of oral and physical movements of six individuals that would typical occur during a 2 hour major orthopaedic surgery, with sampling instruments in place of the patient.

Noble (1962) showed that *Staphylococcus aureus* was capable of rapidly contaminating the environment. During this study a single patient with a distinctive form of *Staphylococcus aureus* was observed. Before entry to the ward the type of *Staphylococcus aureus* the patient was colonised with was not present elsewhere. Upon arrival the patient contaminated the bedding with more than 700 colonies within two hours. Only five hours after arrival the contamination had spread to the curtains surrounding the bed. Two days into the patients stay 14 beds within the 22 bed ward had been contaminated. A week into the stay this had risen to 20 beds, 28 of 30 curtains and all the window ledges and sinks. Activities such as walking (Bethune *et al.*, 1965, Cleyton *et al.*, 1968, Duguid and Wallace, 1948, Hill *et al.*, 1974, May and Pomeroy, 1973, Speers *et al.*, 1965, Speers *et al.*, 1966), undressing and dressing (Duguid and Wallace, 1948, Hambraeus, 1973, Noble and Davies, 1965), and moving patients (Bethune *et al.*, 1965) have been shown to increase the level of bacteria in the air. This bacterium has also been shown to settle out of the air after activity such as walking on the spot (Hare and Ridely, 1958, Hare and Thomas, 1956, Sciple *et al.*, 1967).

There is a large amount of variability in the values recorded as each experiment was carried out differently, using different types of chamber, sampling methods and culture agar. Studies also considered different types of people including healthy people and those with skin diseases, or gender differences. Many of these studies were interested in the effect of different clothing types so these may also have an effect on the levels of airborne micro-organisms released. Details of the individual studies are not given here except where necessary for explaining differences in results.

Walking

Figure 2-2 shows the range of colony forming units per metre cubed ($cfu.m^{-3}$) sampled from the air with the subject walking on the spot. The work by Duguid and Wallace (1948) gives particularly high values compared to the other studies, but in this study activity was carried out in an unventilated chamber for 10 minutes, whereas the activity was only carried out for 0.5-2 minutes in the other studies. Considering the variability within the experiment conducted by Speers *et al* (1965) is over a 1000 $cfu.m^{-3}$, the variability between different studies is minimal, and all show an increase during walking in comparison to background count.

Bedmaking

For many years bedmaking has been thought to contribute to the airborne micro-flora. Davies and Noble (1962) took both measurements of skin particles and the total viable count of bacteria in the air, and the two sets of samples followed the same pattern throughout a period of bedmaking. Peaks and troughs occurred at the same time, as has been reproduced in Figure 2-3, increasing at 12 and 30 minutes when bed disturbance occurred. A similar pattern was also found by Noble (1962). An increase in *Staphylococci* during bedmaking has also been shown by Noble (1962) and Walter (1959), the data for which is presented in Figure 2-4. There is a large variation between the values for those classified as dispersers and normal patients. However all values are higher than at rest, with a minimum threefold increase for normal patients. More recently air sampling showed values of airborne MRSA to be up to 26 times that during the resting period during bedmaking. These did not reduce to the background level for 30 minutes after the activity (Shiomori *et al.*, 2002).

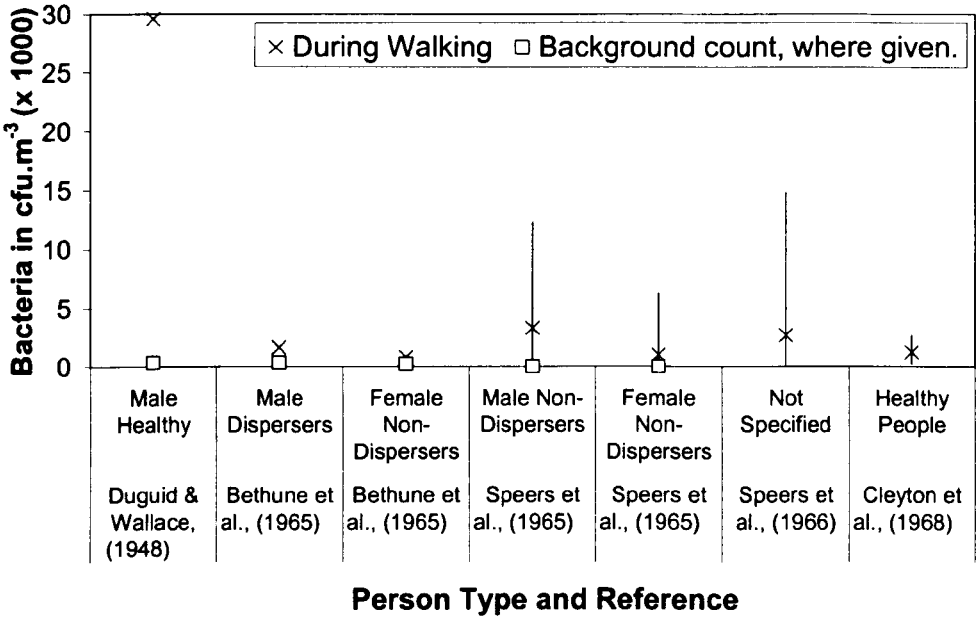

Figure 2-2 Range of colony forming units sampled during walking from different types of people. The background count is either a person standing still, or an empty chamber.

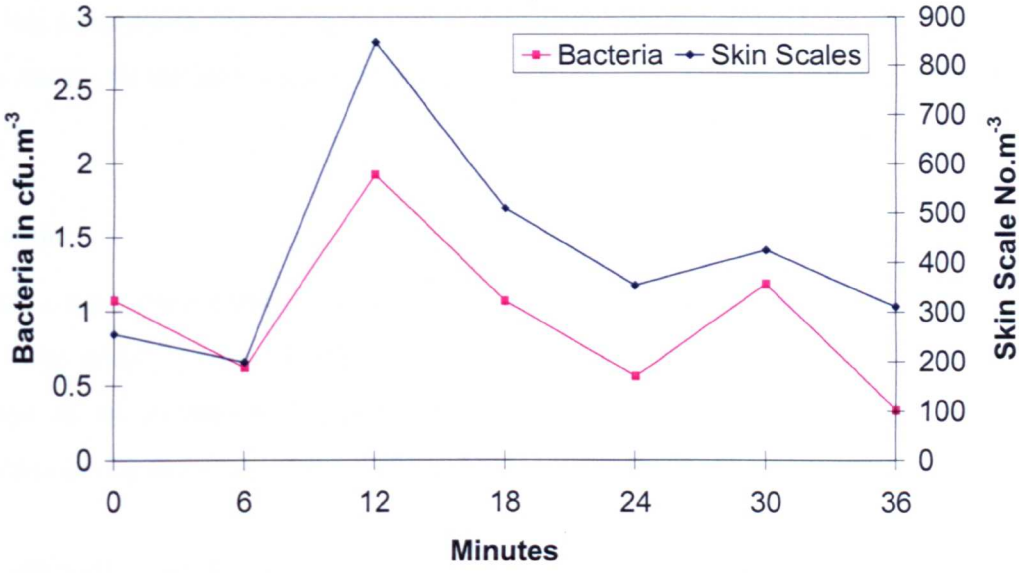

Figure 2-3 Skin scales and bacteria sampled during bed disturbance (at 12 and 30minutes) Data from Davies and Noble (1962)

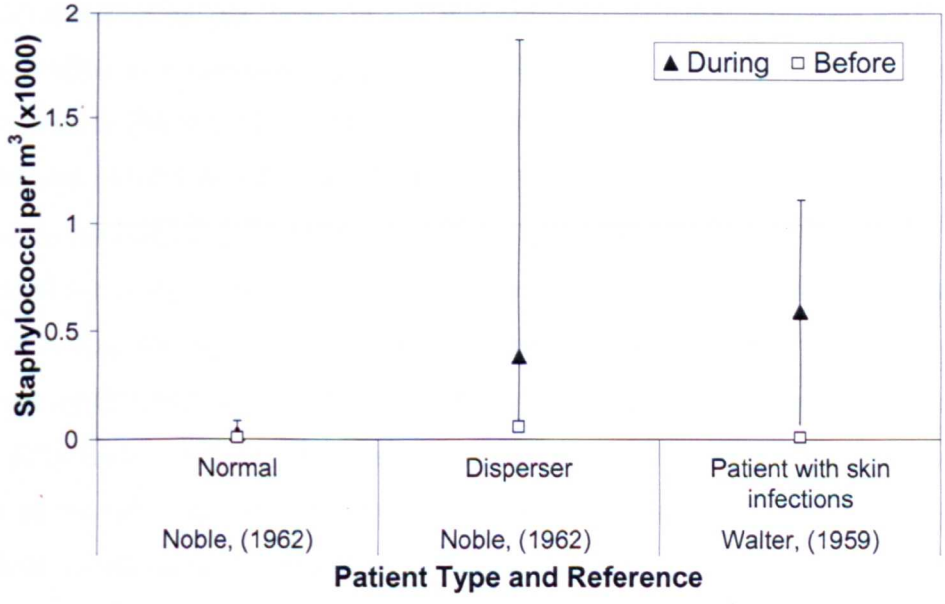

Figure 2-4 Sampled values of *Staphylococci* per m^3 of air for different types of patients during bedmaking.

Undressing and Washing

The work by Duguid and Wallace (1948) (results shown in Figure 2-2) also sampled the air whilst the subject undressed. This showed an even greater increase in cfus sampled than vigorously walking, to almost double that produced when vigorously marking time. As with the results for bedmaking and walking the amount of bacteria dispersed depends on the type of patient, with values between 1836 $cfu.m^{-3}$ for normal females, up to 32843 $cfu.m^{-3}$ for patients with skin diseases (Noble and Davies, 1965). A mock up of

nursing procedures that included washing, bedmaking and tidying, showed an increase in *S. aureus* in the air from a background count of 0.4 per m^3 to 4.2 per m^3 (Hambraeus, 1973).

Curtains

Curtains have been found to become contaminated with bacteria such as *Acinetobacter* spp. (Das *et al.*, 2002) and *Staphylococcus aureus* (Noble, 1962). Noble found that on 36 out of 41 occasions the disturbance of curtains corresponded to an increase in airborne micro-flora and on 26 of these occasions of *Staphylococcus aureus*.

The discussion above demonstrates that there are many studies into the release of bacteria and particles from humans during activity. However there is no comprehensive study of the microbial flora in the air on a general ward, and how general nursing activities during the day effect it. The majority of the studies described were carried out in controlled environments. Some have studied air in hospitals but these are either for short periods (Noble, 1962, Davies and Noble, 1962), or are only concerned with side rooms and individual patients (Shiomori *et al.*, 2002, Walter *et al.*, 1958). Greene *et al* (1962) considered the airborne micro-flora in several areas of two hospitals. This study included the comparison of activity in an operating theatre to the airborne count, and the use of a laundry chute. Nevertheless the majority of the study was concerned with comparing different areas within a hospital, and the airborne contamination between the two institutions, and not the variation of airborne micro-flora within a general ward. Also in the 40 years since Greene's work the way hospitals are run has evolved and medical interventions have advanced, which is likely to change how, where and when bioaerosols are released into the space. This leaves a large gap in knowledge that could impact on the way ward spaces are designed for better infection control. Except for the study by Shiomori *et al* these were carried out pre-genotyping and so relating the sampled bacteria to the source (e.g. an infected patient) was more difficult and uncertain.

2.4 Particle Transport

Within CFD models, as will be discussed later, it is possible to model a pollutant as a passive scalar that follows the air flow, or as particles that possess size and mass. In

order to choose the most efficient modelling technique it is necessary to have an understanding of the passage of particles through the air. The following section discusses the physical laws that control the transport of particles of a size relevant to this study. From the previous review (2.3) it was seen that airborne bacteria are generally associated with particle diameters between 1μm for droplet nuclei and up to 50μm maximum diameter for bacteria carried on a flake of skin squame. Therefore the remainder of this study will focus on airborne particles in this size range.

Once any particle is released into the air its motion will be affected by gravity, resistance from the fluid, electrostatic effects, thermal gradients and turbulent diffusion, and Brownian motion for those smaller than 0.1μm (Cox, 1987). Firstly only the motion of a particle due to gravity and the resistance from the fluid is considered. The following is an outline of the laws of fluid resistance and a discussion of settling velocities of various sized spheres. A more complete derivation can be found in Hinds (1982).

As a particle falls through a still fluid, such as air, it will displace that fluid from its path. It follows that a particle must exert a force in order to accelerate this mass of fluid out of its path. If the particle is a sphere then it will push aside a cylindrical column of air the same diameter, d, as the sphere. If the sphere is falling at v ms^{-1} and the density of the fluid is ρ_f, then it follows that the mass of fluid moved is $\rho_f \frac{\pi}{4} d^2 v$. Since the acceleration of the fluid will be proportional to the velocity of the particle, then the force the sphere imparts on the fluid, and consequently the resistance force acting on the sphere is:

$$F_r = C\rho_f \frac{\pi}{4} d^2 v^2 \qquad 2\text{-}1$$

Equation 2-1 is the general form of Newton's equation of fluid resistance. The co-efficient C in the above equation was assumed to be constant by Newton, and is acceptably so when the Reynolds number Re>1000. At these higher Reynolds numbers the inertial forces are dominant and the viscous forces can be neglected. However for lower values of Re the viscosity of the fluid becomes increasingly important in calculating the resistance it imparts. At the other extreme to Newton's law the inertial forces become negligible when Re <1. In this region Stokes' Law is used. Stokes' law

solves the general equation of fluid motion, the Navier-Stokes equations by making the following assumptions.

- The inertial forces are negligible
- The fluid is incompressible
- The influence of walls or other particles is negligible and therefore not within 10 diameters of the particle
- Velocity is constant
- The particle is a rigid sphere
- Fluid velocity at the particles surface is zero.

The first assumption is the most important; by removing the inertial effects the Navier-Stokes equations can be reduced to only the pressure and viscosity terms enabling them to be solved for a velocity distribution around the sphere. From this velocity the normal and tangential forces on the sphere can be found and integrated over the whole sphere. Summing these forces due to pressure and friction gives the drag on the particle F_D:

$$F_D = 3\pi\eta v d \qquad 2\text{-}2$$

Where η is the viscosity of the fluid. Comparing this to the equation 2-1 the resistance force changes from being proportional to v^2d^2 in Newton's region, to being proportional vd in Stokes' region. In the transition zone, where $1<Re<1000$ the resistance relationship will vary between these values.

Stokes' law (equation 2.2) is valid for spheres of diameters 1.5μm to 75μm. The reason for the lower limit is that as the diameter decreases, it approaches the mean free path of air. When this occurs the assumption of zero velocity at the particles surface becomes invalid and the particle 'slips' between the gas molecules, enabling the particle to move faster than would be predicted with equation 2-2. To enable the equation for drag to be used a correction for this slip is applied, known as the Cunningham Slip Correction factor, C_c, applied as in equation 2-3.

$$F_D = \frac{3\pi\eta V d}{C_c} \qquad 2\text{-}3$$

The value for C_c, at 20°C and 1atm, is 1.11 (Hinds, 1982) for a spherical particle with diameter 1.5μm and the value decreases with increasing diameter. It can be seen from this that for particles > 1.5μm there will be an error of about 10% decreasing for larger particles if slip is ignored, hence for submicron particles the slip cannot be ignored.

Having defined a method of calculating the drag force on a particle then the settling velocity in still air can be determined by equating the drag force to the force due to gravity $F_D = mg$. Still considering a spherical particle with density ρ_p and rearranging for the velocity this becomes:

$$v_{TS} = \frac{\rho_p d^2 g C_c}{18\eta} \qquad 2\text{-}4$$

Transport of spherical particles in an air current

The research in this thesis studies the transport of particles in indoor environments where air currents will be present. The transport of the particles will depend on the velocity of the air and the settling velocity of the particle. The following considers the relative horizontal distance spherical particles may be transported in a typical indoor environment in the size range relative to this study.

Spherical particles of diameters sized 1μm, 5μm, 10μm, and 20μm, density of 1000 kg.m^{-3}, viscosity of 1.8 x 10^{-5} Pa.s, and with a Cunningham slip correction taken from Hinds (1982) were considered. Applying these values to equation 2-4 the settling velocity of each particle diameter was found. This was treated as the vertical velocity vector, whilst a horizontal velocity of 0.06m.s^{-1} was applied giving the solution of particle tracks as shown in Figure 2-5. This current is taken as a typical low flow that has been measured within an office environment (Sekhar and Willem, 2004). The largest sphere shown here with a diameter of 20μm drops 2m in less than 2.5minutes, whereas the 1μm particle is still airborne after four hours.

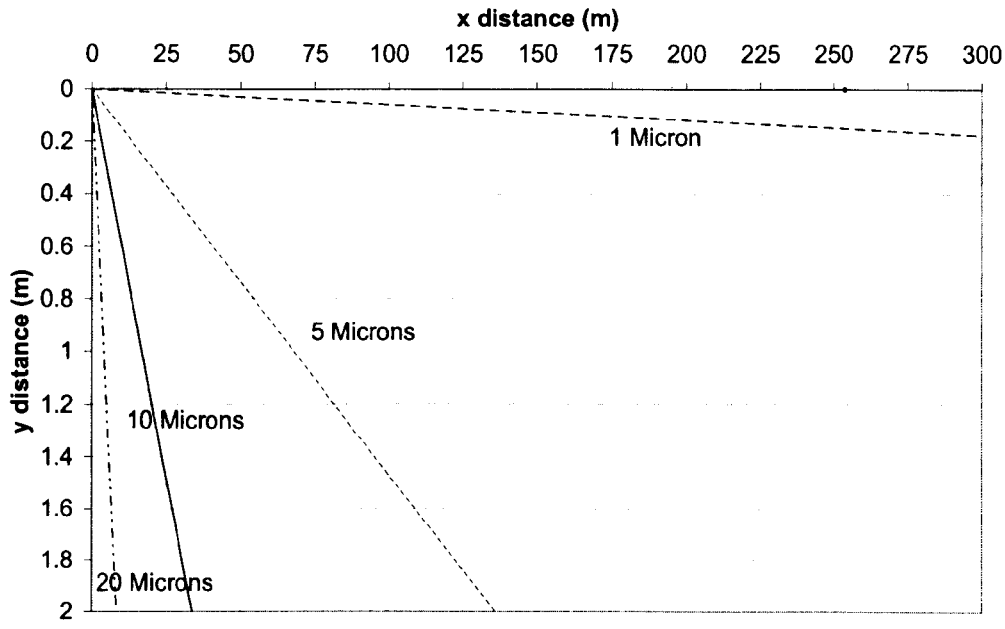

Figure 2-5: Distance 1-20μm particles travel with a horizontal speed of 0.06m.s^{-1} before landing from a height of 2m

The results are presented in Figure 2-5 where the x-axis is the distance travelled horizontally, whilst the y-axis is the vertical distance. This considers that the particles are released 2m above the floor. As can be seen the low settling velocity of the smaller particles enables them to travel very long distances before being deposited from the air stream. It may be possible with a well designed ventilation systems that these may be removed from the ward, however it could also mean that they travel long distances to different bays contaminating surfaces, or become inhaled to cause infection.

Particle Shape

The particles considered here are assumed to be spherical, however as has been discussed a large proportion of *S. aureus* is released on skin squame that is more likely to be flake like in shape. This will affect the motion of the particle and shape factors may be applied to the above equations to allow for this. However shape factors merely alter the equation by considering a spherical particle of equivalent diameter that would have the same particle relaxation time as the required shape. Since the diameters considered here correspond to those found from experimental techniques that size the particles due to their aerodynamic behaviour (2.3.2) it is reasonable to assume spherical particles from these sizes.

2.5 Summary

It is clear that HAIs present a large problem in both the UK, and the rest of the world. The ability of bacteria to travel on air currents and become deposited on surfaces, or become inhaled by susceptible individuals means there is the potential for engineering interventions to be able to go some way towards controlling the problem. *Staphylococcus aureus* and the resistant version MRSA has been identified as being carried on skin particles with dimensions between 3-50μm, or aerodynamic diameters between 4 and 22μm, which are released during bedmaking, walking, undressing, curtain movement and wound dressing. Respiratory diseases will be released on droplets from the mouth, nose and respiratory tract that evaporate quickly to be between <1-10μm. The larger particles will drop out of the air stream quickly whilst the smaller droplets will stay airborne for many hours. This data will be considered in the definition of the particles injected in the zonal source representing the generation of bioaerosols due to activity.

Several specific nursing activities have been identified as causing bioaerosol release, however it was noted that there have been no comprehensive field studies relating daily routines on a hospital ward with the levels of airborne micro-flora. It is important to be able to assess those activities that produce the most bioaerosols and the locations within the ward that they occur in order to use this information within a CFD model. As well as highlighting the lack of a current comprehensive study of the airborne micro-flora within hospitals the literature review in this chapter will aid the design of such a study, and identifies those activities that should be quantified.

Chapter 3

Background to methods of modelling the spread of infections

The following chapter presents a background to methods of modelling the transfer of infection. The majority of work presented in this thesis uses Computational Fluid Dynamics (CFD) as a tool to understand the transport of bioaerosols. However there are many other tools that may be used to understand the spread of infectious disease and it is therefore necessary to present a background to the different types of methods used by both engineers and epidemiologists. Importantly this chapter presents the current state of the art in terms of using CFD to research the design of hospital wards; this highlights why it is felt necessary to develop the zonal model which is described in more detail in Chapter 6. The detail of modelling bioaerosol transport and the background equations used in CFD will be presented in Chapter 5 alongside the test chamber model developed in this study.

3.1 Mathematical Modelling of the Spread of Disease.

In order to control the outbreak of disease, either health-care associated or otherwise, understanding of the transmission process is an important part of implementing any control procedures. Modelling techniques can be a highly useful method to aid this understanding. There are many different factors that affect the spread of infections; including the micro-organism responsible, its virulence and ability to survive in the environment, the design of the environment, temperature and humidity, along with any ventilation that may remove the micro-organism or air cleaning mechanisms such as UV. Finally the host themselves and their susceptibility to the particular micro-organism will also control the probability of an infection occurring. Patients in hospitals are often immuno-compromised due to illness or treatment, dramatically increasing their likelihood of succumbing to an infection.

There are several modelling techniques that can be used to provide insight into the various factors involved in disease transmission either individually or collectively. The traditional models are commonly referred to as epidemiological models, and consider the epidemic potential of an outbreak due to simplified contact between infectious and susceptible people in a community. An alternative approach although not widely adopted is to model directly the movement of infectious particles in the space using fluid modelling techniques (Noakes *et al.*, 2006b) and to infer contagious contact due to the transport of these between one person and another. These infectious particles may be bacteria, fungi and viruses, referred to in their general form when aerosolised as bioaerosols. It is necessary to present here the fundamental equations on which the traditional methods are based to enable understanding of the concepts used to understand epidemics and to carry out infection simulations.

3.1.1 SIR and SIS Epidemic Models

Epidemiological modelling of diseases in populations is a widely used tool to determine the extent of an infection in a population or the likelihood of an epidemic occurring and whether the outbreak is self limiting. It can be used to predict how an epidemic will progress and the impact it will have on a population including the effects of interventions.

Two classic epidemic models are the SIR and the SIS models, both of which consider the dynamics of Susceptible, S and Infective, I people. The SIS model, considers the case where a person may go from susceptible to infective and directly back to susceptible on recovery, whereas in the SIR model an infective person then becomes Removed, R, through isolation, immunity or death. For a closed population of size N, the basic equations for the progression between each state for the SIR model are as follows:

$$\begin{aligned} \frac{dS}{dt} &= -\beta IS \\ \frac{dI}{dt} &= \beta IS - \gamma I \\ \frac{dR}{dt} &= \gamma I \\ N &= S + I + R \end{aligned} \qquad 3\text{-}1$$

Here β is the infectious contact rate, and γ is the recovery rate. The important parameter in these equations is the reproductive ratio:

$$R_o = \frac{\beta N}{\gamma} \qquad 3\text{-}2$$

$R_o < 1$ indicates that the disease will die out, whereas a value of $R_o > 1$ will lead to an epidemic. This ratio can be used to assess the effect of an intervention on the progression of a disease through a population and is commonly used when considering vaccination. In a SIR model this is used by reclassifying a number of susceptible cases as removed due to immunity, carried out by reducing the value of S and by increasing the value R in equation 3-1. Using equations 3-1 and 3-2 the reproductive ratio can be found, which will inform whether the disease is likely to die out (Britton, 2003).

3.1.2 Wells Riley Model

The SIR/SIS epidemiological models described above can explain how an infection spreads through a population, but in this basic form there is no provision for the effect of the environment. Wells (1955) was among the first to describe the effect of the indoor environment on the spread of airborne infections using mathematical models.

Wells introduced the concept of a *quanta* of infection. This is a unit that encompasses the infectiousness of a disease, the susceptibility of uninfected people and the quantity of contagious material present in the air. If each person in the room inhales a quanta of infection then 63.2% (equal to 1-1/e) of them will become infected. The *law of mass action*, which is commonly used in chemistry to express how a reaction is effected by the quantity of reactants (Daley and Gani, 1999), can be used to express the number of new infections C, that will occur in relation to the dilution of infectious particles, r, and the number of infectors, I, or susceptibles in the space, S such that:

$$C = rIS \qquad 3\text{-}3$$

$$r = pqt\ /Q \qquad 3\text{-}4$$

The dilution of infectious particles, r, includes; the quanta of infective material produced per infector per hour q, quanta.h^{-1}, the pulmonary ventilation of the susceptibles p, m^3.h^{-1}, and the volume flow rate of clean air into the space Q, m^3.h^{-1}. With a constant number of susceptibles and infectors in the space, and assuming there is a constant production of quanta, the increase in numbers of infection will be proportional to the inverse of the ventilation rate (Wells, 1955). So instead of simply relating the infection rate to the amount of contact between susceptibles and infectors, the effect of the ventilation regime has been included.

The law of mass action is valid if the infectious material is evenly distributed throughout the room. However quanta is likely to exist in very low concentrations, and to be randomly distributed throughout the internal space. Riley (1978) adapted the law of mass action to this case by introducing a probability of infection:

$$p = 1 - e^{-Ir} \qquad 3\text{-}5$$

Summing the probability of infection for all susceptibles, enables the number of new infection cases to be predicted. This expression is known as the Wells-Riley model:

$$C = S\left(1 - e^{-Ir}\right) \qquad 3\text{-}6$$

The Wells-Riley equation has been used in many instances, particularly in studying the outbreak of measles (Riley *et al.*, 1978) and looking at ventilation efficiency in preventing the spread of TB (Nardell *et al.*, 1991).

Returning to the SIR equation, for airborne diseases the effect of ventilation will affect the contact rate β between infectors and susceptibles. Therefore examining equations 3-1, it is possible to simply include the effect of ventilation using this factor. Noakes *et al* (2006a) compared equation 3-1 with the time derivative of the Wells-Riley Equation:

$$\frac{dS}{dt} = rIS \qquad 3\text{-}7$$

From equation 3-1 and 3-7 it is clear that the value β is equal to r in the Wells-Riley equation. The definition of r is given in equation 3-4 and includes the volume flow rate of clean air into the room. Therefore simply replacing β with r allows the model to be used to study the effect of ventilation rates on the number of susceptibles and infectors, and thus enabling the reproductive number to be discovered.

3.1.3 Multi-Zone Models.

The Wells-Riley equation above depends on the room air being well mixed. In a room with perfect mixing the steady state contaminant concentration, C, is simply a function of contaminant generation rate, q, and the ventilation rate, Q.

$$C = \frac{q}{Q} \qquad 3\text{-}8$$

Since the air flow in rooms rarely reaches perfect mixing this description of contamination concentration may be inadequate in certain ventilation regimes in which strong short circuiting in the flow occurs. One possible method to take this into account is to include a mixing factor on the ventilation rate, but this will still be describing a well mixed room however one with an adjusted ventilation rate that may result in underestimating the risk in certain areas. To improve on the assumption of the room air being well mixed, multi-zone models may be used. The simplest of these is the two-zone model which may be used to assess higher concentrations near a source, or to

include the effect of short circuiting as illustrated in Figure 3-1 (Nicas, 1996). These models may then be extended and used to compare contaminant removal efficiency with different ventilation regimes (inflow and outflow positions) (Brouns and Waters, 1991), or to apply UV irradiation to the upper zone (Noakes *et al.*, 2004a).

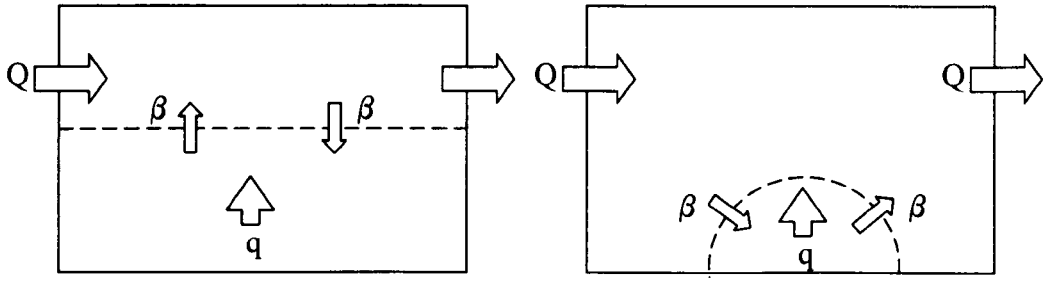

Figure 3-1 Example of two-zone models accounting for a) short circuiting ventilation b) high contaminant levels at source, Q is the flow rate into, and out of whole room, Air exchange between zones β , with a contaminant release q (Nicas, 1996).

Extending this concept the airflow through entire buildings may be modelled by classifying each room as a separate zone and assuming each of these to be well mixed. In order to obtain more detail in one critical area, e.g. where a contaminant is released, any zone may be broken up into smaller "sub-zones" (Ren and Stewart, 2005). Improved accuracy can further be achieved by using CFD techniques to model areas that cannot be assumed to be well mixed. An example of this is modelling the contaminant release point where there are naturally very high gradients, and coupling this to a multi-zone model for the remainder of the building (Wang and Chen, 2007).

The simulation techniques described above are all deterministic in nature, and therefore do not account for any variability in the concentration of the contaminant across a zone. It is possible to account for this using probabilistic methods in the process. The benefit of this is that the results can provide a range of bioaerosol concentrations defined by the probability of that risk occurring. This technique may be very useful when defining the risk to HCWs from patients, or workers from occupational exposures (Nicas, 2000).

The short computing time with multi-zone airflow models compared to CFD means that a whole year can be modelled dynamically. The comfort levels within the space, and energy consumption over a year can then assessed with the different outdoor conditions

that will occur. However for contaminant distribution within a space a shorter timescale is generally of interest. For this study it is the distribution of bioaerosols within a single bay of a hospital ward that is of interest and so multi-zone models are less likely to give the level of spatial detail required due to the high pollutant gradients near a source of infection (Richmond-Bryant *et al.*, 2006). As such CFD is the chosen method of computing the contaminant transport in the majority of the work presented here.

3.2 Computational Fluid Dynamics

CFD modelling involves dividing a flow domain into discrete cells or elements, then finding a numerical solution to the momentum, energy, turbulence and transport equations that govern the fluid flow, heat transfer and movement of contaminants in each cell (see Chapter 5). The converged numerical solution yields values for a range of variables throughout the flow domain, including velocities, pressures, temperatures and contaminant distributions. It is a useful tool for studying indoor air, along with a large number of other fluid applications and as such is useful for determining the transport of bioaerosols within an indoor space (Versteeg and Malalasekera, 1995). This is particularly useful as the measurements of bioaerosols within a space would not be possible in reality to the same level of detail as is possible through the use of CFD. Considering hazardous material such as infectious particles information can be found from CFD that may be dangerous to study in real life situations. (Etheridge and Sandberg, 1996).

CFD is not always the appropriate tool. Within research it can depend on the level of information required from a study, and also the level of assumptions and simplifications that are necessary, that decides the type of modelling that is required. As noted earlier, CFD can be used alongside other methods. When linked with zonal models the pollutant transport throughout a whole ward can be modelled relatively simply but with the required definition in the source region. Because CFD is not always the desired method of modelling contaminant transport in Chapter 7 the zonal source is applied to a pressure driven multi-zone model in order to examine the ability of this method to provide the required information for risk evaluation.

3.2.1 CFD modelling of bioaerosols

Since it is possible to study airflow in spaces under a variety of conditions, it is possible to consider the movement of contaminants along these air flows. Although the particles of interest within this research are bioaerosols, the computational methods of tracking particles will be the same as for most inert particles. There are numerous particle sources in indoor environments for which research has been carried out using CFD analysis. These include combustion due to cooking, smoking, car exhaust fumes entering the building, or chemical release from cleaning materials (Nazaroff, 2004, Holmberg and Li, 1998). The problem of particle levels within homes is of particular interest within large and congested cities in Asia, as such numerical studies published in recent years on the transport of various sized particles sometimes focus on this aspect (Chang *et al.*, 2006, Chang *et al.*, 2007). The definitions of these different sources mainly impact the size of particles considered, however it may also affect the decision to include evaporation and chemical reactions in the transport equations.

There are several methods for monitoring the transport of pollutants within CFD. The three main methods are:

- Passive Scalar
- Particle tracking with a Euler-Lagrangian approach
- Multi-phase models with a Euler-Euler approach

The simplest method is the use of a passive scalar, this can be introduced into the flow at any point in the domain. By assuming the mass of the particle is negligible it will not affect the air flow pattern, therefore the air flow in the room can be established and the bioaerosol transport solved from the converged air flow solution. The scalar is transported simply by convection due to the flow field, and diffusing according to the defined diffusivity as set by the user, and so is popular for modelling contaminant dispersal in room air (Li *et al.*, 2005, Noakes *et al.*, 2006b, Sekhar and Willem, 2004). It may be used for modelling respiratory sized aerosols as the smaller particles produced evaporate quickly to droplet nuclei (section 2.3.1), that will then follow the path of the air (Wells, 1955). In many CFD packages user defined functions (UDFs) can be included to incorporate decay of a biological species, for example through natural death

or an engineering intervention such as filtration or UV irradiation (Noakes *et al.*, 2004b).

For larger particles where mass and size play an important role in the transport dynamics a Lagrangian approach may be more appropriate. The path of the particles through the continuous phase is calculated from the forces acting on them. The effect of evaporation on the particle, collisions between particles, and the heat and mass transfer between the continuous and discrete phase can be modelled (Fluent Inc, 2005). This is useful when studying in more detail the air concentrations allowing for the effect of deposition as well as extraction from the space. The particles can be tracked from source to sink thereby allowing more detail to be studied than would be possible with experimental methods (Zhang and Chen, 2006). The effect of different ventilation systems for studying contaminant removal efficiency can be assessed allowing for the size of the particles, which is particularly important with slow moving flows such as displacement ventilation and large particles (Chang *et al.*, 2007, Zhao *et al.*, 2004b, Chau *et al.*, 2006), as well as studying the transport between different rooms (Lu and Howarth, 1996).

The final method is a multiphase simulation. In this technique the conservation equations governing fluid flow are derived for each phase. Volume fractions are used to describe the quantity of either the fluid, or the bioaerosol phase. Due to the significantly greater number of equations needed this model is more computational intensive and is therefore only used when other methods are unsuitable.

CFD analysis has been shown to be a useful tool in hospital design as highlighted in a review by Chow and Yang (2004) considering the ventilation design of operating theatres. Ventilation in operating theatres is present to protect both the staff and the patient from pathogens. CFD modelling provides a method of designing aspects such as air flow rate and extract hood size to provide the optimal protection possible and enables many different designs to be experimented with, and the most effective designs to be highlighted.

Recently the published use of CFD within hospitals has been extended to multi-bed wards with studies relating to the 2002-03 SARS outbreaks. One model by Li *et al*

(2005) of a hospital ward included fours bays and the corridor, and used a passive tracer to model the spread of bioaerosols. The simulated contagion dispersal was very similar to the infection pattern in the ward, with decreasing risk with distance from the source patient. Wong *et al* (2004) also modelled this ward including the effect of evaporation on the transport of the infectious particles. CFD and multi-zone modelling was also used to simulate the spread of infectious material in the Amoy Gardens Complex from the index patients flat to others both within the same building and nearby blocks. In this simulation the spread of infectious material compared well with the pattern of infection among residents (Yu *et al.*, 2004). In all these cases CFD was used successfully to inform discussion on the transmission mechanisms of a novel disease. By aiding understanding in this way suitable interventions can be assessed.

CFD is also a useful tool for studying the effect of different ventilation regimes within isolation rooms (Walker *et al.*, 2007). This has been used to assess the effect of local exhaust ventilation for reducing the risk to the HCW and the ward as a whole (Chau *et al.*, 2006). The results of this study showed that using the local extract resulted in infectious particles not being transported into the HCW's breathing zone. It also showed that the suspension time of the particles could be greatly reduced, thereby reducing the amount of time the particles are airborne and capable of being inhaled. CFD was used to assess the effect of interventions in a space in a TB ward in Peru (Noakes *et al.*, 2006b). This study modelled the ward with five different cases, each with a different level of complexity and cost for the various interventions. By carrying out these models the risk of infection spreading to HCWs and other patients were evaluated for each design. This enabled the various engineering interventions to be recommended based on cost and efficiency. The effect of different ventilation designs on the transport of particles using a Lagrangian approach has been studied, both in relation to isolation rooms within healthcare facilities (Cheong and Phua, 2006, Kao and Yang, 2006) and more general layouts (Chao and Wan, 2006, Yang *et al.*, 2004, Zhao *et al.*, 2004b, Zhao *et al.*, 2004a).

3.2.2 Bioaerosol Sources with CFD

Studies with similar aims to those described above have been carried out considering different ventilation techniques within isolation rooms and exposure of patients and HCWs to pathogenic material, however, as they consider respiratory diseases, they

consider the release of bioaerosols to occur from a single point source (Wan *et al.*, 2007, Gao and Niu, 2006, Bjorn and Nielsen, 2002, Shih *et al.*, 2007). The purpose of the room, and specified ventilation system may be to isolate a person with an infectious respiratory disease such as TB (2.2.3), in which case the definition of a point source and release of bioaerosols from the mouth is suitable. However it may also be the case that a side room is used to isolate a patient colonised with MRSA, in which case the release may not be from the single point but from the patients skin (section 2.1.1), and this designation of the point source may be unsuitable.

CFD based research into contaminant transport within operating theatres has considered the dispersal of bacteria from sites other than the nose and mouth. As well as the surgical site being considered as a source (Buchanan and Dunn-Rankin, 1998), the ability of people to disperse bacteria from the skin has been recognised in some CFD models of operating theatres (Brohus *et al.*, 2006, Chow and Yang, 2003). Noting that the staff will disperse bacteria from their skin as they work over a patient Chow and Yang (2003) expressed the release from a plane rather than a point source. However they did not carry out any analysis as to the effect of making this decision on potential contaminant distributions within the space. Brohus (2006) considered that the dispersal of bacteria would be from the patients and staffs skin, yet despite including momentum sources across the space to represent movement, described below, the release of bacteria was consigned to the still persons surface.

As discussed in Chapter 2 the aerodynamic diameters of particles released from the skin are in the range of 4-22μm. Zhao *et al* (2008) found at even high air change rates (10ac.h^{-1} and 20ac.h^{-1}) the transport of particles size 10μm was inadequately represented using a passive scalar. Even for particles sized 2μm the rate of deposition can be equivalent to that removed by typical indoor ventilation making it necessary to include this factor in the transport analysis (Fisk, 2008). For these larger particles Lagrangian particle tracking may perform better, as it includes the size and mass of the particle in the trajectory calculations and the same study by Zhao *et al* found that this method performed generally well. A more detailed discussion of the validation of Lagrangian particle tracking is given in section 5.3.2.

3.2.3 Dynamic Simulation of People within CFD Models

CFD models are generally representative situations that highly idealise the indoor space. However real indoor areas are used by people, who will affect the airflow in that space in transient and complicated ways. The effect of human motion on airflow is difficult to calculate, more so considering how these movements will differ from day to day. This can introduce mixing and promote the motion of infectious material into new areas (Tang *et al.*, 2006). Different levels of movement will also have varying effects on the air field in the room. For instance if an individual makes a single pass through the room they will create horizontal air movements, with very few turbulent vortices being created. However when the body moves back and forth repeatedly newly created vortices will interact with those created previously, resulting in higher velocities and turbulence within the room (Mattsson and Sandberg, 1996). It is important to be aware of this as the change in air pattern may affect the ventilation efficiency. This is particularly important in displacement ventilation systems were thermal stratification of the air is the design intent. Moving objects in this situation may break this thermal stratification and return polluted air to lower regions rather than letting it move upwards and become extracted from the space (Matsumoto and Ohba, 2004, Bjorn and Nielsen, 2002).

Most of the work described above on isolation rooms, operating theatres or hospital wards, makes the large assumption that the occupants are standing still. These models are generally steady state models, and as such are a simple snapshot of time. The solution then gives an indication of the risk factors within the room only for this representative situation. In reality indoor spaces are occupied by people who move and have an effect on the air flow, and contaminant distribution, as well as potentially dispersing contaminants as they move. Sekhar and Willem (2004) found that a simulation of a large office space underestimated the velocities of the air. It was suggested that this could be partially explained by the lack of occupant movement in the model, that would potentially increase air velocities.

Direct method of representing movement in CFD models

It is possible with the computer power available nowadays to incorporate the movement of people dynamically within that space. Shih *et al* (2007) simulated an isolation room

using CFD and studied the effect of a person walking and the door opening and closing. They showed that a person moving up and down next to a bed has no effect on the dispersion of the contaminant source, when the ventilation regime involves a local extract with ventilation rate of 12 $ac.h^{-1}$. This simulation required significantly increased complexity with the use of dynamic meshes necessary to model the movement of an object within a room, but actually results in little new information. Although movement is incorporated it is only in a narrow area away from the bed. In practice a HCW would attend to the patient and this movement, close to the bed may result in dispersion of the bacteria away from the extracted air stream, and towards the HCW.

Brohus *et al* (2006) highlights the problems with these 'direct' methods that exactly model the movement of people dynamically within the space. To solve the discretised equations, the flow domain is divided up by the computational mesh. When an object is present in the space the computational mesh is removed from this volume (as the fluid will flow around it, not through it) and boundary conditions are applied around the interface. As an object travels through a space the location of the interface between the object and the fluid will also move. In order to include the moving object one of two methods is generally used; interface-tracking, or interface-capturing techniques.

Interface-tracking is so named because the mesh 'tracks' the interface as it moves through space. The mesh therefore changes when the object moves resulting in frequent remeshing. As a new mesh is having to be created throughout the calculation process, depending on the complexity, this may be computationally very expensive. Due to the constant remeshing this method will take significantly longer to run, than a fixed mesh model. Mazumdar and Chen (2007) simplified a dynamic mesh by only remeshing the 'aisle' the person moved through, yet it still took two and a half weeks to solve 15 seconds of real time.

Interface-capturing does not involve remeshing, but uses a fixed mesh and computes the location of the interface through the use of an interface function. Although this reduces the required computer power it has not been shown to accurately represent the interface (Tezduyar, 2006). Brohus commented on how important the boundary layer was to the flow around the human body when considering the persons exposure. With the interface-capturing technique this would not be resolved adequately. With the interface

tracking techniques the frequent remeshing may require a coarser than desirable mesh to be used, this again would diminish the accuracy of the solution at the boundary. Personal exposure and problems with boundary layers are not just an issue concerned with inhaling bacteria, but also the deposition of bacteria onto a persons skin or clothing. The same problems would provide great uncertainties when modelling this phenomena.

Indirect Method of representing movement in CFD models

Brohus *et al* (2006) recognised the need to represent movement within hospital spaces, moreover this study also recognised the necessity to be able to represent movement within a simple steady state model. In his study a model of an operating theatre was created. In the steady state model the effect of movement was included by adding sources of momentum to a number of zones that the person passes through. The layout of these are shown in Figure 3-2, in plan; the zones themselves are slightly shorter than the computer simulated person. The layout of the zones and intensities were found by trial and error, comparing the CFD model with smoke visualisations and measurements in a real operating theatre. A second indirect way of accounting for movement was also used. This used a volumetric source around the zone where small movements take place over the operating table and added a source of turbulent kinetic energy to this zone. This method was aiming to model the *average influence* of movement on the air field, whereas the momentum sources aimed to model a *worst case* scenario. The momentum source was used to simulate the effect of a nurse moving into the clean zone around the operating table, and to find how contaminants were dragged by this airflow. Turbulent kinetic energy sources were used to simulate the average effect from the small movements that take place from the surgeons arms above the operating table. Both these simulations were not intended to provide accurate quantitative data, but to provide good qualitative data to enhance knowledge of air flow fields within operating rooms.

Once a method of representing movement is developed this can be incorporated into many models at the design stage of building hospitals. If a quick and simple method is found this can be used to assess different design approaches, to gain an idea of the risk to patients and HCWs, and highlight any benefits, or dangerous situations. It would have to be recognised that this will not be an accurate model of the airflow, and contaminant distribution in the space but a tool to give an approximate idea of the

mechanisms of contaminant transport which is useful for comparing different interventions, or to highlight areas that may require more study.

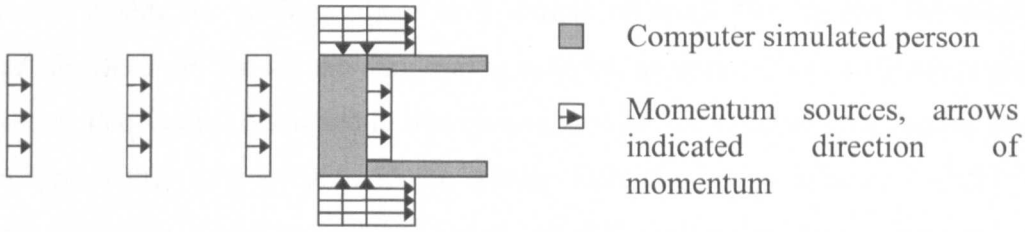

Figure 3-2 Schematic representation of the position and direction of momentum sources as shown in Brohus *et al* (2006)

The method described above is an interesting option for expressing the effect of motion on the airflow. However methods to express the release of bacteria due to movement have not been broached previously. A reasonable definition of a bioaerosol source is likely to be necessary to solve the subsequent transport through the space.

As argued by Brohus both modelling the movement directly in the flow domain, or using indirect representations of movement require assumptions to be made. Uncertainties will exist in both simulations, yet the indirect method is simpler and quicker to produce. Being simpler to produce it is also less prone to inaccuracies due to the user.

As the industry use of CFD becomes more common, the graphical user interface becomes simpler to understand and the software easier to use. Hence, it is increasingly possible to use CFD to inform designs with little validation of the results, other than personal judgement. In these instances, complicated mesh generation, or transient simulations will create more factors that may incorporate potential errors, which will be undesirable to the user. Results will be needed in a short time scale, in order to compare potential designs. In this situation a simple way of representing bacterial sources from activity and other moving phenomena within the model that is simple to run is beneficial.

3.3 Summary

Despite the interest in expressing movement within CFD models and the use of CFD to describe healthcare settings, there is a deficit of work that studies the release of contaminants from the human skin during activity, as opposed to that from respiratory diseases. The studies discussed in this chapter that have considered the release from the skin have either only considered the release from the body surface of a still object within the space, or did not analyse the effect of changing their source type to a plane, as opposed to a point source. It was also noted that this release from the skin was only represented in models of operating theatres and not general wards or isolation rooms. From Chapter 2 it is clear that the release of bacteria from general nursing activity is an important factor in the microbial levels of hospital air and this should therefore be represented when considering the effect of ventilation regimes and other interventions. However, as has been discussed, there is always an element of error within CFD and a simple model to express this release would be beneficial, both since it is quicker and easier but it also avoids giving the impression of accuracy when many assumptions are still being made, as may occur using time dependant models.

Chapter 4
Observational and Sampling Study in a Respiratory Ward

The literature discussed in Chapter 2 provided evidence that activities such as bedmaking and walking can result in the dispersal of bioaerosols, including MRSA, into the air in a hospital. In order to further understand how activities may affect the bio-burden of hospital air, and therefore potentially the transfer of infection, an air sampling and observational study was carried out on a four-bed bay on the respiratory ward at St James's University Hospital, Leeds. The zonal source modelling methodology that is introduced and validated in Chapter 6 is developed on the basis that activities can significantly affect the bio-burden of hospital air. It is therefore necessary to first study how the dispersal outlined in the literature review affects the hospital ward environment and to understand where the 'zones' of dispersal may occur.

This chapter commences with a description of different bioaerosol sampling methods and the justification for the chosen methods used in this study. This section is also relevant to the experimental work carried out to validate the CFD models, described in Chapter 5.

Following this introduction to the general sampling and analysis methods, the specific methodology carried out in the observational and air sampling study is presented. The statistical methods used in both this study, and in the CFD validation are then described in detail followed by the results and discussion. These results are used to inform the modelling carried out in Chapter 7, where the zonal source model developed in Chapter 6 is applied in simulations of hospital wards.

The work presented in this Chapter is based on two observational studies. The first was published as Roberts *et al* (2006) and carried out jointly with the lead author as outlined at the beginning of this thesis. However all the statistical analysis presented here, except that comparing similarities between the fluctuations of different sizes of particles, has been carried out independently and subsequent to that publication.

4.1 Sampling Equipment and Methodology

This section describes different methods for sampling bioaerosols, explains the particular choices of equipment for this study and outlines the sampling and culturing methodologies used to quantify bioaerosols and particles in the hospital ward air.

4.1.1 Bioaerosol Sampling

Many different air samplers are available that are designed to quantify the number of viable micro-organisms within an air sample. No air sampler will perfectly sample the total number of micro-organisms in the air, and the relative positive and negative aspects of each need to be taken into account when choosing the best sampler for the study (Griffiths and Stewart, 1999).

The sampling efficiency of a device can be split into two distinct parts, the physical efficiency, and the bio-efficiency. The physical efficiency incorporates the ability to collect the particle from the air, into the device, and to store it. The bio-efficiency relates to the difficulties in maintaining a micro-organism's viability during the sampling process and to create growth from this sample. Unfortunately increasing one of these factors often results in a decrease in the other. For example improving the physical efficiency, by drawing in air at a greater rate, often results in reduced bio-efficiency due to increased shear forces which may damage, kill, or render the micro-organism unculturable (Cox, 1987).

Impactor Samplers

Impactor samplers work on the principle of a particle deviating from an airstream that changes direction, due to the particle momentum. A jet of air, as shown in Figure 4-1, changes direction due to the presence of a plate that forces it around a 90° bend. The momentum of the particles entrained in the air flow results in them travelling across air

streams due to their mass, velocity and the drag force acting on them due to the changing air current. The particle trajectory will therefore be as shown in the figure, and if the particle deviates sufficiently it will be collected on the plate. This can be used to collect viable particles by using an agar plate to provide suitable conditions for colony growth.

It therefore follows that the efficiency of the sampler will depend on the density and volume of the particle. The sampling efficiency can be quantified for different particles that are defined by their behaviour in the air using the aerodynamic diameter. This is the diameter of a spherical particle of unit density ($1 g.cm^{-3}$, equivalent to $1000 kg.m^{-3}$) that has the same aerodynamic properties as the particle of interest. Using this definition the sampling efficiency, E, can be shown to be a function of the aerodynamic diameter of the particle and the velocity of air through the sampler nozzle. The sampling efficiency can be estimated using (Hinds, 1982):

$$E = \frac{\pi.U}{2.r}\left(\frac{\rho.d^2.C}{18.\eta}\right) \qquad \text{4-1}$$

Where U is the velocity through the nozzle and r is the radius of curvature of the streamline; which may be assumed to be the same as the nozzle radius in this instance. ρ is the density of the particle, (taken as $1000 kg.m^{-3}$ for this study as the micro-organisms were suspended in distilled water), d is the diameter of the particles and η is the viscosity of the room air, taken as $1.8x10^{-5} kg.m^{-1}.s^{-1}$. The most common method for describing a sampling efficiency is to quote the particle diameter at which a 50% collection efficiency is achieved; the D_{50} particle size.

Since the D_{50} particle size of an impactor will vary according to the jet velocity and the distance x (Figure 4-1) to the surface of the plate, a sampler may be designed to sample for a specific size range. Cascade samplers use different sized nozzles, and therefore different velocities to sample for different particle sizes on separate plates.

The sampler nozzle shown in Figure 4-1 may be created by either a long slit or a series of holes to form a "sieve" impactor. Most of the air sampling reviewed in section 2.3.2 used a slit sampler. However the sieve impactors provide many more individual jets,

and therefore deposition sites, improving the quantification of airborne bioaerosols. More than one micro-organism may land on a individual site, however standard methods exist to account for this (e.g. *positive hole correction* – see below).

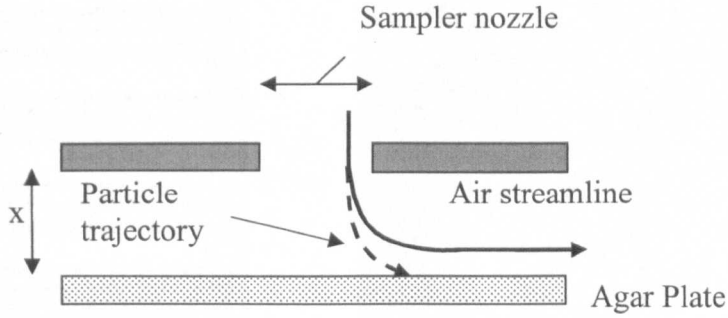

Figure 4-1: Diagram indicating how particles deviate from the air flow to become impacted on the plate within impactor samplers.

Andersen Sampler

The Andersen sampler is a multi-level impactor. It was developed after it was recognised that the human respiratory tract consecutively filtered out particles with decreasing size, preventing them reaching the lungs. Hence, to understand whether sampled micro-organisms had the potential to reach the lungs or where in the bronchial tract they would become trapped, a method of separating *viable* particles into size groups as they are sampled was devised (Andersen, 1958).

As shown in Figure 4-2 the Andersen Sampler (Westech Ltd, UK) used in this study is split into 6 sections, or stages. Each section contains an agar plate and the sections are separated by a metal 'sieve' plates, each with 400 holes. The plate at the top of the sampler has the largest diameter holes, with the diameter progressively decreasing down the sampler. As the hole size decreases the velocity of the air jet passing though them increases enabling increasingly smaller particles to gain sufficient momentum to leave the air stream. Consequently it successively samples particles in decreasing size from the air. A photograph of the sampler with the stages separated is shown in Figure 4-3. Table 4-1 shows both the D_{50} as described by Martinez *et al* (2004) and the size range found by Andersen (1958) sampling spherical wax particles if the sampler is run at 28 $l.min^{-1}$. There are differences in the values because Andersen quotes the size range for 95% of the particles collected and not the D_{50} size.

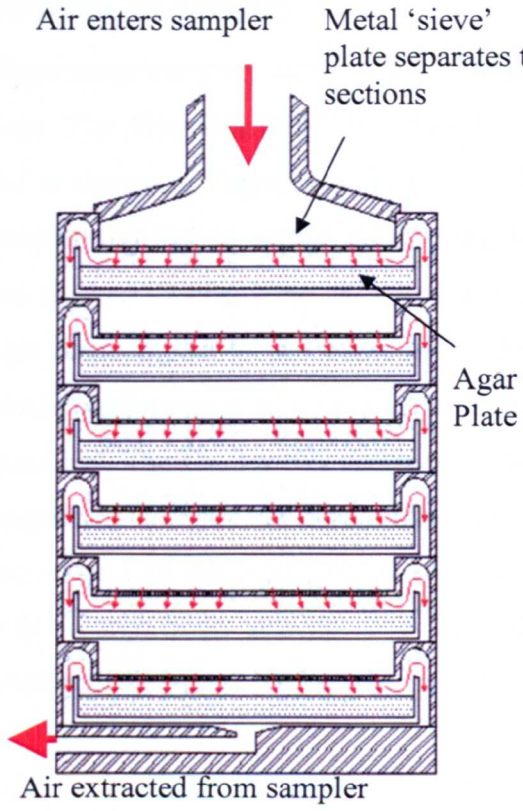

Figure 4-2: Schematic of the Andersen sampler in section. Red arrows indicate air flow.

Figure 4-3: Photograph of Andersen Sampler showing how the levels stack together

Table 4-1: Size ranges of particles sampled on each level of the Andersen Sampler, theoretical D_{50} and experimentally collected spherical wax particles.

		(Martinez *et al.*, 2004)	(Andersen, 1958)
Stage	Hole Diameter (inches/mm)	D_{50} (μm)	Spherical wax particles 95% collected (μm)
1	0.0405/1.028	7.0	>8.2
2	0.031/0.787	4.7	5.0-10.4
3	0.028/0.711	3.3	3.0-6.0
4	0.021/0.533	2.1	2.0-3.5
5	0.0135/0.343	1.1	1.0-2.0
6	0.01/0.254	0.65	1.0

MicroBio Air Sampler

Single stage samplers work on the same impaction principle but with only one sampling stage. The MicroBio MB2 (F.D.Parrett Ltd, UK) is an example of this type of sampler and is shown in Figure 4-4. This type of sampler is much smaller than the Andersen sampler and has an inbuilt pump. Despite the obvious 'front' to the sampler Griffiths and Stewart (1999) have shown that the orientation of the sampler does not have a significant impact on the collection of micro-organisms. They also found that it has a similar performance to a cyclone sampler and the Andersen sampler at 70 % Relative Humidity. The D_{50} for this sampler is 1.8μm, similar to stage 4 and 5 on the Andersen sampler. A comparison during this study found similar counts for the MicroBio MB2 and stage 5 of the Andersen sampler for concurrent indoor sampling during a period with no significant activity. The MicroBio samples at 100 $l.min^{-1}$ through 220 holes 1mm in diameter.

Figure 4-4: Photograph of MicroBio MB2 Air Sampler, showing the sieve head (left) and the positioning of the Agar plate (right)

Positive hole correction

Samples taken with the Andersen Sampler, or the MicroBio, may result in more than one colony forming particle impacting through the same hole. As the colonies grow they will overlap and appear as one single colony when counting. The greater the number of micro-organisms sampled the greater the likelihood of this occurring. In order to allow for this error *positive hole correction* is applied to the results (Macher, 1989). This adjustment takes into account the fact that when a larger number of viable micro-organisms are collected they become less likely to enter the sampler through empty holes. Therefore the correction scales up the count to include the probability of more than more viable micro-organism being sampled from different holes. The level of scaling up increases the higher the value sampled. Positive hole correction is applied using the following formula:

$$P_r = N\left[\frac{1}{N} + \frac{1}{N-1} + \frac{1}{N-2} + \ldots + \frac{1}{N-r+1}\right] \qquad 4\text{-}2$$

Where P_r is the corrected value, r is the number of colonies counted, and N is the number of holes in the plate.

Cyclone Samplers

Cyclone samples also work by creating a situation whereby a particle leaves the sampled air stream due to their own momentum. Instead of impacting these particles on an agar plate, Cyclone samplers inject air tangentially into a sampling cylinder, forcing the air to spiral down into a collection vessel containing liquid for bioaerosol sampling, returning up the centre and exiting from the top. The momentum of the particles causes them to deposit from the spiralling air stream into the liquid. Centrifugal samplers also operate on a similar principle but impact the particles onto an agar strip, or other medium on the inner wall of the cylinder. The advantage of the cyclone sampler is that the biological particles are sampled directly into a liquid, which may help to maintain viability for later culturing. By swirling the particles into a liquid any clumps of more than one viable micro-organism may be broken up, thereby increasing the count of viable particles. This may be a positive outcome as it will be a more realistic measure of the total count of micro-organisms in the air, however it may over estimate the number

of viable particles capable of causing disease (Cox, 1987, Crook, 1995). The Burkard sampler is a cyclone sampler which samples into a small Eppendorf tube that is usually filled with 1ml Ringers solution (Oxoid, UK) (Figure 4-5). This enables the viable particles to be stored during the sampling period, and then spread onto a series of individual agar plates after the sampling period. Typically 0.1ml of the liquid is plated out onto the surface of an agar plate. This has the added advantage that it is possible to plate the solution onto several different media in order to determine the presence of specific micro-organism species. Sampling into a liquid, as opposed to directly onto a hard agar surface may mean the bioaerosol has a greater chance of survival due to less stress on the particle.

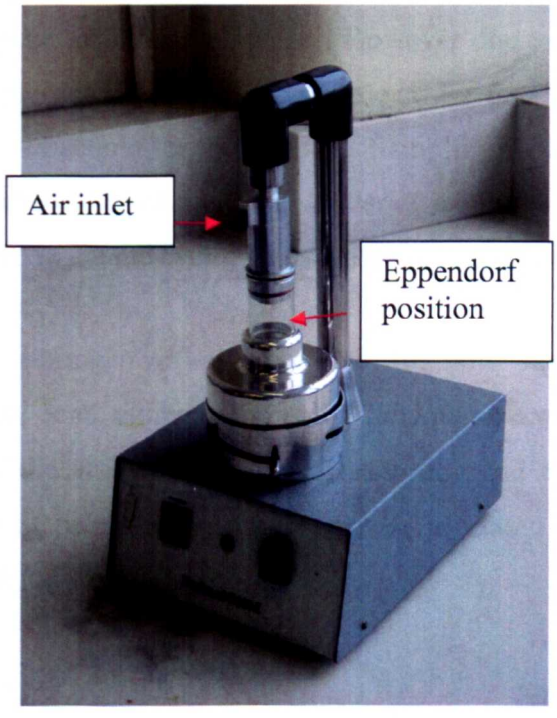

Figure 4-5: Burkard Cyclone Sampler indicating where the air enters the sampler and the positioning of the ependorf tube for sample collection

These samplers operate at a much lower flow rate, 16.6 $l.min^{-1}$ for the Burkard cyclone sampler. This again increases the chances of the particles remaining viable due to the lower shear stresses in the fluid from the lower velocity, however it reduces the total number of particles which can be collected from the air within a given time period. In order to sample the same volume of air as the MicroBio MB2 it would need to be operated for just over six times the sampling period. Not only is the sampling time

increased but the volume of the collection liquid can be significantly reduced during the extended sampling period due to evaporation.

4.1.2 Chosen Sampling Methodology

The MicroBio MB2 was used for the bioaerosol sampling in this study. This sampler has similar characteristics to the Anderson sampler, however importantly it uses a much smaller pump, and is therefore much quieter. This is an important consideration particularly when sampling around sensitive people within a hospital ward.

The initial intention was to use the Burkard Cyclone sampler in order to be able to plate the sampled micro-organisms onto a variety of media to gain an understanding of the concentration fluctuations of different species. However due to the lower flow rate, as mentioned above, it was found necessary to sample air for four hours in order to sample a reasonable quantity of bacteria for this purpose. Sampling for this period of time made it impossible to characterise changes in bacterial concentrations during different activities, and therefore made the cyclone unsuitable for this study.

The main bacterial pathogen of interest due to skin squame release was the *Staphylococci* species, and more specifically *Staphylococcus aureus* (Chapter 2). Therefore for part of the study in addition to sampling and enumerating for a *Total Viable Count* (TVC) of micro-organisms in the air a second MicroBio was used to sample and enumerate for *Staphylococci.*

Culture Media

TVC enables an overall picture of the general bioaerosol concentration in the air to be obtained. This will include pathogenic and non-pathogenic micro-organisms and will not select for or differentiate micro-organisms. Tryptone Soya Agar (TSA) (Oxoid, UK), a general purpose media was used to sample for the bioaerosol TVC. This is made from Tryptone, Peptone, Glucose, Sodium Chloride and Dipotassium phosphate (Prescott *et al.*, 2005).

Mannitol Salt Agar (MSA) (Oxoid, UK), a selective and differential medium, was chosen to selectively sample for *Staphylococci* and to differentiate *S. aureus*. This agar contains a high salt content to inhibit most bacteria except *Staphylococci.* Phenol red is

included in the agar; this is an indicator that is red above pH 7.4 and yellow below pH 6.8. S. *aureus* ferments mannitol creating acidic by-products and thereby lowering the pH. This turns the agar yellow enabling the species to be identified and counted.

For all cases agar plates from the sampler were incubated for 24 hours at 37°C. After this time visible colonies had grown up on the agar. On the TSA all visible colonies regardless of colour or morphology were counted and the number of *colony forming units* (cfu) sampled from the air was determined. On the MSA plate all visible colonies were counted to find the number of *Staphylococci* spp. In both cases positive hole correction was applied and the corrected counts recorded.

Although the high salt content in this agar should inhibit most bacteria other than *Staphylococcus*, *Bacillus* has been documented to grow on it (Han *et al.*, 2007) and some other halophillic species may also survive. Bacillus is often clearly identified on observation of the colonies, as it has a very distinctive appearance. However this was not deemed vigorous enough and therefore, each visually different colony on all the plates was tested using gram staining (Prescott *et al.*, 2005), in order to ascertain the construction of the cell wall. *Staphylococcus* and *Baccilus* are both gram positive having a thick peptidoglycan layer in their cell wall. This traps the purple crystal violet stain, holding it through decolourisation with ethanol, enabling identification. The stained samples were then viewed using a light micro-scope at 1000x magnification to view whether the bacterium was cocci, *(Staphylococci)*, or bacilli *(Bacillus)*. All colonies, except those originally thought to be *Bacillus*, were found to be gram positive cocci. When a bacterium was grown on MSA, tested gram positive, and visually identified as being cocci it was deemed sufficient to identify it as *Staphylococcus spp.*

The organisms grown on MSA and thought to be *S. aureus* due to yellow growth, and the change of colour in the agar from red to yellow were checked using the Staphylase test (Oxoid, UK). *S. aureus* is differentiated by the presence of coagulase and this tests for the presence of coagulase (otherwise known as the clumping factor) using fibrinogen-sensitised sheep red blood cells. By mixing a small colony sample into a drop of the Staphylase test aggluniation occurs for coagulase positive bacteria, but none will occur for coagulase negative bacteria (e.g. *S. epidermis*). Those colonies showing

yellow growth, a colour change in the agar and a positive response to the Staphylase test were recorded as *S. aureus*.

Figure 4-6 shows a typical air sample onto MSA taken during a busy period on the study bay and the range of colonies that can be observed growing on the media. As can be seen there are several colonies that could be characterised as showing 'yellow' growth. Therefore in order to determine which were *S. aureus* a sample of all colonies that were cream, yellow, or orange, were tested for the presence of coagulase. As only one visually different type of colony tested positive this could be taken as being *S. aureus*. All colonies then suspected of being *S. aureus* were tested and found positive for the presence of coagulase.

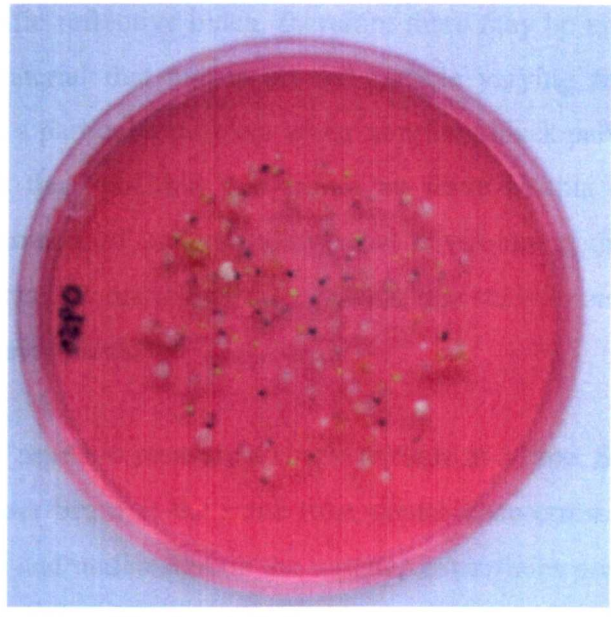

Figure 4-6: Typical air sample taken during a busy period during Study 2 onto MSA.

4.1.3 Inert Particle Sampling

In addition to sampling for micro-organisms, the number of airborne particles over 5 size ranges were also quantified. The size ranges considered were 0.3-0.5μm, 0.5-1μm, 1-3μm, 3-5μm, >5μm. These dimensions are assumed to be the particles aerodynamic diameter. Sampling was carried out using a Kanomax 3886 Laser particle counter (Optical Sciences Ltd, UK), shown in Figure 4-7 which has a flow rate of 2.83 $l.min^{-1}$. With this sampler the particles are directed to pass through a beam of light, created by a laser diode. The particles are assigned a size based on the intensity of the light scattered

by them. As only particles greater than 0.3μm are counted, the Mie theory is used to relate the intensity of light to the diameter (Mitchell, 1995b). The Mie theory specifies that the relationship of the scattered light intensity $I(\theta)$ is proportional to the distance, R , in direction θ from the particle and the particle diameter along with the wavelength of light λ.

$$I(\theta) = \frac{I_0 \lambda^2 (i_1 + i_2)}{8\pi^2 R^2} \qquad 4\text{-}3$$

The diameter, d is incorporated into the Mie intensity parameters i_1 and i_2, these are also based on the θ and the refractive index, m, of the particles relative to the fluid. Since the refractive index is included in the sizing theory the particle counters need to be calibrated to a specific refractive index, therefore there may be errors in the calculated sizes due to the material that makes up the particle varying from that used in the calibration. There is a particular problem when sampling black particles (such as carbon dust) which absorb the light, but this is not an issue in this study. However this highlights the importance of understanding what environment the particle counter is designed for and hence the particle counter used in this study is one specified for use in indoor air quality assessments.

The particle counter needs to measure a single particle at a time. Should more than one particle enter the laser beam at the same time coincidence errors will occur, this will oversize the particle and underestimate the number of particles present. This will occur at times of high concentrations and at such concentrations the particle counter indicates there may be errors. When this occurred in this study the results were discounted.

The scattering of the light by irregularly shaped particles and hence the sizing of such particles can be highly dependant on the rotation of the particle in respect to the light source. This is an issue with all particle counters and is difficult to resolve. However the number of particles summed every 5 minutes is in the region of 1 x 10^5 for the largest particles and so the effect of some particles being sized incorrectly is not considered to have a great effect on the overall results.

Figure 4-7: Photograph of Kanomax 3886 Laser Particle Counter

4.2 Observational and Sampling Study Objectives

Two studies were carried out on a respiratory ward at St. James University Hospital Leeds in December 2004 and August 2007. Both involved air sampling to quantify inert particle and bioaerosol concentrations, along with observations carried out to record all the activities taking place within a single four-bed bay. The aim of these studies was to address the following three objectives:

1. To determine whether there are significant similarities in activity and airborne contamination between days, and establish whether a 'typical' day can be described.

2. To evaluate the typical size of particles likely to be carrying micro-organisms within a hospital ward.

3. To identify the important activities for releasing micro-organisms into the air and the spatial zones in which they occur. This would highlight those activities that may require definition as a zonal source within a CFD model of a hospital ward, and would enable definition of the location of that zone.

4.3 Observational Study Methodology

4.3.1 Definition of Activities

Before describing the main study methodology this section first defines the activities that were monitored during the studies. The term "activities" in the context of the studies refers to a range of factors as detailed below.

- *People* – The number of people in the bay was used as a marker for general activity. This is a very simplistic approach which assumes that since people are needed to be present in the bay to perform activities then the more people present the more activity is occurring. When counting the number of people within the bay only staff were considered; this included healthcare workers (HCWs) and housekeeping staff. Visitors to the bay were not considered under this activity.

- *Washing* – The majority of patients within this bay were either washed by a HCW, or washed themselves, in the bay and this usually occurred behind closed curtains. Since dressing and undressing has been associated with large bioaerosol concentrations (section 2.3.2) and since this is necessary to carry out washing it was recorded as a specific activity that may contribute to the airborne micro-flora.

- *Bedmaking* – This has also been shown to disperse bacteria into the air by several authors (section 2.3.2). As patients shed skin particles into the bed clothing, when the sheets are disturbed during bedmaking the particles are released into the air. Since new bedding should be clean and mattresses are vinyl covered, only the stripping of beds was recorded, not the process of making up the new bed.

- *Commode* – Depending upon the health of the patients the commode was sometimes used within the hospital bay. When this occurred it was noted as it is a potential source of faecal related micro-organisms.

- *Curtains* – The activities of washing, bedmaking, commode use, and also moving a patient out of their bed, all usually occurred behind closed curtains. Hence the movement of curtains was chosen as a general marker for this group of different types of activities. Curtains are also known to become contaminated by micro-organisms (Das *et al.*, 2002) which may be released into the air with vigorous movements.

- *Specialist Equipment* - As this study was carried out on a respiratory ward the patients used various pieces of respiratory equipment. In these studies Non-invasive Ventilators (NIV), Oxygen and Nebulisers were used. NIV provided ventilation aid to the patients either through a whole face mask or nasal plugs. The oxygen tended to be given to the patient through nasal plugs but occasionally from face masks. The nebulisers covered the patients mouth and nose and nebulised drugs to open the airways of the patients. The mask has holes in the side and when in use small particles were visibly emitted into the air. The use of the NIV and nebulisers were recorded as an activity since it was hypothesised that they may be responsible for increasing airborne micro-flora.

- *Visitors* - Since visitors to patients tended to sit when they visited and did not make any vigorous movements it was thought that they would not be responsible for releasing large number of bioaerosols or particles. However visiting time does equate to an increase in people in the bay which may lead to increased bioaerosol counts so this was considered.

4.3.2 Overview

Both the studies were carried out over eight hour periods with sampling at regular intervals and monitoring of all activities as explained above. Ethical approval was acquired for the study from Leeds Teaching Hospitals NHS Trust. The two studies are detailed below and both were carried out in a four-bed bay on the same respiratory support ward. A schematic of the ward is shown in Figure 4-8. The ward was supplied with natural ventilation from opening windows assisted by mechanical extracts provided in the corridors. The windows were opened on occasion during both studies and this was noted and accounted for when it occurred

Study 1

The initial scoping study was carried out in December 2004 over a period of two days. On the first day sampling was carried out in a high dependency bay (HD), and the second day in a separate non-HD bay. Due to the more dependant nature of the patients on the HD bay there was greater activity in this area and hence the two sites could be compared as a *busy* and a *quiet* bay. The layout of each bay was identical and the location of the two bays within the ward is shown in Figure 4-8.

During this study sampling was carried out between 09:00 and 17:00 hours on both days. The MicroBio MB2 (section 4.2.1) was used to sample the air for a Total Viable Count (TVC) (section 4.2.2) onto TSA in order to quantify the total bioaerosol level in the space. The particle counter was used to sample for particles (both viable and inert) in five size ranges as described above (section 4.2.3). The location of the MicroBio and the particle counter within the bay is shown in Figure 4-8 as the sampling position. For this study the MicroBio sampled consecutively three times every 30 minutes in order to provide three repeated measurements, and the particle counter summed the number of particles over 5 minute intervals continuously. This is shown in Table 4-2

Observations were carried out to record when the specified activities described above were carried out as well as noting the number of people passing through the doorway (both in and out). The temperature and humidity were checked once every hour at the bay entrance in order to see if there were any changes in the environmental conditions that may have affected the airborne count of particles or micro-organisms.

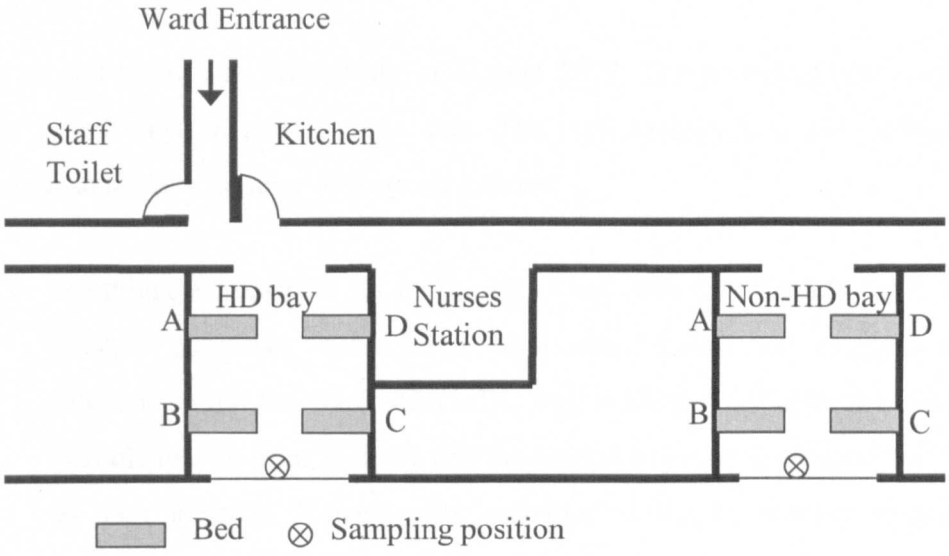

Figure 4-8: Layout of Ward for observational study. Study 1 used both bays, whereas Study 2 only sampled in the HD bay.

Table 4-2: Showing the different sampling methods used on each day of the observational study

Study N° & Dates		Bay Sampled	Particle Counter		MicroBio with TSA		MicroBio with MSA	
Study 1: 2004	Dec 16th	HD Bay	✓	Summed over every 5 minutes	✓	3 consecutive 5 min samples every 30 mins		
	Dec 17th	Non-HD Bay	✓		✓			
Study 2:2007	Aug 7th	Non-HD Bay	✓					
	Aug 8th		✓					
	Aug 14th		✓		✓	5 min sample every 15mins and in periods of high activity		
	Aug 21st		✓		✓			
	Aug 22nd		✓		✓			
	Aug 28th		✓		✓		✓	5 min sample every 15mins and in periods of high activity
	Aug 29th		✓		✓		✓	

Study 2

The second study was carried out in August 2007. The period of study was extended from 2 to 7 days to collect more data. The methodology was also refined from the previous study in a number of ways as follows:

1. Sampling was carried out on the HDU bay only for all study days. This was to prevent excessive interference from other particulate sources, mainly the kitchen, within the ward. The HDU bay is located opposite the kitchen and so particle results from this bay and the second bay sampled may have differed due to their location. However the activities within the kitchen should follow a regular pattern and so the effect on an individual bay, if there is one, that has a constant proximity to the source can be negated. Therefore instead of having a *busy* and *quiet* day across two bays, two days of the week were chosen using the same bay with different rotas and hence levels of activities, Tuesdays were chosen as the *busy* days, and Wednesdays as the *quiet* days.

2. The sampling and observations took place between 08:00 and 16:00 as the initial study highlighted that by 09:00 most activity had begun in the bay, and that the levels of activity tailed off into the afternoon

3. The results of the Study 1 showed that over the 15 minute period in which the three consecutive bioaerosol samples were taken there were noteworthy differences in activity levels that appeared to translate into microbial and particulate counts. Therefore in the second study the bioaerosol samples were taken once every 15 minutes and more frequently when a large amount of activity was occurring. In the initial assessment of the results each sample was treated as an individual case instead of as a replicate, as had been the intention with the 15 minute sampling periods in Study 1. This thereby increased the sampling frequency to at least once every 15 minutes, and enabled the mean for 30 minutes to be taken from samples spaced apart rather than clustered at one end of the period.

4. The number of people present in the bay were counted every minute, rather than just as they passed the doorway. This reduced the chance of errors, as if one

person was missed leaving the bay in the initial method this could impact the count for the remainder of the day.

5. On the final two days of Study 2 two MicroBio samplers were used in tandem to sample specifically for the presence of *S. aureus* as well the bioaerosol TVC.

The first two days of this study were used to assess the practicality of utilising a Burkard Cyclone Sampler (section 4.2.1) for this study. Unfortunately it was found to collect an inadequately small number of bioaerosols and so was not used on subsequent study days. However the results from observations and particle counts on these two days are still considered in section 4.5.4. Table 4-2 shows the relative sampling times and methods for each day of the two studies.

4.3.3 Statistical Methodology

The objectives stated at the beginning of this chapter all involve the correlation of different variables. Objective 1 requires measured data on each day to be related to each other day to see how strong the similarities are in activity and airborne contamination between days. Objective 2 requires particle production to be related to bioaerosol production, and Objective 3 requires that the relationship between activities and bioaerosol production is considered. The latter involves the analysis of a larger quantity of data than the other two objectives since there are many activities and fluctuations to take into consideration. Various activities have been outlined as possibly contributing to the airborne micro-flora. In order to initially test the bioaerosol release from these activities graphs were plotted in order to view, over time, the variation in bioaerosol and particle concentrations, alongside the occurrence of activities. The relationships considered in the three objectives were then analysed using bi-variate correlation with the objective of establishing where significant relationships exist.

In order to analyse data with a Pearson's correlation test, the standard parametric correlation test for two variables, the data should be normally distributed. Therefore the distribution of each variable was checked for normality using the One-Sample Kolmogorov-Smirnov tests, a goodness of fit test that compares the distribution of the variables with a normal distribution (Hinton, 2004). The results were also visualised using histograms. It was found through this that normality could not be assumed in

either of the studies using correlation analysis in this thesis (both this data and in Chapter 5), and so the following method was adopted.

Data that is not normally distributed may be analysed using the Spearman's correlation test. This is a non-parametric test that does not use the real values of the variables at each point, but instead uses ranks. Ranks are calculated for each variable by giving the lowest measurement a value of 1 and moving up through the values increasing the rank each time. Where there are several scores with the same value these will be given the same rank which is calculated as:

$$rank = \frac{r + (r+1) + ... + (r+s-1)}{s} \qquad 4\text{-}4$$

Where s is the number of original values and r is the rank the first data point with the value would have received. As well as being suitable for use with non-normal data this method reduces the effect of outliers, useful in this study as a high peak in bioaerosols/particles corresponding to an activity can skew the results and falsely provide strong correlations, or equally a lack of correlation. The results from this correlation are Spearman's Rho, a value between -1 and 1 that indicates the strength of a relationship and whether it is positive or negative. This is quoted along with the significance level; the smaller the significance level the higher the probability that the two variables are related linearly. The number of cases is also shown with the results as a small number may result in a falsely significant correlation due to the impact of a single point.

During the study it was found that several activities occurred at the same time on the bay, and therefore in order to correlate the results it was necessary to control for certain values. This was done using partial correlation on some specific occasions in this study in order to improve the understanding of the results. However this method uses Pearson's correlation and since normality cannot be assumed for this data the results should be treated with caution. Because of this issue each partial test was related to a similar test using Spearman's Rho and plotted on graphs to confirm the findings.

Quantifying the Observations

In order to carry out the statistical analysis described above, it was necessary to assign numerical values to each variable, including the activities, and ensure they corresponded in time. The variables were treated differently in the two studies, due to the refinement in the methodology carried out for Study 2. These are described below.

Study 1

During this study the particle counter was used to sum particles over 5 minute intervals, while the MicroBio sampler was used to take three 5 minute replicate samples every 30 minutes (Table 4-2). The results were therefore compared over 30 minute intervals. The activities were quantified in this time by assigning each occurrence with a value of 1, multiplying this by the number of minutes over which it occurs and summing all activities of the same type occurring at the same time. For example if two HCWs are in the bay for 15 minutes the value for the activity 'people' would be 30. The totals of each activity category were summed up over each 30 minute interval. The 5 minute samples for the particle counts were also summed in this time. The bioaerosol data was based on results from the MicroBio over the final 15 minutes of this half hour, and was the average of the three values.

Study 2

After the method of analysing the results was defined for Study 2 the frequency of sampling with the MicroBio was changed (Table 4-2). In this study the activities and particle counts were still summed over 30 minute intervals. The average of the bioaerosol samples in this period were found from one taken at 10 minutes and 25 minutes. When more samples are taken, such as periods of high activity the average of all samples taken in the period were considered.

4.4 Results and Discussion

In this section results and discussion are presented in three sections corresponding to the three main objectives outlined in section 4.3. The main analysis methods for these three aspects are described below:

1) A description of the day's activities and the main changes in particulate and bioaerosol count are described with diagrams of the fluctuations. Correlation is then attempted between the days to see how similar they are in respect to the particle and bioaerosol counts.

2) Correlations are drawn between the fluctuation in each size range of particles and bioaerosol counts in the air in order to establish what size of particle within the bay are most likely to be carrying micro-organisms.

3) Correlations between activities and bioaerosols are carried out in order to identify the activities that have the greatest effect on the bioaerosol count within the bay and the zones in which they occur.

Following this a general discussion concludes the section.

4.4.1 Objective 1: Daily Patterns of Activity and Airborne Contamination on a Ward

To determine whether there are significant similarities in activity and airborne contamination between days, and establishing whether a 'typical' day can be described.

A description of the general daily routine in the bay is presented followed by the findings for each separate study. The fluctuations of particle and bioaerosols sampled throughout the day are only shown for one study for succinctness. Study 2 is chosen because it provided more data than other days and it refers to a single bay only.

Overview of Observations

On all the days during both studies the morning tended to be the busiest period. At this time the patients were woken, given breakfast and the ward round took place, when patients were examined by doctors. The number of HCWs involved in the ward round varied between 2 and 8. Washing took place at this time, and often bedmaking was carried out during the same period although this varied. The washing was either independent, or with the aid of a nurse, the time taken varied according to this

dependence. The literature reviewed in section 2.3.2 showed that activities typical of those occurring in the morning period can generate large amounts of bioaerosols.

Meal times and visiting hours caused little disturbance in comparison. Meal times usually involved a single member of staff entering the bay to deliver meals. At visiting times there could be 1-8 extra people in the bay, but generally visitors remained seated and there was little increase in activity.

Study 1

The first study took place on two different bays: one a HD bay, the other a non-HD bay. Table 4-3 gives a general outline of the timing of activities on these days. On the HD bay the patients required the use of NIV, and these were used throughout the day by several of the patients. Except for a short period over lunch at least one NIV was in operation throughout the day. During the lunch period nebulisers were usually used. In the non-HD bay NIV were not used and there was a greater use of nebulisers particularly between 12:30 and 14:30. On both days the floor was mopped and the surfaces cleaned, bedmaking took place in both the morning and in the afternoon in the HD-Bay.

Table 4-3: Typical time line for observational Study 1 for both the busy (HD) and quiet (non-HD Bay).

<table>
<tr><th></th><th>09:00</th><th>10:00</th><th>11:00</th><th>12:00</th><th>13:00</th><th>14:00</th><th>15:00</th><th>16:00</th><th>17:00</th></tr>
<tr><td rowspan="2">Busy</td><td colspan="2">HCW Activity</td><td>Mopping</td><td colspan="2"></td><td colspan="4">Visiting</td></tr>
<tr><td colspan="5">NIV</td><td>Nebuliser</td><td colspan="3">NIV</td></tr>
<tr><td rowspan="2">Quiet</td><td>HCW</td><td>Mopping</td><td>HCW</td><td colspan="2"></td><td colspan="4">Visiting</td></tr>
<tr><td>Nebuliser</td><td colspan="3"></td><td>Nebuliser</td><td colspan="4"></td></tr>
</table>

Study 2

The high level of activity from HCWs in the morning also occurred in this study and is shown on the time line in Table 4-4. There was a noticeable decrease in the frequency of NIV and nebuliser use compared to Study 1. The table also shows the occurrence of cleaning in the afternoons of the quiet days. This reduced visitor hours as the ward was closed until 16:00, although there were still occasional visitors coming onto the bay during the day. On the three occasions observed here the cleaning began in the sampled

bay at approximately 13:30 (+/- 20mins). In order to clean the bay any unoccupied beds (e.g. empty beds or a patient sitting in their chair) were removed and placed in the corridor. Wet mopping was then carried out, followed by polishing.

Table 4-4: Typical time line for observational Study 2 for both the busy and quiet days.

	08:00	09:00	10:00	11:00	12:00	13:00	14:00	15:00	16:00
Busy		HCW Activity					Visiting		
Quiet		HCW Activity				Cleaning			Visiting

Quantitative Results

This section presents quantitative results from Study 2. The number of people in the bay (summed as explained in section 4.4.1) is shown as fluctuations in 15 minute intervals in Figure 4-9. Data is shown for three weeks with sampling carried out on Tuesdays and Wednesdays, to study *busy* and *quiet* days. Blue and red lines are used on the chart to distinguish between the busy and quiet days respectively. The peaks of activity occurred at similar times on all days but the recorded values are higher on the busy days. The peak then drops more quickly, whereas on quiet days the lower value is extended for a longer period.

The fluctuation of airborne micro-organisms in terms of TVC is shown in Figure 4-10 for the 5 days of Study 2. Figure 4-11 shows the measured daily fluctuation of particles with diameter > 5μm, while Figure 4-12 shows the daily fluctuation for particles in the range 0.3-0.5μm, illustrating the smallest and largest particles sampled. Figures 4-10 and 4-11 show that both the large particles and the TVC peak in the morning for the busy days. However the quiet days have higher values of 5μm particles in the afternoon when cleaning of the bay occurs. The 0.3-0.5μm particles generally follow a cyclic pattern with a peak in the morning and a second peak in the afternoon.

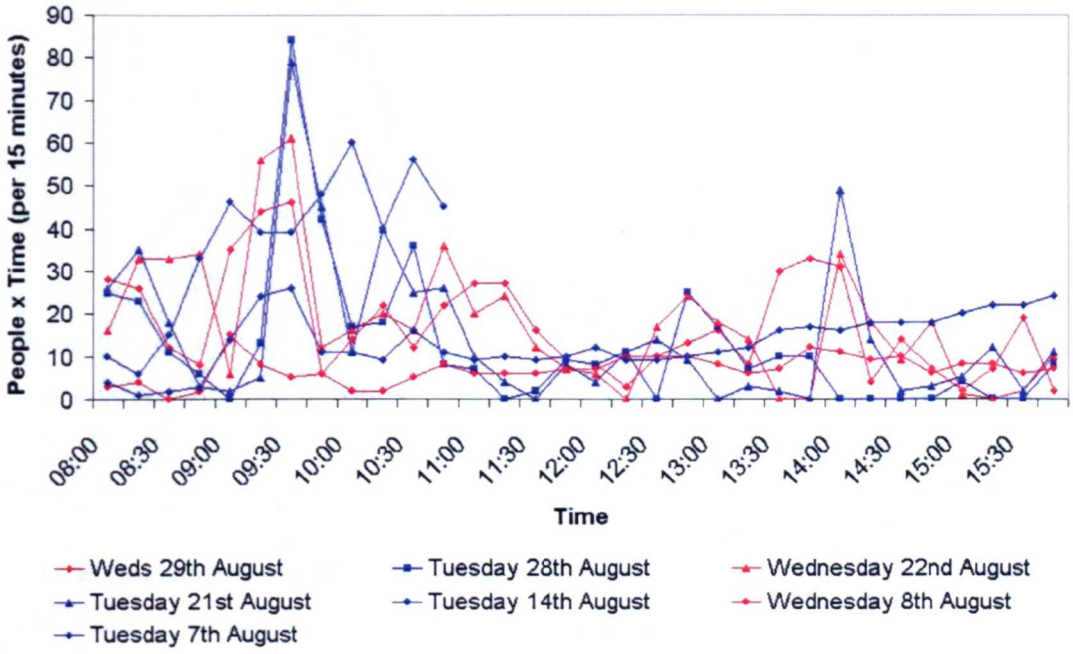

Figure 4-9: Fluctuation of hospital staff in the bay during Study 2. Blue lines show Tuesdays, the busy day, whereas red lines show Wednesdays, the quiet days. These values are used as a general marker for the level of activity in the bay.

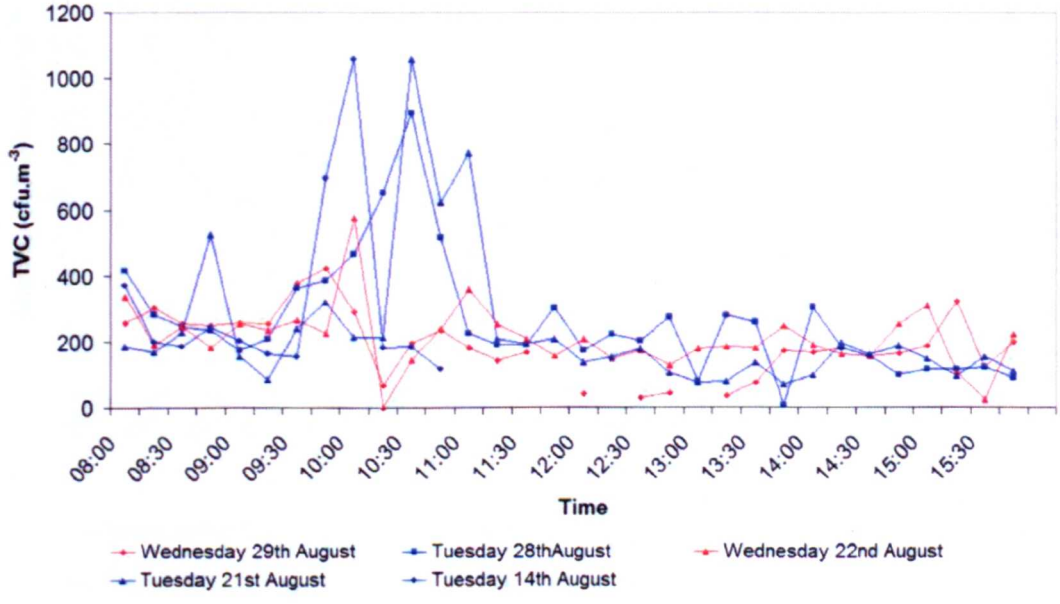

Figure 4-10: Fluctuation of TVC in Study 2. As in Figure 4-12 the blue lines show the busy days, and the red lines the quiet days.

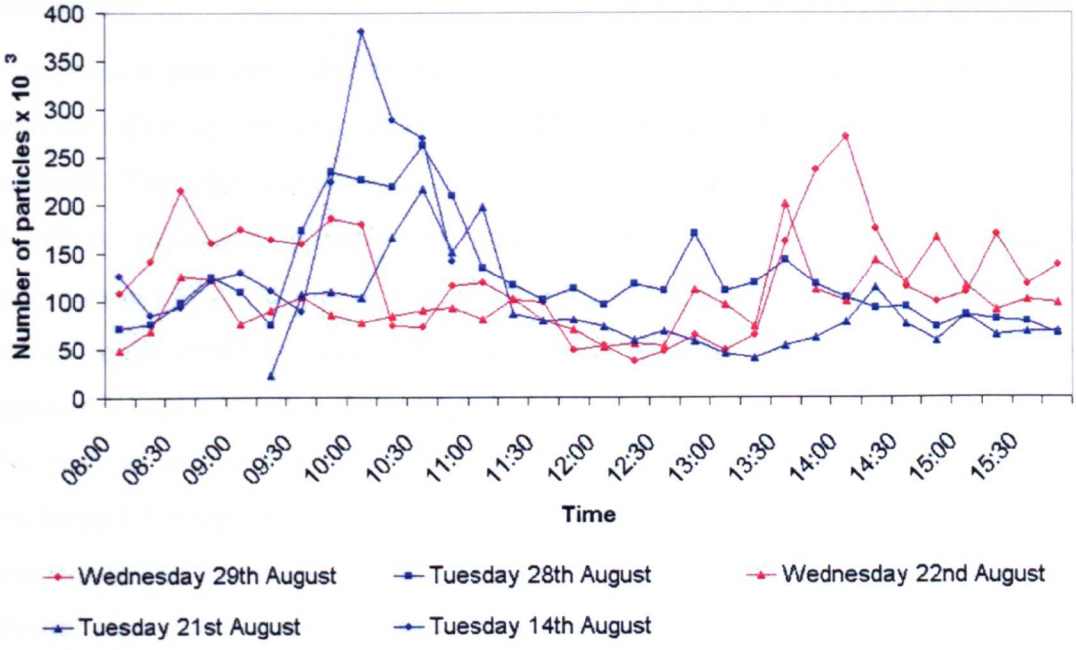

Figure 4-11 Fluctuation of particles > 5μm in Study 2. Blues lines show the busy days, red lines the quiet days.

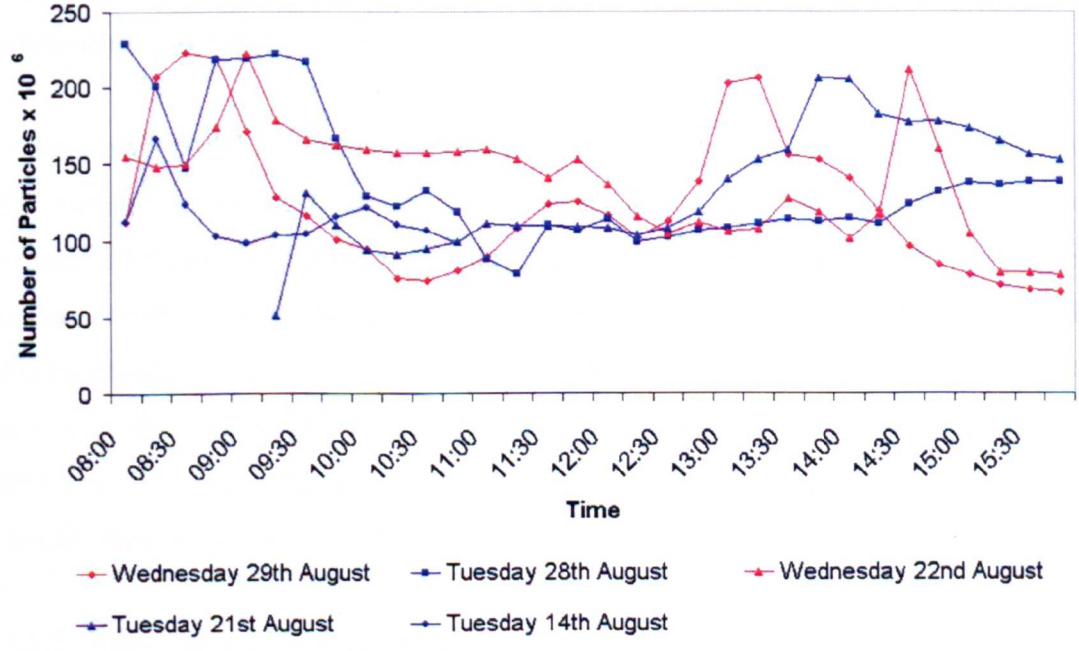

Figure 4-12: Fluctuation of particles 0.3-0.5μm particles in Study 2. Blues lines show the busy days, red lines the quiet days.

Discussion

The studies presented above only considered one ward, so conclusions about the activities of a typical day can only be drawn for this single ward and not the entire hospital. The observations carried out in both studies indicated that for general activities, such as ward round and patient washing, there was a daily pattern to the activities as shown in Figure 4-9. The similarities are greater when the days are split into *busy* and *quiet* days. Segregating the results into *busy* and *quiet* days shows how the periods of high activity are condensed into shorter time frames on *busy* days, whereas the peak on the quiet days is lower but is spread over a longer time period. This was confirmed by the observations which noted that on the busy days more HCWs participated in the ward rounds and that the nursing activity was condensed into a shorter time frame. This meant that activities such as bedmaking and patient washing would occur at the same time for multiple patients.

There are also differences between each type of day for the TVC and the large particles. The peaks of bioaerosols and particles in the morning are higher for the busy days, whereas the smaller particles have a similar cyclic pattern for all days.

Although there are similarities between the days there is a large amount of variance. The variance in the results meant that considering that summed values in 15, 30 and 60 minute intervals there were few significant correlations between the days. This is understandable viewing the difference in peak values and spread in Figures 4-9 to 4-12. The patients in the bay also changed during the three weeks of the study, and since the activities are due to human behaviour there will always be variance in the result. Although statistically significant correlations cannot be drawn there are general patterns that are repeated on several days and are evident in the figures.

4.4.2 Objective 2: Sizing of particles carrying Micro-organisms

To evaluate the typical size of particles likely to be carrying micro-organisms within a hospital ward.

To efficiently carry out the correlations both in this section and in section 4.5.3 it is necessary to define particular particle and microbial data for analysis, rather than

carrying out the entire analysis on all particle ranges and bioaerosols sampled during the studies. In order to decide which data are most suitable the following section first compares all the particle ranges sampled to find the cut-off diameter where behaviour differs between the measured data sets. Correlations are also carried out with the microbial data to determine whether the fluctuation of the TVC will adequately represent the release of *Staphylococci* and *Staphylococci aureus*. Following this preliminary analysis the particle data are correlated to the production of bioaerosols to assess which size of particles are most likely to carry the majority of micro-organisms within the hospital bay.

Comparing fluctuations of each particle size range

As described in section 4.2.3 the particles were sized in five different ranges. If different sources of particle generation produced different sized particles at un-coordinated times then the sampled data should reveal variation between the particle sizes. This section considers the relationship of each size range to each other, to see how each differs in its fluctuations over time. By comparing each size range, and grouping those that behave similarly, a selection of representative particle sizes can be used in the following analysis, rather than carrying out correlations on each size range sampled. It is also useful to understand which particle sizes relate to different release mechanisms. To understand where this difference occurs correlation coefficients were found between each particle size range. These correlation coefficients are shown in Table 4-5 and Table 4-6 for Study 1 and 2 respectively, along with the significance of the correlation and the number of samples. Underlined values are significant to at least the 0.05 level. For this analysis, since only the particle data was considered, the 5 minute particle summations were used thereby providing a greater number samples on which to apply the statistical methods.

From this analysis it is likely that particles with a characteristic diameter greater than 5μm are generally generated from a different source than those with a smaller diameter. The results in Table 4-5 and 4-6 show that the 1-3μm range has a high significant positive correlation coefficient with both particles down to 0.3μm and up to 5μm. The sampled data in the 1-3μm size range can therefore be used to describe the general behaviour of particles between 0.3 and 5μm with reasonable accuracy. The correlation to the smallest particles between 0.3 and 0.5μm was low compared to the other ranges

and therefore some of the analysis was also carried out using this size range. However this did not yield any extra information and is therefore not presented.

There is significant positive correlation between particles in the >5μm size range and 3-5μm range. However the correlation to 1-3μm particles is very low and there is no significant correlation below this size. Therefore this size range is treated separately.

For the remainder of the analysis only the behaviour of the particles sized 1-3μm and >5μm will be used in the analysis as it is felt that these adequately represent all the size ranges sampled.

Table 4-5: Study 1: Comparison of particle concentration fluctuations between different size ranges using Spearman's Rho correlation coefficients (those significant at the 0.05 level are underlined).

Characteristic Particle Diameter (μm)		**0.3-0.5**	**0.5-1**	**1-3**	**3-5**	**>5**
0.5-1	r	0.991				
	Sig (2-tailed)	0.01				
	No. of Samples	192				
1-3	r	0.983	0.997			
	Sig (2-tailed)	0.01	0.01			
	No. of Samples	192	192			
3-5	r	0.909	0.918	0.924		
	Sig (2-tailed)	0.01	0.01	0.01		
	No. of Samples	192	192	192		
>5	r	0.209	0.203	0.206	0.446	
	Sig (2-tailed)	0.01	0.01	0.01	0.01	
	No. of Samples	192	192	192	192	

Table 4-6: Study 2: Comparison of particle concentration fluctuations between different size ranges using Spearman's Rho correlation coefficients (those significant at the 0.05 level are underlined).

Characteristic Particle Diameter (μm)		0.3-0.5	0.5-1	1-3	3-5	>5
0.5-1	r	0.806				
	Sig (2-tailed)	0.01				
	No. of Samples	601				
1-3	r	0.676	0.965			
	Sig (2-tailed)	0.01	0.01			
	No. of Samples	601	601			
3-5	r	0.414	0.689	0.800		
	Sig (2-tailed)	0.01	0.01	0.01		
	No. of Samples	601	601	601		
>5	r	-0.065	0.177	0.289	0.698	
	Sig (2-tailed)	0.111	0.01	0.01	0.01	
	No. of Samples	601	601	601	601	

Relationship between selective and non selective bioaerosol sampling.

On the final two days of Study 2 selective agar was used to sample for *Staphylococcus spp.*, particularly *S. aureus,* as described in section 4.2.2. Analysis was therefore carried out to determine whether there were relationships between the microbial counts sampled on selective media and the TVC samples taken using a general purpose media.

The correlation between TVC and *Staphylococci* or *S. aureus* is positive with r=0.770; p<0.01; n=31 and r=0.535; p<0.01; n=31 respectively. The correlation between TVC and *Staphylococcus spp.* is significant to the 0.01 level with a high positive correlation coefficient. The total number of bacteria colonies grown on mannitol salt agar were of a similar magnitude to that on the general agar so this seems a reasonable result. However the number of *S. aureus* colonies collected in each sample was approximately 100 times lower than the TVC or all *Staphylococcal spp,* with 1 or 2 colonies counted as opposed

to hundreds. Since only a few *S. aureus* colonies were sampled the correlation to the others is likely to be low as there is a large difference in numbers from the presence of only one extra colony. Although the correlation is not as strong as with the *Staphylococci spp.* Figure 4-13 shows the larger values of *S. aureus* tend to occur around similar times to sampling a high TVC. As such the values of TVC are used in the later analysis as a good indicator of *Staphylococci spp.* The difference in the quantity of *S. aureus* and general bacteria sampled from the air is similar to other studies discussed in section 2.3.2 particularly Bethune *et al* (1965) and Hambraeus (1973).

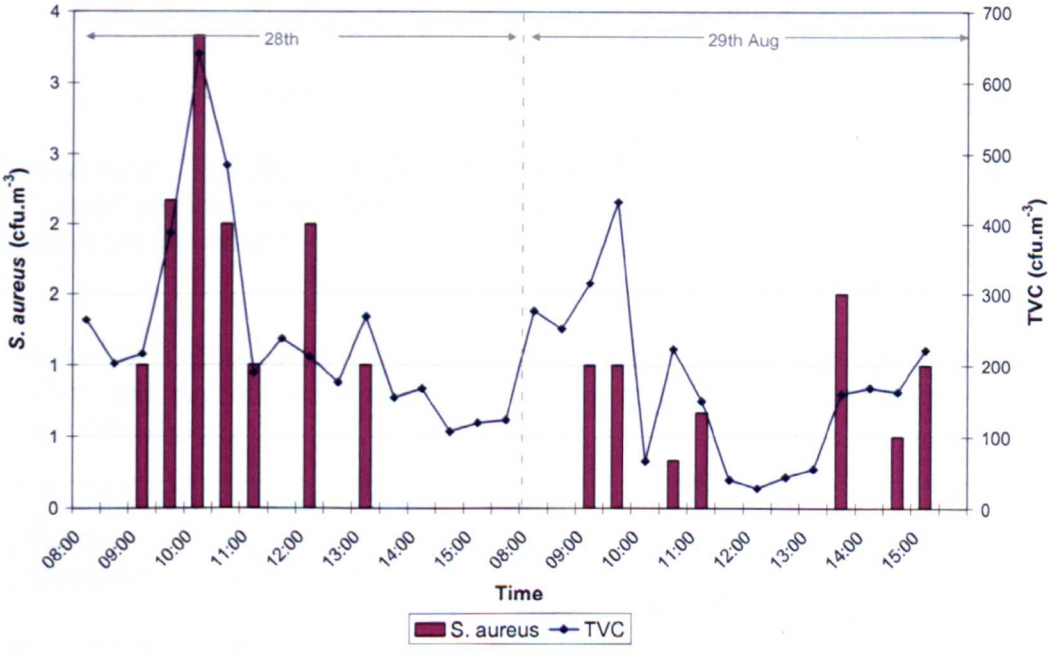

Figure 4-13: Fluctuations in *S. aureus* (bars) and TVC (line) over two days in Study 2. Showing how the higher values of TVC correspond to sampling *S. aureus.*

Defining size ranges for bioaerosol release.

The two particle size groups, 1-3μm and >5μm, were correlated against the TVC for all the study days. This was carried out in an attempt to ascertain the size of particles most likely to be responsible for the transport of bacteria within general hospital wards. Since there were differences in the levels of activity and the production of particles and bioaerosols on the days labelled *busy* and *quiet* the following analysis is split between these types of day, and the two studies.

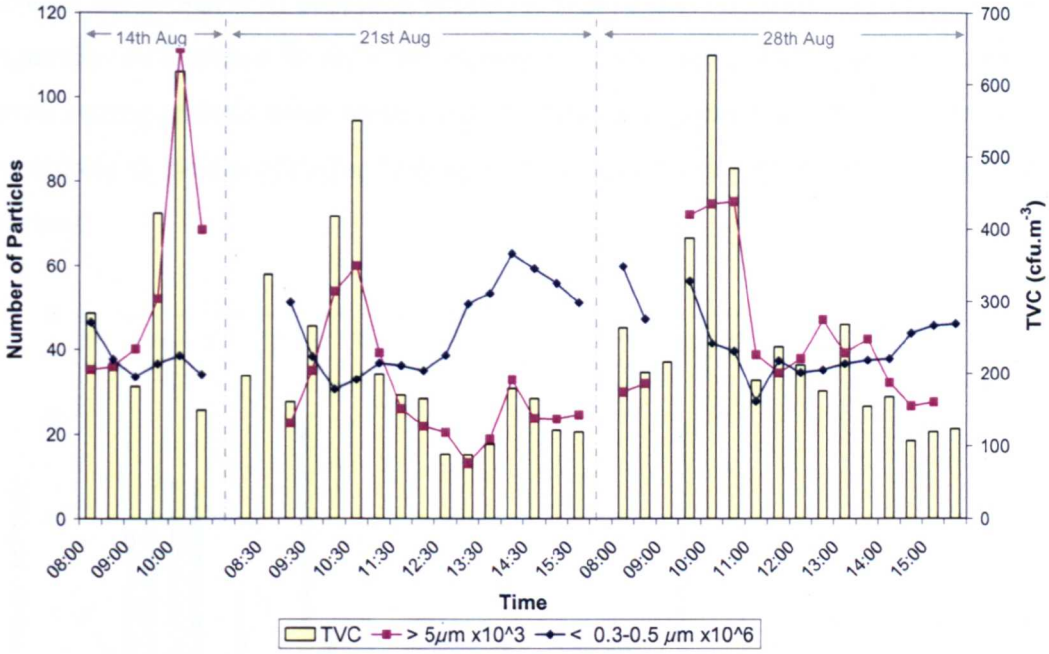

Figure 4-14: Fluctuation of TVC and Particle Counts for the busy days of Study 2. Values of particles 0.3-0.5μm characteristic diameter are shown at 10^6 and >5μm particles are shown at 10^{-3} on the left y axis.

Table 4-7: Correlation Coefficients (Spearmann's Rho) between fluctuations of TVC and particle sizes >5μm and 1-3μm (those significant to 0.05 level are underlined).

Characteristic Particle Diameter	Study	1		2	
	Day Type	Busy HD	Quiet Non-HD	Busy Tues	Quiet Weds
5 μm	r	0.725	0.214	0.771	0.450
	Sig (2-tailed)	0.02	0.443	0.01	0.011
	No. of Samples	15	15	35	31
1-3 μm	r	0.536	0.207	0.139	0.347
	Sig (2-tailed)	0.04	0.459	0.426	0.056
	No. of Samples	15	15	35	31

As can be seen in Table 4-7 there are high correlation coefficients between 5μm particles and sampled micro-organisms during the busy days. The correlation coefficient is less on quieter days of Study 2 and there is no significant correlation on the quiet day

Overall the presence of people in the bay is a good indication for activity, and there was generally an increase in airborne micro-organisms and particles greater than 5μm at times during periods when more hospital staff were present. However other factors can contribute to the fluctuations, such as windows being opened and venting particles from the bay.

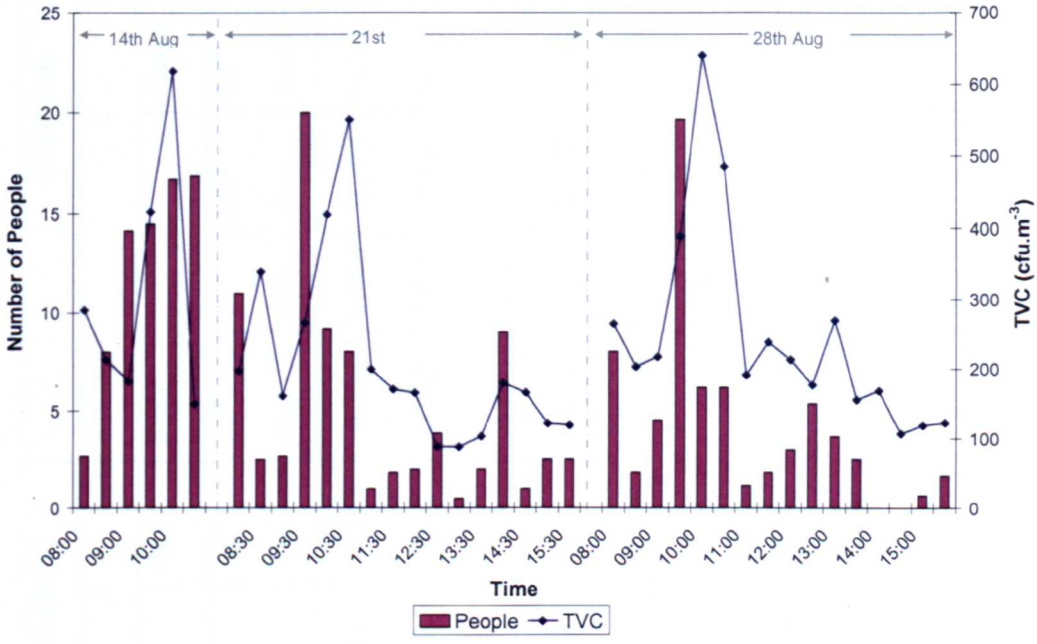

Figure 4-15 Fluctuations of hospital staff (bars) and TVC (line) shown for the busy days of Study 2

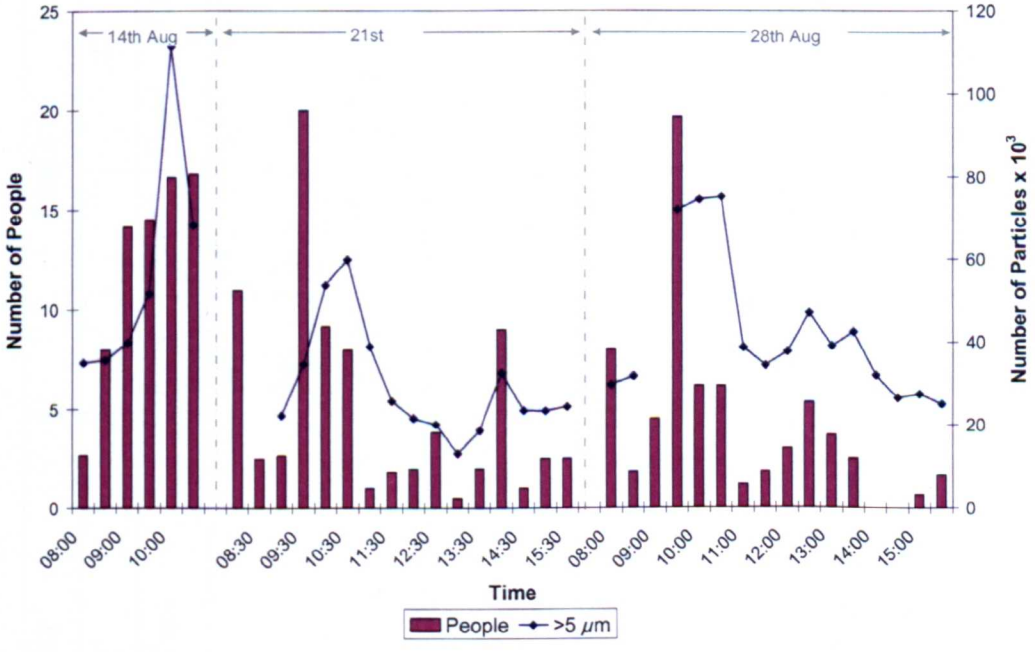

Figure 4-16: Fluctuations of hospital staff (bars) and Particles > 5μm characteristic diameter (line). Shown for the busy days of Study 2.

Table 4-8: Correlation Coefficients (Spearman's Rho) between TVC or particles and all observed activities. Those significant to the 0.05 level are underlined. (p) indicates where partial correlation is used as described in the text.

Activity		People				Washing		Commode					
Study		1		2		2		2					
Day Type		Busy	Quiet	Busy	Quiet	Busy	Quiet	Busy			Quiet		
Date		16th Dec	17th Dec	All	All	All	22nd Aug	14th Aug	21st Aug	28th Aug	22nd Aug	29th Aug	29th Aug(p)
TVC cfu.m^3	r	0.563	0.232	0.552	0.421	0.644	0.437	0.828	0.064	0.754	0.252	0.433	0.668
	Sig (2-tailed)	0.029	0.405	0.01	0.018	0.01	0.09	0.042	0.730	0.01	0.346	0.107	0.01
	No. of Samples	15	15	38	31	38	16	6	32	16	16	15	12
>5 μm	r	0.822	0.687	0.605	0.166	0.686	-0.412	0.621	0.259	0.695	0.028	0.308	0.246
	Sig (2-tailed)	0.01	0.01	0.01	0.124	0.01	0.113	0.188	0.201	0.01	0.918	0.2246	0.396
	No. of Samples	15	15	35	32	35	16	6	26	15	16	16	12
1-3 μm	r	0.316	-0.142	-0.018	0.208	-0.039	-0.349	0.001	0.423	0.220	0.364	0.028	-0.183
	Sig (2-tailed)	0.252	0.613	0.919	0.253	0.825	0.185	0.99	0.031	0.430	0.166	0.918	0.530
	No. of Samples	15	15	35	32	35	16	6	26	15	16	16	12

Table 4-8 cont.

Activity		Bedmaking				Curtains				Nebuliser		NIV	Cleaning
Study		1		2		1		2		2	1	1	2
Day Type		Busy	Quiet	Busy	Quiet	Busy	Quiet	Busy	Quiet	Quiet	Quiet	Busy	Quiet
Date		16th Dec	17th Dec	All	22nd Aug	16th Dec	17th Dec	All	8th,29th Aug	29th Aug	17th Dec	16th Dec	Weds
TVC cfu.m^3	r	0.452	0.432	0.458	0.530	0.565	0.525	0.405	0.516	0.307	0.010	0.117	-0.094
	Sig (2-tailed)	0.091	0.108	0.01	0.077	0.028	0.045	0.012	0.004	0.266	0.973	0.690	0.614
	No. of Samples	15	15	37	12	15	15	38	30	15	15	14	31
>5 μm	r	0.678	0.448	0.624	-0.362	0.663	0.255	0.443	0.133	-0.754	-0.242	-0.179	0.418
	Sig (2-tailed)	0.01	0.094	0.01	0.247	0.007	0.358	0.008	0.380	0.103	0.384	0.540	0.003
	No. of Samples	15	15	34	12	15	15	35	46	6	15	14	47
1-3 μm	r	0.198	-0.079	-0.184	-0.195	0.219	0.284	0.013	0.100	0.812	0.650	-0.902	0.269
	Sig (2-tailed)	0.479	0.779	0.298	0.543	0.433	0.304	0.939	0.507	0.01	0.09	0.01	0.067
	No. of Samples	15	15	34	12	15	15	35	46	16	15	14	47

Washing

Observations of patients washing were only carried out in Study 2 therefore only these results are shown in Table 4-8. The analysis indicates that on the busy days the correlation between washing and TVC or >5μm particles is very strong. On the quiet days the correlation of washing to TVC is significant to the 0.1 level, however similarly to the analysis with people, this is not reflected in the particle data (See Appendix Figure A1-2 and A1-3).

Wednesday 29th August is not included in the results in Table 4-8 as the window in the bay was opened at 10:30 coinciding with the start of washing. Partial correlation controlling for the window being opened was carried out giving $r = 0.471$, $df = 12$, $p < 0.1$ for TVC and washing and for *Staphylococci* the correlation improves to give $r = 0.574$, $df = 12$, $p < 0.05$. The production of particles sized 5μm or greater does not correlate well due to the occurrence of cleaning in the afternoon.

As a result of the lower concentrations of TVC on the quiet days the correlation with washing on the busy days was found individually to ensure one day was not skewing the results. Similar results were found for both days suggesting that this was not the case.

Since washing occurred at a similar time to peaks in the number of people in the bay partial correlation was carried out for people controlling for washing and vice versa. Even when controlling for the number of people, washing correlates to the TVC with a coefficient $r=0.672$, $df=32$, $p<0.01$, and to >5μm particles with $r=0.780$, $df=32$, $p<0.01$ for busy days. However when controlling for washing and correlating people to TVC the correlation coefficient drops to $r=-0.1232$, $df=32$, $p<0.48$ which is not considered to be significant. Correlation between people and large particles is still significant with coefficient of $r=0.428$, $df=32$, $p<0.01$ showing that the specific activity of washing may release more bioaerosols than just considering the general activity of people. Section 2.3.2 presented studies that found undressing and dressing resulted in a large production of micro-organisms. It follows that washing is then also likely to be responsible for releasing bacteria into the air in large quantities as this may incorporate undressing and towelling, both of which can cause friction across the skin releasing particles into the air. It has also been shown that the human body releases more bacteria after showering

as the skin flakes lose their natural oils and dry out (Speers *et al.*, 1965); this may also be the case after washing.

These results suggest that it is not simply the presence of people in the bay that results in high particle and bioaerosol counts, but that the specific activities they carry out have a strong influence on the airborne micro-flora. The difference in the correlation coefficients when applying partial correlation to compare people and TVC emphasises this. Although this suggests that washing is responsible for a large release of micro-organisms several other activities occurred during the same period, such as commode use and bedmaking.

Commode Use

As with washing, the use of the commode was only recorded in Study 2 and so only these results are shown in Table 4-8. The individual days are shown separately as Tuesday 21st August correlates very poorly and since the commode was used during a period when the window was open on Wednesday 29th August then partial correlation is carried out using the window as a control.

The use of the commode tends to occur at a time when there is a peak in TVC, and significant positive correlation is found on the days 14th, 28th and 29th August between the commode use and the TVC. On the 28th and 29th of August the use of the commode also gives a high correlation to the sampled *S. aureus* with $r= 0.720$; $p< 0.01$; $n=12$ and $r=0.727$; $p<0.3$; $n=16$ respectively. However the weak correlations between commode use and particle counts show there is little indication that commode use is responsible for the release of a particular size range of particles.

On 21st August there is no significant correlation between commode use and bioaerosol counts. It is possible that the effect of the commode on the airborne micro-flora varied between each patient and instance. Also the time the curtains were kept closed after use may have affected the quantity sampled as the curtains remained closed for longer on the 21st August. Although the correlation analysis does not show any significant correlation on the 21st the occurrence of commode use is generally followed by an increase in the TVC sampled, although the increase may be very small and it does not occur immediately (Appendix 1. Figure A1-4 and A1-5).

Bedmaking

Bedmaking does appear to correspond to peaks in bioaerosols as can be seen in the figures in the Appendix (Figure A1-6), although the correlation is not significant to $p<0.05$ on most days they are close to $p<0.1$. Data from Wednesday 29th is again not shown here as there was only one occurrence of bedmaking on this day and this took place during a period when the window was open. Data from Tuesday 14th is also not included as there was a very small number of samples. Correlations with the TVC bioaerosol data are considered reasonable as they are all close to the 0.1 significance level, although this is higher than usually considered as a significant result. This is also the case for most of the correlations with the >5μm particle data, however like the other activities presented so far there is no significant correlation with the 1-3μm particles.

Due to the low occurrence of bedmaking there are not many occasions to correlate values over and there are difficulties in carrying out reasonable statistical analysis. However this is worth considering as an important activity as it has been shown on other occasions to be responsible for the release of airborne bacteria (Noble, 1962, Shiomori *et al.*, 2002, Walter *et al.*, 1958) and there are further indications from the results presented in this thesis that it is responsible for the generation of bioaerosols as part of the morning activities within the bay (Appendix 1. Figure A1-6 and A1-7). On Tuesday 28th August there is a clear significant correlation to the sampling of *S. aureus* with a $r = 0.6$; $p< 0.05$; $n=13$.

Curtains

The activities, *washing, bedmaking,* and *commode use* all took place behind closed curtains. Curtain movement gives significant positive correlation to TVC as shown in Table 4-8. Also as part of the ward round when patients were being examined and if a patient was moved out of the bed the curtains were closed. As such the movement of curtains tended to indicate the occurrence of an activity. Since curtains may become contaminated with micro-flora (Das *et al.*, 2002) it was desirable to see if any of the observed increase in TVC was due to the activities or the movement of the curtains.

During a quiet period the curtains were vigorously moved by opening and closing them 3 times in the 5 minute sampling period to see if this contributed to the airborne micro-flora. This did not seem to have a noticeable affect on the levels although swabs from

the curtains onto TSA showed them to be colonised with bacteria. However a previous study by Noble (1962) noticed that disturbance of curtains did release bioaerosols, this however may be due to the possible difference in curtain material between the two studies. Also the difference in the two studies may be related to the background count at the time the disturbance takes place.

A further possibility is that the curtains would 'contain' the effects of the activity until they were opened at which point the bacteria could be released into the wider bay environment. The data presented here sometimes showed an increase in both TVC and particles after opening, but also on other occasions did not. As the length of time after the activity before the curtains were opened would vary, and there are other factors within the bay affecting the airborne count there was not enough data to either support, or reject this hypothesis.

Nebulisers and Ventilators

Since visible particles were released into the air when a nebuliser was in use it was of concern that these may carry micro-organisms as the particles impact with the skin and mouth of the patient before being released into the air. The results in Table 4-8 show insignificant correlations between TVC and the use of nebulisers, indicating they are unlikely to be responsible for increasing the airborne micro-flora. However they do appear to increase the levels of particles in the air that are in the 0.3-3μm size ranges. The production of viable particles from the use of nebulisers may be an issue for specific infections, as they were banned from use in Hong Kong hospitals in 2003 for patients with SARS as they were thought to be responsible for aggravating the spread of the infection (Li *et al.*, 2005). However in this case, on a general hospital ward, they do not appear to increase the bacterial bio-burden of the air.

NIV was only used intermittently, and as such correlations with use could only be carried out on one day of the study where the data was sufficient (Study 1, busy day). The ventilator seems to have no effect on either the micro-organisms in the air or larger particles, but there are very strong negative correlations to particles within the size range 0.3-3μm. Since these particles may be small enough to follow the air flow the ventilators may pull in these particles and they are either filtered out by the device or inhaled by the patients. The lack of correlation with the larger particles indicates that the

ability of the ventilator to draw in particles from the surrounding air is not extended to the larger particles. These correlations were only found for one day as on the other day (Study 2, 22nd August) that the ventilators were in use they were on for the whole day. Comparing the particle counts from this day to the other days in the study there does not appear to be fewer smaller particles in the air.

In Study 2 on the 22nd August 2007 a ventilator was in use all day. The results for the correlations to particle size differ on this day to the results from the other days. The correlation between TVC production and particles 5μm characteristic diameter is not statistically significant, whereas the correlation to the smaller particles in the range 0.3-0.5μm is significant with $r=0.764$; $p<0.01$; $n=16$. This is echoed in Study 1 where the ventilator is used intermittently and although the correlation to particles > 5μm is much higher than the 22nd August the correlation to the smaller particles is much improved with significant correlation to 1-3μm particles (Table 4-7) and nearly significant correlation to 0.3-0.5μm particles with $r=0.500$; $p< 0.06$; $n=15$. The average value of bioaerosols, or smaller particles sampled from the air on these days did not increase. Although the number of smaller particles and TVC did not appear to increase when the ventilator was in operation, it seems that there may be greater carriage of the bioaerosols on smaller particles. Although this data is limited and therefore the carriage on smaller particles could be coincidental this may have implications on the transfer of infection; the smaller the particle size the further it may be travel down the respiratory tract and thereby cause infection.

Cleaning

Cleaning occurred on the Wednesdays in Study 2 for the whole ward, and the dust thrown up during polishing was visible at times. Table 4-8 shows the correlation coefficients for this activity. Mopping and polishing were not considered separately in these coefficients as they occur so close in time it would not be possible to make any sensible conclusions as to which was affecting the counts (Appendix Figure A1-8). There was significant correlation with the particle data greater than 5μm but not for smaller particles or the TVC bioaerosol samples.

Visitors

As can be seen in Figure 4-17 visitors came to the bay in the afternoon, when the concentration of bioaerosols were generally decreasing. The lack of effect that visitors have on the production of bioaerosols may be due to their lack of activity. Although the number of people in the bay increased visitors tended to remain sedentary and during this time there was less health care related activity.

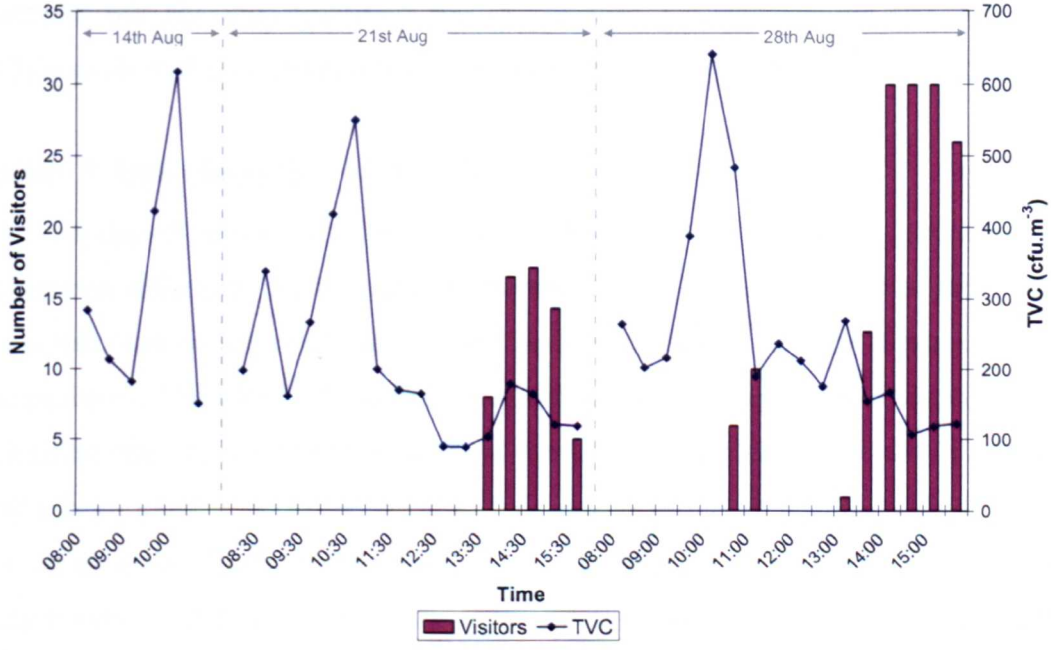

Figure 4-17: The fluctuations in TVC compared to the number of visitors for Study 2 on busy days

4.4.4 General Discussion

Although some days show very strong correlations for specific activities, this does not occur over all the days sampled. The results show that the correlations of bioaerosols to particles, number of people or washing is not as strong on quiet days. A simple reason could be the smaller fluctuations resulting in correlations that are not as clear. For example, washing on busy days always occurred within a short time frame whereas on the quiet days it was spread out over a longer period, hence the sharp peaks in both activity and particle production are not present. Three of the quiet days also have other individual reasons for poor correlations; these are described below.

Study 1: Quiet Day (17th December 2004)

This day of Study 1 shows no significant correlation between bioaerosols and people or bedmaking, although there is significant correlation between >5μm particles and the number of people in the bay. There is also no significant correlation between the bioaerosols data and any of the particle ranges. On this day the average concentration of TVC at 13:30 is much higher than the rest of the day at 885cfu.m^3; this occurred much later than the peak values on other days and occurred when a patient situated near the sampler was shaving. Removing this sample from the analysis, the TVC and particles >5μm peak in the morning, fluctuating in a similar manner (Appendix 1. Figure A1-9)

Study 2: Quiet Day (22nd August 2007)

As mentioned previously, on the quiet days of Study 2 cleaning occurred in the afternoon affecting the correlations between 5μm particles to either the bioaerosol concentration or activities, as cleaning produced a large number of particles but few bioaerosols. The effect of cleaning may not just have affected the afternoon period as cleaning was carried out on the rest of the ward during the whole day. Particles may have been transported to the sampled bay, and affected the results, without an activity being observed. Even considering this the correlation to any activities on this particular day is very poor. The ventilator was in use all day and this may have affected the burden of the air. The peak value on this day for bioaerosols does occur during the busy period of the morning, as occurs on the other days. However a much higher concentration was sampled than during the rest of the day (Appendix 1. Figure A1-10) and so this will skew the data when attempting to draw correlations.

Study 2: Quiet Day (29nd August 2007)

On the 29th August there is a lack of correlation between TVC and large particles due to cleaning. The window in the bay was open between 10:00 and 13:30; the time the highest production of particles and bioaerosols would be expected. Instead of the expected increase, as the window is opened the quantity of both decrease, and the expected effect of activity is not shown.

Study 2: Preliminary particle and activity data

On the 7th and 8th of August a study was carried out measuring particle concentrations, but the TVC was not quantified. This data has not been included in the analysis above where the focus has been on bioaerosols. However the data provides some interesting results in regard to the particle data. On the 7th August there was a very large peak at 9:30am for particles > 5μm (Appendix Figure A1-11), this is almost ten times higher than any other day from both studies. At this time there were also high counts for the other particles, but of the same order of magnitude as was found in the other studies. There was no error registered in the particle counter at this time.

From observations in the bay there did not appear to be anything special about this day, or time. In the morning there were typical nursing activities. Patient A was washed, the bed made and patient D was washing themselves. At 09:21, just as the increase begins, both sets of curtains were opened. The peak on the 8th occurs at 9:45, this is not as large, but is greater than on any other sampling days (Appendix 1. Figure A1-12). At this time the curtains at D were opened, after washing, only on the side facing the sampler. At patient A nurses moved through the curtains whilst washing was being carried out. Also at this time patient B, near the sampler was spraying an aerosol behind curtains.

These high peaks occurred during the morning when nursing activities such as washing, commode use and bedmaking took place, however they give much greater quantities of particles than on other days. Noble (1975) noted that some patients were capable of dispersing much larger quantities of *S. aureus*. Unfortunately no samples of bacteria were taken on these days but it is possible that a single patient may also be responsible for greater release of particles either due to natural shedding, or a specific disease. No other observations were made of activities at this time that may have affected the airborne micro-flora so significantly. Although only particle data, these counts highlight how much the level of airborne contamination within a hospital bay may vary from day to day. A previous study on the same ward also found large variations in the data for specific bioaerosols (Thornton *et al.*, 2004).

4.5 Summary

Objective 1

Generally the days specified as *busy* and *quiet* followed a similar pattern for level of activity, which was correspondingly reflected in the levels of particles and bioaerosols sampled. Although visually the fluctuations were similar with 30 minute intervals significant correlations between the different days could not be drawn. The different types of days resulted in different quantities of release of particles/bioaerosols and the occurrence of different activities (cleaning). Specific factors such as use of medical equipment and the opening of the windows can result in large variations away from the typical pattern.

Objective 2

The behaviour of all particles sampled could be represented in analysis by only using data in the 1-3μm and > 5μm particle size ranges. In addition the microbial samples taken on general purpose media to give a TVC correlated well with samples taken on selective media to identify *Staphylococcus spp.*

The sampled bioaerosols generally correlated very well to the collection of particles greater than 5μm in diameter but not with smaller particles. However when NIV was in use in the bay significant correlation with the smaller sized particles was found.

Objective 3

The number of hospital staff within a bay can be used as an indicator to quantify the activity level, as the important activities take place when they are in the bay. The total number of people within the bay should not be used as this would also include visitors who do not have a significant effect on the airborne micro-flora or particle concentrations.

Although number of people is a good indicator for activity, and the presence of staff within the bay relates to an increase in particles and bioaerosols, the generation of both depends on specific activities occuring. Washing, commode use and bedmaking occur at similar times when higher concentrations of bioaerosols and particles > 5μm are sampled. These all occur near to the patients beds, usually with the curtains closed.

Although cleaning, via floor polishing and mopping, is shown to increase the numbers of large particles in the air it does not appear to contribute to the level of micro-organisms in the air.

Chapter 5
CFD Methods and Test Chamber Model Validation

This chapter describes the CFD methodology used to develop and validate the zonal source concept to be described in Chapter 6. Following a general description of the CFD process, a model of the airflow in a mechanically ventilated chamber is presented. The geometry and boundary conditions are based on the climatically controlled bioaerosol test chamber at the University of Leeds, which is used in the experimental validation of the model. The two methods used to model the injection and transportation of bioaerosols in the space are described in detail. These methods are then applied to the airflow model of the test chamber. Experiments carried out within the test chamber to validate both the methods are described. The results from these are then compared to those from the CFD models to assess the ability of the methods to model bioaerosol transport to reasonable reflect reality. This completes the first part of the second objective stated in the introduction to this thesis; to validate the ability of the chosen methods to simulate bioaerosol transport and deposition within CFD model.

5.1 Governing Equations of Fluid Flow

This section provides an overview of the CFD methodology used in this study. As the study is carried out using a commercial CFD code and the CFD process is well documented elsewhere only a brief description of the governing equations and numerical methods are given here. The reader is referred to other texts such as Versteeg and Malalasekera (1995), for further details.

Airflow in a room is governed by the conservation laws of physics. In order to describe the behaviour of a fluid a small fluid element is considered. Any changes in mass, momentum and energy must be due to flow across the surfaces of the element, or sources within the element to obey the three conservation laws:

- Conservation of Mass: The continuity equation.
- Conservation of Momentum: Newton's Second Law.
- Conservation of Energy: The first Law of Thermodynamics.

Conservation of Mass

Conservation of mass, also known as the continuity equation, expresses that any increase of mass in a fluid element is equal to the rate of flow of mass in to that fluid element. Figure 5.1 illustrates this mass flow into and out of a fluid element. For incompressible flow the density of the fluid will remain constant and any change in mass within a fluid element is due to the mass flow rate across the elements face. The continuity equation for incompressible flow can therefore be written as:

$$\frac{\partial(u)}{\partial x}+\frac{\partial(v)}{\partial y}+\frac{\partial(w)}{\partial z}=0 \qquad 5\text{-}1$$

In vector notation:

$$div(\mathbf{u})=0 \qquad 5\text{-}2$$

Where **u** is the vector value of velocity *(u, w, z)*.

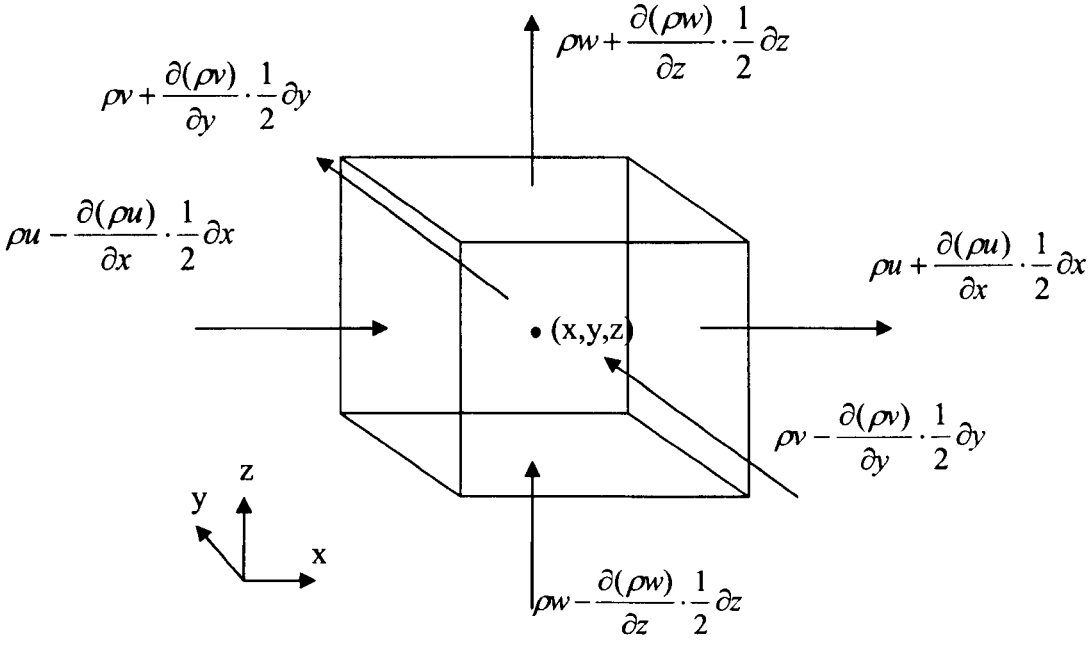

Figure 5-1: Mass flow rate through a fluid element

Conservation of Momentum

The equation for the conservation of momentum, Newton's second law, states that the rate of increase of momentum of a particle equals the sum of forces acting on that particle. This law relates equally to fluid particles as it does solids.

For the purposes of demonstration the x component of the momentum equation is given (equation 5-3). Similar equations can be derived for the y and z direction. Equation 5-3 is derived from Newton's second law. The left hand side of the equation expresses the increase in momentum on the fluid particle; the rate of change of velocity u, with time t multiplied by the density ρ of the fluid.

On the right hand side of the equation the forces that act on the fluid particle are summed up. These forces are split into surface and body forces. Gravity is treated as a body force, included as a source term S_{My} in the y momentum equation. The surface forces comprise of pressure forces p acting normal to surface, and viscous stress components that are split into the normal stresses τ_{xx} and the shear stresses τ_{yx} and τ_{zx}

that act across the surface. These are illustrated in Figure 5-2. The subscripts refer, in order, to the direction normal to the surface affected *(x,y,z)* and the direction in which the force acts, *x*.

$$\rho\frac{Du}{Dt}=\frac{\partial(-p+\tau_{xx})}{\partial x}+\frac{\partial\tau_{yx}}{\partial y}+\frac{\partial\tau_{zx}}{\partial z}+S_{Mx} \qquad 5\text{-}3$$

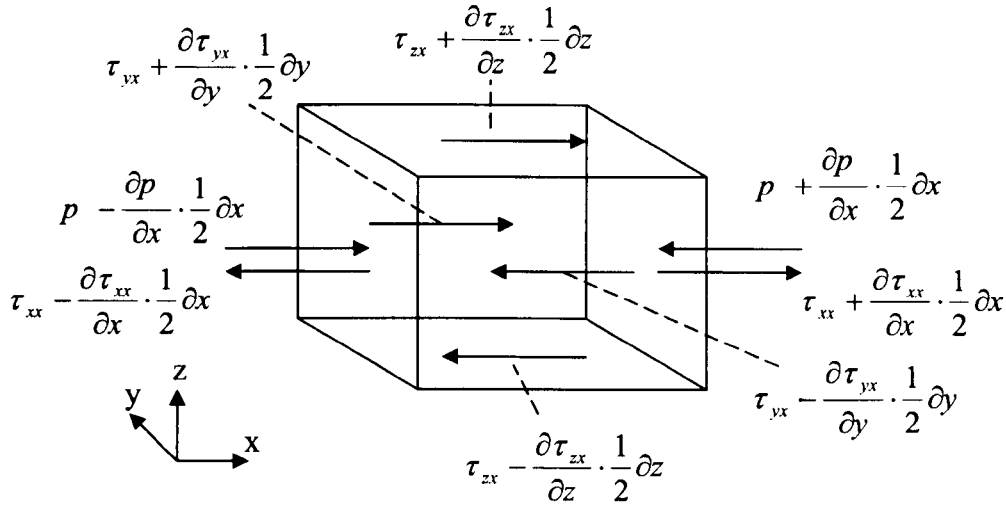

Figure 5-2: Forces acting on a fluid particle in the x-direction.

In order to use equation 5-3 a suitable model needs to be applied for the viscous stress components. Applying Newton's Law of viscosity, that viscous stresses are proportional to the rate of deformation and equation 5-3 can be re-written:

$$\rho\frac{Du}{Dt}=-\frac{\partial p}{\partial x}+div(\mu\quad grad\quad u)+S_{Mx} \qquad 5\text{-}4$$

Where μ is the dynamic viscosity. This is known as the Navier-Stokes equation, and similar equations can be derived for the y and z direction.

Conservation of Energy

The energy equation is derived from the first law of thermodynamics. This states that the rate of increase of energy on a fluid particle is equal to the net rate of heat added and

the net rate of work done on that particle. Replacing the viscous stresses using Newton's law of viscosity, as was carried out for momentum in equation 5-4, the energy equation becomes:

$$\rho \frac{Di}{Dt} = -p \quad div \quad \mathbf{u} + div(k \quad grad \quad T) + \Phi + S_E \qquad 5\text{-}5$$

Where i is the internal energy, p pressure and **u** the velocity vector. The heat flux into the fluid particle is expressed with $div(k \quad grad \quad T)$. Where T is the temperature and k is the thermal conductivity. The term Φ is the dissipation function which includes the effects of viscous stresses changing mechanical work into internal energy. Finally S_E is a source term.

5.1.1 Finite Volume method

The Finite Volume Method is the basis of most commercial CFD packages, including Fluent used in this study. Originally designed as a special finite difference formulation, the method discretises the integral equations of the conservation laws (equations 5-2, 5-4, and 5-5) directly in physical space. The calculation domain is divided into a grid, or mesh, with each point on this grid surrounded by a control volume, Figure 5-3. The differential equations for fluid flow are then integrated over each control volume (Versteeg and Malalasekera, 1995). Using this method the discretised equations adhere to the conservation principles for each control volume, and therefore the entire domain. These principles will be satisfied with any size of mesh (Patanker, 1980), although it is still necessary to use a mesh fine enough to capture all the physics of the flow. This use of cell volume rather than grid intersections to numerically discretise the equations enables unstructured grids to be easily used and therefore allows greater flexibility with complex and varying geometry (Fluent Inc, 2005, Versteeg and Malalasekera, 1995).

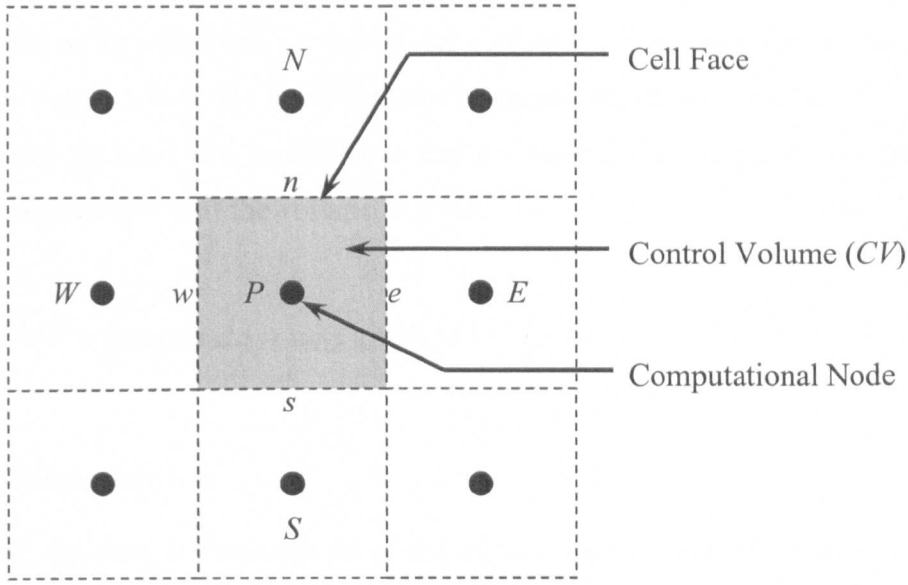

Figure 5-3: Computational mesh for a two dimensional structured grid. Showing the computational node and the control volume that would surround it. The cell face, or boundary of the volume is required to consider the transport of properties into and out of the cell.

In the finite volume method the equations of flow are integrated over the control volume surrounding the computational node. Using Gauss' divergence theorem the integration of the convective flux and the diffusive flux are rewritten as integrals over the bounding surface. This is demonstrated using the general transport equation, equation 5-6. This states that the increase of the value of the transported property ϕ over time plus the decrease due to convective transport of ϕ out of the space is equal to the increase of ϕ due to diffusion, where Γ is the diffusivity and any sources S_ϕ.

$$\frac{\partial \rho\phi}{\partial t} + div(\rho\phi\mathbf{u}) = div(\Gamma grad\phi) + S_\phi \qquad 5\text{-}6$$

Integrating this over the control volume (CV) shown in Figure 5-3 gives equation 5-7

$$\int_{CV} \frac{\partial(\rho\phi)}{\partial t} dV + \int_{CV} div(\rho\phi\mathbf{u}) dV = \int_{CV} div(grad\phi) dV + \int_{CV} S_\phi dV \qquad 5\text{-}7$$

The convective term, $div(\rho\phi\mathbf{u})$, and the diffusive term, $div(\Gamma grad\phi)$, need to be considered as they pass into, or out of, the control volume across the cell face shown in Figure 5-3 with area A. By applying the divergence theorem to equation 5-7 the rate of increase or decrease due to diffusive and convective flux along the normal vector **n** across the boundaries of the volume is given:

$$\int_{CV}\frac{\partial(\rho\phi)}{\partial t}dV+\int_{A}\mathbf{n}.(\rho\phi\mathbf{u})dA=\int_{A}\mathbf{n}.(\Gamma grad\phi)dA+\int_{CV}S_{\phi}dV \qquad 5\text{-}8$$

5.1.2 Discretisation

Since all the flow information is stored at the central node of the cell, a method is needed to find the values of the flow variables at the cell face. Diffusive transport alone results in the movement of properties in all directions and so it is reasonable to assume the value at each face of the cell will be equivalent to the difference between the nodes to each side. For diffusion a central differencing method may be applied; this finds the value at the interface between two cells by using the weighted average of the values at the adjacent nodes, in Figure 5-3 for face e the nodes P and E would be averaged. However, for convection the direction of flow is important, and needs to be taken into account when approximating the cell face values. The simplest scheme, upwind differencing, uses the value from the upstream cell to approximate the value at the cell face. For instance in Figure 5-3 if the flow was travelling from west to east then the value at the west cell face of the control volume w would be taken as the value at the node W, and at the face e, the value from P would be taken.

Since only the node upstream is used this scheme is only of first order accuracy. It assumes that the entire cell volume is well mixed with the same value of the transported property and is therefore prone to false numerical diffusion. This occurs when the convective flow moves diagonally with respect to the grid lines. In a situation with no diffusion there should be no movement of the transported scalars normal to the flow. However with a coarse grid and a first order upwinding differencing scheme diffusion will occur due to the gradient of that property in the direction of the gridlines, even though the gradient is zero in the direction of the convection. As the value at the cell face will be taken as that at the upstream node, which is half the cell length away, with a

coarse mesh this can cause significant false diffusion. Using a finer mesh reduces this error, however it is also necessary to use higher order discretisation methods, usually second order upwinding. The more accurate second order scheme used in this study evaluates the value of the transported property at the face using not only the value at the upstream node but also using more neighbouring points, by incorporating the gradient through the upstream cell. Discussion of the mesh used in this study, and the explanation of the choice, are given in section 5.2.7 after a description of the general model geometry and boundary conditions.

5.2 Test Chamber Air Flow Model

This section describes the CFD model developed to simulate the airflow in a ventilated test chamber. The airflow solutions from this model are then used in the experimental validation of the CFD method, and the numerical validation of the zonal source method in the following chapter.

5.2.1 CFD Process

The commercial CFD package Fluent 6.2 (Ansys Inc.) is used to carry out the modelling in this study. This is a robust code that has been used widely in industry and academia for a diverse range of fluid flow problems. This includes research into contaminant transport within indoor air flows by several authors (e.g. Beggs *et al.*, 2007, Chau *et al.*, 2006, Khan *et al.*, 2006, Lee *et al.*, 2002, Noakes *et al*,. 2006b , Richmond-Bryant *et al.*, 2006). The software incorporates a method of enabling user defined functions (UDFs) where external subroutines can be used to define model specific physics or control the solution process and outputs. This feature was essential to this study and has been used widely in order to specify inlet boundary condition profiles, sources over spatial zones, transient sources and particle injection positions as well as to output data in the required form.

To carry out the simulation of airflow using CFD incorporates three stages: pre-processing, numerical solution and post-processing of the results. Pre-processing involves defining the geometry of the flow domain and the mesh that specifies node points for the fluid, the physical and chemical properties of the fluid and the boundary conditions. The solver performs the numerical solution, in the case of Fluent using a

finite volume method. In the post-processor, visualisation software is available which includes the ability to create vector and contour plots of variables, trace particle paths through the flow, as well as extracting values at any point within the flow domain.

5.2.2 Model Overview

The geometry of the chamber was defined as shown in Figure 5-4. Two different ventilation regimes were simulated, indicated by Inlet/Outlet A and Inlet/Outlet B in the figure. There are no heat sources in the actual room and the simulated flow is therefore treated as isothermal. In all cases the airflow in the chamber was assumed to be steady-state at a constant air change rate with boundary conditions as described in section 5.2.3.

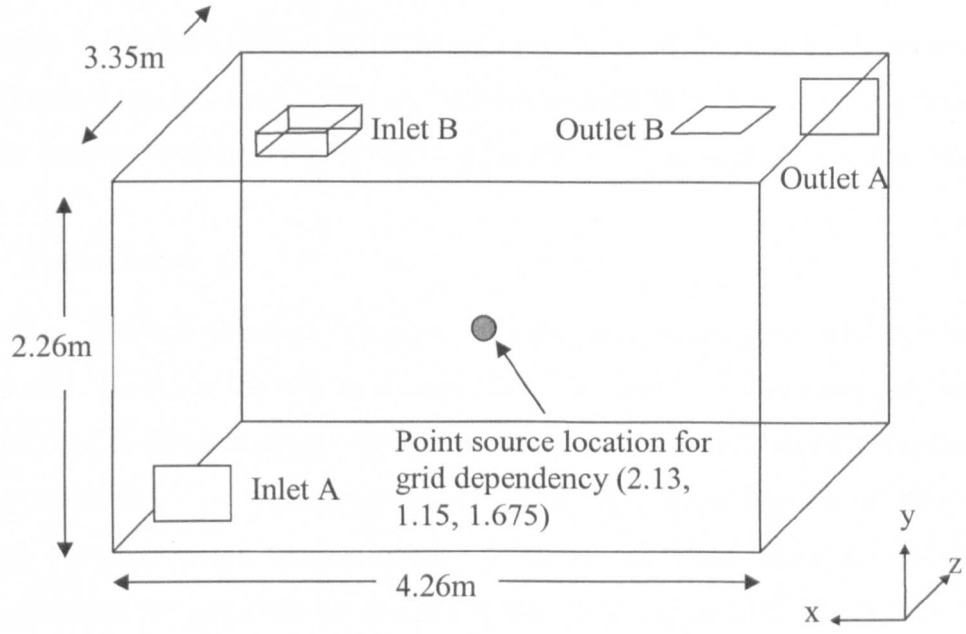

Figure 5-4: Geometry of the chamber created in the CFD model and equivalent to the bioaerosol test chamber used for the validation experiments.

5.2.3 Boundary Conditions

For both ventilation regimes there was a single supply air inlet and extract as shown in Figure 5-4. Ventilation regime A has a low level wall mounted air supply inlet with an identical high level wall mounted extract on the opposite wall of the chamber. This is the same ventilation regime used in the experiments described in section 5-4. In order to

describe the air entering the space through the louvered diffuser in the real room a series of parabolic velocity profiles were defined across the inlet boundary (Noakes *et al.*, 2006c). This provides a more realistic inlet velocity boundary than defining only a single value (Lee *et al.*, 2002). To represent the actual diffuser the velocity profile was angled downwards at 45° and injected along 13 lines evenly-spaced vertically across the inlet area. This was implemented using a UDF within Fluent.

For ventilation regime B a four-way ceiling supply diffuser was simulated by defining the velocity around the sides of a shallow box that projects into the room. Air was injected into the space at a constant velocity of $0.45 m.s^{-1}$ at 15° to the horizontal from all 4 sides of the box. This is a simpler method than defining the exact velocity information at the grille and has been shown to give similar results in the occupied zone (Srebic and Chen, 2002).

The supply velocities in both ventilation regimes were calculated to be representative of an air change rate of $6 ac.h^{-1}$. The extract boundaries in both cases were defined as constant pressure extracts with a value of 0 Pa. The walls were set to a no slip condition.

5.2.4 Turbulence

Most room airflow is turbulent in nature, and this needed to be accounted for within the CFD model. However the effects of turbulence in modelling the flow can be highly complex. The smallest turbulent eddies may be as small as $10\mu m$, and a suitable grid for solving these would be unfeasibly small due to the large amount of computation required. For engineering applications the detail of individual eddies are not required, and considering the assumptions that are made about the general situation, modelling this detail would be unnecessary. Therefore instead of exactly simulating these effects, engineering approximations may be used and the affect of these turbulent fluctuations on the mean flow calculated. The velocity at any point in space and time u is made up of the mean $\overline{u}$ and the unsteady fluctuations u'; $u = \overline{u} + u'$. Applying this averaging to the Navier-Stokes equations gives the Reynolds-averaged Navier-Stokes equations (RANS) (Ferziger and Peric, 2002).

The most popular turbulence model for room air flow is the RANS k-ϵ model (Sorensen and Nielsen, 2003). This is a two equation model in which the diffusion coefficient due

to turbulence is calculated independently for each cell using the values for turbulent kinetic energy, k and its dissipation rate, ϵ. It is simple to use requiring only inputs for k and ϵ at the inlets which can be found from the turbulence intensity and the characteristic length of the inlet.

Although the k-ϵ model is valid for the bulk flow in the room, near the wall the model needs to take into account both the viscous sub-layer and the transition layer where the flow progresses towards fully turbulent. Standard wall functions provide a method of bridging the gap between the wall and the fully turbulent region. However this requires that the first node near the boundary is placed within the fully developed turbulent region. This was not achievable with the mesh required with this model and so enhanced wall treatment was applied instead. With this method the domain is split into a turbulent region and viscosity affected near wall region, a blending function is then used to merge the regions across the transition zone.

Turbulence is of interest in a vast number of fluid dynamics applications, not only room air flow, and there has been a great deal of research on improving these turbulent models. For room air flow the Renormalised Group (RNG) k-ϵ model is growing in popularity as it has been shown in certain situations to provide better accuracy than the standard k-ϵ model (Chen, 1995) however the increase in accuracy is not great and the standard model has been shown to be robust over many different room air applications by several authors (Versteeg and Malalasekera, 1995, Awbi, 1989).

There is also growing interest in the use of Large Eddy Simulation (LES) within indoor air simulations, as this enables the effect of large turbulent eddies to be directly modelled in space. These models provide much greater detail of the turbulence, as they do not average all the turbulent effects but use filters to separate out the large and small eddies. The large eddies are then solved directly, and a sub-grid scale model is used only for the smaller turbulent eddies. Although this is much more feasible to carry out than a direct numerical simulation of the turbulence it still requires a fine enough grid to be used to capture the large eddies, and is computationally much more expensive than using a RANS model. For the calculation of the bulk air flow it is not recommended (Sorensen and Nielsen, 2003) but interest is growing in its use when particle tracking is to be carried out (Bouilly *et al.*, 2005, Chang *et al.*, 2006, Tian *et al.*, 2006). This

interest is due to the effect turbulent diffusion has on the transport of small particles, which is discussed further in section 5.3.2.

Although the use of LES and RNG models show promising results, both are still relatively new and have not been validated over a large number of different ventilation regimes. As the standard RANS k- ϵ model has been shown to be robust over many different room air applications it is chosen for this study (Versteeg and Malalasekera, 1995). Also since the aim of this model is to produce a simple method of representing dispersal of activity it is more appropriate to use the traditional simple turbulence model than an LES model, that would result in the need for a finer grid and more computation time.

5.2.5 Solution Controls

The second order upwind discretisation scheme was used for the momentum, turbulence, and scalar transport equations and pressure velocity coupling was carried out using the SIMPLE (Semi-implicit Method for Pressure-Linked Equations) method. In this algorithm an initial guess of the pressure field is used to find a solution to the momentum equations. Continuity will not be satisfied as values at this stage have just been guessed. By substituting for the correction of velocity and pressure into the continuity equation a *pressure correction* equation is derived. This equation is used to find the corrected pressure field and hence the velocity fields. An iterative process, as shown in Figure 5-5 is then followed until the value of pressure correction is sufficiently small.

5.2.6 Convergence criteria

In this study the iterative solution process was carried out using a segregated solver that treats the equations sequentially. Global residuals were monitored at each iteration in order to monitor the convergence of the solution. In all cases the solution was taken to be converged when the residuals showed no visible decrease for between 200-300 iterations and the residuals of all equations were less than 10^{-3}. The solution convergence was then checked by monitoring the mass flux within the space and ensuring a difference of less than 0.01% across the whole domain.

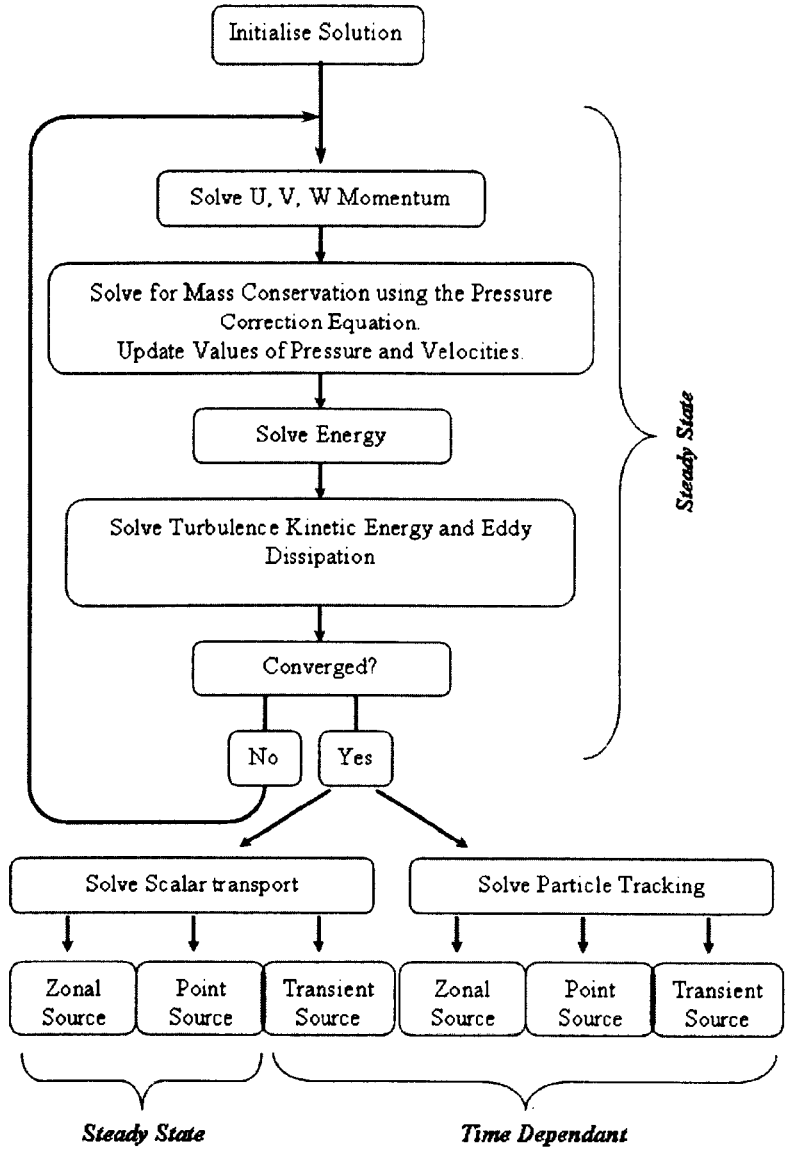

Figure 5-5: Solution Process using SIMPLE algorithm and Segregated Solver, including the solution of bioaerosol transport as carried out in this study. Adapted from Fluent Inc (2005).

5.2.7 Computational Mesh

In order to define a suitable mesh for the model a grid dependency study was carried out to ensure the solution will not significantly change by further refinement of the grid. Three grids were considered as given in Table 5-1. These grids were created in the Gambit automatic meshing tool using a "tet/hybrid" scheme. This generates a mesh composed mainly of tetrahedral elements, but with other shapes used when required. This method was chosen due to the asymmetrical location of inlet and outlet A that would have made the use of a hexahedral mesh prohibitively fine.

Table 5-1: Grid dependency for test chamber model using ventilation regime A. Table shows the 3 mesh sizes and results for the average scalar concentration and iteration time.

Parameter	Mesh a	Mesh b	Mesh c
Number of Cells	**313,892**	**648,857**	**1,436,352**
Volume Average Scalar Concentration. (quantity.m^{-3})	6.72	6.86	6.83
Average Iteration Time (Seconds)	06	10	23

To enable a comparison between grids that was relevant to the zonal source model developed in chapter 6, a point source scalar was defined positioned as shown in Figure 5-4. This released a passive scalar contaminant into the space at a concentration of 500 per m^{-3} using the methodology described in section 5.3.1.

The computational time per iteration approximately doubled with a doubling of cell numbers within the space. Since an average of 4000 iterations were required to achieve a converged airflow for each model the difference in time between grids for the whole model to run is significant. As shown in Table 5-1, the variation in average scalar concentration in the space is very small between all three meshes. Figure 5-6 shows plumes of equivalent scalar concentration for each grid size. With further refinement of the grid the scalar concentration remains higher over a greater distance from the source, seen by the lengthening plume. However the overall behaviour is very similar, particularly for meshes b, and c. Considering all these factors, a global grid size between 300,000 and 600,000 cells was chosen with additional cell refinement at the

boundaries where there are high gradients in the properties of the flow. This boundary layer was four cells deep, with the first cell centroid being 5mm from the boundary wall and a ratio between cells of 1.2. Large changes in cell size will result in larger truncation errors when obtaining the discrete approximations to the equations of flow and a ratio of 1.2 is the recommended limit between adjacent cells (Fluent Inc, 2005). This boundary layer also enables a hexahedral grid to be used close to the boundary where there are high gradients.

The quality of the grid was checked using the skewness and the aspect ratio of the cells. The skewness of the cells is found using equiangle skew (Q_{EAS}), that relates the internal angles of the element (Minimum angle θ_{min}: Maximum angle θ_{max}) to that of an equilateral cell (60° for tetrahedral cells) using equation 5-9 below.

$$Q_{EAS} = \max\left\{\frac{\theta_{\max} - 60}{120}, \frac{60 - \theta_{\min}}{60}\right\} \qquad 5\text{-}9$$

This value is between 0 and 1, where 0 is a equilateral cell, and 1 is a very thin sliver of a cell. In practical terms some cells in the mesh will be highly skewed, therefore some judgement is needed to chose an adequate mesh. The mesh may be assumed adequate if the majority of the cells have low values of equi-angle skew, and the maximum value is less than 0.9. For this model the highest value of equi-angle skew was 0.83, and 99% of the cells have a value less than 0.68, which is considered reasonable (Fluent Inc, 2001).

The second quality check, the aspect ratio, is a measure of the stretching of the cell. This is found by using a ratio of the circumferences of spheres that would enclose (R) or fit into (r) the cell with equation 5.10 for tetrahedral elements.

$$Q_{AR} = \frac{1}{3}\left(\frac{R}{r}\right) \qquad 5\text{-}10$$

The aspect ratio should be no greater than 5:1 for most of the domain but, again, it is important to have the majority of cells with a good aspect ratio. In this model the worst cell has a ratio of 4.3:1 but 99% of cells have ratios below 2.4.

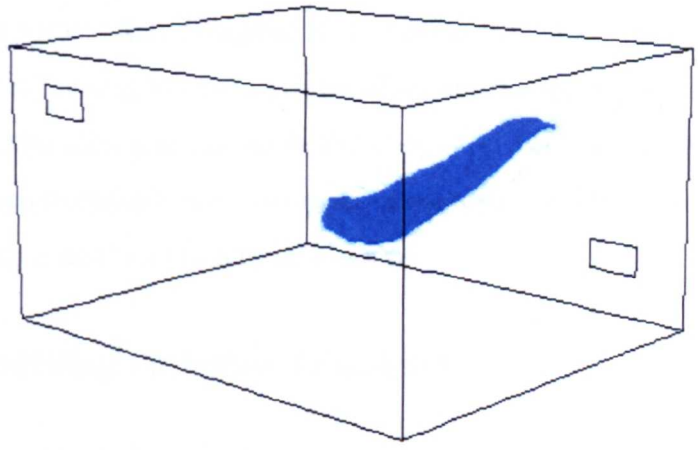

a) ~ 300 000 cells

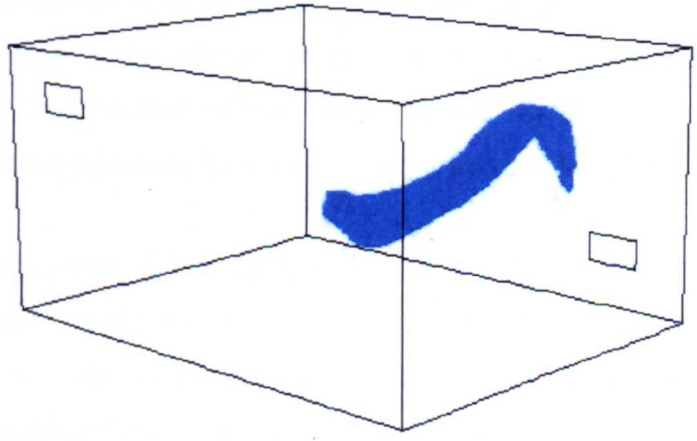

b) ~ 600 000 cells

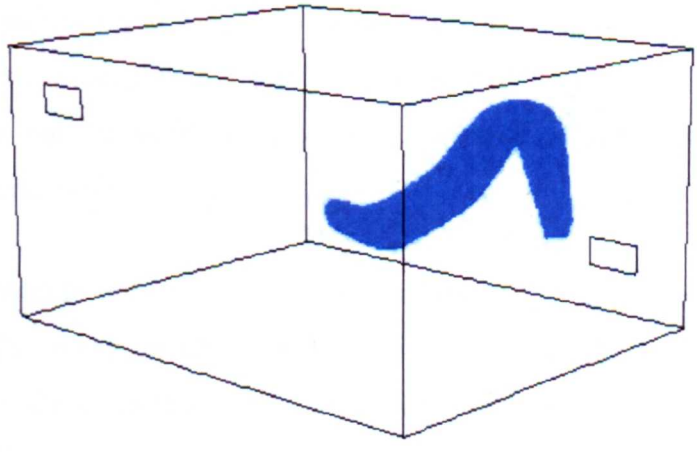

c) ~1400 000 cells

Figure 5-6: Plumes of scalar concentration >35(volume.m^{-3}) for the 3 mesh sizes used to assess grid dependency. Using ventilation regime A

The final meshes have approximately 850,000 cells for ventilation regime A and 450,000 cells for ventilation regime B. The difference in the mesh sizes was largely due to the ability of Gambit to create a mesh of acceptable quality with the desired boundary layer near to the inlet and extract in the corners in ventilation regime A. This led to a finer mesh than necessary across most of the domain for ventilation regime A, however a coarser mesh was of an unacceptable quality.

5.3 Modelling Pathogen Transport

Two methods of modelling the airborne transport of bioaerosols were used in this thesis; the Euler-Euler approach of injecting a passive scalar into the domain that follows the bulk air movement, and an Euler-Lagrangian method that solves the transport of a particle through the domain by considering momentum, drag and gravity forces. Both methods are used in this and the following two chapters to simulate steady-state and transient release of bioaerosols from a range of source locations.

In both cases a steady-state airflow solution was found separately prior to solving for the bioaerosol transport (Figure 5-5). This method was adopted for practical considerations. The airflow simulation took significantly longer to solve than the bioaerosol transport as six equations were solved at each iteration (three momentum equations, continuity, turbulence kinetic energy and dissipation rate) instead of a single transport equation or set of particle tracks. Since the same airflow was used for the point, zonal and transient source in two orientations within the room, this reduced the number of airflow runs from six to one. As each solution of airflow took between 12 and 24 hours and the steady-state scalar a matter of minutes, this saved a significant amount of computational time.

Lagrangian particle tracking was also carried out using the previously solved bulk air movement. This was possible as the transport of the particles was modelled using one–way coupling; the air flow impacts the particle transport, but the particles do not affect the air flow. This is a reasonable assumption at the low particle volume fractions used in this study and for room air in general. For all the models in this thesis the particle volume fraction is $<10^{-8}$, much less than would be considered to affect turbulence production in the air (Elghobashi, 1994) , as shown in Figure 5-7.

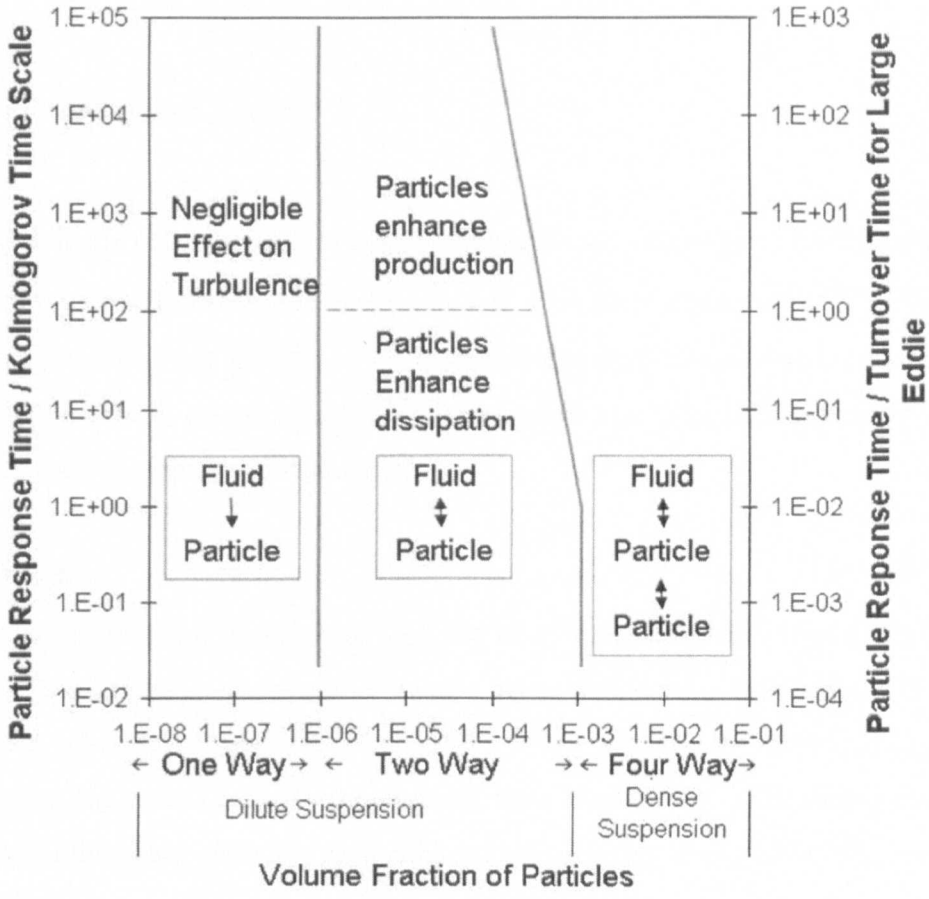

Figure 5-7: Effect of particle volume fraction on the production of turbulence as presented by Elghobashi, 1994.

5.3.1 Passive Scalar transport

Theory

Passive scalar transport may be used to simulate the distribution of airborne contaminants when it can be assumed that the particles are small enough to remain airborne for long periods of time and the influence of the particle mass is minimal. This is a valid assumption for many bioaerosol particles, particularly respiratory particles which are expelled through coughing and rapidly evaporate to droplet nuclei with a diameter of 1-2μm (Wells, 1955). Skin particles have a larger range in size, with a typical average diameter of 14μm (Noble *et al.*, 1963). Although this is larger than would be usually acceptable for treatment as a passive scalar as an initial case it was assumed the all the particles moved with the air flow to enable development and validation of the zonal source methodology

The transport of a scalar is solved using equation 5-11:

$$\frac{\partial \phi}{\partial t} + div(\phi \mathbf{u}) - div(\Gamma grad\phi) = 0 \qquad 5\text{-}11$$

Here ϕ is the concentration of micro-organisms per unit volume (quantity.m^{-3}); **u** is the velocity vector (u,v,w) of the air (m.s^{-1}); and Γ is the diffusivity (m^2.s^{-1}). The diffusivity in this case was set to 10^{-7} m^{2}s^{-1}, a sensitivity study showed that reducing this had negligible effects on the results. A second order upwinding discretisation scheme was used for solving the scalar transport.

Validation

The use of the passive scalar method has been validated with experiments using tracer gases. Scalars have shown good results when comparing ventilation efficiencies for various schemes (Chung and Hsu, 2001). More importantly measurements at several points within rooms have been compared with simulations, with readings taken at 6-30 points in the space showing reasonable results (Huang *et al.*, 2004, Khan *et al.*, 2006). Simulations have been shown to over estimate the values very close to the source, where there are high gradients in concentration, however, despite the errors in the values, the location of these points correspond well, and further from the source the results show good correlation (Zhang *et al.*, 2007). Validation against a controlled bioaerosol source has not, to the authors knowledge, been carried out prior to the work presented in this thesis.

5.3.2 Lagrangian Particle Tracking

Theory

Lagrangian particle tracking is carried out using the Discrete Phase Model (DPM) available in Fluent. This method is suitable for modelling the behaviour of larger particles, and in this study is used to model the distribution of pathogens carried on skin squame or dust particles. The DPM uses a Lagrangian approach to the track the path of a number of individually defined particles through the continuous phase. The particle trajectory is computed and hence path lines can be visualised, and importantly for this study, the end point of the trajectory determined. This will indicate whether a particle is

extracted from the space by the airflow or deposited on a surface. This type of model is suitable only for cases where there is a definite start and end point, and the particles are heavily diluted in the air with a volume fraction less than 12% (Fluent Inc, 2005). The boundaries in the space are labelled as either *trap*, *reflect*, or *escape*. When the particle reaches the boundary then the state of the particle is changed depending on this specification.

The trajectory of a particle is found considering the change in particle velocity due to the particles inertia, gravity, and drag forces (equation 5-12).

$$\frac{\partial u_p}{\partial t} = F_D(u - u_p) + \frac{g_x(\rho_p - \rho)}{\rho_p} + F_x \qquad 5\text{-}12$$

The first term on the right hand side $F_D(u-u_p)$ is the drag force per unit of particle mass where u is velocity, the subscript p refers the particles; non-subscripted terms refer to the air. The second term represents the gravitational force where ρ is the density and g the gravitational acceleration. F_x is used to incorporate any additional forces and is not used for those forces considered in this study.

F_D may vary depending on the drag law that is most appropriate. This study uses the spherical drag law in which F_D is defined as:

$$F_D = \frac{18\mu}{\rho_p d_p^2} \frac{C_D \mathrm{Re}}{24} \qquad 5\text{-}13$$

Where μ is the molecular viscosity of the fluid, ρ_p is the density of the particle, and d_p the diameter of the particle. Re is the Reynolds number and C_D is the drag co-efficient. For spherical particles, as assumed in this study, C_D *is*

$$C_D = a + \frac{a_2}{\mathrm{Re}} + \frac{a_3}{\mathrm{Re}^2} \qquad 5\text{-}14$$

The values of a, a_2 and a_3 vary with the Reynolds number and are given in Morsi and Alexander (1972).

The Lagrangian approach is by its nature time dependant. The particles are tracked as they move through the domain and hence a specific number of time steps need to be applied to ensure the entire required trajectory is simulated. The solved trajectory of the particle is sensitive to the chosen time step as this will affect the distance the particle will travel before a new solution is found for the velocity. The time step for the Lagrangian particle tracking is defined with a step length factor λ using:

$$\Delta t = \frac{\Delta t^*}{\lambda} \qquad 5\text{-}15$$

Where Δt is the time step and Δt^* is the estimated time it will take for the particle to traverse the current cell. The step length factor is set to 5 in order to ensure that the particle motion is solved at least three times in one cell as recommended (Fluent Inc, 2005).

Validation

The use of this Lagrangian method to simulate particle transport has been shown to adequately represent particle mass concentrations within room air, provided a large enough number of particles are injected (Chang *et al.*, 2007, Lu and Howarth, 1996, Zhao *et al.*, 2004b). Zhang and Chen (2006) compared particle concentrations at several positions within a room with a simulation and found generally good correlations for particles sized 0.3, 0.7 and 4.5μm. Similar to the passive scalar studies the discrepancies occurred near to the source positions. In this case there were fluctuations in the experimental methods due to the particle generator so this may be due to errors in the experimental work. The validation of Lagrangian methods for deposition within indoor spaces is not well documented despite the method being used to quantify this effect in many publications (Wan *et al.*, 2007, Lu and Howarth, 1996). The reason for this may be due to the difficulties in carrying out experimental studies. Studies on particle deposition are either conducted over long periods of time, in order to sample sufficiently to be able to reliably detect and count them, or determined using an indirect method. The latter calculates deposition from the reduction in airborne counts corrected for a known extraction (Thatcher and Layton, 1994). Leduc and Fredriksson (2006) attempted to validate the Lagrangian particle tracking method by simulating a particle sampler that differentiates between sizes (similar in design to the Anderson Sampler

section 4.2.1) The two dimensional simulation of deposition on each level was compared to experimentally collected particles onto each impaction stage. The results showed that for 3μm particles and above the standard k-ϵ turbulence model gives acceptable results with an error of around 10%. However for experimental sized particles of 2.4μm the error was 15%, and for 1μm particles the error was 80%. Below 1μm particles the deposition error was greater than 100%. A second simulation with the RNG turbulence model did show better results with a 22% error for 1μm particles and similar results to the k-ε model for particles 3μm diameter and greater. A similar comparison between the k-ε and RNG turbulence models was carried out in this study for the test chamber model described in section 5.2.2. An airflow solution was calculated for both the standard k-ϵ and RNG model and six thousand particles were injected from a point in the centre of the chamber as described in section 5.3.4. The fraction either deposited on horizontal and vertical surfaces, or extracted, was then found. This showed only very small differences between the two turbulence models, even for 1μm particles, as shown in Figure 5-8. Since the equivalent aerodynamic diameters found for skin squame in section 2.3.2 ranged between 4 and 22 μm (section 2.3.2) the turbulence model is unlikely to have any significant impact on simulated deposition patterns. However it should be noted that once the particles considered are 1μm or less then severe errors in the deposition may be incurred. This error is likely to be due to the turbulent dispersion of the particles which will now be discussed in more detail.

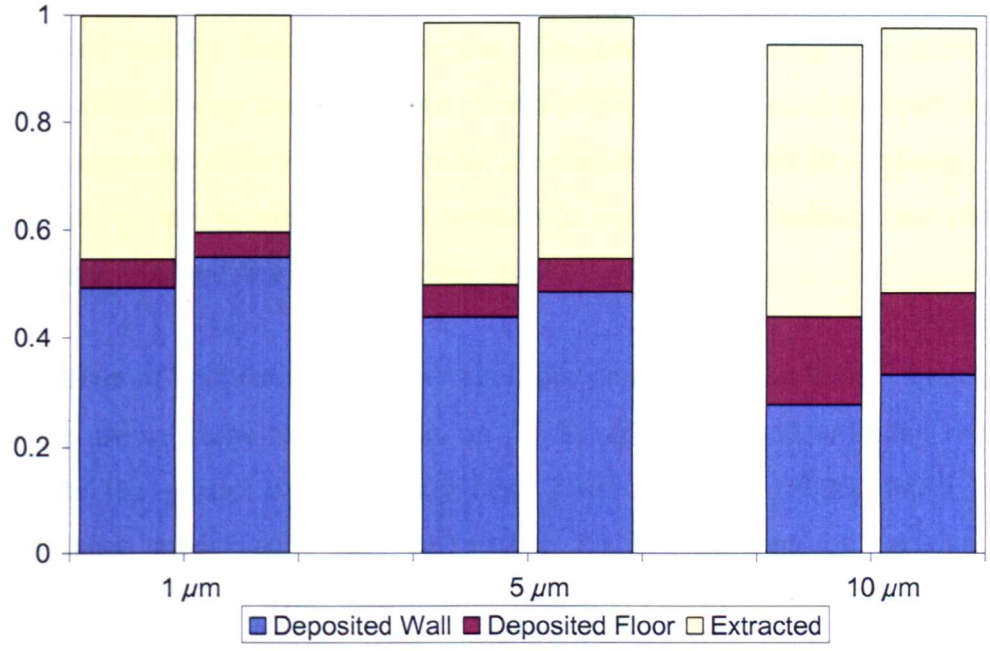

Figure 5-8: Comparison of deposited and extracted fractions using the standard (left) and RNG (right) k-ϵ turbulence model.

Turbulent Dispersion

It is necessary to include the effects of turbulent dispersion when tracking particles through the domain as this can have a significant influence on the transport (Richmond-Bryant *et al.*, 2006). The use of the k-ϵ turbulence model means these randomly fluctuating turbulent eddies within a room are not simulated. It is therefore necessary to model the effects of turbulent dispersion separately. In order to include this, a discrete random walk model (DRW) is used. This specifies that the instantaneous fluid velocity, u in equation 5-12, is expressed as:

$$u = u + u' \qquad 5\text{-}16$$

where u' is the fluctuating component due to turbulence. This is assumed to follow a Gaussian distribution and can therefore be expressed using the kinetic energy of turbulence k and a randomly generated number ζ as:

$$u' = \zeta\sqrt{\overline{u'^2}} = \zeta\sqrt{\overline{v'^2}} = \zeta\sqrt{\overline{w'^2}} = \zeta\sqrt{2k/3} \qquad 5\text{-}17$$

The velocity fluctuation is assumed to be isotropic in this instance. In the region near the wall this can result in a much higher velocity normal to the wall. Due to the higher

velocities acting on the particle this can over predict the particle deposition for small particles, usually around 1μm or less (Lai and Chen, 2006). The problem of over deposition is being improved with research being carried out into functions to reduce the magnitude of the normal velocity fluctuation to the wall. By reducing the normal velocity to the boundary the deposition is significantly reduced for particles with diameter 1μm and less (Lai and Chen, 2007).

The effect of turbulence on the particle diffusion is one reason there is increased interest in the use of Large Eddy Simulation (LES) turbulence models within room air flow despite the greater computational cost. Tian, Tu *et* al (2006) found that a LES turbulence model gave different results for the numbers of particles remaining suspended in the air over time when compared to RANS models. The difference though was very small compared to the total number of particles injected. No details were given for the total deposition.

Lai and Chen (2006) have shown that the solution for particle tracking is much more mesh dependant than the airflow when solving the transport of particles with diameter 1μm or less. Decreasing the nearest centroid distance to the wall from 5mm to 1mm changes the deposition of 1μm particles from 48% to 11% of the total injected, despite the air flow solution being independent of mesh size. However, as the inertial forces become more dominant than the turbulent diffusion this is not so important. For 7μm particles and the same grid the difference is only 3%, which would be an acceptable error (Lai and Chen, 2006). Even for particles as small as 1.5μm Wan and Chao (2007) showed that the DRW model gives good representation of the vertical and horizontal distribution of particles in the air. It seems reasonable then to use this model as although deposition may be increased the model should provide a reasonable representation of the spatial positions. Due to the size range considered when modelling the dispersion of skin squame using Lagrangian particle tracking with DRW for turbulent dispersion should give reasonable results, however the problems with over deposition should be considered, particularly if the model is extended to cover smaller particle sizes.

There is very little work attempting to validate numerical studies to bioaerosol deposition available in the open literature. Rui *et al* (2008) simulated an operating room, modelling the particle dispersion with the DRW model, they attempted to validate the

particle transport with results from bacteria deposition. The simulation corresponded very poorly to the results, however the bacteria deposition was found from measurements during a knee replacement surgery, and not from a controlled experiment, as such there was a large amount of movement within the field study that was not represented in the simulation. It was therefore necessary to test the reasonableness of the Lagrangian particle tracking in simulating bioaerosol transport through controlled experiments, in order to compare equivalent situations. This is presented in section 5.5.

5.3.3 Transient simulation of Moving Bioaerosol sources.

To carry out the validation of the bioaerosol zonal source method (Chapter 6) it was necessary to consider bioaerosol sources that move spatially over a period of time. As illustrated in Figure 5-5 both scalar transport or discrete phase models can be carried out with a transient source. For both steady state and transient simulations the discretisation through space is carried out in the same way. The only difference between the two states is the addition, or removal, of the term for discretisation over time.

Scalar Source Time Stepping

The time integration for the transient bioaerosol source was carried out using the first order implicit method. This method requires that a set of simultaneous equations for the whole domain is solved at each time step, since for the calculation at a single node the values at the surrounding nodes at that time are used. In order to ensure that the time step was sufficiently small to avoid false approximations, a series of simulations using progressively smaller time steps were carried out. The scalar source was injected into the test chamber airflow model. The source was defined to move across the chamber along the line x=2.13, y=1.15 for the entire width of the room in the z direction (Figure 5-4) at a speed of $1.2x10^{-3}m.s^{-1}$. The simulation was carried out for 2800 seconds, enough time for the source to traverse the entire space. The results were used to determine the correlation coefficients (section 4.4.2) between scalar contours on a plane at y =1.15m using 1s time steps and either 10s or 100s time steps. These are shown in Table 5-2. It was decided to use a 10s time step for subsequent transient simulations as this provided a reasonable solution even in the first 100s.

Table 5-2 : Time step dependency for the test chamber model. Spearman's Rho correlation coefficient to a 1s time step. All values significant to 0.05 level.

Time	10s	100s
100	0.646	0.498
200	0.919	0.835
300	0.973	0.909

Lagrangian Time Stepping

With Lagrangian particle tracking all solutions were carried out transiently in order to solve the entire trajectory of the individual particles through the space. This method is described in section 5.3.2. For the transient source a transient method for injecting the particle was also required. This was set to 1s, during the period the bioaerosols are released, increasing to 100s after. The use of two time steps meant a courser one could be used for the greater part of the solution process, but there was adequate refinement during the injection.

5.3.4 Source Definition for Experimental Validation

The bioaerosol sources were defined to represent the equivalent sources within the test chamber experiments which are described in the next section.

Passive Scalar definition for experimental validation

CFD simulations using a passive scalar to represent the distribution of bioaerosols were carried out with two different source volumes to compare with experimental results. Within a CFD model a scalar may be injected into a space using a UDF which defines the scalar source over a small volume. The definition is "small volume" rather than point as the source must be defined to cover a least one computational cell. In addition the bioaerosol injection in the experiments was from the surface of a pipe, and not an individual point. In order to emit the scalar into the air flow of the room a small momentum source of 0.1 $N.m^{-3}$ was added in the y and x direction, to represent how the bioaerosols are dispersed in the experiment (section 5.4). The location of the source in the CFD simulations was equivalent to that in the experiments. A 10cm cube with the

centre at coordinates (2.13, 1.15, 1.675) was defined to represent the small volume release at the centre of the room in the experiments. A linear source was defined with a dimension of 10 cm in the x and y direction with the centre at x=2.13 and y=1.1. In the z direction the source spans from 0.42 to 1.725m (co-ordinate system and dimensions of chamber shown in Figure 5-4) and represents experimental injection of bioaerosols from a series of holes located along the length of a pipe.

Lagrangian Particle Tracking definition for experimental validation

This part of the validation study is of particular importance as Lagrangian particle tracking, and the DRW model are not well validated in the literature (5.3.2). This is particularly the case when attempting to represent the transport of bioaerosols.

The CFD simulations involving particle tracking injected the particles from a single point. The validation of the Lagrangian particle tracking model was carried out assuming a central point source, and the particles were therefore injected at co-ordinates (2.13, 1.15, 1.675). The diameters of the particles used in the CFD model were taken from the manufacturers literature for the nebuliser (BGI Collison Nebuliser, 2007) (5.4.2), and converted to equivalent particle numbers which are shown in Table 5-3. A density of 1000 $kg.m^{-3}$ was assumed. The mass flow rate for each particle was set to $5x10^{-13}$ $kg.s^{-1}$, a sensitivity study showed that with mass flows below 10^{-9} $kg.s^{-1}$ there is a negligible effect with a change in the value, therefore it was deemed adequate to set each particle range to the same mass flow rate.

Table 5-3: Quantities of particles injected in each of the 7 size ranges for experimental validation of Lagrangian particle tracking model

Size Range (μm)	Number of Particles
0.78-1.4	1200
1-4-2	7000
2-3	1400
3-4	1000
4-4.5	300
4.5-9	200

Three CFD simulations were carried out. The first did not take into account the effects of turbulent dispersion and the second used the DRW model to simulate these effects (section 5.3.2), both using a steady state airflow simulation. The third simulation used the DRW model and a transient air flow simulation to see if this would affect the results. The transient model used a fairly coarse time step of 100s in order to simulate the whole experiment. The simulation started at the equivalent of 00:10 (hours:seconds) in the experiment, when the nebuliser was turned on, the injection was stopped at the equivalent of 01:30 and the simulation halted at 3:00. Details of the experiment are given in 5.4.

5.4 Experimental Methods

The following section describes the experimental methods carried out to in order to assess the reasonableness of the CFD model. The experiments were carried out in a test chamber with equivalent geometry to that described previously in section 5.2.2. using ventilation regime A. Bioaerosols were injected into the chamber and the concentrations in the air measured at 12 positions. Firstly the test chamber will be described in more detail along with the method for bioaerosol generation. The particular sampling methods used in this experiment are then presented before the general methodology is outlined. Two methods are presented, one to validate the passive scalar transport model, and a separate experiment used to validate the Lagrangian particle tracking.

5.4.1 Test Chamber

All the experiments were carried out in a climatically controlled aerobiological test chamber at The University of Leeds (see photographs in Figure 5-9 and a schematic Figure 5-4). This is a hermetically sealed 32.25m^3 (3.35 x 4.26 x 2.26m) room with a controlled, HEPA filtered mechanical ventilation system. The ventilation was controlled to keep a steady ventilation rate together with close control of both the temperature and relative humidity throughout the experiments. The only potential heat sources within the space were the lights which were maintained switched off during experimental procedures. The bioaerosols were created externally using a nebuliser, and injected into the chamber through a 34mm diameter pipe and released through 2mm diameter holes spaced equally around the circumference. Two different sized sources were used; a centrally located source consisting of 3 parallel sets of 4 holes at 90° to each other

spaced 1cm apart along the length of the pipe, and a linear source. The linear source was created by repeating the central source 6 times at a spacing of 20cm between centres. A separate anteroom provides controlled access to the chamber and houses sampling and monitoring equipment.

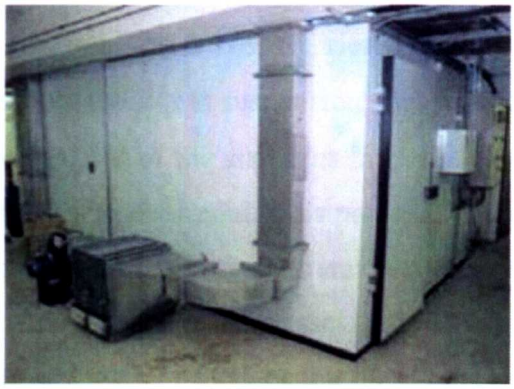

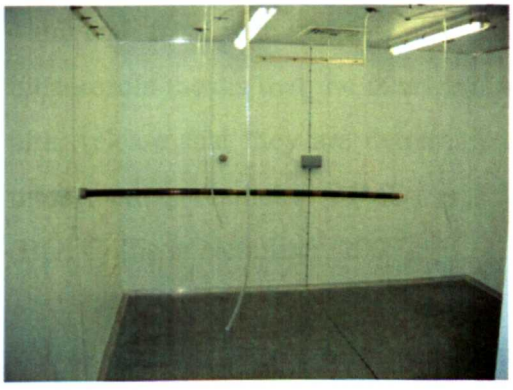

A

B

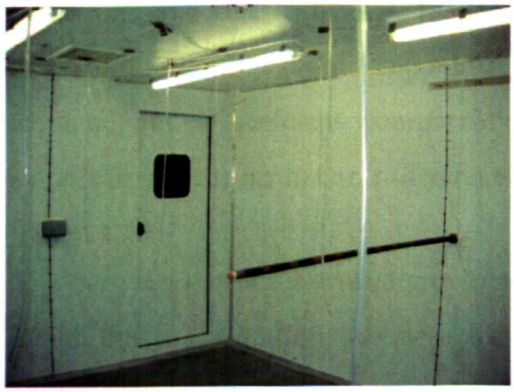

C

D

Figure 5-9: Photographs of the test chamber showing the exterior and the interior (A-D). The interior images are for camera positions A,B,C,D as labelled and shown in Figure 5-12

5.4.2 Bioaerosol Generation

In order to generate bioaerosols within the test chamber a solution containing the pure bacterial culture and distilled water was aerosolised into the room. This was achieved using a six jet Collinson Nebuliser (CN 25, BGI Inc, USA) (Figure 5-11) connected to the inlet port of the chamber. The nebuliser had its own air pump, pressure regulator and flow meter and was operated at a flow rate of 12 $l.min^{-1}$ with the pressure maintained at 20 psi (139kPa). The air pump (B100DE, Charles Austen) pumps air through a HEPA filter, to ensure sterility into the liquid suspension, and results in liquid being sucked up into the nozzle and sprayed out of the six holes into the vessel. Approximately 99% of this hits the wall and returns to the liquid. This process is shown in Figure 5-10. A very small portion of the smallest droplets created remain suspended and are ejected from the nebuliser due to the higher pressure in the vessel. This enables a fine spray to be created with size distributions showing that 90% of the mass released having diameters below 4μm and 60% with diameters smaller than 2μm (May, 1973). Evaporation of the bioaerosols means that the measured size distribution will vary depending on the time after release that they are determined. Data from the manufacturer indicates that the mass median diameter (MMD) is 2.5μm with a geometric standard deviation of 1.8 (BGI Collison Nebuliser, 2007).

The bioaerosols were created using a pure culture of *Serratia marcescens* (ATCC 274). This is a non-fastidious micro-organism that grows easily on general purpose media, poses minimal risk to healthy humans and the incubated colonies turn pink after 2-3 hours in the light at room temperature, enabling any contamination from other sources to stand out. It performs comparably to other vegetative cells in terms of numbers sampled from the air in controlled tests (Rosebury, 1947).

The *Serratia marcescens* was grown up for 24-48 hours in nutrient broth at 37°C after which the concentration was approximately 1 $x10^9$ per ml. A 2ml aliquot of the pure culture was aseptically removed and suspended in 100ml of sterile distilled water in the pre-autoclaved nebuliser. Sterile distilled water was the preferred suspension medium since it did not produce foaming of the suspension during nebulisation. The nebuliser was sterilised by autoclaving between experimental runs.

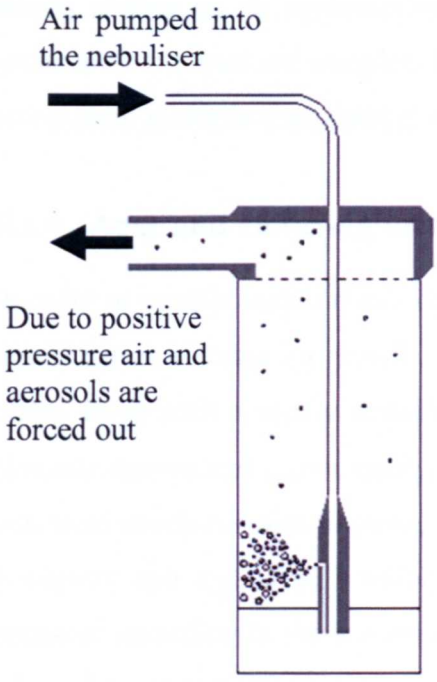

Figure 5-10: Simple schematic of the nebuliser. Air travelling down the tube forces the solution up into the nebuliser head creating an aerosol.

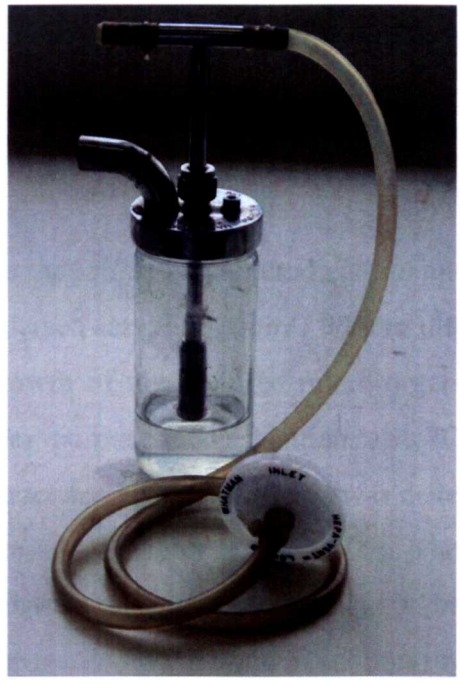

Figure 5-11: Photograph of the Collison Nebuliser

5.4.3 Bioaerosol Sampler

A description of the different bioaerosol sampling techniques was given in Chapter 4. The Andersen sampler was used for all the bioaerosol sampling in the test chamber experiments. The MMD of bioaerosols created in the experiments is 2.5μm (5.4.2) and these will evaporate in the room air, so it is important to have a high sampling efficiency at small particle sizes. Sampling from the test chamber with the Andersen Sampler has shown that bioaerosols are sampled in large numbers on the lower two stages. It was therefore more appropriate to use this sampler with higher efficiencies for the smaller sizes. Since previous sampling studies have shown the lower stages to be the only ones with significant colony growth only these were used in this study.

Since the micro-organism being sampled was a pure culture introduced artificially into the space, no speciation was required and samples could be cultured on one general purpose media. This overrides one of the main benefits of using the Burkard sampler which is that a single sample can be plated onto a variety of selective media. Using the Andersen sampler removes the chance of potential false counts due to contamination

during plating up, or agglomeration or break up of particles within the liquid as can occur with the Burkard sampler. Positive hole correction can be applied to reduce the errors from multiple impaction at one location.

5.4.4 Agar and culturing methods

In order to sample viable micro-organisms they must be captured and maintained alive in a situation suitable for growth. The Andersen sampler requires 90 mm diameter agar plates filled with a media suitable for growth of the required micro-organism. Since *Serratia marcescens* grows easily on general purpose media Nutrient agar (Oxoid, UK) was used which contains peptone, beef extract and agar. This media was developed over a century ago and is still widely used today (Prescott *et al.*, 2005). The agar was prepared according to the manufacturers instructions, autoclaved at 121°C before being allowed to cool slightly and poured into the sterile Petri dishes. After pouring the plates were left to cool and solidify before being refrigerated until required.

After sampling the agar plates were incubated for 24 hours at 37°C after which time visible colonies had grown up. After incubation the number of colonies on each of the plates was counted and subjected to positive hole correction in order to account for multiple impaction (4.2.1). The corrected counts for each pair of plates (stages 5 and 6) were added together to give a total count and multiplied by the volumetric sample rate and sample time to give a count per m^3 of test chamber air.

5.4.5 Validation Methodology

Experiments to Compare with Passive Scalar Transport Simulations

The experiments were carried out at two chamber ventilation rates; 6 and 12 $ac.h^{-1}$ In both cases bioaerosols were injected through the central source as described above (5.4.1) with co-ordinates: 2.13, 1.15, 1.675. Experiments conducted at 6 $ac.h^{-1}$ also considered the linear source that spanned from z= 0.42 to 1.725m in the z direction (Figure 5-12). The bioaerosol concentration in the room was determined at 12 points by drawing air out through 5mm diameter pipes and into the Anderson sampler located in the anteroom. The locations of the sampling positions are shown in Figure 5-12. The experiments were carried out with the room in steady-state by maintaining a constant airflow rate and a constant injection of bioaerosols.

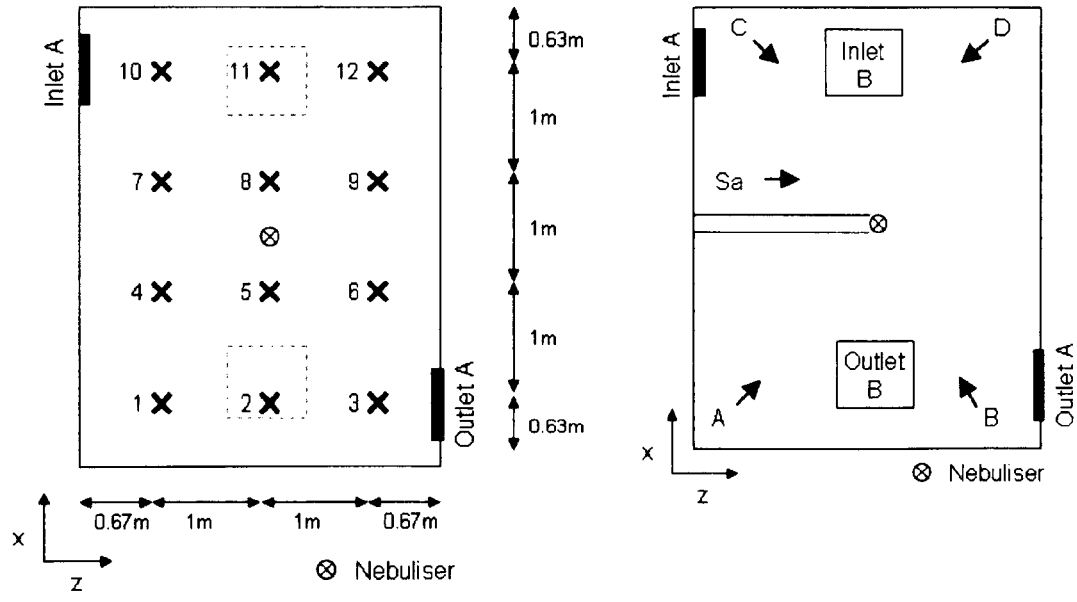

a) b)

Figure 5-12: a) Plan view of the test chamber showing sampling positions and the central nebuliser position b) Camera locations for photographs in Figure 5-9 (A,B,C,D) and the smoke images in Figure 5-18 (Sa)

At each ventilation rate the room was allowed to stabilise for one hour after switching on the nebuliser in order to ensure steady state was reached, as the air filling the volume of the room should have been replaced at least six times. This condition was then maintained for the duration of the sampling period.

Each sample was taken over a 2 minute period, at a sampler flow rate of 22 $l.min^{-1}$. Between samples the room air was left for 10 minutes, equivalent to 1 air change, in order for the bioaerosol concentrations to return to the steady state concentrations. The order in which the samples were taken was varied for each run. For each experimental run four repeated samples were taken at each point and three runs were carried out for each of the three regimes. Therefore each position was sampled 12 times.

The sampling pipes were arranged such that it was necessary to bend them in two positions in order to reach the Andersen sampler. There was concern that this would result in the bioaerosols impacting on the pipe walls around the bends and lead to sampling losses. However the bioaerosols are sufficiently small to deviate only

minimally from the air stream due to their own momentum at a bend. To ensure this was the case the particle relaxation time for a 2μm diameter spherical particle was found. This is the length of time for a particle to 'relax' to equilibrium after the forces acting upon it change. Therefore this is the length of time for which the particle will deviate from the air current. The equation to calculate the relaxation time (τ) is given in equation 5-18 below (Hinds, 1982). For a 2μm particle this results in 1.4 x10^{-5} seconds.

$$\tau = \frac{d^2 \rho_p C_c}{18\mu} \qquad 5\text{-}18$$

Here d is the diameter of the particle, ρ is the density of the particle, μ the viscosity of the air, C_c the Cunningham correction factor (taken as 1.1).

If the velocity of the particle is due to the volume flow rate through the sampler then the particle will only travel 0.25mm before rejoining the air stream and therefore losses inside the pipe should be minimal.

Flow visualisation

In order to obtain some qualitative results to compare to simulated bioaerosol transport within the test chamber, flow visualisation was carried out by injecting smoke at the central source location. The smoke was generated using a smoke canister (Orange-9 Hi Viz Orange Smoke Cannisters, Hayes UK) located within a 60 litre container. Once the canister was lit, the smoke entered the chamber through the same port and tube as the bioaerosols, entering the chamber at the central source location. Initially to start the flow of smoke into the chamber a pump was used to pass 1 l.min^{-1} of air over the container into the chamber. Once the smoke had started flowing into the chamber the pump was switched off. A video camera was set to record the movement of smoke in the test chamber. A still from this is shown in the results (Figure 5-18). The flow visualisation test was carried out at an airflow set up with ventilation regime A at 6ac.h^{-1}.

Experiments to Compare with Lagrangian Particle Tracking

Experiments in the test chamber to compare with Lagrangian particle tracking simulation were conducted at an air change rate of 3 ac.h^{-1}. This air change rate is lower

than previous studies and was chosen in order to reduce the bioaerosol deposition rate due to turbulent dispersion (Lu *et al.*, 1996). This would minimise the risk of the agar plates being overloaded with micro-organisms, affecting the ability to quantify the deposition spatially. In order to quantify the level of deposition 21 agar plates containing nutrient agar were spaced out over the floor of the test chamber as shown in Figure 5-13.

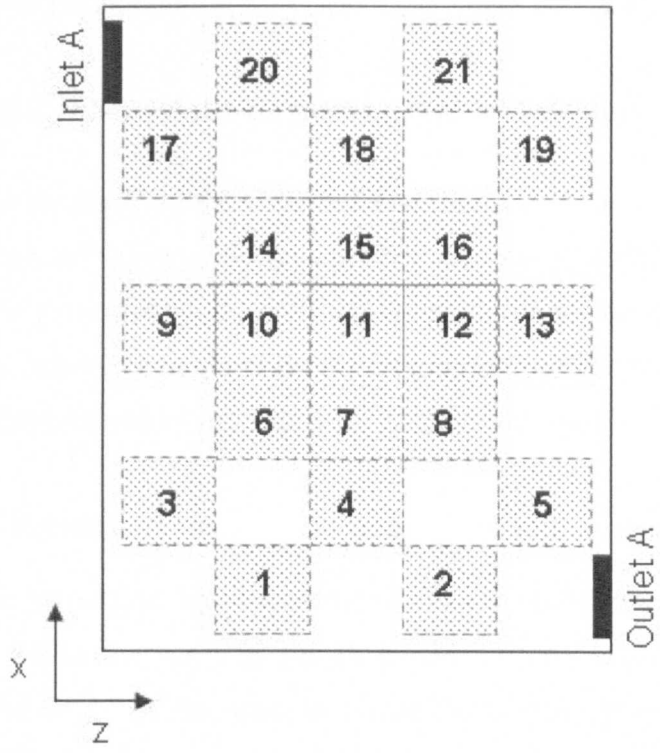

Figure 5-13: Positions on floor where particles are collected for validation of Lagrangian particle tracking model. The areas indicated are those used in the CFD post-processing, each with an area of 0.5 x 0.5 m. The experimental plates are placed at the centroid of each square.

The lids were removed from these agar plates starting at the far corner and moving towards the door, in order to reduce contamination from particles off the skin. Once all the lids had been removed and the chamber vacated and sealed a pure culture of *S. aureus* was nebulised into the chamber using the same method as described above (5.4.2), and injected from the central point source (5.4.4). It was envisaged that the Lagrangian particle tracking could be used to simulate bioaerosols released from the skin depositing on surfaces within a ward. Since the pathogen of interest in these

situation is *S. aureus* (Chapter 2) this was chosen for these experiments. Air samples were taken every 20 minutes, as this was equivalent to one complete air change in the chamber. The first sample was taken before the nebuliser was activated in order to determine the background count due to the presence of the person removing the plate lids. The nebuliser was then operated continuously for 80 minutes. After this time the nebuliser was switched off and the chamber airflow was maintained at $3ac.h^{-1}$ for a further 90 minutes to reduce the airborne concentration of *S. aureus* and thereby ensure a very low risk from airborne pathogens when entering the chamber. The agar plates were then incubated for 24 hours at 37°C and the colonies counted.

5.5 Results and Discussion: Experimental Validation

Firstly the airflow results from the CFD model of the test chamber using two different ventilation regimes are shown. Following this the results from the passive scalar transport model is presented along with the comparisons to the experimental results. Finally a similar comparison is given for the Lagrangian particle tracking. Results from smoke tests are also presented to qualitatively visualise the results.

5.5.1 Airflow Results

The two different ventilation layouts used in the CFD model result in quite different velocity profiles within the space as shown by the velocity vectors on perpendicular planes through the centre of the room in Figure 5-14. These planes show clearly the difference in air flow patterns, with regime A showing the circling airflow in the y-z plane. The x-y plane also indicates this recirculation in the flow is towards the inlet side of the chamber. Regime B has two areas of recirculation on the two sides of the room, and a more direct flow from inlet to extract. As a result of these differences, the two cases provide two distinct ventilation profiles for validating the zonal source method in Chapter 6. Since the air change rate is the same in both models the maximum velocity within the space is the same, $0.6\ m.s^{-1}$, with the volume average velocities being $0.05\ m.s^{-1}$ and $0.03\ m.s^{-1}$ for regime A and B respectively. Although the patterns differ quite considerably the velocities are of similar magnitude.

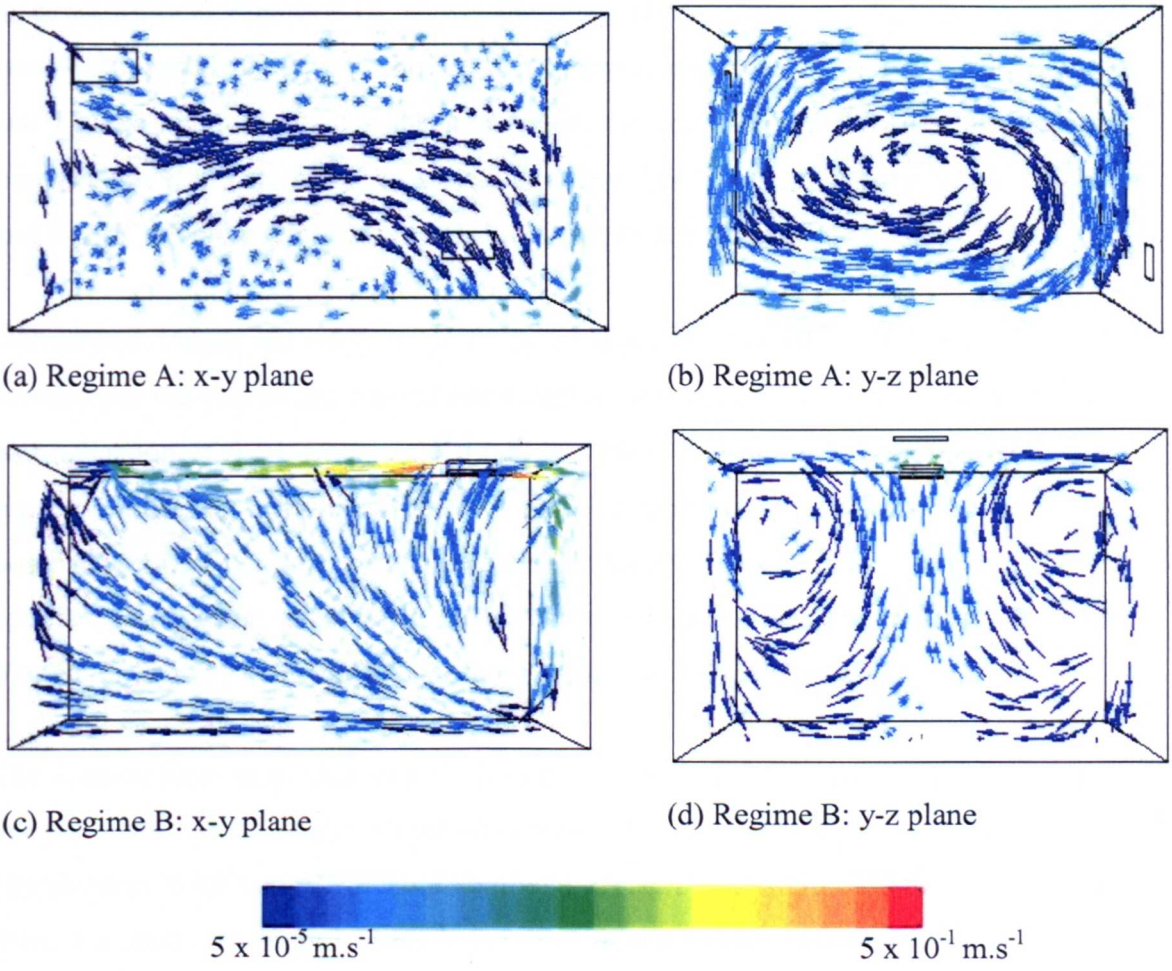

Figure 5-14: Velocity profiles for ventilation regimes A (a, b) and B (c,d) of the test chamber model on central planes in the x-y or y-z direction.

5.5.2 Experimental Validation of Passive Scalar Transport

In order to validate the CFD test chamber model, and to ensure the results were realistic, bioaerosol transport simulations were compared against experimental results for three scenarios:

- Point source bioaerosol injection with ventilation rate of 6 $ac.h^{-1}$
- Point source bioaerosol injection with ventilation rate of 12 $ac.h^{-1}$
- Linear source bioaerosol injection with ventilation rate of 6 $ac.h^{-1}$

The results from these comparisons are shown in Figures 5-15 and 5-16. Figure 5-15 shows the contour plots of bioaerosol concentration for both the CFD simulation (on a plane y=1.15m) and the experiment. The experimental values were interpolated at 10 points between each sampled position assuming zero at the walls and a linear variation

in concentration. Figure 5-16, shows the point experimental values with the relevant error bars plotted across the room on lines between positions 1 and 10, 2 and 11, and 3 and 12 (see Figure 5-12). On the same graph the simulated results on a line spanning from wall to wall from x=0.0 to x=4.26 at a height of 1.15m are plotted at z=0.67, 1.67, and 2.67m, which would cross through the represented experimental points.

Normalised values are used in order to compare the results at each point. For the simulations the results are normalised based on the arithmetic mean of all three lines. Normalisation of the experimental results is treated differently as they consist of three runs with differing nebuliser concentrations. For each experiment, which sampled each point four times, the average concentration is found, and this is used to normalise the results at each point, resulting in three normalised values for each position. The value plotted on Figure 5-16 is then the arithmetic mean of these three values.

The contour plots show that in both the simulations and the experiment the bioaerosols are entrained towards the inlet air stream and that the entrainment increases with air change rate. With both the central source at 12 $ac.h^{-1}$ and the linear source at 6 $ac.h^{-1}$ there is a much greater pull towards the inlet, than the central source at 6 $ac.h^{-1}$. This is shown in both the experimental and CFD results. With the linear source this is due to the different air currents near the wall away from the centre of the room. Figure 5-16 is much clearer for direct comparisons. There is generally a good representation of the bioaerosol transport by the CFD model. The results suggest that the model possibly over estimates the concentration at the source as has been found previously (Zhang *et al.*, 2007), but since no measurements could be taken precisely at the source this is not confirmed.

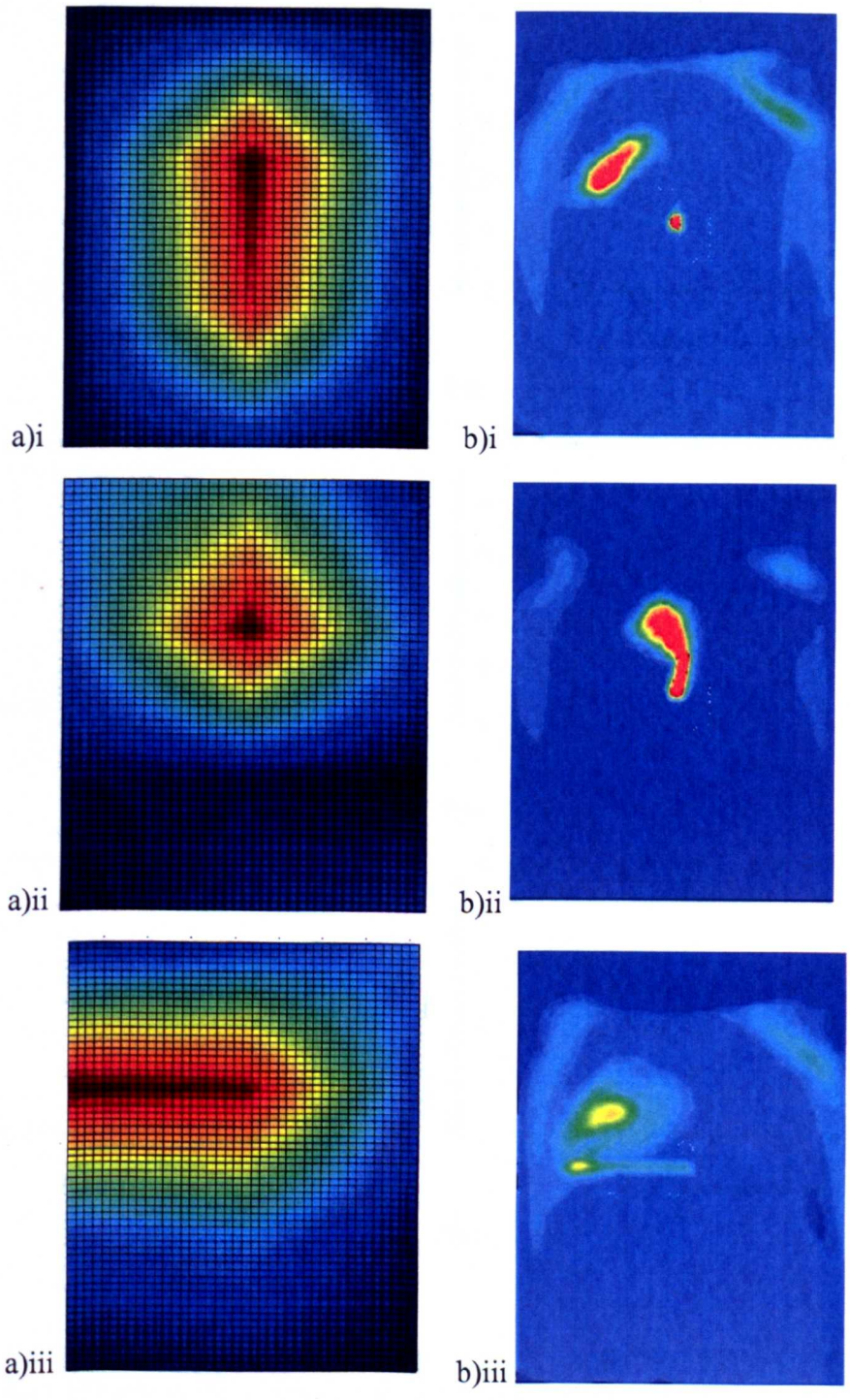

Figure 5-15: Contours of experimental bioaerosol concentrations (a) and the CFD simulated passive scalar (b) plotted at y = 1.15m for central source (i) at 6ac.h^{-1} (ii) at 12 ac.h^{-1} and (iii) linear source at 6 ac.h^{-1}.

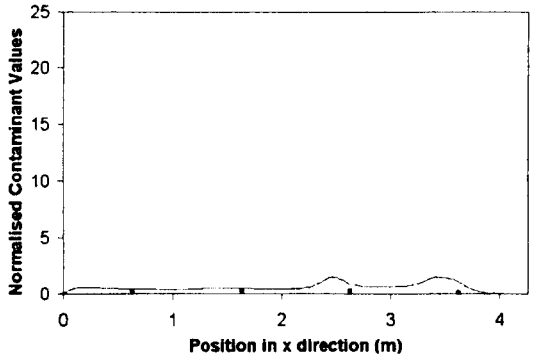

a)i

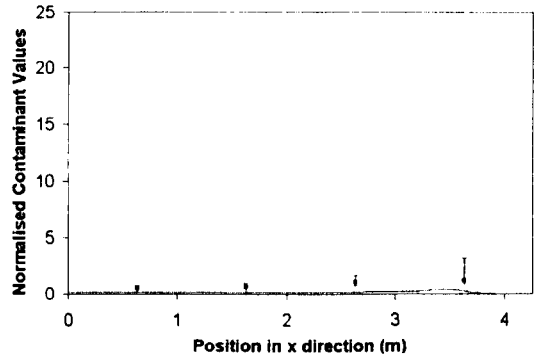

b)i

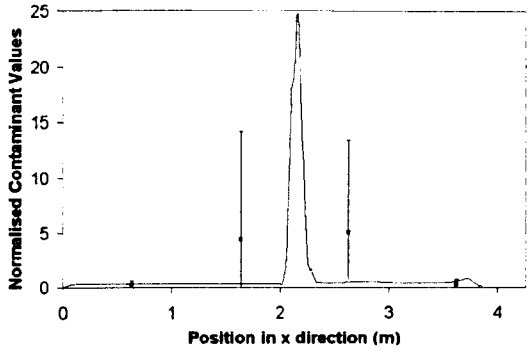

a)ii

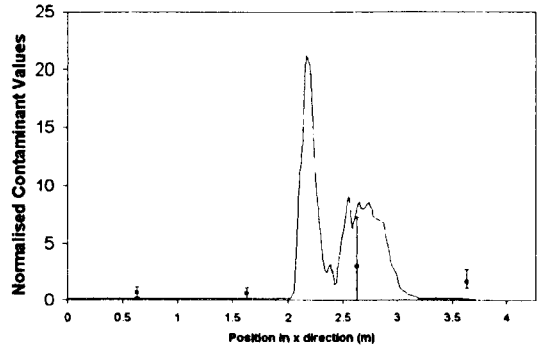

b)ii

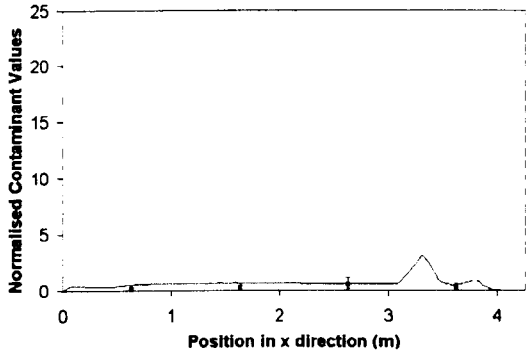

a)iii

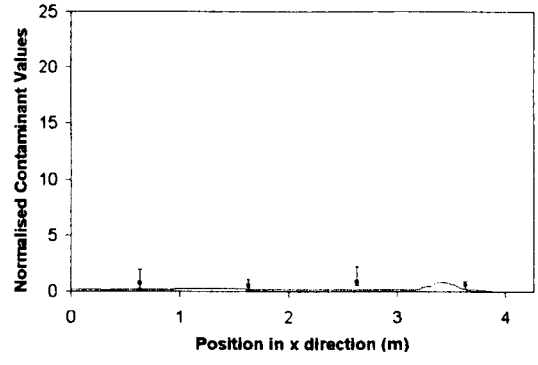

b)iii

Figure 5-16 Normalised concentrations on lines (i) z=0.67m, (ii) z=1.67m and (iii) z=2.67m for CFD simulations and at points on this line for experimental results, shown for (a) 6 ac.h-1 (b) 12 ac.h-1 and (c) linear source at 6 ac.h-1. The positions of the experimental samples are plotted relative to the x axis.

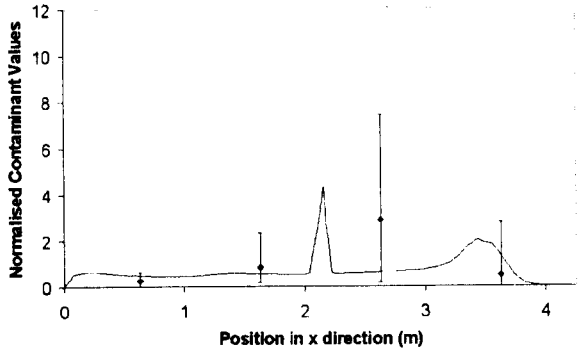

c)i

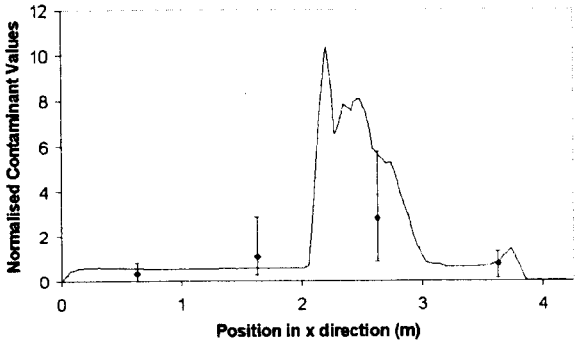

c)ii

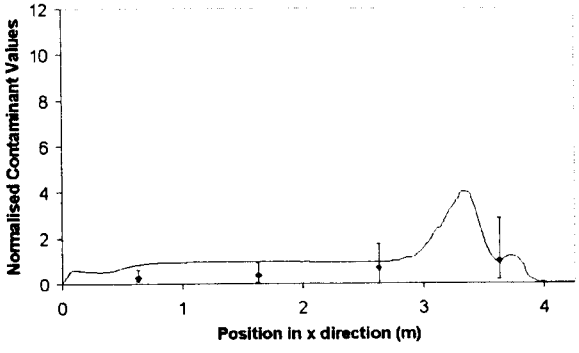

c)iii

Figure 5-16 cont. Normalised concentrations on lines (i) z=0.67m, (ii) z=1.67m and (iii) z=2.67m for CFD simulations and at points on this line for experimental results shown for (a) 6 ac.h-1 (b) 12 ac.h-1 and (c) linear source at 6 ac.h-1. The positions of the experimental samples are plotted relative to the x axis.

Close to the source there is a very large variation in sampled values from the experimental results. It is possible this is due to an unstable generation of bioaerosols from the nebuliser, or local variation in the room air flow. At 6 $ac.h^{-1}$ this variation was significant on both sides of the source (positions 5 and 8 in Figure 5-12). It was desirable to establish if these points varied consistently with each other, or if an increase at one position meant a decrease at the other, possibly indicating that the transport of the bioaerosols had a time dependent nature. In order to study this two Andersen samplers were used in an experiment to sample positions 5 and 8 simultaneously, following the same method as described in 5.4. The results are shown in Figure 5-17. With the exception of one sampling time the bioaerosol concentrations were similar at both positions. It is therefore likely that the large variation near the source is due to an unsteady generation of bioaerosols, rather than a time dependant airflow.

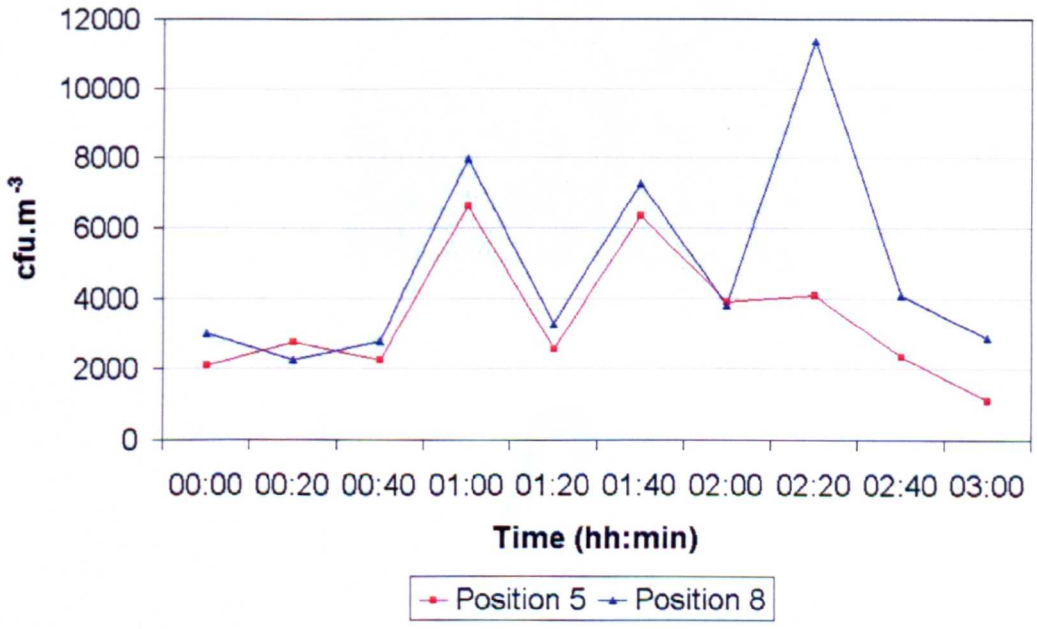

Figure 5-17: Experimental bioaerosol concentration ($cfu.m^{-3}$) at position 5 and position 8, sampled concurrently

It was of concern that over the course of an experiment the bioaerosol suspension in the nebuliser would become more concentrated and so the concentration injected into the room air would not remain at steady state over the entire experiment. The concentration in the nebuliser was determined before and after each experiment, and although there were variations in the counts these were all of similar magnitude. In order to reduce the

effect this may have on the results the samples at each position were carried out in a different order each time.

An attempt was made to repeat these experiments using CO_2 as a tracer. It was considered that this may provide more stable results, as this would eliminate any errors due to the death, or loss of viability of the bioaerosols. However it was found that CO_2 diffused too quickly within the space to measure any reasonable patterns of dispersion that could relate to a bioaerosol distribution. The aim of this study was to validate the transport of bioaerosols in the CFD model, and since the dispersion patterns shown in the bioaerosol experiment were not shown in the CO_2 experiment due to this rapid diffusion it seemed more appropriate to use bioaerosols to validate the CFD model.

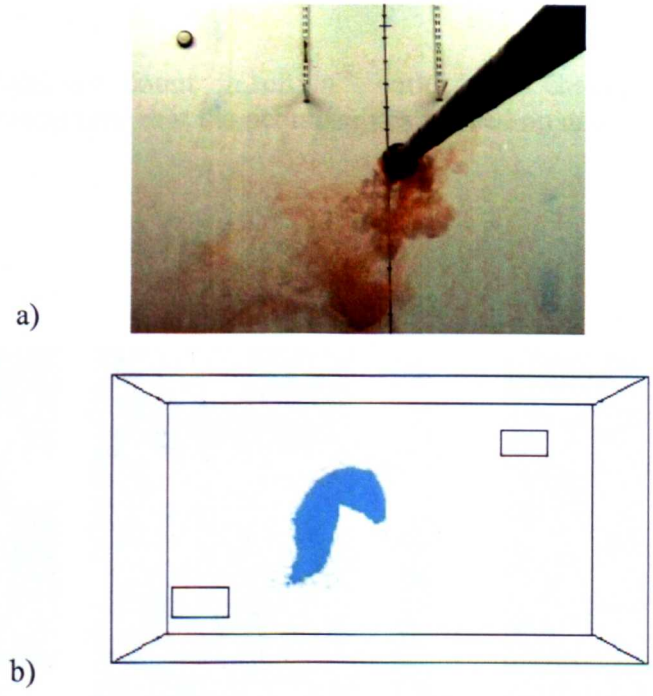

Figure 5-18: Comparison of CFD simulations with a smoke tracer. a) Smoke released from centre source, with camera position Sa shown in Figure 5-12, b) simulated CFD scalar plume from the same view point.

Flow Visualisation

The entrainment of the contaminant towards the air supply inlet that was shown in the CFD simulations, was also seen with the smoke tests. The smoke particles drop downwards immediately on injection into the room, which does not occur with the CFD

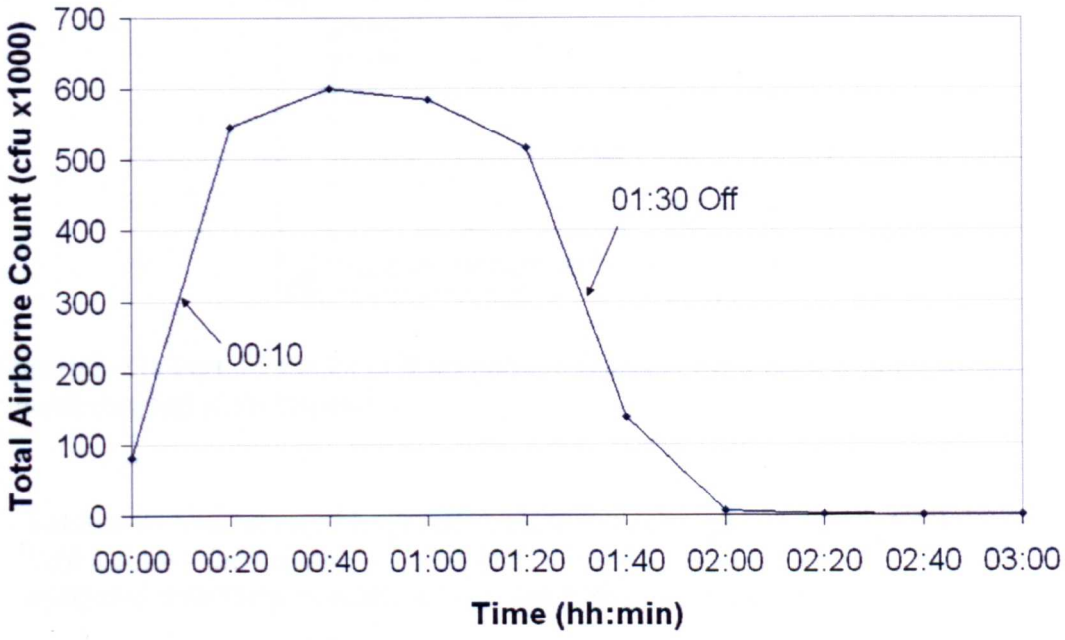

Figure 5-19: Total air count in cfu.m^{-3} within test chamber during deposition experiment. Indicating time that the nebuliser is switched on and off.

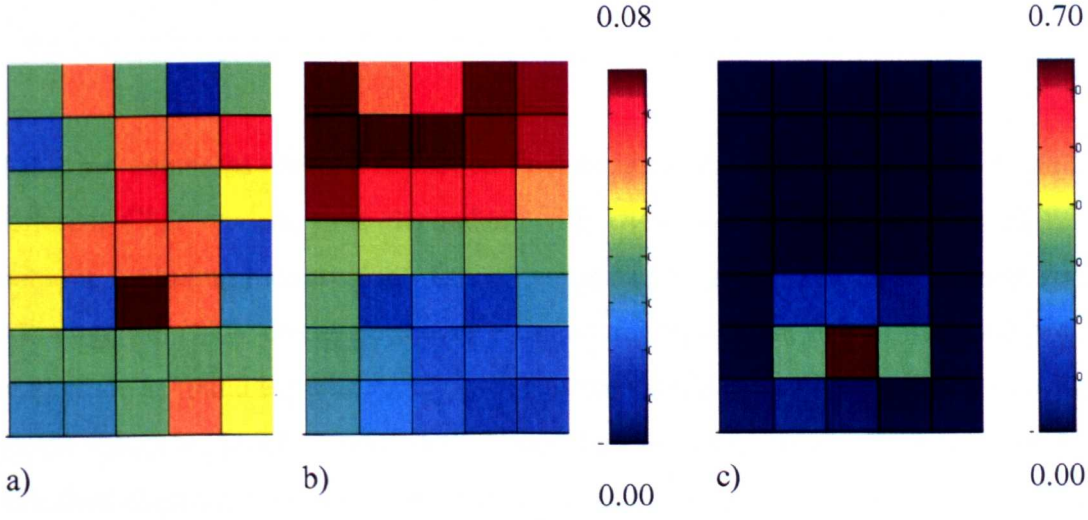

Figure 5-20: Plots of deposition for a) experimental, b) DRW particle tracking c) Bulk flow particle tracking. The values shown in the keys are the fraction of particles in that location with respect to the total floor deposition. c) uses a different key from a) and b)

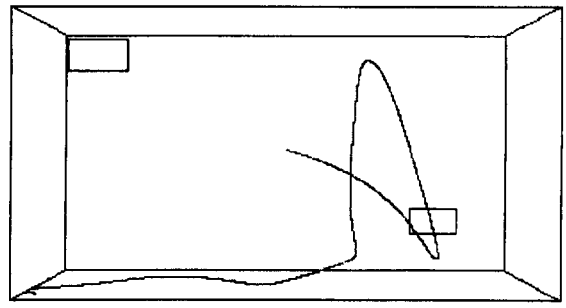

Figure 5-21: Particle tracks of 9μm particle released from central point source without considering turbulent dispersion.

Table 5-4: Validation of Lagrangian particle tracking model using total deposition. Table shows percentage of airborne bioaerosol count deposited on the floor compared with the percentage of injected particles for the three CFD models.

	Experimental	**Bulk Flow**	**DRW**	**Time dependent (DRW)**
Percentage deposited	9.1	0.4	14.2	13.6

Table 5-4 compares the total deposited fraction in the experiments with that in the three different CFD models, time dependant with DRW and steady-state with DRW and without. Including the turbulent dispersion appears to give much more realistic results. Although the DRW model does over estimate the deposition, it is of the same order of magnitude as found experimentally, whereas the simulation without turbulent dispersion yields values an order of magnitude lower than the experiments. Without considering turbulent dispersion the majority of the predicted deposition is in one position, as there is no stochastic nature to the transport and all particles of the same size and mass follow the same trajectory. The tracks for the largest size, 9μm, are shown in Figure 5-21. The results of the experimental study in Figure 5-20 show that it is highly unrealistic that deposition should occur in one small location. Neglecting turbulent dispersion has the effect of creating a much clearer cut off diameter between the number of particles being extracted, and those that become deposited. Accounting for turbulent dispersion results in a greater number of particles that are deposited and a large range of particle sizes that

are both extracted and deposited in varying quantities. This appears to be more representative of a real situation.

The CFD model created is expected to differ from the experiment since evaporation is not included, and the particles are assumed to be the same diameter throughout their transport. As the experimental method nebulises a liquid suspension made with distilled water, this will evaporate and the sizes of the particles in the air, after a few minutes, may be smaller than those defined in the simulation. The need for a person to be present in the room to remove the plate lids in the experiment also differs from the CFD simulation. However any release from a person is negligible as can be seen by the difference in airborne concentrations shown in Figure 5-16. At the beginning of the experiment there is a count of 60 x 10^3 cfu in the room before the nebuliser is switched on which rises 10 fold during the experiment. The use of plastic Petri dishes may also affect the count due to the build up of electrostatic charge on the plate. This may either attract more particles to the plate because of the surrounding plastic, or more particles may land on the exterior plastic part of the plate. The bioaerosols were injected into the space using a plastic pipe, which may also attract particles to it, thereby preventing them from depositing on the floor (Andersen, 1958). In addition all particles hitting the floor in the CFD model are counted whereas in the experiment only those that deposit and remain viable are counted. However since the airborne concentration was used to express the results as a deposited fraction this should reduce this error.

Despite the many assumptions necessary in the CFD model the DRW model is considered to give a very good overall comparison with total deposition and reasonable results for the deposition pattern, with a greater number deposited near the inlet end of the room than the extract side. The main cause for concern is near to the inlet where the CFD model predicts much higher deposition rate than is found experimentally. This may be due to the high turbulence as the air enters the space and an over estimate of the velocity component acting normal to the floor resulting in higher deposition than reality (section 5.3.2). Problems with simulating dispersion due to turbulence with the DRW model near to inlets has also been found by Zhao *et al* (2008). Since the problem of over deposition is recognised and there is current work to improve this (Lai and Chen, 2007) it was considered that the results from this current study demonstrate that the techniques are satisfactory to use for demonstrating and validating the zonal source.

5.6 Summary

The general equations of fluid flow used within CFD are presented, along with a discussion of the discretisation methods used in Fluent. The test chamber model used to validate the zonal source (Chapter 6) is described. The fundamentals of passive scalar transport and Lagrangian particle tracking have been described.

Through measurements of the spatial variance in bioaerosol concentration and qualitative visualisation using smoke tests the passive scalar transport model was found to give reasonable results to represent bioaerosol transport. Validation of the Lagrangian particle tracking showed that it was necessary to consider the effects of turbulent dispersion on the particle behaviour. The DRW model was found to give generally reasonable results of spatial variation in deposition, although possibly overestimating deposited values near the inlet. This type of validation of bioaerosol deposition in controlled conditions has not previously been published and shows very positive results. Overall both models were deemed to be of sufficient quality for use in validating the zonal source presented in the following chapter.

Chapter 6

Development and Validation of a Zonal Source Model

This chapter outlines the development and validation of a zonal source method for developing CFD models of pathogen release in a hospital ward due to activities. The chapter begins by explaining the rational for the method and the aims of the validation study. This is followed by a description of how the separate bioaerosol sources were set up in the study and how the results are then compared for three sources; a point source, a zonal source and a transient source. Following this validation study, Chapter 7 applies the methodology to a side room and a multi-bed hospital ward in order to demonstrate the application and evaluate the sensitivity of the model and to compare CFD simulations to other modelling techniques.

6.1 Objectives of the Zonal Source Model

Through the literature review in Chapter 2 and the observational study described in Chapter 4 it is clear that general nursing activities, such as washing patients, can be responsible for the release of bioaerosols, and that this significantly contributes to the concentration of micro-organisms in the air of a hospital ward. Since it was found that some of these bacteria are potentially pathogenic *S. aureus* it is possible that the bioaerosols released in this manner may lead to further infection. However as discussed in Chapter 3 this type of release from activities is rarely represented in CFD models when considering the efficiency of ventilation. Although some researchers are presently attempting to represent movement of people in some detail within CFD, intensity and pattern of this movement will vary day to day. As such it may give an unrealistic sense of reality to create transient models including the release from movement. Also steady state models are often more convenient to set up and post process the results to enable comparison of different engineering interventions. As such it was deemed necessary to develop a method of representing the transient dispersal due to activities within a steady state model framework.

The zonal source was developed for this purpose and is presented in this chapter. It is hypothesised that a zonal bioaerosol source, within a steady state model, that encompasses the entire region bioaerosols are released from during an activity can reasonably represent the time averaged release of bioaerosols from said activity. For instance an activity such as bedmaking may release bioaerosols from across the entire top of the bed when contaminated sheets are removed. To model this as a point source seems unrealistic; however the variation in release across the bed top will vary spatially and in intensity on each occasion bedmaking takes place. It is unfeasible to represent all the possible variations of release in a CFD model. Using a zonal source encompassing the region in which this activity takes place, as illustrated in Figure 1.1 enables the release to be simplified. The simplicity of the source conveys the assumptions made and the model may be able to achieve it's objective of providing a reasonable representation of a transient release. This is a similar concept to that used by Brohus (2006) who represents the increase in turbulence created by movement in a steady state model as

discussed in section 3.2.3. If this model is found to be suitable for simulating release of bioaerosols from activity it would enable these to be represented simply in a steady state model. The risk associated with these sources can then be considered when using CFD to more realistically research hospital ward design which may include transport of airborne contamination.

The aim of this chapter is to use numerical methods to validate whether a CFD model using a zonal source can reasonably represent the time averaged release from activity within the same spatial region. The zonal source model provides a simpler alternative to carrying out transient models, providing a more general view of the average behaviour rather than occasion specific results. To achieve this, the dispersion results from a CFD model using a zonal source were compared to the time averaged dispersion results from a transient model with a source that moves through the space. The transient model was also compared to a central point source in order to establish if this method, typically used to represent a respiratory disease, was adequate to also represent the release from activity.

The numerical models used in this chapter were based on the converged airflow for the test chamber model developed in Chapter 5 and the bioaerosol transport models validated in the same chapter.

6.2 Modelling Bioaerosol Sources

The zonal source intends to encompass the spatial region in which an activity occurs. In order to carry out validation of this a zonal source was set up that encompasses the whole region a transient point source passes through as it moves across the room. The time averaged dispersion from this transient source as it moves through the space was compared to that from a zonal source and a point source. The point source in this case was situated at the centre of the zone.

Figure 6-1 illustrates these three sources. Figure 6-1 a) shows a transient source. This is a point source that traverses once across the room and is created by defining a new source location at each time step. The zonal source is shown in Figure 6-1 b) and is defined by a volume that encompasses the entire zone traversed by the transient source.

Figure 6-1 c) shows the point source located in the centre of the room. All three sources were applied in simulations for the two ventilation regimes developed in Chapter 5. The zonal and transient source simulations were carried out for two source orientations i) the x-x source which spans the room in the x direction and ii) z-z source which spans in the z direction.

There were differences in the injection properties for the scalar and Lagrangian methods and so these are described separately below.

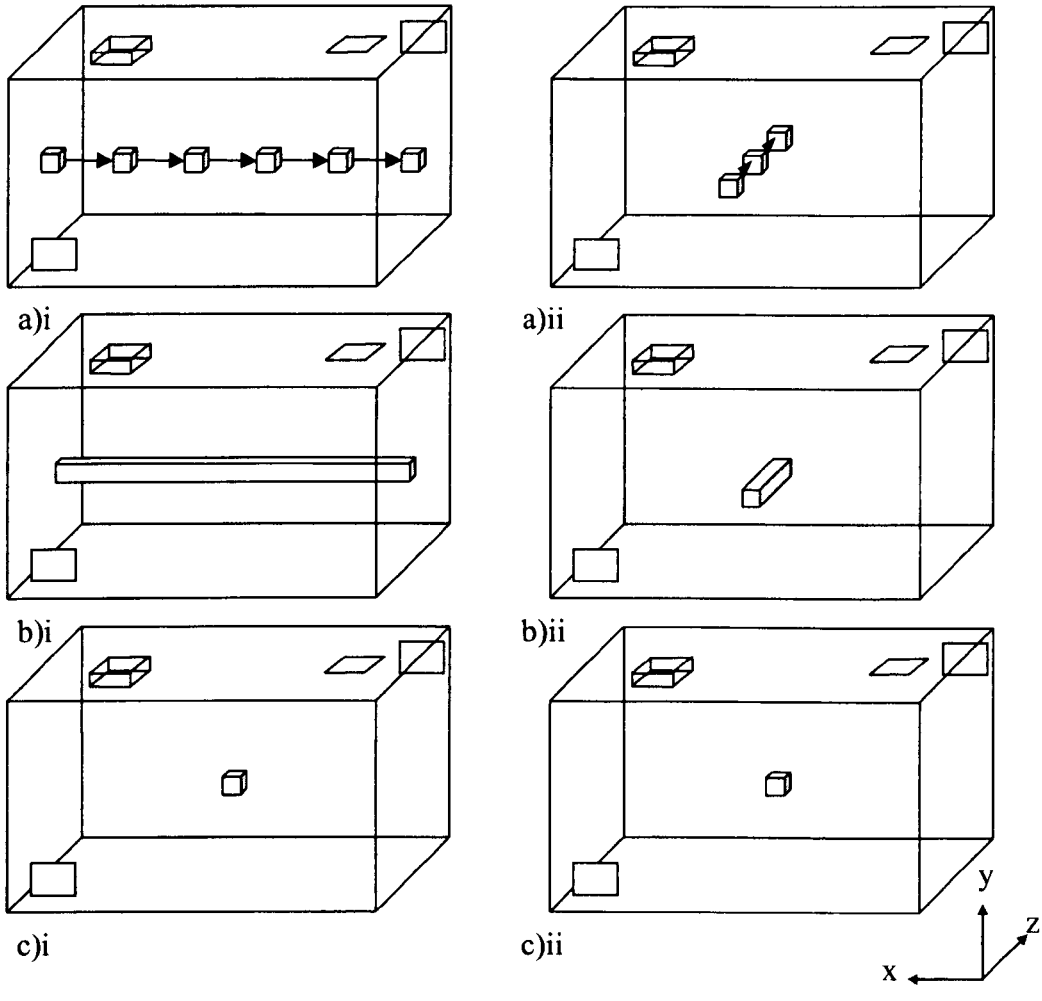

Figure 6-1: The geometry of the three sources a) transient b) zonal and c) point, for the i) x-x source and ii) z-z source. The number of positions shown for the transient source is not representative of the number of steps and is merely used for illustrative purposes.

6.2.1 Source Definition

Passive Scalar

The source was injected into the space as described in Section 5.3.4 although in this case the momentum source of 0.1 $N.m^{-3}$ was applied to all six sides of the volume. The locations of the three sources are given in Table 6-1. The time stepping of the transient source has been described in section 5.3.3. The Point and Zonal source were set up to release the same overall quantity as the transient source injects per time step.

Lagrangian Particle Tracking

The injection points for the Lagrangian particle tracking model were defined at the centroids of the volumes given in Table 6-1 for the simulations with a point source. The zonal and transient sources were defined by a line that spanned through the centre of the zone described in Table 6-1. Both the zonal and the transient sources spanned the entire length of the room from x=0 to x=4.26m and z=0 to z=3.35m for the x-x and z-z sources respectively. In all cases particles were modelled as spherical objects with a density of 1000 $kg.m^{-3}$ injected with a velocity of 0.1 $m.s^{-1}$. This small initial velocity was applied only to allow the particles into the room, and would have little effect on the overall behaviour as the small size of the particles means they have a very short relaxation time (section 5.4.5), and therefore only accelerate for a short period before they reach equilibrium with gravity and drag forces (Hinds, 1982). The definition of the particle diameters and respective mass flow rates are given in Table 6-2. A hundred particles were injected per times step, and the total number of particles injected for the transient source was injected with the Point and Zonal Sources. The value was chosen after carrying out a sensitivity study using 100, 1000, and 10,000 5μm particles injected from a point source.

The zonal and point source solutions were run for 1.5 x 10^6 steps (see section 5.3.2), which ensured less than 10% of the particles remained suspended in the air. The simulations with a transient source injected particles at a new position along the zonal injection line every second, moving with a speed of 0.05$m.s^{-1}$. After the final injection the model was run for a further 18000 seconds.

Table 6-1: Location and geometry of bioaerosol sources for zonal source validation using the passive scalar model. This method requires the use of small volumes rather than single points or lines. The positions for Lagrangian particle tracking are at the centre of these volumes as either a point (point and transient) or a line (zonal).

x-x source			
Dimension (m)	**Point Source**	**Zonal Source**	**Transient Source**
Minimum x value	2.08	0.33	Moving from 0.33 to 3.83
Maximum x value	2.18	3.93	Moving from 0.43 to 3.93
Minimum y value	1.1	1.1	1.1
Maximum y value	1.2	1.2	1.2
Minimum z value	1.625	1.625	1.625
Maximum z value	1.725	1.725	1.725
z-z source			
Dimension (m)	**Point Source**	**Zonal Source**	**Transient Source**
Minimum x value	2.08	2.08	2.08
Maximum x value	2.18	2.18	2.18
Minimum y value	1.1	1.1	1.1
Maximum y value	1.2	1.2	1.2
Minimum z value	1.625	0.42	Moving from 0.42 to 2.83
Maximum z value	1.725	2.93	Moving from 0.52 to 2.93

Table 6-2: Mass Flow rate associated with each particle diameter used to inject particles in the Lagrangian particle tracking model.

Particle Diameter: (μm)	**Mass Flow Rate: (kg.s^{-1})**
1	1×10^{-15}
5	6×10^{-13}
10	5×10^{-12}
20	4×10^{-11}
30	1×10^{-10}
40	3×10^{-10}
50	6×10^{-10}

The model describing particle impaction on a surface defines the particle state as either reflected, trapped, or escaped. For this study particles were assumed to be "trapped" when they collided with the wall, ceiling or floor, and were designated as "escaped" at the outlet. The inlet was set to reflect; however the designation of this makes negligible difference to the results as the momentum of the inlet flow prevents the particles impacting on it. A UDF was used at the boundaries to terminate the particles transport and count the number depositing in each floor zone.

As stated above, all particles were assumed to be spherical in shape, while (as stated in 2.3.2) a skin squame is flake like in appearance. It was assumed here that the shape of the particles has little effect on their transport and since most of the studies described in section 2.3.2. found sizes based on the aerodynamic behaviour of particles, the values used in the CFD model are an equivalent description of particle size to these. The chosen particle diameters (Table 6-2) reflect those found in indoor air from the literature reviewed, however larger particles (30-50μm) were also considered in order to study their possible behaviour. Neither coagulation nor evaporation of the particles were modelled.

Figure 6-2 illustrates a plume of particles injected for ventilation regime A (section 4.2) and source z-z defined in Table 6-1. The image for the transient source (a) displays the situation just after the last particle has been injected, at 67 seconds, while the point (b) and zonal (c) sources show the situation after tracking the particles for 200 seconds. The difference in time is used for clarity. Only a representative number of particles are plotted.

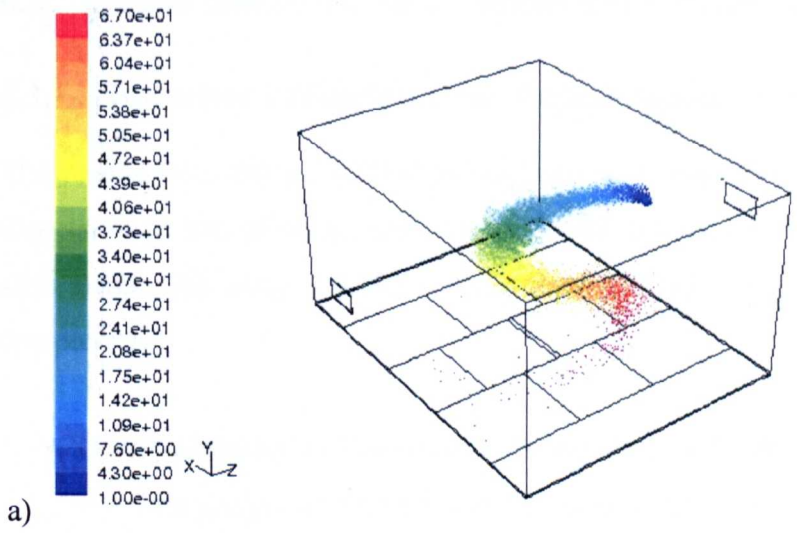

a)

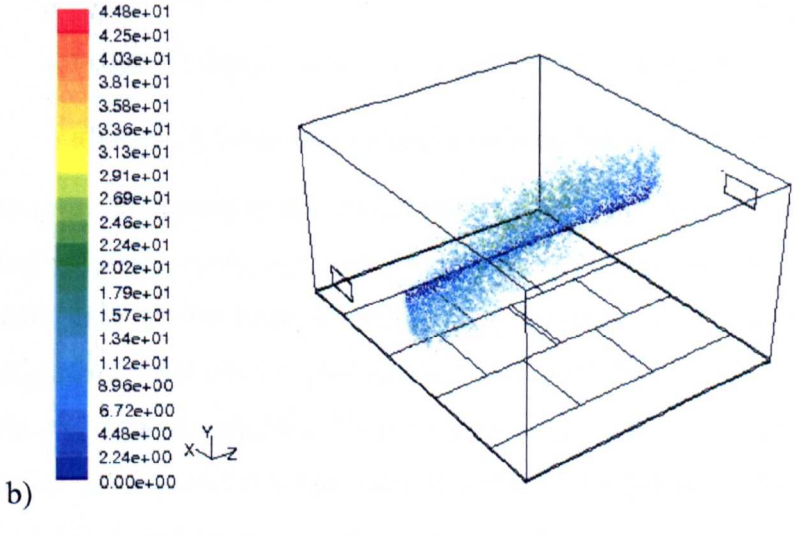

b)

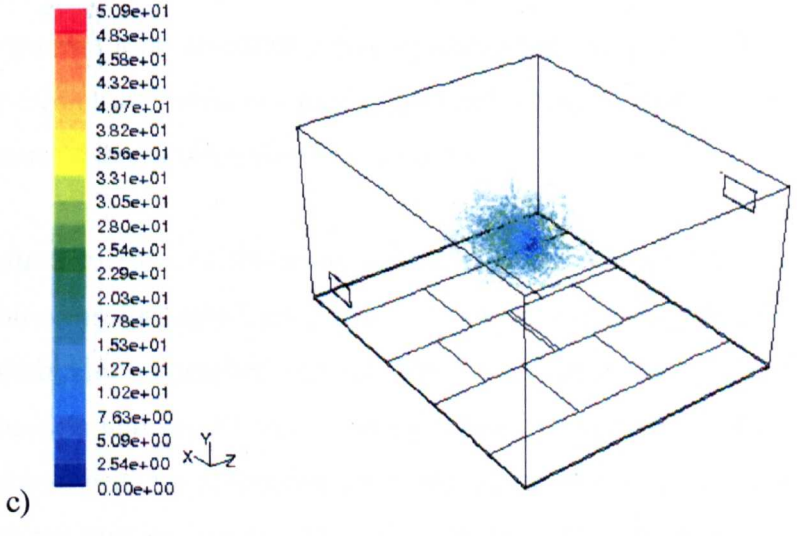

c)

Figure 6-2: Visual representation of the injection of particles from a) transient source, b) zonal source, c) point source. The length of time (s) since the particle is injected is shown on the colour scale in seconds. The transient source is shown after 67 seconds, the point and zonal source are shown after 200 seconds for clarity

6.3 Results and Discussion: Numerical Validation

6.3.1 Numerical Validation using Passive Scalar Transport

The results from the three CFD simulations were used to compare the time averaged dispersion pattern of bioaerosols from a transient source to the dispersion from steady state zonal and point sources. The following results were used to carry out this comparison

- Spatial variations of bioaerosol concentration modelled as a scalar on x-z planes at y=1.15m (height of injection) and y=1.60m (approximate breathing zone) (Figure 6-3; Table 6-3).
- Volume averaged bioaerosol concentration in the domain (Table 6-4).
- Maximum bioaerosol concentration on the plane at height y=1.15m (Figure 6-5).

In order to determine the spatial variations in bioaerosol concentrations for comparison, the values at every node on the two horizontal planes were exported for simulations with each of the three sources; zonal, transient and point. Comparison of bioaerosol dispersion between two simulations was quantified by applying bivariate correlation to the two sets of variables. Comparisons were made between the transient source and the zonal source, and the transient source and the point source. The ability of either the point or zonal source to represent the transient source was then studied by comparing concentration distributions using scatter plots (Figure 6-3) and quantified using the non-parametric correlation test Spearmann's Rho (Table 6-3) as the data did not follow a normal distribution (see Section 4.4.1).

Since the aim of the zonal source is to provide a time averaged representation of the bioaerosol release from a transient source it is necessary to compare steady state results with time dependent results. The zonal source and the point source are steady state models and so the values at each node were simply exported once the solution was converged. For simulations with the transient source the values on the output plane vary as the time progresses. The transient simulations were run for the entire time it took for the source to traverse the space, which was 3600 and 2600 seconds for the x-x and z-z sources respectively. The bioaerosol concentrations on the plane were exported every 100 seconds, over the entire run, and the average at each point in the space found. The

volume averaged bioaerosol concentration was also output every 100s, and the average and the maximum value for this found over the simulation time. This is shown along with the results for the point and zonal source simulations in Table 6-4. The maximum concentration is found from all the exported data for the plane y=1.15m.

Spatial Variations in Bioaerosol Concentration

Figure 6-3 shows scatter plots for ventilation regime A that compare the time averaged scalar dispersion patterns from the transient source with the dispersion patterns from the steady state release from either a point or a zonal source. Each graph shows the time averaged concentration at each node on the plane from the transient source plotted on the y axis, and for exactly the same position in the computational grid, the value extracted from the model using a point or zonal source plotted on the x axis. The scales on both the y and x axes are equal. The plots comparing the zonal source to the transient source have a very small amount of spread, being very close to line at almost 45 degrees. This demonstrates that the values at each position are very similar for both models. However the graphs showing the point source in relation to the transient source have a much shallower gradient correlation line which indicates that the concentrations at each point are much higher with the point source than the averaged transient source. More importantly there is also a much greater spread away from the line, indicating that as well as the values being different the variation between different points, and the pattern of dispersal in the space also varies.

Table 6-3 gives the correlation coefficients generated from these scatter plots for ventilation regime A and the equivalent for ventilation regime B. These values show how well the two variables can be represented by a straight line on the graph, and, equivalently, how well they represent each other. This is not affected by the slope of the line but by the spread of the values away from a straight line result. Values close to 1 indicate that the solution is close to linear, and therefore the spatial variation in concentration is similar for both models. The comparison with the zonal source all have values of 0.94 or greater showing the two solutions have very similar dispersal patterns; they are close to 1 and therefore close to a linear relationship. However for the point source the difference between the spatial dispersion for the two models is shown by the varying correlation coefficients, dropping lower than 0.5.

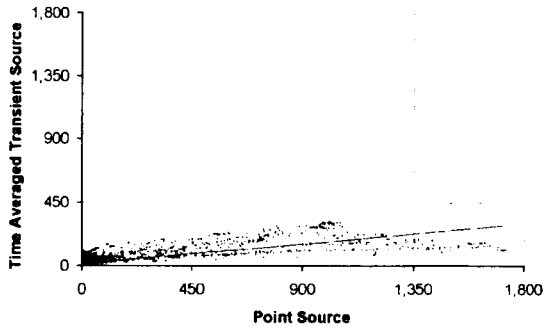

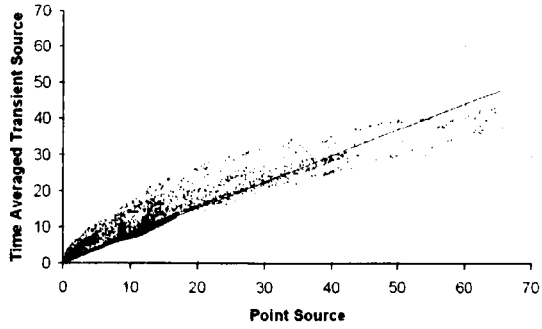

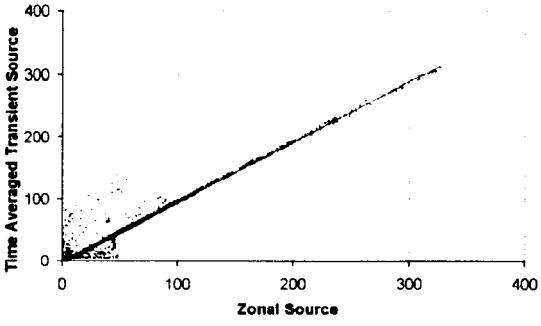

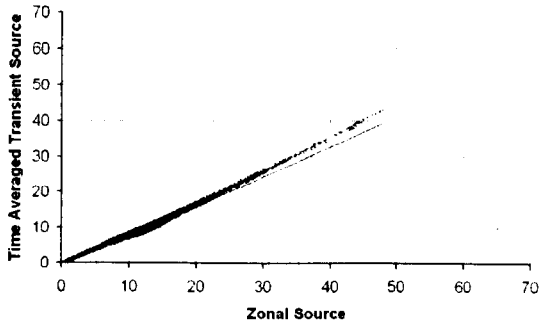

a)i a)ii

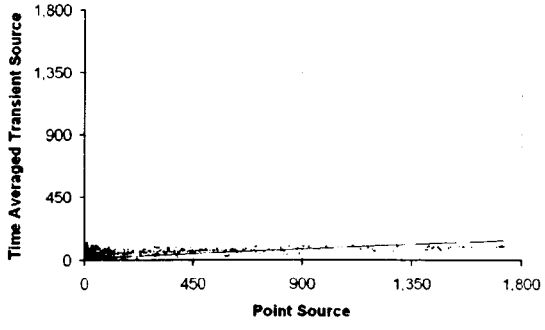

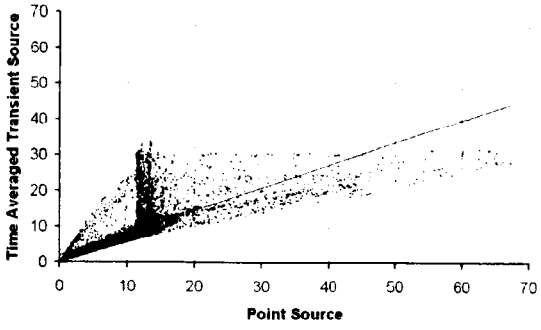

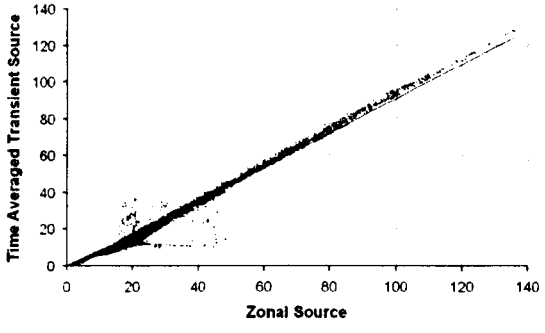

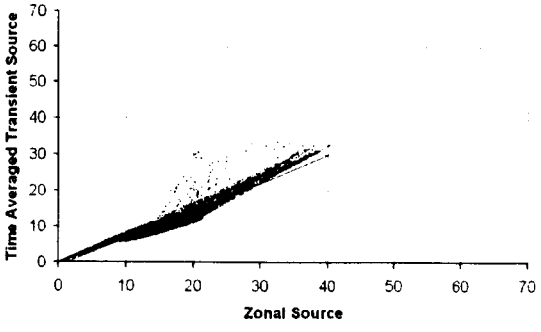

b)i b)ii

Figure 6-3 Scatter plots comparing the variation in bioaerosol concentration for ventilation regime A, with (a) x-x source and (b) z-z source, on planes (i) y=1.15m, (ii) y=1.60m. Each point represents one position in space with the value on the y axis being the transient solution and the x axis being from either the zonal or the point source. The values are bioaerosol concentration $\times 10^3$ (cfu.m^{-3}).

Table 6-3: Comparison of concentration contours between Transient source and Zonal or Point source models using Spearmann's Rho correlation coefficients. The number of nodes used in the calculation is shown in the table, and all values are significant to less than 0.05 level. The values for ventilation regime A are illustrated on scatter plots in Figure 6-3.

		Number of Nodes	Zonal and Transient Source Spearmann's Rho	Point and Transient Source Spearmann's Rho
Ventilation Regime A				
z-z Source	Y=1.15m	13405	0.97	0.75
	Y=1.60m	10688	0.98	0.81
x-x Source	Y=1.15m	13800	0.96	0.54
	Y=1.60m	10690	0.94	0.67
Ventilation Regime B				
z-z Source	Y=1.15m	11180	0.97	0.67
	Y=1.60m	9111	0.97	0.65
x-x Source	Y=1.15m	11800	0.99	0.55
	Y=1.60m	9111	0.99	0.45

Table 6-4: Volume averaged bioaerosol concentrations ($cfu.m^{-3}$) from simulations of each source definition for all cases in the test chamber model.

	Point	Zone	Transient	
Ventilation Regime A				
z-z Source	12497	13104	Ave	9304
			Max	12463
x-x Source	11736	12399	Ave	9840
			Max	11664
Ventilation Regime B				
z-z Source	2488	5884	Ave	9840
			Max	11664
x-x Source	2468	13201	Ave	9222
			Max	13929

These results show clearly that the dispersion from a zonal source provides a much improved representation of the time averaged dispersion from a transient source than a central point source is able to. The correlation with the zonal source has consistently high values; whereas the ability of the point source to represent the transient source varies greatly, depending on the source location and the ventilation regime. Contours of bioaerosol concentrations on a plane y=1.15m for the point and zonal source simulations are shown in Figure 6-4 for regime B in which the point source shows the worst comparison with the transient source. The colours represent equivalent concentrations on each image and it can be seen that this is not just variation close to the source due to the different source geometry but also that the values across the whole plane vary greatly between the two sources. From these images it seems that there is much greater mixing with the zonal source, but that bioaerosols from a central point source are extracted more efficiently from the space.

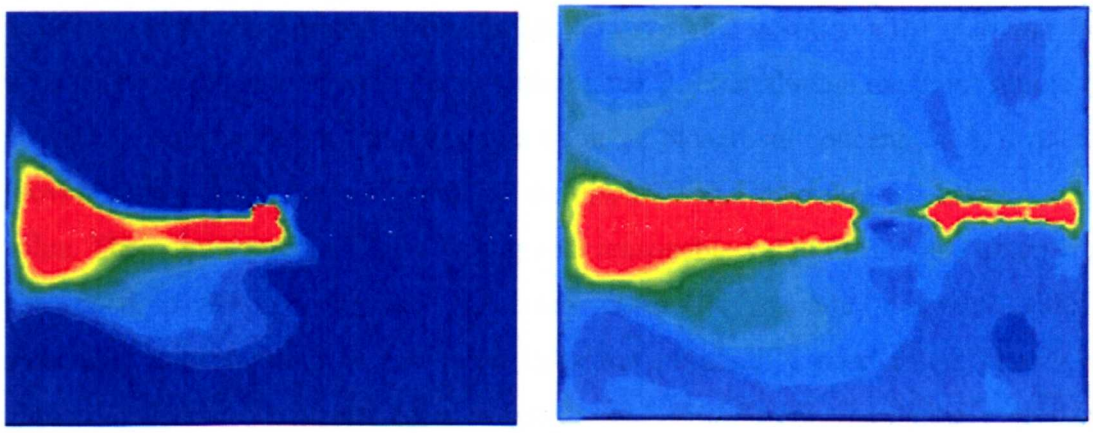

a) b)

Figure 6-4: Contours of Passive Scalar Transport with ventilation regime B source x-x from a) point source and b) zonal source. The red shows areas of high concentration, and the dark blue the lowest.

Volume Averaged Bioaerosol Concentration

Table 6-4 shows the volume averaged concentration of bioaerosols within the space for simulations with all three sources. For the models using the transient source, both the volume averaged concentration over time and the maximum value is given. Table 6-4 shows that the volume averaged concentration within the space is similar for all sources with ventilation regime A, however the simulation using the zonal source still provides a better representation of that from the transient source. In regime B the resulting concentrations from the point source are much lower than those with the other two

sources. It seems in this case the ventilation extract directly pulls a large amount of the bioaerosols from the room. However with a transient source there is greater dispersion of bioaerosols as they are not all injected in an ideal position to be drawn into the extract, and this behaviour is reflected by using the zonal source. For ventilation regime B the central point source provides a very poor representation of the transient source, both in terms of the dispersion pattern (Table 6-3) and the volume averaged bioaerosol concentration (Table 6-4). When there is improved mixing in the room air the point source is better at representing this transient source.

Maximum Bioaerosol Concentration

Despite its ability to better represent the dispersion pattern of a time averaged transient source, the zonal source greatly under estimates the maximum value at any point, as shown in Figure 6-5. This may be due to bioaerosols getting caught in areas of recirculation and building up over time with the transient source. The point source provides a higher maximum concentration; however this is still smaller than that found with the transient source, particularly with regime B. Even though the point source does provide a better value for the maximum value of bioaerosol concentration, it does not provide a reasonable representation of the dispersal and therefore the location of that value. The point source will also only give a reasonable value for the maximum if it is positioned in the *correct* place. In many cases the absolute maximum value of bioaerosol concentration in the room does not necessarily need to be known, and relative differences between cases are sufficient. If different ventilation regimes are being compared then an increase or decrease in concentration will still be shown, and the local extraction of the source, or level of mixing in the space will be demonstrated with reasonable accuracy using a zonal source to represent a transient source, and with considerably less resources than a full transient simulation.

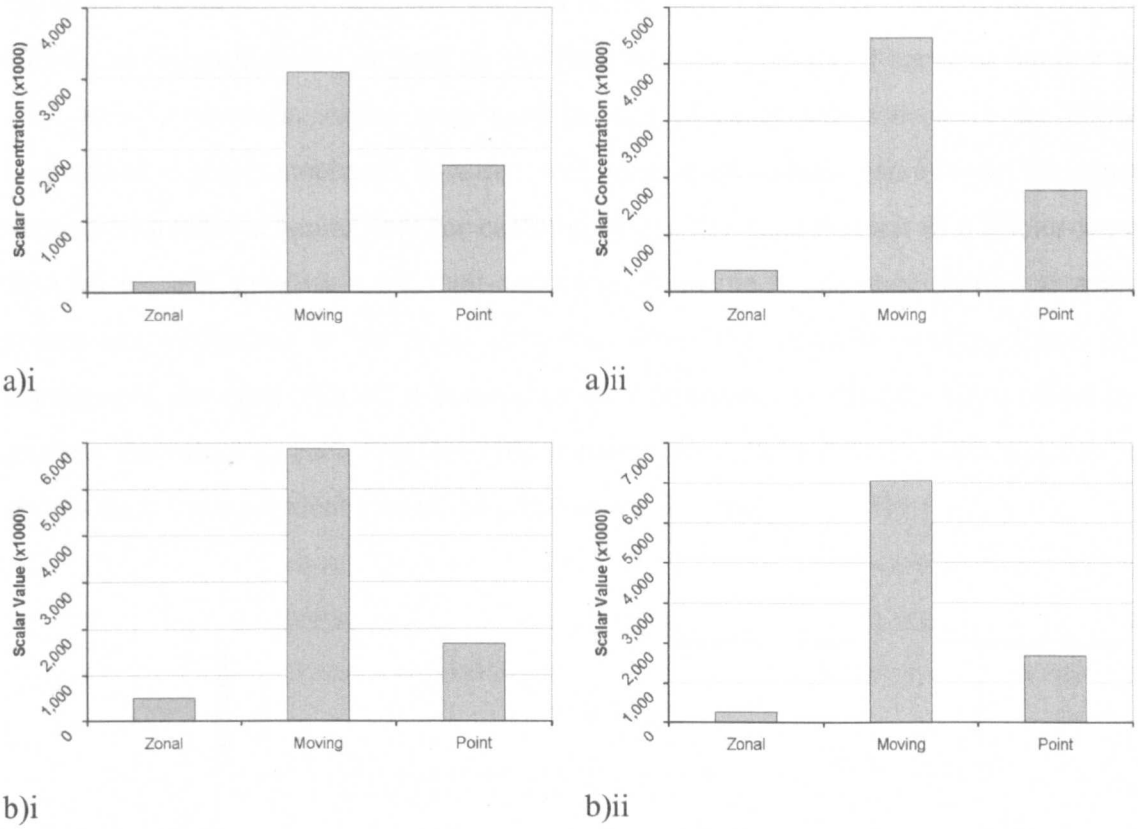

Figure 6-5: Maximum value of bioaerosol concentration (cfu.m^{-3}) on plane y=1.35 for a) regime A, b) regime B; z-z source (i) and x-x source (ii)

6.3.2 Numerical Validation using Lagrangian Particle Tracking

Lagrangian particle tracking was used to assess the ability of a zonal source to represent the spatial deposition that would occur from a transient source. This study differs from that in the previous section in that it considers the total deposition over time, rather than the average dispersal. The total number of particles deposited or extracted from the room for the three different sources were the parameters of interest, along with the locations of deposited particles.

Validation of the zonal source was carried out by considering:

- The total floor deposition from simulations using each source (Table 6-5).
- Correlations between the particle deposition over 12 zones on the floor for simulations of each source (Table 6-6, Figure 6-7 and 6-8).

The method to correlate the deposition patterns is similar to that used to compare the dispersion on individual planes in the room in the passive scalar experiments. However

the exact locations where the particles land is not used, and instead a series of 12 areas (shown in Figure 6-6) are defined on the floor and the quantity of particles landing in each area is summed. Areas were used instead of exact points because the DRW Lagrangian model is stochastic in nature, and hence even with the same model the exact deposition locations would vary for each run. Since the same number of particles were injected in each simulation the total deposition from the steady state point and zonal source are compared to the total deposited from the transient source. Once the summations for each area were completed the correlation coefficients were found by plotting the values in each area from the transient source simulation results against the results from the equivalent area in the point or zonal model.

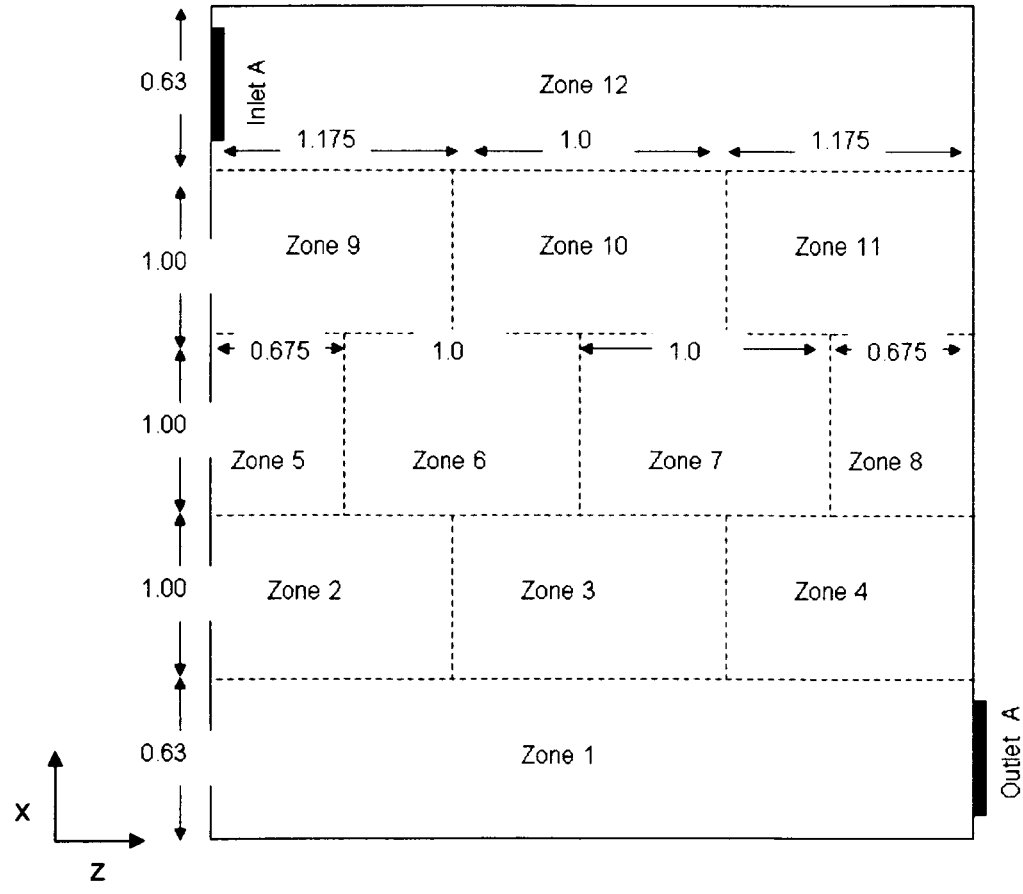

Figure 6-6: Definition of floor zones used in the Lagrangian particle tracking model to compare deposition patterns from the three different sources.

Total Floor Deposition

Table 6-5 gives the summation of bioaerosols that deposited on the floor as a percentage of the number injected for each of the three sources. The values are similar for the majority of the cases, however, with ventilation regime B and the x-x source the results from the point source indicate much less deposition than either the transient or the zonal source. The results from the zonal and point source are also lower than the transient source for both cases in ventilation regime B. This is the same regime that gave the greatest differences in the passive scalar study.

The total number of particles deposited for regime B is much greater with the transient source than for either of the other two sources. This is not the case with regime A where the total deposited is comparable between all three sources (Table 6-5). This may be due to better mixing by regime A. That there are differences between the particles behaviour in the two regimes is to be expected as different ventilation regimes have been shown to have a large influence on the quantity of particles deposited or extracted (Zhao *et al.*, 2004b).

Table 6-5: Deposition of particles from simulations of each source definition within the test chamber model. Shown as a percentage of the injected quantity.

	Zonal	**Transient**	**Point**
Regime A			
Source x-x	54	54	56
Source z-z	70	69	71
Regime B			
Source x-x	67	94	55
Source z-z	59	68	56

Correlation of Deposition Patterns

Table 6-6 shows the Spearmann's Rho correlation coefficients between the total deposited values in each area for simulations using the transient source against those using the point or zonal source, using the same technique as in section 6.3.1. The results are segregated by size of particle studied. For the particles < 20μm the correlation

coefficients are generally quite high, greater than 0.8, including comparisons between the transient and the point source models. The exception is with the correlations between the models using the transient and point source with ventilation regime B and the z-z source. This is the ceiling ventilation regime, which also saw the lowest correlation with the point source in the passive scalar results. For the larger particles the distinction between the ability of a point and zonal source to represent a transient source becomes more apparent with much lower correlations between the transient and the point source models.

Overall these results show the point source performed much better at representing the deposition associated with a transient source than was seen with the passive scalar model. This is likely to be due to the length of time the particles are airborne before deposition, allowing them to mix with the room air and become more evenly distributed through turbulent diffusion. For very large particles, 40μm and 50μm diameter, the time spent suspended in the air is much shorter. The definition of the source therefore becomes much more important as the correlation coefficients between the point source model and transient source model decrease. As with the passive scalar simulations, with ventilation regime B the ability of the point source to represent the transient source is particularly poor for the z-z source. However the zonal source model always performs as well as the point source or better. For the majority of cases the comparison of the zonal source model to the transient source results is reasonable with most correlation coefficients over 0.69.

In order to visualise the meaning of these correlation coefficients the deposition patterns for ventilation regime B are shown in Figures 6-7 and 6-8. These illustrate the differences between using the point source and using the zonal and transient sources. The plots are created by taking the number of particles deposited in each zone and distributing them evenly throughout that zone on a grid of 0.5 x 0.5m. This was then interpolated onto a 0.1 x 0.1m grid assuming a linear variation to create smooth contours. Although for the z-z source (Figure 6-7) the number of smaller particles deposited is much greater with the transient source, the predicted patterns of deposition are similar to the zonal source. The deposition from both the zonal and transient source is greater towards the side of the room where the ventilation supply inlet is located,

whereas with a point source the overall deposition is much less with the lowest deposition towards the supply inlet.

In the deposition simulations, some of the particles landing on the ground may have been in the air for a long period of time. This may explain why at low particle diameters the difference in deposition when simulating the three different sources is not as pronounced as occurs in the airborne dispersion patterns predicted by the scalar transport model. When there is good mixing of the room air the location of the source is not of such importance as the bioaerosols will become well distributed throughout the space. However it is clear that for certain cases, such as with ventilation regime B, specification of the source is very important in order to represent the correct bioaerosol transport. Since the ability of a point source to represent a transient source within a certain ventilation regime will not be known until a simulation has been carried out it is important to choose the method of representing bioaerosol sources correctly.

Table 6-6: Comparison of particle deposition positions for simulations with each source definition. Table shows Spearmann's Rho correlation coefficient between the transient source and either the zone or point source as specified. This is shown for 7 particle sizes, the two ventilation regimes and two source locations. All values are significant to 0.05 level except where highlighted. Each correlation coefficient is calculated from 12 values for each source.

	Regime A				**Regime B**			
	z-z Source		**x-x Source**		**z-z Source**		**x-x Source**	
	Zone	Point	Zone	Point	Zone	Point	Zone	Point
1 μm	0.85	0.95	0.83	0.80	0.95	0.93	0.88	0.75
5 μm	0.95	0.89	0.91	0.89	0.69	0.10	0.89	0.79
10 μm	0.97	0.97	0.99	0.99	0.92	0.014	0.93	0.90
20 μm	0.91	0.88	0.98	0.90	0.81	0.021	0.89	0.92
30 μm	0.94	0.74	0.98	0.94	0.99	0.55	0.98	0.73
40 μm	0.92	0.62	0.97	0.62	0.91	0.45	0.56*	0.58
50 μm	0.94	0.67	0.95	0.51	0.70	0.58	0.97	0.46

*Not significant

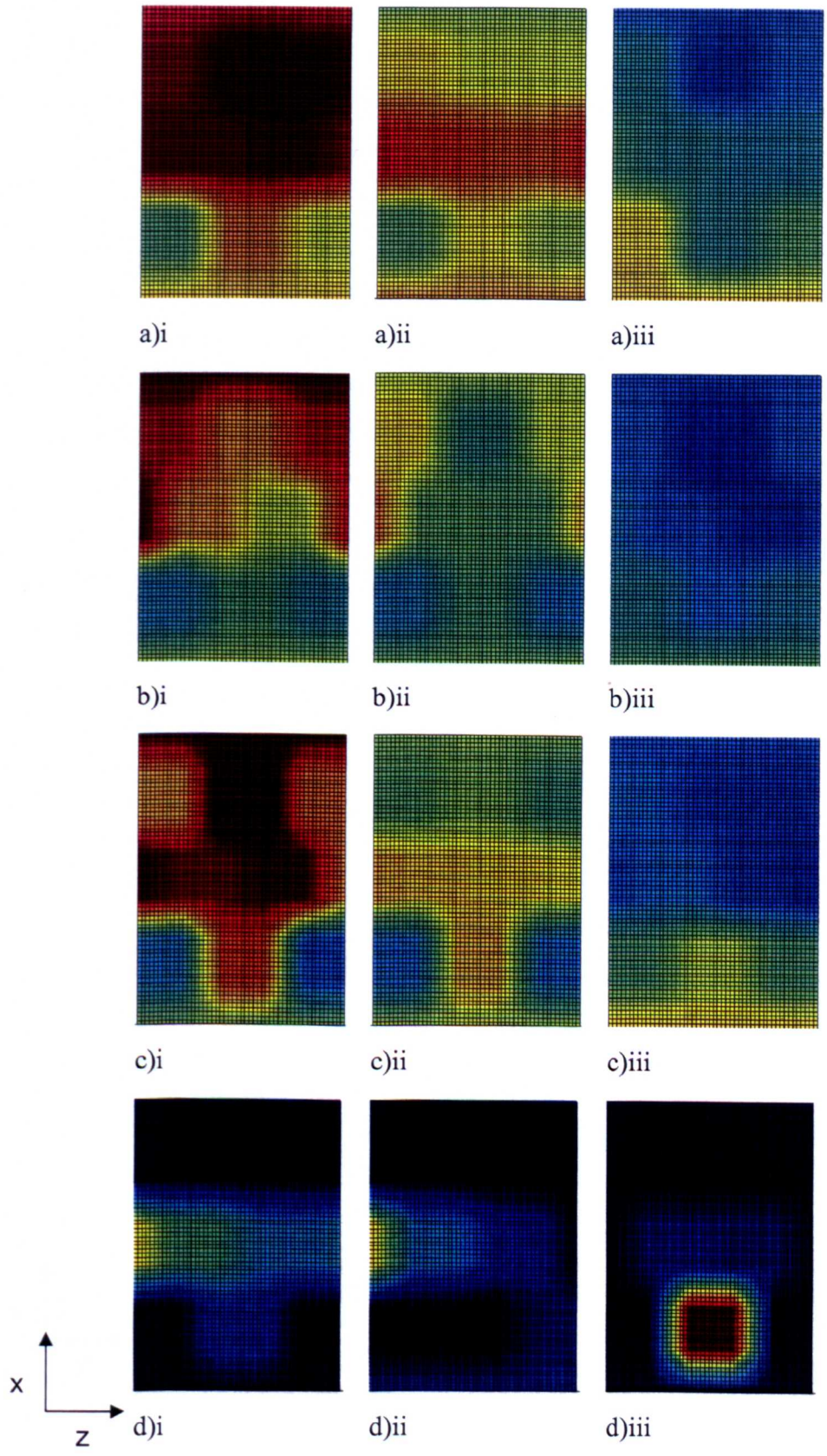

Figure 6-7: Floor deposition patterns for ventilation regime B, source z-z for particles size a) 5μm, b) 10μm c) 20μm and d) 50μm and for transient (i), zonal (ii) and point (iii) sources. Dark red indicates high deposition through to low deposition shown by dark blue.

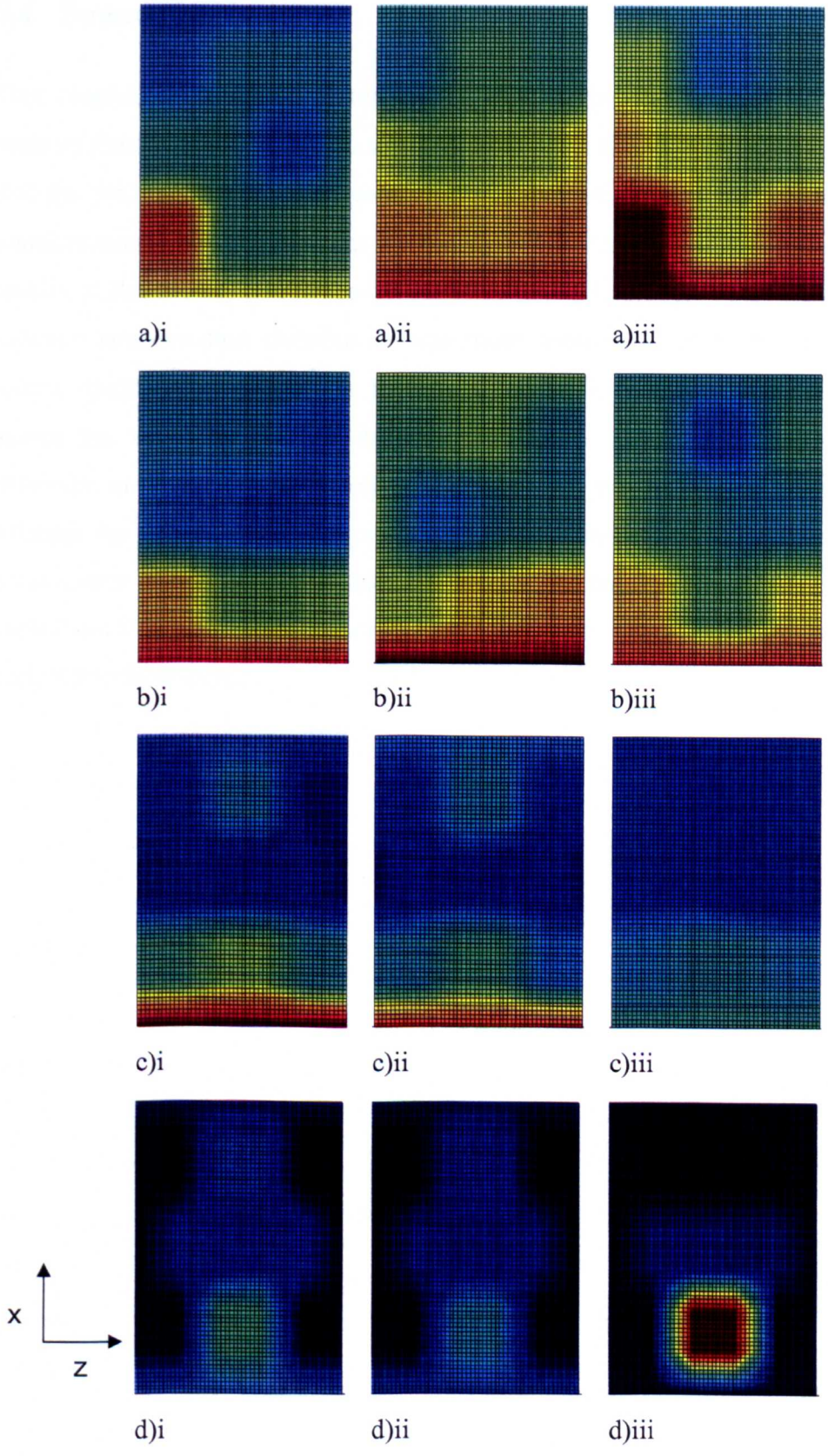

Figure 6-8: Floor deposition patterns for ventilation regime B, source x-x for particles size a) 5μm, b) 10μm c) 20μm and d)50μm and for transient (i), zonal (ii) and point (iii) sources. Dark red indicates high deposition through to low deposition shown by dark blue.

6.4 Summary

This chapter used numerical techniques to compare the time averaged dispersion patterns from a transient source to those from a zonal and point source. This showed that the zonal source provided good representation of the time average behaviour of a transient source moving at a constant speed, both in contours of concentrations (using a passive scalar model) and deposited particles (using Lagrangian particle tracking). The airborne concentration distribution was more sensitive than floor deposition to the source specification. Where the mixing of the air is improved, the definition of the source has less effect on the deposition positions of particles smaller than 30μm. However, in certain airflow regimes, the point source was found to perform very poorly, whereas the zonal source always showed reasonable results. Since the ability of the point source to represent the transient source would not be known until a simulation is carried out it is better to use a zonal source to represent the dispersion from a spatially variant transient source.

Chapter 7
Application of the Zonal Source Model

The hospital observation and sampling study (Chapter 4) and the literature review (Chapter 2) highlighted a number of activities that may not be well represented by a point source within CFD models. The previous chapter introduced the zonal source model and validated the concept of defining a spatial zone in a steady state model to represent the time averaged behaviour from a transient source. This chapter draws on the findings of Chapters 2 and 4, to demonstrate the zonal source method, (validated in Chapter 6,) within CFD models of a single occupancy hospital side room and a four-bed bay on a ward. The side room model is used to carry out a sensitivity study on the size of the zonal source which is compared to the sensitivity of the results from a point source to the injection location. Since the zonal source intends partially to provide a simpler method of representing transient sources, the CFD study of the four-bed bay is compared to results from a simpler pressure driven multi-zone model. This is carried out in order to assess the potential benefits of using CFD, or whether simpler models can provide adequate levels of detail. Finally levels of risk from both respiratory and activity based sources within the four-bed hospital bay are presented.

7.1 Source Sensitivity: Hospital Side Room Model

As outlined previously the release of bioaerosols due to activity will vary spatially and quantitatively over the zone the activity occurs in. Chapter 6 showed how a constant source moving across a space is represented more realistically by a zonal source than a point source located in the centre of the activity zone. However the zone of activity within a hospital will vary in both the quantity of released bacteria and the size of the zone it occurs in. The following considers the sensitivity of the zonal source to its volume and the sensitivity of the point source to its location. Currently when CFD simulations are used to model bioaerosol dispersion, assumptions must be made about the source location. It is therefore desirable to see what effect this assumption can have, and how assumptions that are required in the definition of the zonal source compare to current assumptions in the definition of the point source location. Within an operating theatre Chow and Yang (2004) found that the dispersion from a point source had a great dependency on location. This study will consider how important the source location is within a side room.

Since the results in Chapter 4 showed that the main activities that dispersed bacteria into the air occurred around a patient's bed when the curtains where closed, this section considers the bioaerosol release over a zone encompassing the patient on the bed. This will study the effect of changing the size of a zone that may be considered to encompass this region.

7.1.1 Side Room Model description

The definition of the model is very similar to that described in Chapters 5 and 6. The room is the same size and shape as the test chamber described in Section 5.2 and the ventilation is similar to regime B with air supplied through a four-way ceiling diffuser and extracted via a ceiling mounted grille. As the model is designed to represent a side room it includes a simplified geometry of a bed with patient located on top, a bedside table and a sink, as shown in Figure 7-1. Although the model includes a representative patient, health-care workers are not included in the room as their location will vary depending on activity. It therefore seemed more reasonable to remove them from the space, rather than guess a position. This is a major assumption and does need to be

considered, but is in line with similar studies of isolation rooms (Cheong and Phua, 2006, Kao and Yang, 2006).

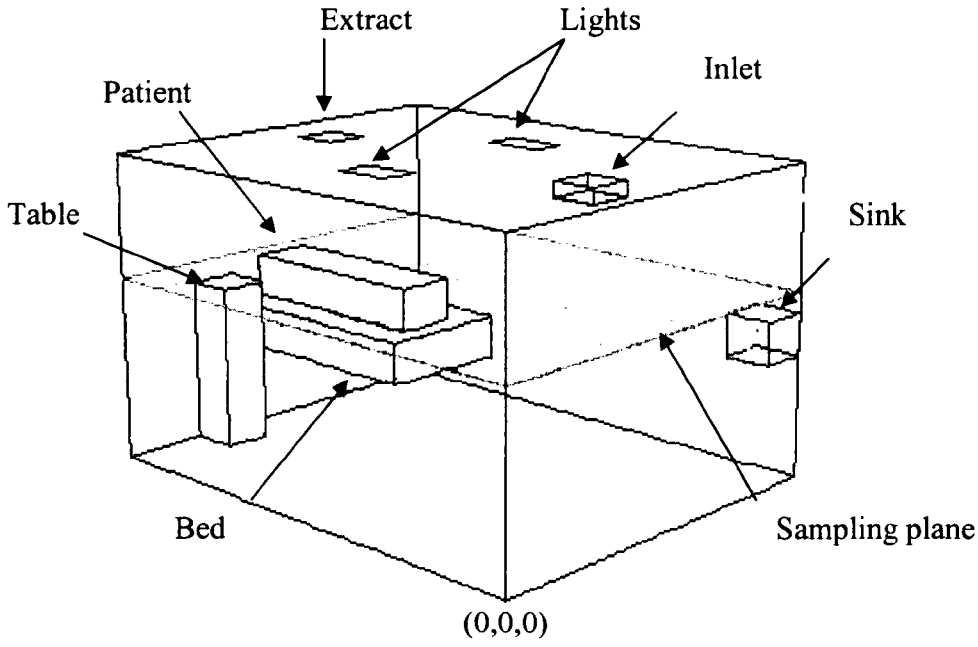

Figure 7-1: Geometry of the Side Room Model.

Boundary Conditions

The inlet and extract are in the same locations as the model described in Chapter 5, and the inlet boundary is projected into the room as described in Section 5.2.2. Table 7-1 gives the values defined at the boundaries. As far as possible these are based on recommended values, with the data source indicated in the table. Since this model attempts to represent a realistic situation, heat flux boundary conditions are applied to the lights and the patient and therefore the energy equation (equation 5-5) is solved. The values for heat flux are also given in Table 7-1.

Since a review of the literature showed a range of heat sources being used to simulate the heat produced by a patient (Bjorn and Nielsen, 2002, Cheong and Phua, 2006, Chow and Yang, 2003) the model was run initially with three different heat fluxes applied to the patient; 25, 60 and 100 $W.m^{-2}$. These were applied to the entire surface of the patient with a comparison carried out using the same convergence criteria as described in Section 5.2.6. The variation in heat flux was found to have a negligible effect on the simulated bioaerosol transport, possibly due to the high pressure differential at the extract located above the bed. Therefore 60 $W.m^{-2}$ was applied to the patient during the

side room study. This concurs with Chau *et al* (2006) who also assumed that heat flux was negligible when simulating the effect of using an extract system local to the patients head.

Table 7-1: Boundary Conditions for Side Room Model.

Inlet	10 $ac.h^{-1}$ (NHS Estates, 2005) angled at -10° to the ceiling, 20°C
Extract	-10 pa (NHS Estates, 2005)
Patient	60 $W.m^{-2}$
Lighting	50 $W.m^{-2}$

Mesh

Since the model has a similar airflow and geometry to the previous test chamber model, the grid dependency studies described in Section 5.2.7 were used to choose a suitable mesh for this model. This mesh had approximately 600, 000 cells, with 99% having values of equiangle skew less than 0.63, 87% of the mesh having an aspect ratio less than 5 and the first boundary layer having a depth of 0.012m.

7.1.2 Bioaerosol Injections

Passive Scalar

The injections were carried out in the same manner as described previously in Section 5.3.4. Point sources were represented by bioaerosol injections from a 10cm cube located in nine different locations above the bed. In the zonal source models, the same total quantity was evenly injected over six zones of different sizes. Both point and zone sources also included a momentum source of 1 $N.m^{-3}$ applied in the positive y direction. The geometries of all the source locations considered are given in Table 7-2.

Lagrangian Particle Tracking

In the Lagrangian particle tracking simulations the point source was injected from a single position in space at the centroid of the nine cubes given in Table 7-2. For the

zonal source cases the injection position for each particle was spaced evenly over the spatial zones defined in Table 7-2. Approximately 10,000 particles were injected for all the cases, imported into Fluent by prior definition in a text file.

Table 7-2: Geometry and location of the Point and Zonal Sources in Side Room Model. Point sources are a small cube, hence minimum and maximum values are given. These locations are illustrated in Figure 7-4. The zonal sources vary in depth and width, either with the lowest surface placed above and covering the width of the patient (u), or the bed (l), as indicated in Figure 7-2.

	x (m)		y (m)		z (m)	
	min	**max**	**min**	**max**	**min**	**max**
Point Sources						
A	3.85	3.95	1.35	1.45	1.125	1.225
B					1.65	1.75
C					2.175	2.275
D	3.21	3.31	1.35	1.45	1.125	1.225
E					1.65	1.75
F					2.175	2.275
G	2.26	2.36	1.15	1.25	1.125	1.225
H					1.65	1.75
I					2.175	2.275
Zonal Sources						
z(u)1	2.46	4.23	1.3	1.4	1.425	1.925
z(u)2				1.7		
z(u)3				2.0		
z(l)4	2.26	4.26	1.0	1.4	1.175	2.275
z(l)5				1.7		
z(l)6				2.0		

In order to space the particles evenly across the zonal sources the numbers of particles vary slightly between each case. The final results are therefore normalised around the injection quantity and treated as a percentage of this maximum so they are directly comparable between cases. The number of particles required was chosen by injecting

1000, 10,000 or 100,0000 particles with diameter 5μm at point source A and quantifying the deposition on the floor and the other surfaces in the room as shown in Figure 7-1. The difference in deposition, or the quantity extracted varied less than 1% between 10,000 and 100,000 particles. The zonal source z(u)1 was run five times with injections of 10,000 particles, with errors of less than 1% between the maximum and minimum deposition values on the individual surfaces. For the final source comparisons particles of three sizes; 5μm, 14μm and 20μm were considered. These were chosen based on the size of skin squame found in studies discussed in Section 2.3.2.

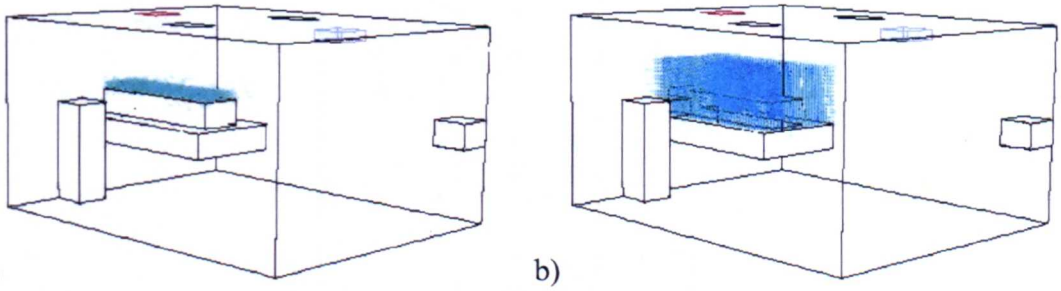

Figure 7-2: Particle injections for a) z(u)1 and b) z(l)5. The exact dimensions are given in Table 7-2

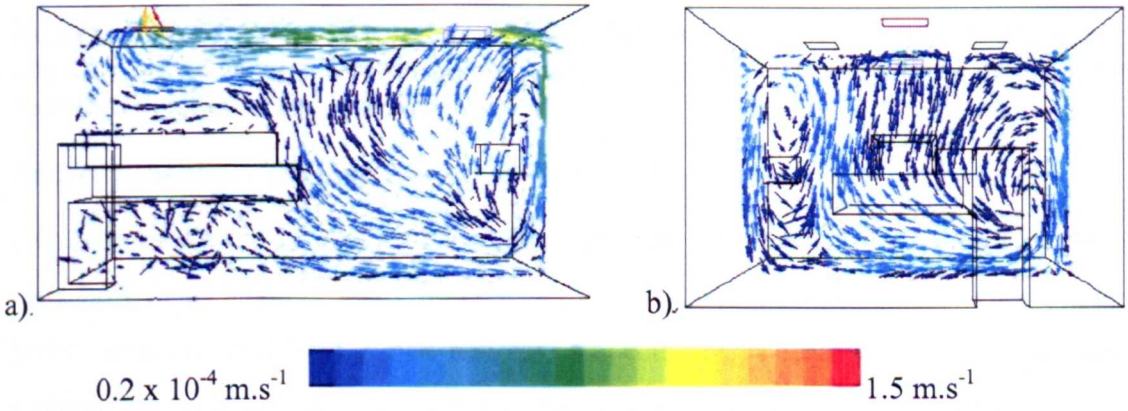

Figure 7-3: Vectors of airflow velocity in the side room model on two vertical planes a) z=1.675m and b) x=1.8m.

7.1.3 Results

Airflow

The airflow in the room is illustrated in Figure 7-3 by showing the velocity vectors on the vertical planes at z= 1.675m and x=1.80m. The air enters the room at 1 m.s^{-1} and travels along the ceiling due to the Coanda effect. The air then drops down the walls into the occupied zone at a much slower speed; less than 0.25m.s^{-1} over the patient as

required by ASHRAE (1992) to avoid drafts. Two significant areas of recirculation occur, on each side of the bed, as shown in Figure 7-3b.

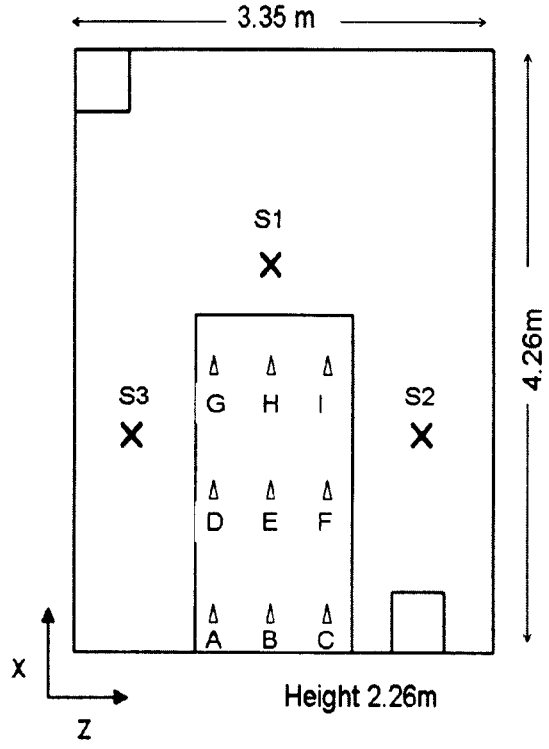

Figure 7-4: Sampling Positions (S1, S2, S3) on a horizontal plane y=1.4m for comparison between different scalar sources. Figures also show nine point source locations detailed in Table 7-2 (A-I)

Source Sensitivity Results: Passive Scalar

Contours of the transported scalar used to represent a bioaerosol distribution are shown on a horizontal plane at y=1.65m (see Figure 7-1) in Figures 7-5 and 7-6 for the nine point sources, and six zonal sources respectively. These provide a qualitative comparison between all the different bioaerosol release cases. The distribution of bioaerosols from different point source locations on top of the bed seems to vary considerably depending on the position of the source (Figure 7-5). In some cases there is a large amount of dispersion giving high concentrations to the side of the bed where the table is located (Figures 7-5 (a),(b),(c)). In other cases the source dispersion on the sample plane is very well contained (Figures 7-5 (d),(h),(i)). The dispersal from different sized zones to represent bed based activity is shown in Figure 7-6. Unlike the point source simulations, the zonal source results show similar dispersion patterns for all six cases.

Quantitative comparisons are made by comparing the volume of air in the room with a concentration greater than 5 cfu.m^{-3} for each simulation (Figure 7-7) with the average concentrations at three sample positions, S1, S2 and S3 (see Figure 7-4), around the bed (Figure 7-8). These are intended to be representative of the locations that may be occupied by a HCW dealing with the patient. The positions around the bed were chosen to be similar to work by Cheong and Phua (2006) that studied the relative risk to HCWs in different ventilation regimes. The assessment using a concentration of 5 cfu.m^{-3} was chosen as a suitable comparator for the study here, as for all cases the calculated volume is less than 50% of the room volume, yet is large enough to not be affected by the difference in the sizes of the source zone alone. The actual value allocated to the bioaerosol source is an arbitrary number and as such the results should only be compared in terms of relative values. The concentration of 5 cfu.m^{-3} does not represent either a significant risk, or little risk, it is chosen only for the reasons specified above.

The measurements presented in Figure 7-7 show there are some considerable differences in the volume of room air with a bioaerosol concentration equal to or greater than 5cfu.m^{-3} between the cases. In the case of the point source simulations, these differences vary more significantly as the distance between the point source and the head of the bed increases, as the bioaerosols become entrained into the air being extracted from the space. To examine the effect this has at specific positions, Figure 7-8 shows concentrations at the three defined sample locations. This figure shows the average concentration for that source type (e.g. point or zone) and the range of concentrations from the different source position and sizes. It can been seen in this figure how at position S2 there is much greater range in concentrations sampled between all the point source releases than with the zonal source release.

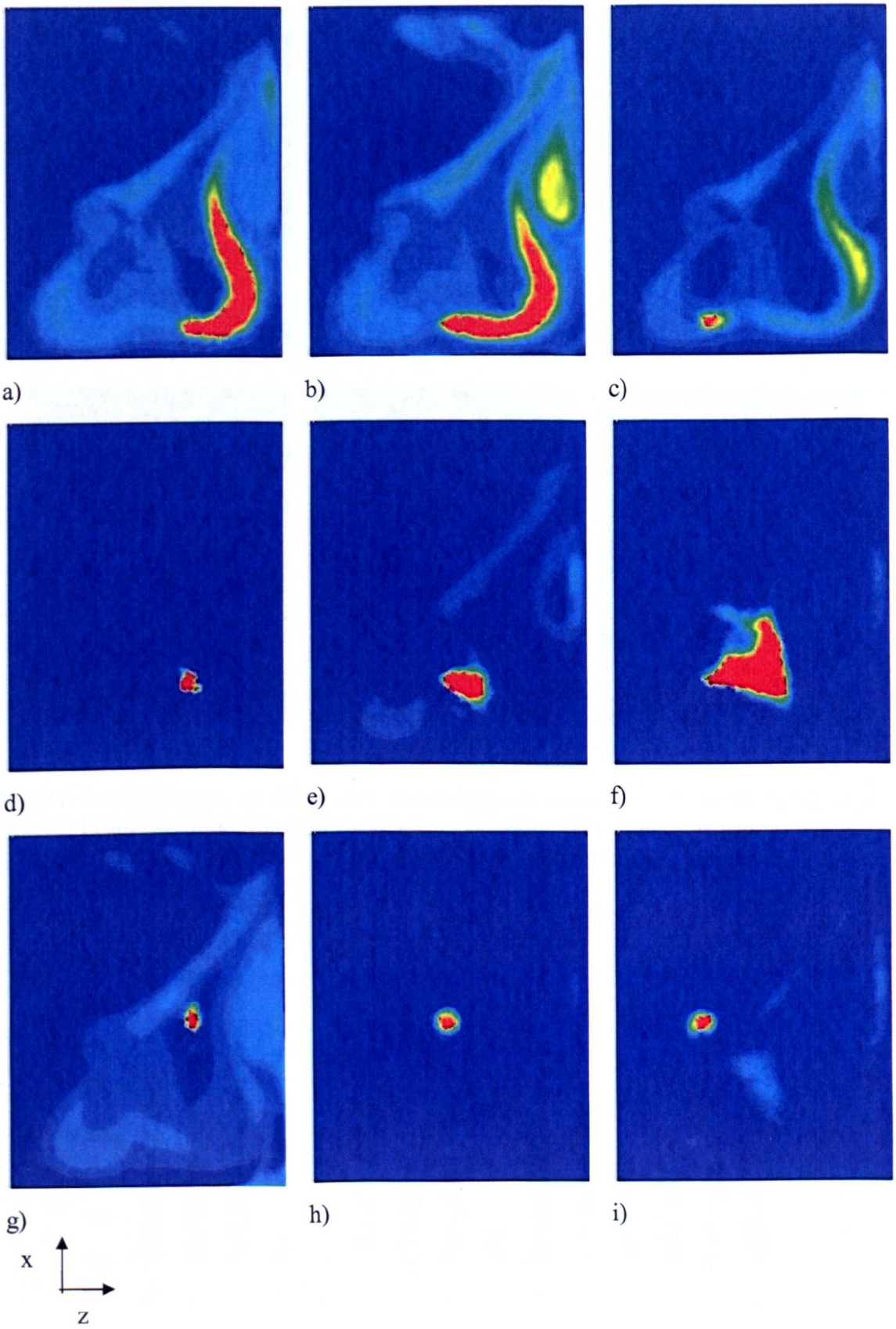

Figure 7-5: Contours of bioaerosol concentration from point sources located in different positions over the bed on a horizontal plane at y=1.65m above floor level. Red indicates the highest value of concentration, through to the lowest in dark blue. The colours relate to the same value in all plots. See Table 7-2 for source positions.

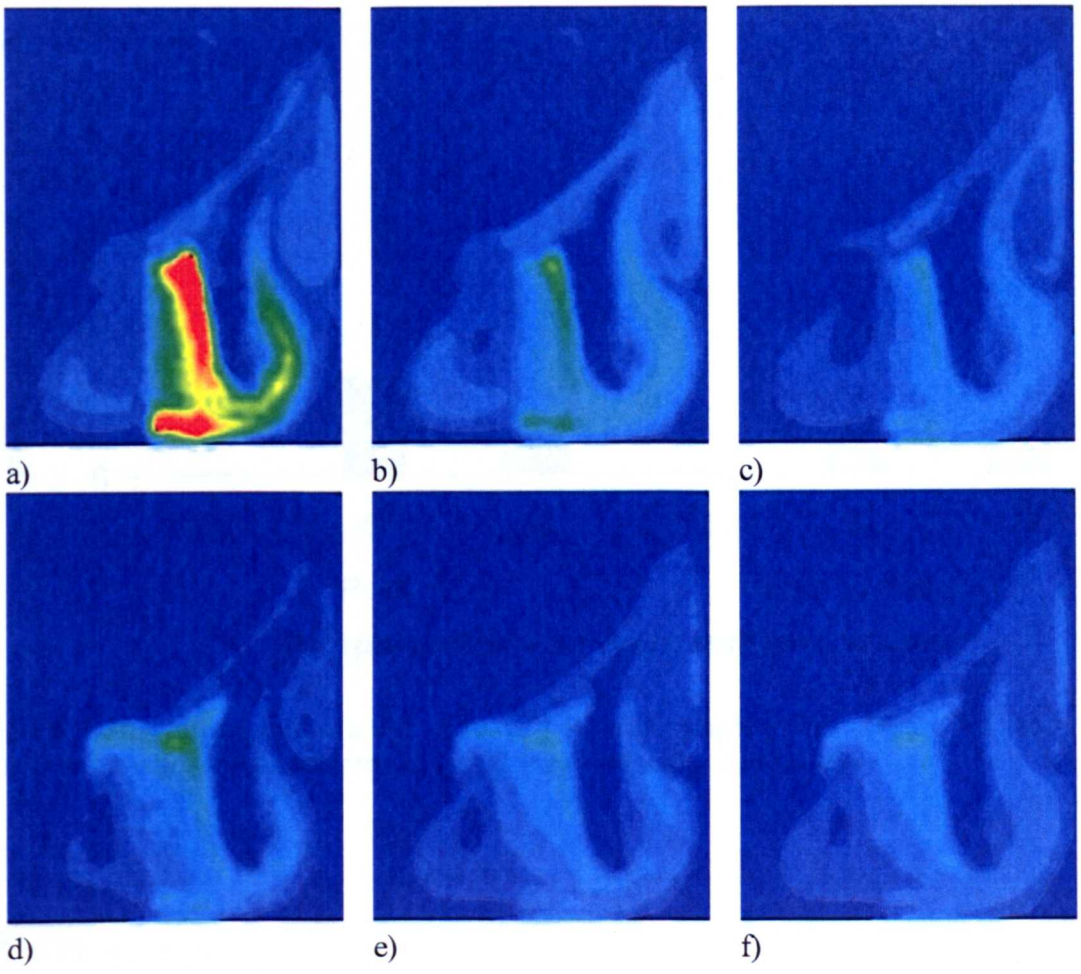

Figure 7-6: Contours of bioaerosol concentrations from six differently sized zonal sources (Table 7-2), on a horizontal plane at y=1.65m. The colours equate to the same concentrations in all plots with red being the highest and dark blue the lowest.

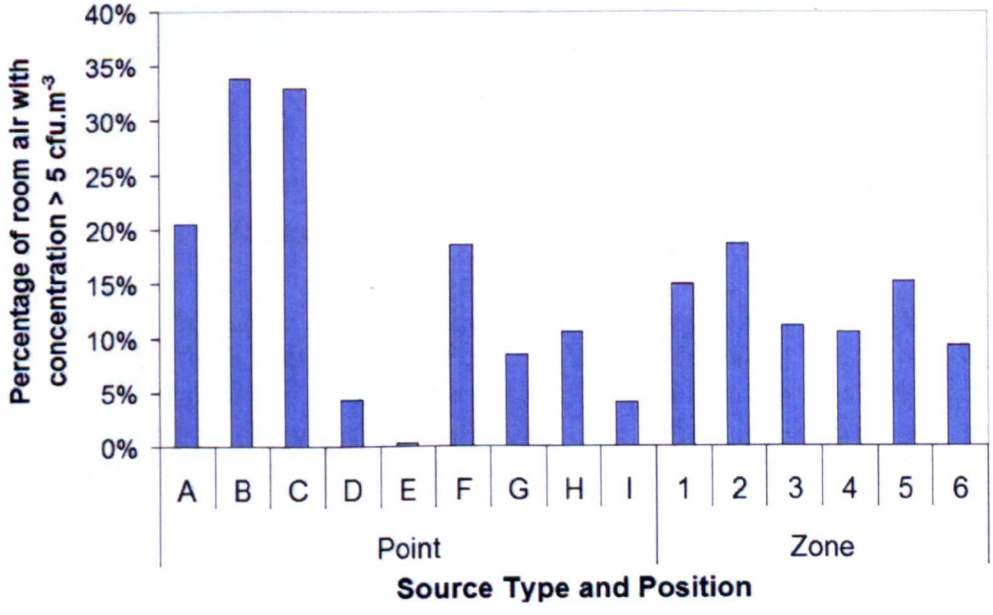

Figure 7-7: Percentage of room air with a concentration > 5cfu.m^{-3} for all simulated sources.

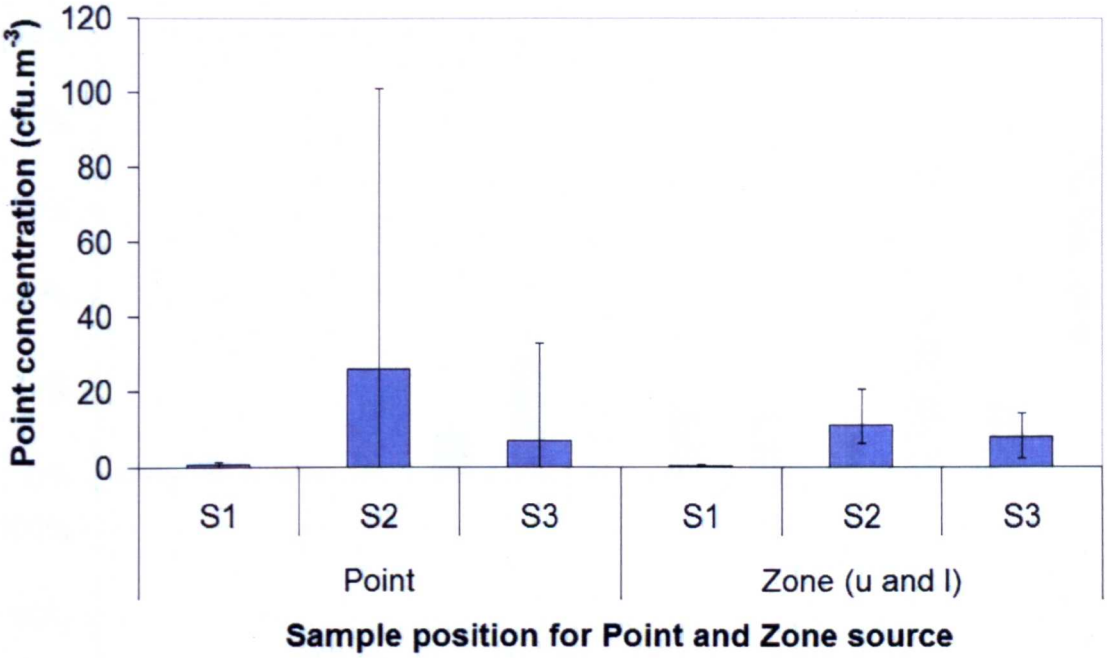

Figure 7-8: Average concentration ($cfu.m^{-3}$) at three sample points (Figure 7-4) and the respective ranges of concentrations for all the point and zonal sources.

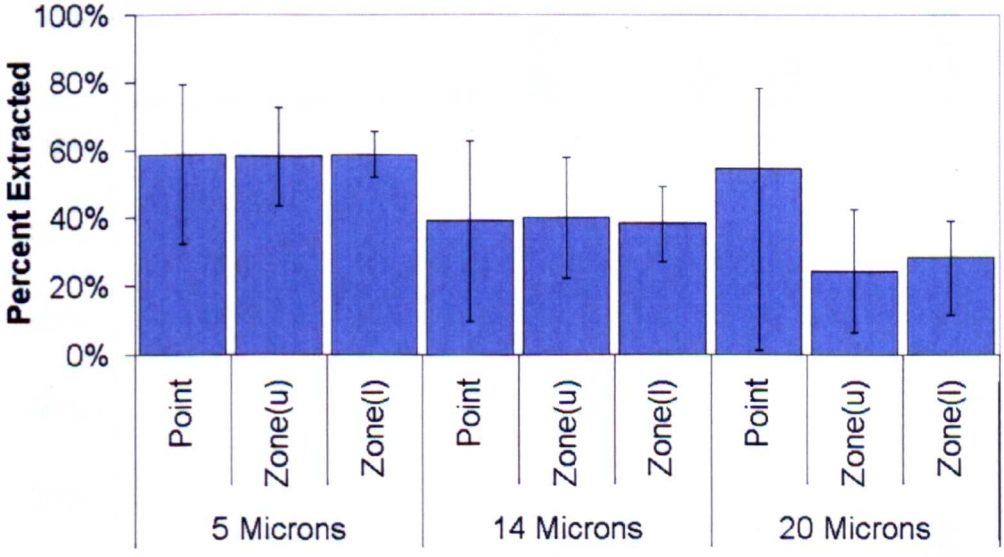

Figure 7-9: Percentage of the number of particles injected that are extracted from the space for the three source types (Point, Zone (u), Zone(l)). The error bars show the range of results for the point source position or zonal source size. The zonal source is presented for both the upper zone, on top of the patient (u) or the lower zone starting from the bed top and extending to the top of the patient and beyond (l).

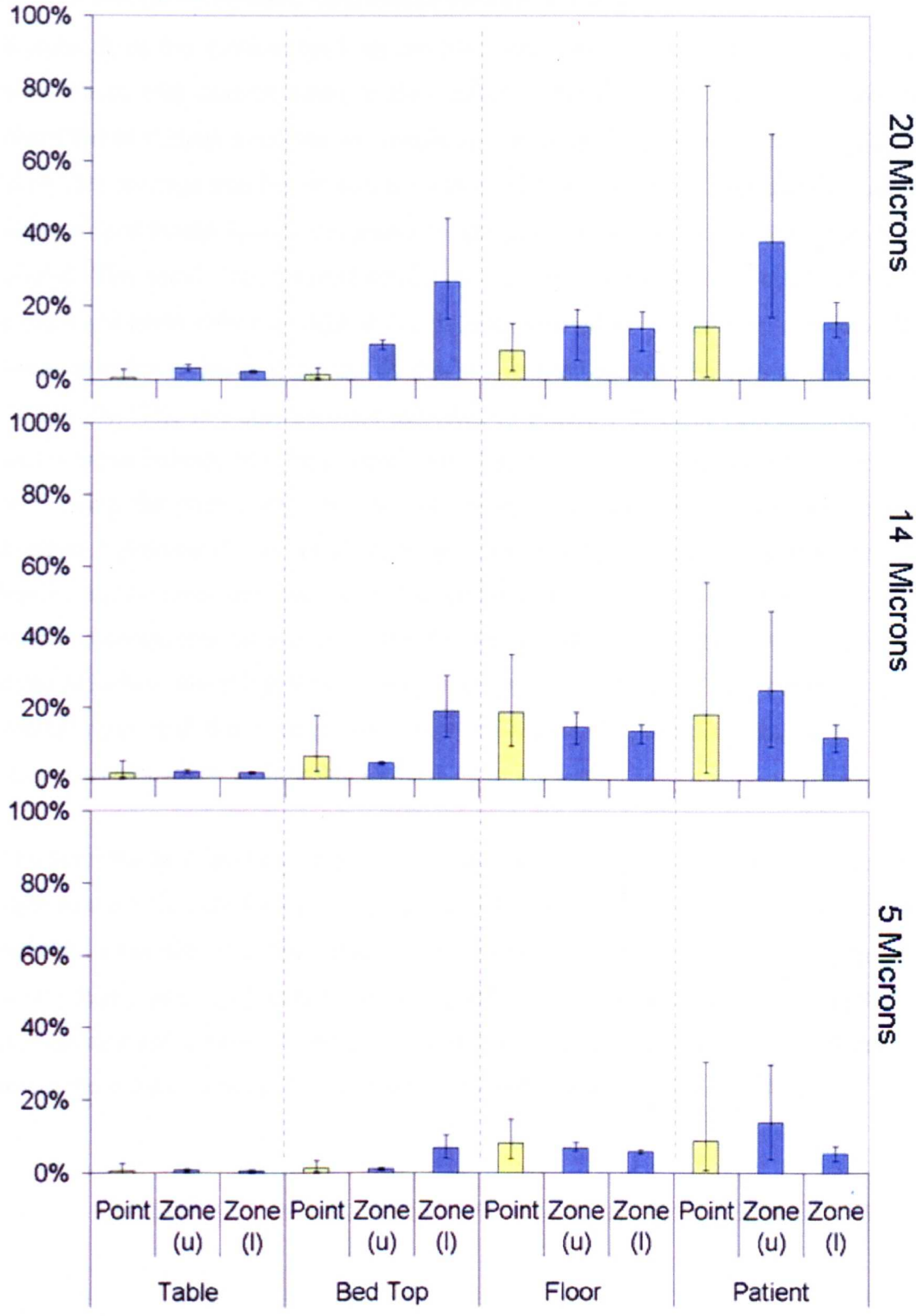

Figure 7-10: Average deposition of particles on several surfaces in the space from the point or zonal sources as a percentage of injected particles. The error bars show the range of values for that particular source type. The zonal source is presented for both the upper zone, on top of the patient (u) or the lower zone starting from the bed top and extending to the top of the patient and beyond (l).

Source Sensitivity Results: Lagrangian Particle Tracking

Results from the particle tracking models were treated differently from the scalar simulations, with analysis based on the number of particles extracted from the space or deposited at various locations for simulations with each source definition. Figure 7-9 shows the average number of particles extracted from the space averaged over all the point source model results, compared to the averages for zonal sources z(u)1-3 and z(l)4-6. The zonal source model results are split into the zones that occur above the patient and cover only the width of the patient (denoted as 'upper' (u)), and zones that begin at a lower position on top of the bed and encompass the patient (denoted as 'lower' (l)). The two scenarios are indicated in Figure 7-2. Error bars are plotted for each case to indicate the range (maximum to minimum) of deposition values obtained by moving the point source location or changing the size of the zonal source. The average deposition values for all cases for 5μm and 14μm diameter particle are very similar but the range of values is smaller for the zonal source, and smaller too when the source encompasses the entire patient. For the 20 μm particles the range of particles extracted when modelling the nine point sources is much larger than either of the zonal source types, and the average percentage deposition is quite different for the point source in comparison to the zonal source.

The percentages of particles deposited on four surfaces; the bedside table, the bed, the floor or the patient are shown in Figure 7-10. Deposition on the sink was also quantified but this is not shown as the results were less than 1% in all cases. Between the two source types (point and zonal) there are similar ranges for each case with a particular particle size and deposition locations. However there is greater deposition on the bed top in the zonal source models, particularly from the 'lower' zones (z(l) 4-6).

7.1.4 Discussion

Passive Scalar Transport

To define a zonal source, the spatial volume over which the dispersion from activity occurs in needs to be identified. This geometry will differ for each activity and also for different occasions of the same activity. For example, each time a bed is made the zone will change. Since this concept of the zonal source is a time averaged behaviour the zone should encompass the entire volume the activity occurs in. Figure 7-6 showed how the different sizes of zonal source do not have a particularly strong effect on the dispersion patterns. There are however some differences; zone z(u)1, the smallest zone, results in a much higher concentration across the bed. This is due to the higher concentration at all these points than in the larger zones due to averaging the total source concentration over a smaller space. Although there is some variation in the predicted dispersion between the zonal sources this is not as great as the effect of placing a point source in different locations. As shown by Figure 7-7 the variation in volume of air with a concentration greater than 5 cfu.m^{-3} is only 10% points between the zonal source results compared to 34% points between the point source simulations.

The dispersion of bioaerosols from a point seems to be highly sensitive to the source location. Figure 7-7 indicates the largest difference is between source location at B and E. The dispersion in these two cases are shown in Figure 7-11 as iso-surfaces of bioaerosol concentration with a value of 15 cfu.m^{-3}. These plots show how much smaller the dispersion is for case E, due to a large proportion of the bioaerosols being directly extracted rather than circulating in the room. Locating the source in position B not only results in much higher concentrations of bioaerosols over a larger volume of the room, it also results in higher concentrations within the likely occupied zone.

Cheong and Phua (2006) assessed the risk to HCWs at different locations by considering the bioaerosol distribution, and concentrations at three points similar to those shown here. However they only considered the release from a single point, and did not consider the sensitivity of the model to the definition of the source location. The results presented here indicate that very different concentrations may have been obtained from small differences in the source position, Figure 7-8 shows a wide range of concentrations sampled from position S2 depending on the location of the point

source. A relocation of the source from position B to A (Figure 7-4), a movement of only 50cm, gives a reduction in concentration at S2 from 96 to 24 cfu.m^{-3}, whereas the distribution from the zonal sources remain similar for all cases simulated. Overall the distribution of a scalar concentration from a zonal source has less dependence on size than a point source does on location. The greatest differences occur for the thinner sources, however errors in the thickness of the specification of the zonal source will still not impact on the results as significantly as an incorrect placement of a point source. In addition, since the release of bioaerosols from activity within a zone could occur at any point, and will vary during the activity, if a point source is used to represent the greatest release and is located incorrectly this will not give an accurate description of the resulting dispersion.

Despite this, the results shown here indicate that a point source located near to the head of the bed (A, D, and G) results in much higher concentrations than the other point sources or the zonal source for a HCW located at sampling position S2. Therefore to consider infectious particles in a respiratory disease, released from the mouth of the patient (i.e. a small point), then the zonal source is not representative of the release. It is suggested that a point source should be used in these cases as it enables the peak risk to the HCW to be better evaluated. However it may be necessary to simulate the dispersal from a selection of locations within a region that the mouth may be located as a relatively small movement can lead to large changes in the result.

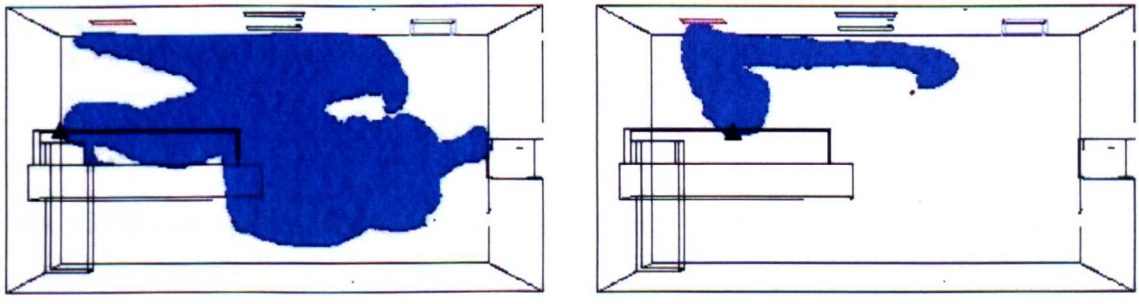

▲ Approximate release point

Figure 7-11: Dispersal of bioaerosols from point source B (left) and E (right) shown using iso-surfaces with concentration 15 cfu.m^{-3}. The source locations are on the central axis of the bed with the two positions approximately shown by the black triangle.

Lagrangian Particle Tracking

Figure 7-9 shows how the range of particles extracted from the space is greater for the zonal source of type u compared to type l. However this is mainly due to the results with zone z(u)1 which is a very thin layer on top of the patient and results in much higher deposition onto the patient than the other zone definitions (Figure 7-10). This zone is only 0.1m thick, compared to the cell dimensions in the main domain being around 0.08m. Having such a relatively thin layer on top of the patient results in a larger number of particles in the near wall region where there may be numerical issues that cause higher deposition (see Section 4.3.2). Similarly for simulations with the lower zones (l) there is a much greater influence of zone size on the number of particles that are deposited onto the top of the bed. Again the biggest difference is due to the smallest zone and the larger the zone the smaller the deposition onto the surface below the zone. This is logical, particularly for larger particles, as having further to fall is likely to result in a greater chance of particles being transported away from the source zone before depositing.

These results suggest that when choosing the geometry and location of a source, either point or zonal, that it is important to consider the quantity of particles that will be injected close to a surface. Even for a zonal source the size and shape of the source can affect the numerical solution of the transportation and so some thought needs to be given to how this is defined. Despite this, the results from the Lagrangian particle tracking models concur with the passive scalar models with the extraction and deposition of particles not as sensitive to an increase in size of a zonal source, as the point source is to location.

Summary

The dispersion patterns from a point source release of bioaerosols modelled as either a passive scalar or discrete particle can be very sensitive to the location of the source. The dispersion due to a zonal source in comparison provides similar results for a range of depths of zone. Different widths of source were also shown to only affect the dispersion patterns by a small amount for the two widths considered in this model.

However the results showed that if a zonal source definition is too thin then it may result in higher concentrations at the source in the case of the passive scalar method and

a greater deposition at surfaces directly below the source when using particle tracking. With a computational grid and airflow as defined here, once the zonal source has a thickness greater than 0.3 m, an increase in size has only a small effect on the predicted distribution of the bioaerosols.

7.2 Application of Zonal Source: Four-Bed Bay

This section presents the application of the zonal source model to bioaerosol dispersion in a four-bed bay, using the CFD methodology outlined previously and an alternative approach; multi-zone simulation. This is a quicker and simpler model than CFD simulation and inherently requires any sources to be released across a whole zone. The two methods are compared to see if the multi-zone methods would provide reasonable results to assess the risk to staff and patients in the bay.

First a description of the theory behind the multi-zone method is presented, followed by model specific data for both this model and the CFD model. The results of the comparisons between the models are presented followed by a more detailed study into the bioaerosol transport in the hospital bay using the CFD simulation.

7.2.1 Multi-Zone Methodology

The use of multi-zone models for building services applications can enable the solution of time dependant problems to be obtained more easily and quickly than with CFD simulations (3.1.3). Although this thesis has focused on CFD it is useful to examine how this technique compares to a multi-zone model, particularly one including the use of a zonal source for a bioaerosol release. Multi-zone models divide an indoor environment into a number of regions and assume that each zone is fully mixed, with only partial mixing occurring between zones defined by an inter-zonal flow rate (Brouns and Waters, 1991). These flow rates can be defined using different techniques, for example, from CFD models (Noakes *et al.*, 2004a). In classical multi-zone methods the concentrations in individual cells are solved using principles of the conservation of mass, whereas the flow between individual cells is derived from pressure differences. Other methods have been introduced to better represent the flow due to thermal plumes and air jets (Mora *et al.*, 2003, Ren and Stewart, 2005).

In this study an in-house code, VENT, developed by the engineering consultancy Arup (Building London Group. Fitzroy Street, London) was used to analyse the airflow and bioaerosol transport in a four-bed hospital bay. This uses the classical method of pressure differences to solve the inter-zonal flow rates (Arup, 2001). These pressure differences can be defined from mechanical ventilation, external wind pressures and temperature differences between zones. As with the CFD method, the continuity equation must be satisfied for each individual zone, therefore the mass flow rate into a zone from all the openings must equal the mass flow rate out of the zone. This can be expressed as equation 7-1 where $\dot{m}$ is the mass flow rate across 1 to n openings.

$$\sum_{1}^{n} \dot{m} = 0 \qquad 7\text{-}1$$

The mass flow rate through each opening is defined by the pressure difference across it:

$$\dot{m} = ACd\Delta p^{n}\rho \qquad 7\text{-}2$$

A is the area of the opening, Cd the coefficient of discharge and n is a constant related to the aperture type, usually given a value of 0.5 (Mora *et al.*, 2003). The density of the air, ρ, is defined based on the temperature of the air in the room using the ideal gas equation:

$$\rho = \frac{p}{RT} \qquad 7\text{-}3$$

Here T is the temperature (K) of the air in the space and R is the gas constant, 287 $J.kg^{-1}.K^{-1}$ for air. Since within a building the density of the air is affected to a much greater degree by the temperature than due to the height, the pressure is taken as being constant at 101,325 Pa throughout.

The pressure difference between the zones Δp in equation 7-2 is defined differently for either internal or external connections. For internal connections the pressure at the opening, p_h, within one zone is corrected for the height, h, from the pressure at the floor, p_f:

$$p_h = p_f + \rho g h \qquad 7\text{-}4$$

For external connections the pressure is also corrected for wind speed.

$$p_h = p_f + \rho g h + Cp\left(\frac{1}{2}\rho U^2\right) \qquad 7\text{-}5$$

Here U is the wind speed which may also need to be corrected for height if the values are taken from those provided by the meteorological office U_{met} which are measured at a height of 10m. The correction equation is:

$$U = CU_{met}h^p \qquad 7\text{-}6$$

where p is the pressure at height h, and C is a constant.

Defining the mass flow rate across each opening due to the pressure difference between them using equation 7-2 and then using the continuity equation for each space gives a set of non-linear equations. These are solved iteratively using the Newton Raphson method.

The geometry of the ward studied is shown in Figure 7-12 and the boundary conditions are given in Table 7-3. The geometry and boundary conditions are equivalent to the CFD model that is described below in Section 7.2.2. Within the model the bay is split into 12 zones and the corridor into 6 zones. The bay is divided in half vertically, and so half the zones are at ground level and half have a base at 1.3m high. These zones are shown in Figure 7-13. Each of these zones is considered to be well mixed, and the connections between the zones are treated by defining the whole 'wall' of adjacent volumes as a two way hole; air can flow in both directions through the hole. The bioaerosol source is injected into zone 7 and is assumed to be fully mixed into this zone. The zones were defined in this layout in order to provide an individual zone around each bed space which can be treated as an activity source, and to allow the central area of the bay to be treated separately. This also allows the results to be compared at different points in the bay, not just the average concentration across the entire room.

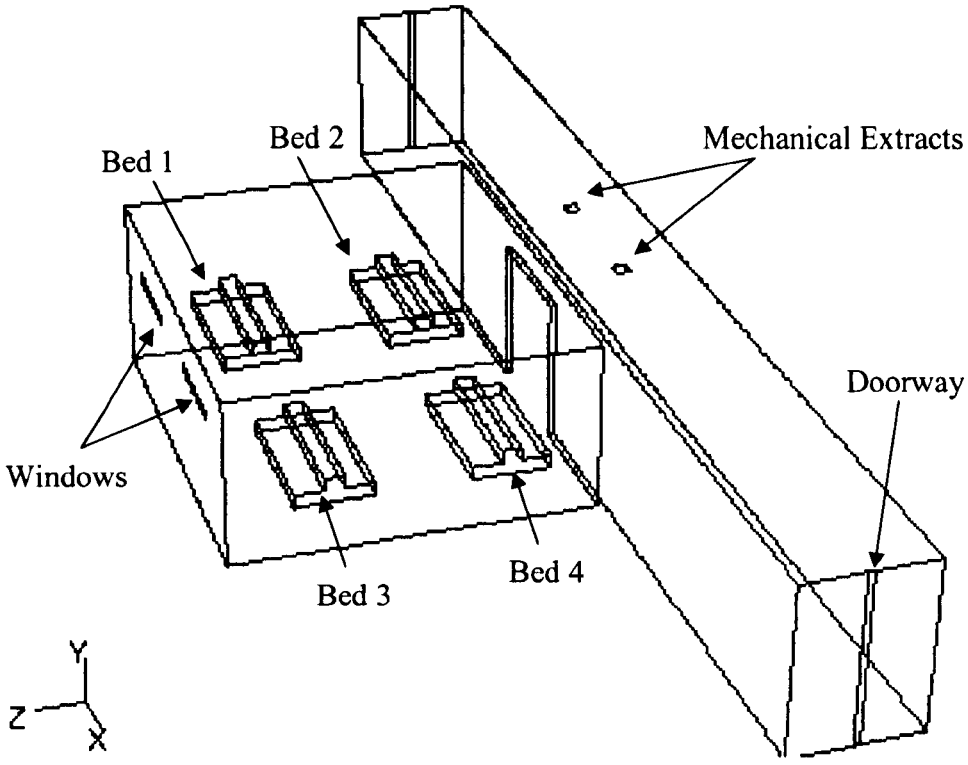

Figure 7-12: Schematic of four –bed bay on a hospital ward.

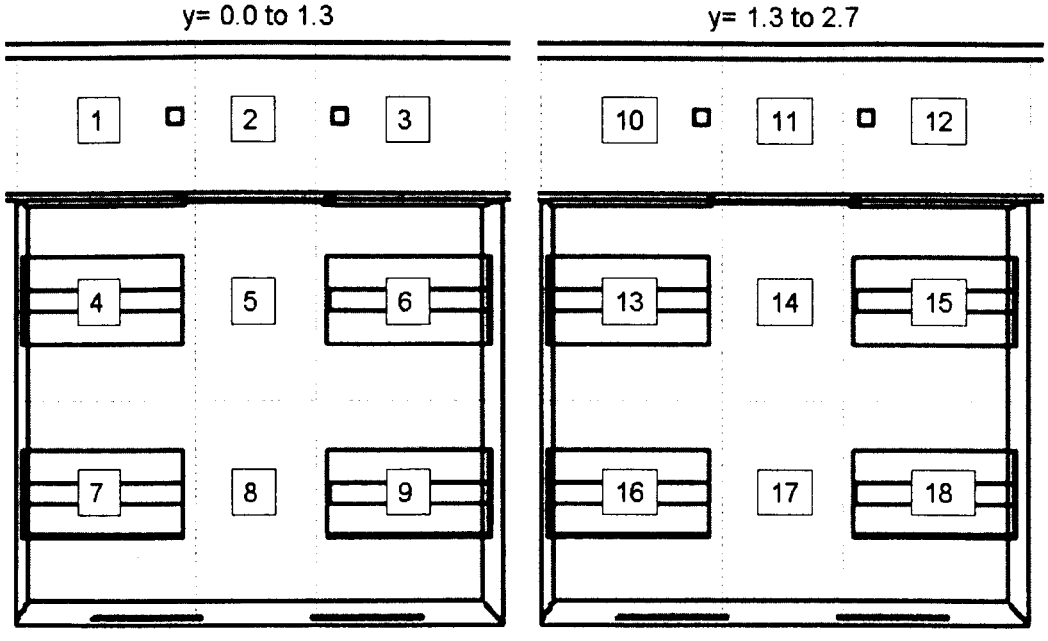

Figure 7-13: Zones as defined in VENT, equivalent to the zones used for post processing in the CFD model to compare the results. The zones are split over two levels, as shown, with zones 1-9 at y<1.3m and zones 10-18 above at y<1.3m.

Table 7-3: Boundary Conditions for CFD and VENT Models of a four-bed hospital bay.

Boundary	CFD	VENT
Inlet	Air Speed = 0.26m.s^{-1} Temp=294 K	Air flow in = 39 l.s^{-1} Temp 21°C
Extract	Pressure differential = -0.1pa	Extracted 30 l.s^{-1}
Doorway	Pressure differential = 0pa Return Flow Temp = 296K	Two way hole Pressure = 0pa Return Temp = 23 °C
Heat Flux	20 W.m^{-2} on each patient Patient surface area = 2.13 m^2	Average temperature for each zone taken from CFD inputted into VENT.
Time Steps	1 s time steps. Results out put every 12s	0.017minutes

Time Stepping

A transient solution to the bioaerosol transport throughout the space was found to enable direct comparisons with VENT which is designed to study the decay of contaminants over time. The program is set up to have 24 time steps for which the input parameters can be changed. The solution for each major time step is carried out using 12 quasi-time steps with a fixed data set. Each of these are set to a value of 1s, resulting in a total solution time of 12x24=288 seconds. Bioaerosols are injected with an arbitrary value of 500cfu.s^{-1} for the first 12s, which is reduced to zero for the remaining major time steps. The other boundary conditions remain constant for the entire duration of solution time.

7.2.2 CFD Methodology

The geometry of the ward is shown in Figure 7-12 and the boundary conditions are given in Table 7-3. Only one bay is considered, and the corridor is extended with a thin neutral pressure boundary at either end to simulate the crack between the door way. Other bays are ignored to reduce the mesh size, but the extension of the corridor is used to reduce the effect the boundary conditions at the end have on the flow in the bay itself. The situation modelled is similar to Ward 8 at St James's University Hospital, Leeds,

where the air sampling study described in Chapter 4 was carried out. This has mechanical extracts in the corridor and receives fresh air into the ward by natural ventilation via opening windows at the end of the bay opposite the corridor. This model considers typical summer conditions with both windows open. The windows are sized the same as those on Ward 8 and are defined as being open to a gap of 10cm, the maximum allowable opening of windows in hospital wards (NHS Estates, 1989). The inlet velocity is taken using typical summer conditions where a pressure differential between the interior and exterior is likely to be between 0-1pa (CIBSE, 2005). A pressure difference of 0.1pa is chosen to simulate a lower airflow, and hence the 'worst case' scenario with less dilution of bioaerosols. The flow rate through the opening is found using equation 7-7 taken from CIBSE (2005)

$$Q = C_d A \sqrt{\frac{2|\Delta p|}{\rho}} \qquad 7\text{-}7$$

Here Q is the flow rate through the opening, $m^3.s^{-1}$, C_d the discharge co-efficient (0.65), A the area of the opening, m^3, Δp is the pressure difference across the opening, Pa, and ρ is the air density, $kg.m^{-3}$. The resulting volume flow rate for the opening is given in Table 7-3 and this is converted to a velocity for input into the CFD model. The temperatures of the patients are taken from the values used by Brohus (2006) adapted to the surface area of patients in this model but rounded up to account for hospital equipment surrounding the bed. The temperature in the final model fits within the design conditions for hospital wards at an average of 22.5°C (CIBSE, 2006). The temperatures in the VENT model are taken as the averaged values for each zone from the CFD simulation.

Bioaerosol Source

Two different bioaerosol sources were used within the CFD model for comparison to the VENT model. A zonal source was set up with the same dimensions as in the VENT model, filling the entire volume of zone 7, and a point source was injected at the head of bed 1 (located in zone 7). In these cases no momentum source was included to eject the bioaerosols into the space, as it was not possible to define in the VENT model and so was also neglected in the CFD case for better comparison. The transport of bioaerosols through the domain is modelled transiently in both cases, with the injection occurring

over the first 12 seconds of the simulation. The time steps for the simulations are given in Table 7-3. There is significant computational time difference between running the two models. The VENT model takes a matter of minutes to achieve a solution, while the CFD model required 24 hours to solve for the transient bioaerosol transport, in addition to 48 hours required for the airflow convergence.

Convergence

The VENT model converged with an overall volume flux of 0.2% of the inlet values. The same convergence criteria was used for the CFD model as specified in Section 4.2.6.

A fully mixed analytical model is also applied to the space by applying the equation below to the whole bay to find the concentration C at time t..

$$C_t = C_o e^{\frac{-Qt}{V}} \qquad 7\text{-}8$$

Here C_o is the original concentration, Q the volume flow rate of air $m^3.s^{-1}$, and the volume of the bay V.

CFD Grid Dependence

Grid dependency was carried out for the CFD hospital ward model with the three meshes shown in Table 7-4. In all cases these are Tet-hybrid meshes defined in the same manner as in the previous models. A point source bioaerosol release was placed at the head of bed 1 (see Figure 7-12) and the scalar transport method was used to simulate bioaerosol transport for the three meshes. Bioaerosol concentration contours on a horizontal plane at y=1.35m are shown in Figure 7-14 for the three meshes. As well as considering the volume average scalar concentrations for each mesh, the bioaerosol concentration at patient 2, and hence the risk to that patient, or the concentration that remains in the cells immediately above patient 1, the source patient, was also found (Table 7-4). From this dependency study mesh 2 with approximately 1,510,000 cells was chosen; this is equivalent of a cell sized approximately 0.08m in the centre of the domain and a wall-cell distance of 0.01m. As before the k-ϵ turbulence mode is used with enhanced wall treatment.

Table 7-4: Grid dependency for CFD model of four-bed bay. For each mesh the number of cells, the volume average scalar concentration and the scalar concentration on a plane directly above patient A and B are given.

Parameter	Mesh 1	Mesh 2	Mesh 3
Number of Cells	914732	1515361	1928199
Volume Average Scalar (cfu.m^{-3})	8.1	5.9	6.1
Concentration above Patient A (cfu.m^{-3})	19.4	13.3	13.9
Concentration above Patient B (cfu.m^{-3})	14.7	10.8	10.6

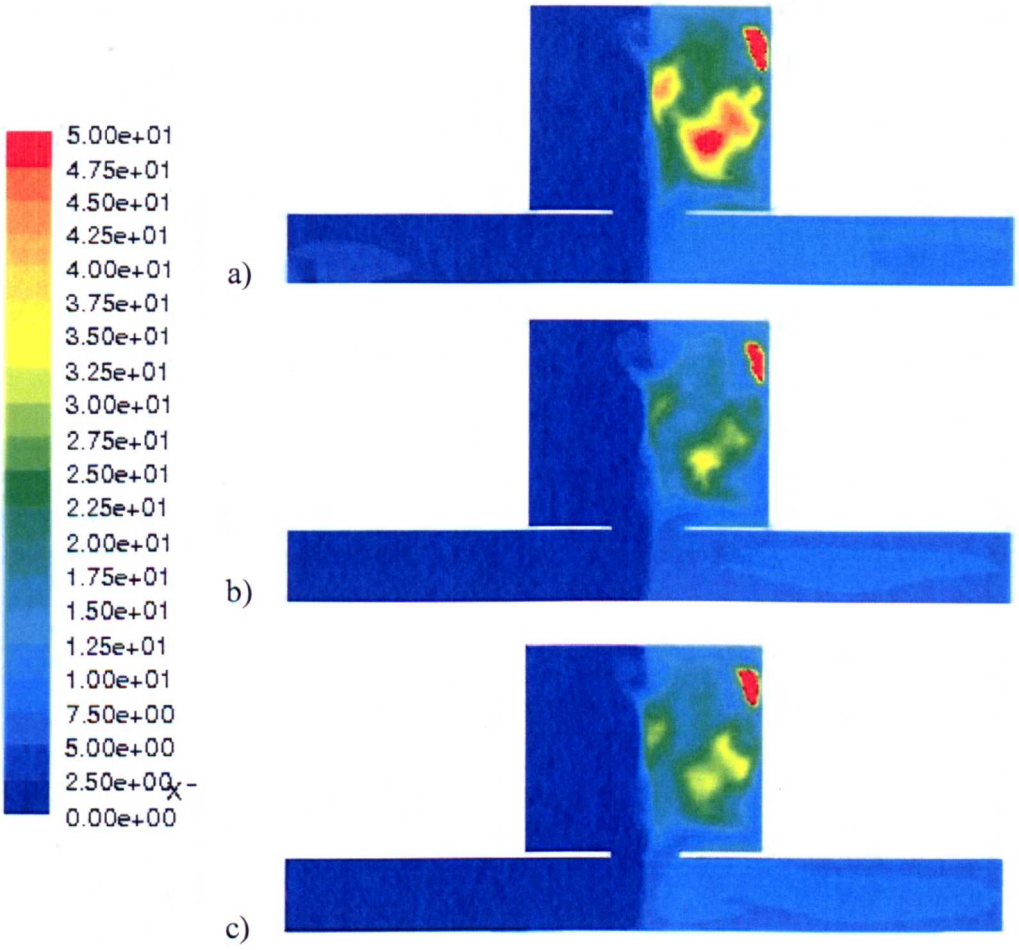

Figure 7-14: Contours of bioaerosol concentration (cfu.m^{-3}) on horizontal plane y=1.35m with approximately (a) 900, 000 (b) 1,500,000 and (c) 1,900,000cells

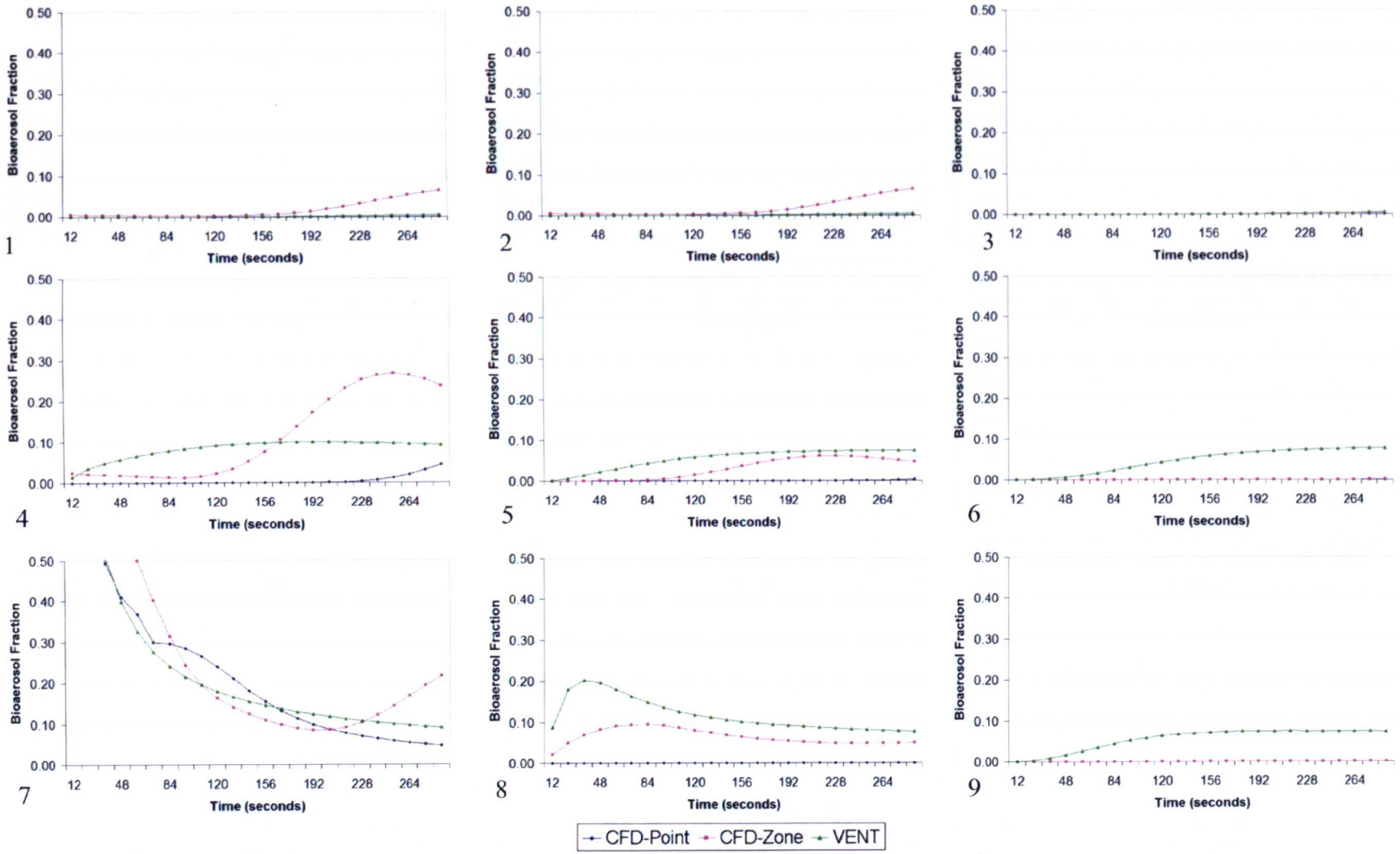

Figure 7-15(a): The variation of bioaerosol concentrations, represented as a fraction of the source concentration, in zones 1-9 as labelled over time. Figures show the difference between the CFD models with point and zonal sources and using the VENT model.

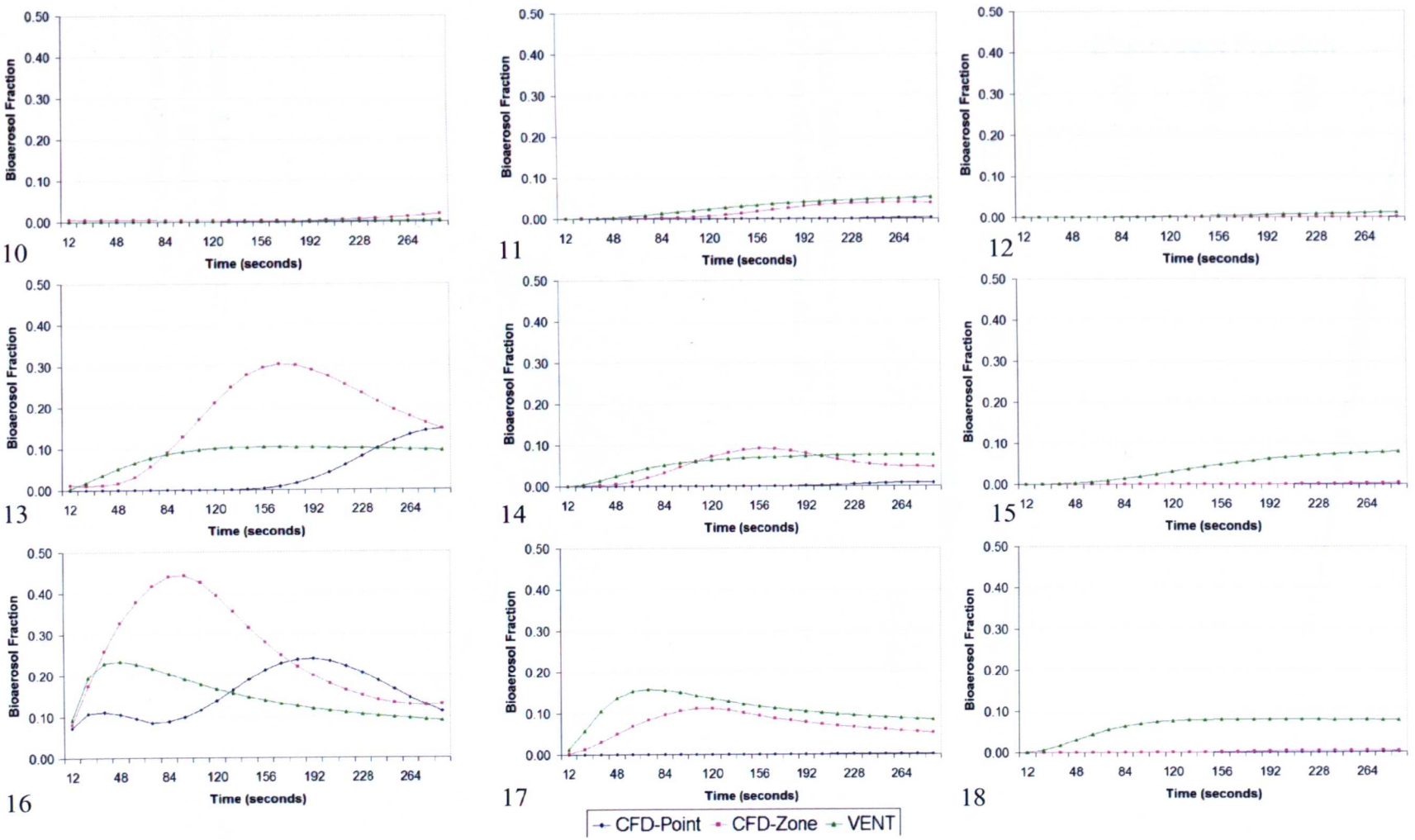

Figure 7-15 (b): The variation of bioaerosol concentrations, represented as a fraction of the initial source concentration, in zones 10-18 as labelled over time.

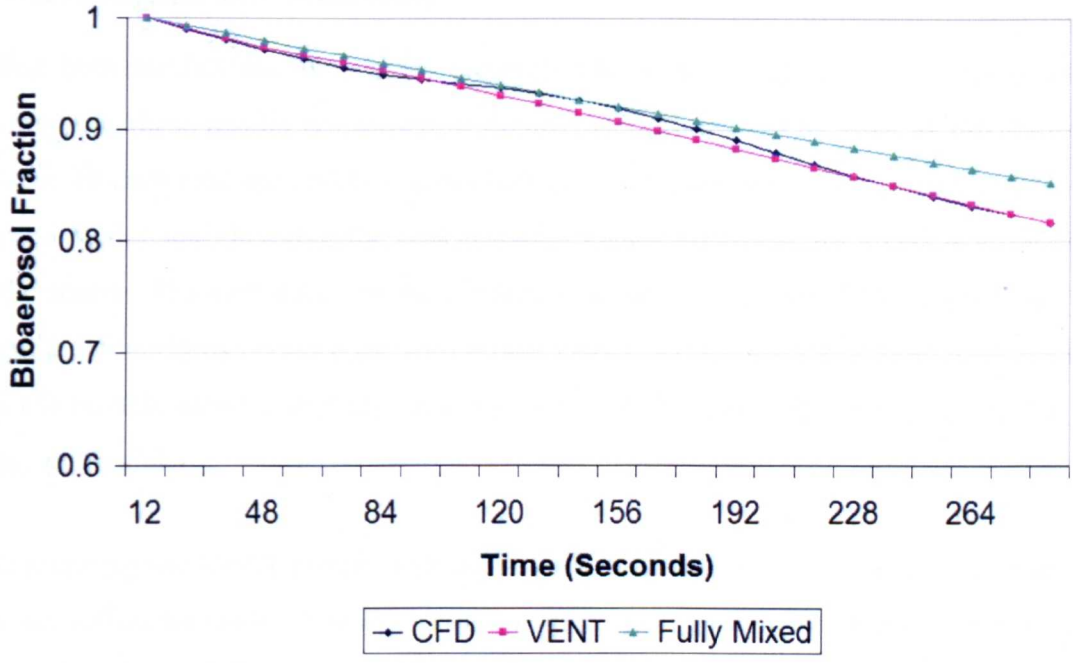

Figure 7-16: The decay of bioaerosol concentration over the entire four-bed bay for the CFD model with zonal source, VENT model, and for a fully mixed model.

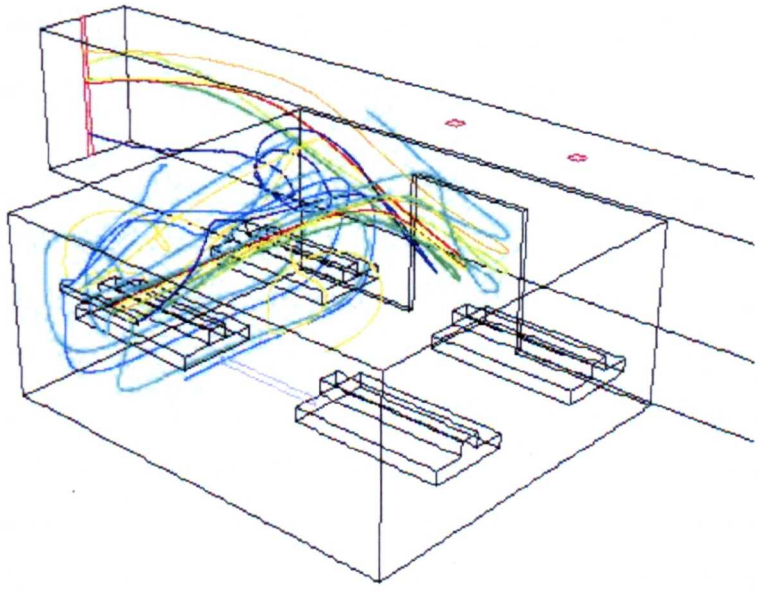

Figure 7-17: Stream lines from the CFD model with a zonal source, originating at patient 1 and showing the transport of bioaerosols from the source zone over time. Each colour represents a different stream line.

7.2.3 Results and Discussion

For both models the bioaerosol concentration within each zone was found at 12s intervals; these results are shown in Figure 7-15 (a) and (b) by zone as fluctuations in time. In each case the results are normalised around the initial source concentration for each model, and therefore the concentration values presented are given as a fraction of the source. The total decay in the entire bay is shown in Figure 7-16 which shows very good comparisons between the well mixed model, VENT and CFD. Both the VENT and CFD models show a slightly increased decay in the space in comparison to the fully mixed model.

Comparing the VENT model with the two CFD models in Figure 7-15 shows there is a clear difference between using a point source or a zonal source when considering the variation in each zone. The CFD results from an injection at a single point show an initial increase within the injection zone (zone 7) which then disperses to neighbouring zones. Because of this behaviour, the build up in adjacent zones (e.g. zone 16) takes much longer than in the CFD model with a zonal source or the VENT model. This can be seen particularly in the plot for zone 16 in Figure 7-15 (b).

Considering a coarse overview of the bay, the general pattern of dispersal is consistent between the VENT model and the CFD model using the zonal source, and the decay rate for the whole bay is similar in each case. Both CFD and VENT models maintain a 'clean zone' down one side of the bay, however looking at the bioaerosol transport in more detail reveals several differences in the transport between the zones. This can be seen in Figure 7-15 particularly in the zones closest to the source. Initially there is a much greater increase in concentration in zone 16 with the CFD model, whereas the VENT model shows a greater increase in zone 8. This is due to the different methods of solving the airflow in the CFD models compared to the VENT model, which results in different flow patterns between the individual zones. The inlet air flow is defined in a different manner for each modelling method due to the individual constraints of the software programs. Within the CFD models the velocity of the air is specified over an inlet surface and a direction and turbulence intensity is defined. Within the VENT model the airflow is defined as an extra mass flow rate supplied into the zone that the inlet is attached to, however there is no directional component. In the CFD models the horizontal air flow from the inlet results in bioaerosols from the source zone (zone 7)

becoming entrained into zone 16 located directly above; this transport of bioaerosols from the patient is shown by stream lines in Figure 7-17. However in the VENT model the mass flow included in zone 16 results in a flow out of this zone into the source zone so in the VENT model the bioaerosol decay in the source zone is due to a sideways transport into the two adjacent zones, with most of the flow into zone 8. The CFD results also show there to be an increase in the concentration in zone 7 (the source zone) towards the end of the transient simulation. This can be explained by examining the plots in Figure 7-18 which show iso-surfaces of contaminant concentration of 750 cfu.m^{-3} at six times between 1s and 23s. This shows how the bioaerosols travel upwards across to bed 2 (zone 4) and then recirculate down and around back to zone 7. This detail is not apparent in the VENT model as the simulation method cannot fully resolve such details of the airflow paths. The theory behind the VENT model assumes that all the zones are fully mixed, including zone 16. However the CFD models show there is a strong direction to the airflow in this zone, and therefore the VENT model predicts a false transport of bioaerosols from zone 7.

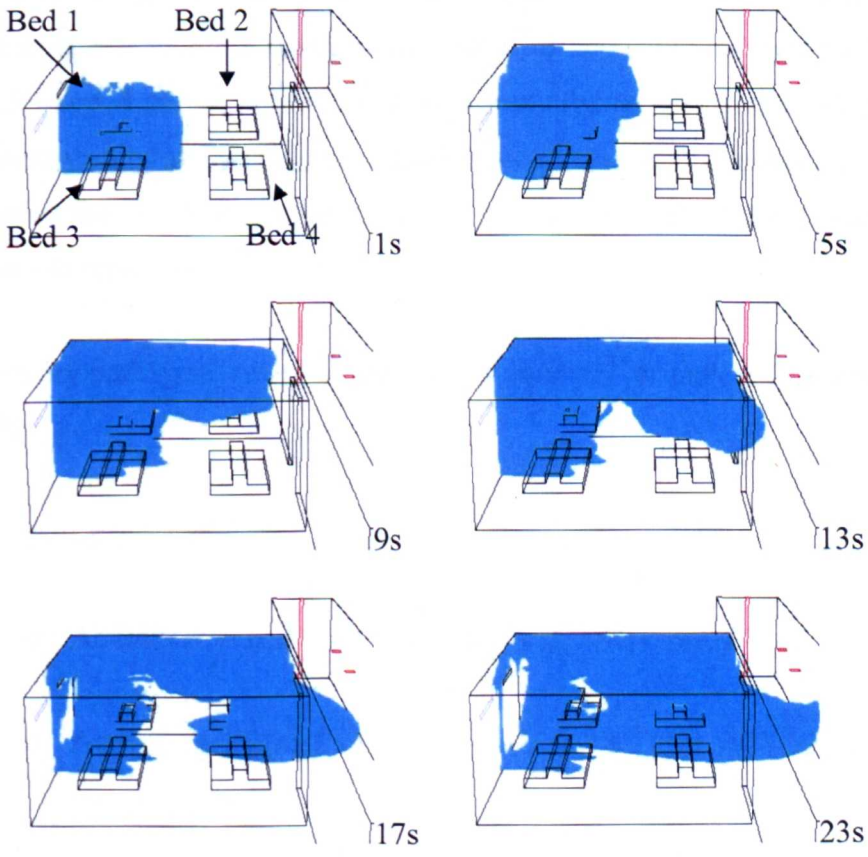

Figure 7-18: Iso-surfaces of bioaerosol concentration 750 cfu.m^{-3} at times shown, representing how the bioaerosols are transported throughout the ward.

Although VENT is a useful tool for this time dependant analysis, providing results much more quickly than the CFD model, a reasonable amount of mixing must be present in the zones specified for the model to produce contaminant transport with any accuracy. It may be useful when considering a whole ward with many bays, as a solution is found in a much shorter timescale than with CFD, and as Figure 7-16 shows, the overall VENT solution is similar to the CFD results. However for transport within one bay, and between adjacent beds, detailed consideration of the airflow is required. VENT is not capable of providing the level of detail to consider differing health risks within a single bay, whereas CFD can provide this information. Mora *et al* (2003) also showed that certain zonal models did not accurately express the recirculation of contaminants in indoor spaces, and so this model may also have the same limitations for studying pollutant transport within rooms.

7.3 Risk to Patients and Staff

The results above indicate the improved performance of CFD simulations over a multi-zone model to deliver the level of detail required to assess risks from sources of bacteria to staff and patients within a hospital bay. The CFD simulation of air flow on the four-bed bay developed above is now used in this section to assess the risk to staff and patients from respiratory and activity based sources, considering patient 1 or 2 (Figure 7-12) as being the location of the infectious source. Several simulations were carried out with sources to represent:

- Respiratory pathogens released from either patient 1 or patient 2 as point sources: (P1, P2)

- Bioaerosols generated from activity

    - Activity over bed 1 or 2 (B1, B2) (e.g. bedmaking)

    - Activity adjacent to the bed 1 or 2 (HCW1, HCW2) (e.g washing, commode use)

The activity based sources were chosen in these areas following results from the hospital study (Chapter 4) which showed higher bioaerosol concentrations during

activities that occurred near the bed (e.g. washing). Past studies have also shown bedmaking to be an important factor in the release of bioaerosols (Chapter 2) and so both a zone above the bed, and immediately adjacent are used here.

Locations of the zonal sources are shown on the plan in Figure 7-19, together with five sampling locations labelled A to E which are used in the analysis of the results.

Both models of bioaerosol transport are considered; passive scalar concentration and Lagrangian particle tracking. The respiratory source models are studied with a scalar to assess the potential airborne droplet nuclei dispersal and the Lagrangian particle tracking is used to study droplet spread. The source injections are created as described in Section 5.3, however in this case 10,000 particles are injected for Lagrangian particle tracking and 500 $cfu.m^{-3}$ is defined for the passive scalar source. In the zonal source models the primary spread is assumed to be via skin squame. Passive scalar transport is initially used for the activity source to get a general description of transport patterns with particle tracking then used to properly represent the larger skin squame particles and study the length of time particles remain airborne and the distance they could travel.

7.3.1 Results

Airflow

The airflow in the ward model has been partially discussed in Section 7.2.3 in reference to the comparison with the VENT model. A lower air exchange rate is used in this model than the previous studies resulting in a velocity over the beds of $0.04m.s^{-1}$ and an average velocity of $0.02m.s^{-1}$ through the entire domain. Vectors of velocity on a horizontal plane y=1.3m are shown in Figure 7-20. This shows the symmetrical air flow that is created by having the same flow specified at both the windows. The effect of this airflow can be seen in the contours of bioaerosol concentration which indicate a 'clean' half of the bay. This is due to the wind, defined as a velocity at the inlet, entering the space perpendicular to the window. Non-symmetric results would be achievable if the wind was given an angle on entry to the space. This would then direct the air into the other half of the room, promoting mixing across the whole space rather than the airflow in the space being separated into two halves.

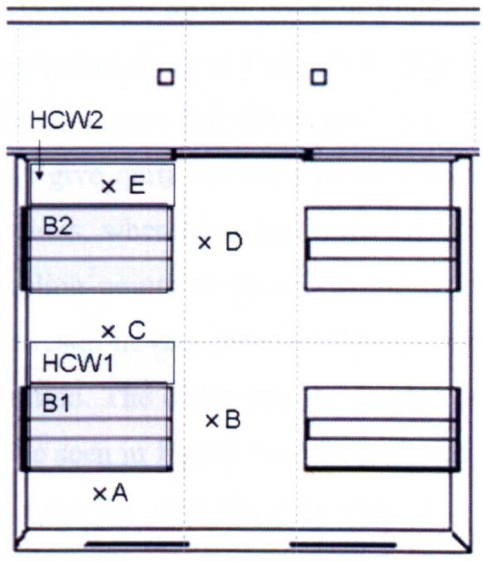

Figure 7-19: The location of the four zonal sources in the four-bed bay model. These have a height to 1.7m, from the floor for HCW1 and HCW2 and from the bed top for B1 and B2. The sampling positions A,B,C,D and E are all at a height of y=1.5m.

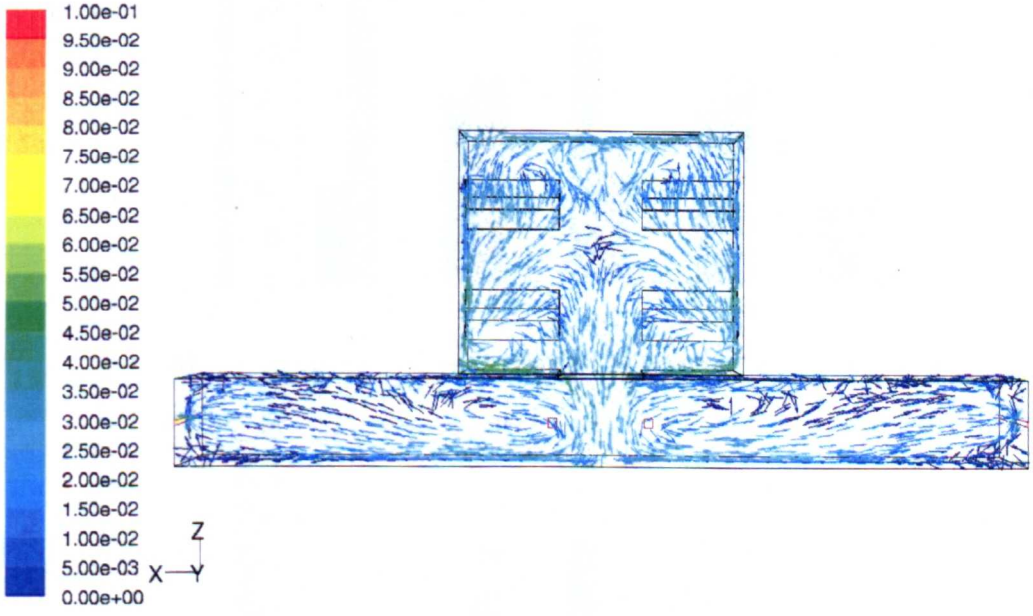

Figure 7-20: Velocity vectors on a horizontal plane y=1.3m. Colour of arrows represents the velocity magnitude ($m.s^{-1}$) according to the key shown.

Relative Risks Determined from Passive Scalar Transport Models

As discussed above and with respect to the VENT model, airflow entering the space tends to recirculate within each side of the bay, and not across the whole room. As such there is little mixing between the two sides of the room. To evaluate the risk from the specified sources contours of bioaerosol concentration are considered and the concentration at six points in the bay compared. The location of these sampling points

are as shown in Figure 7-19 and the results given in Figure 7-21. These are illustrated with the contours of concentration given in Figure 7-22. Figure 7-21 shows how there is variation between the different source definitions and sampling locations. For bed 1 the different source definitions give quite different concentration at A and C but similar results at the other 3 locations, whereas at bed 2 the HCW zone results in very little spread to any of the sampling points compared to the other two sources. Simulated releases from this bed also result in very different concentrations sampled at position C depending on source definition. The difference in sampled concentration at position A with sources at bed 1 can be seen in Figure 7-22 through the contours of concentration. As can be seen with the zone B1, over the bed, there is a much high concentration within this area spreading across the adjacent patient's bed.

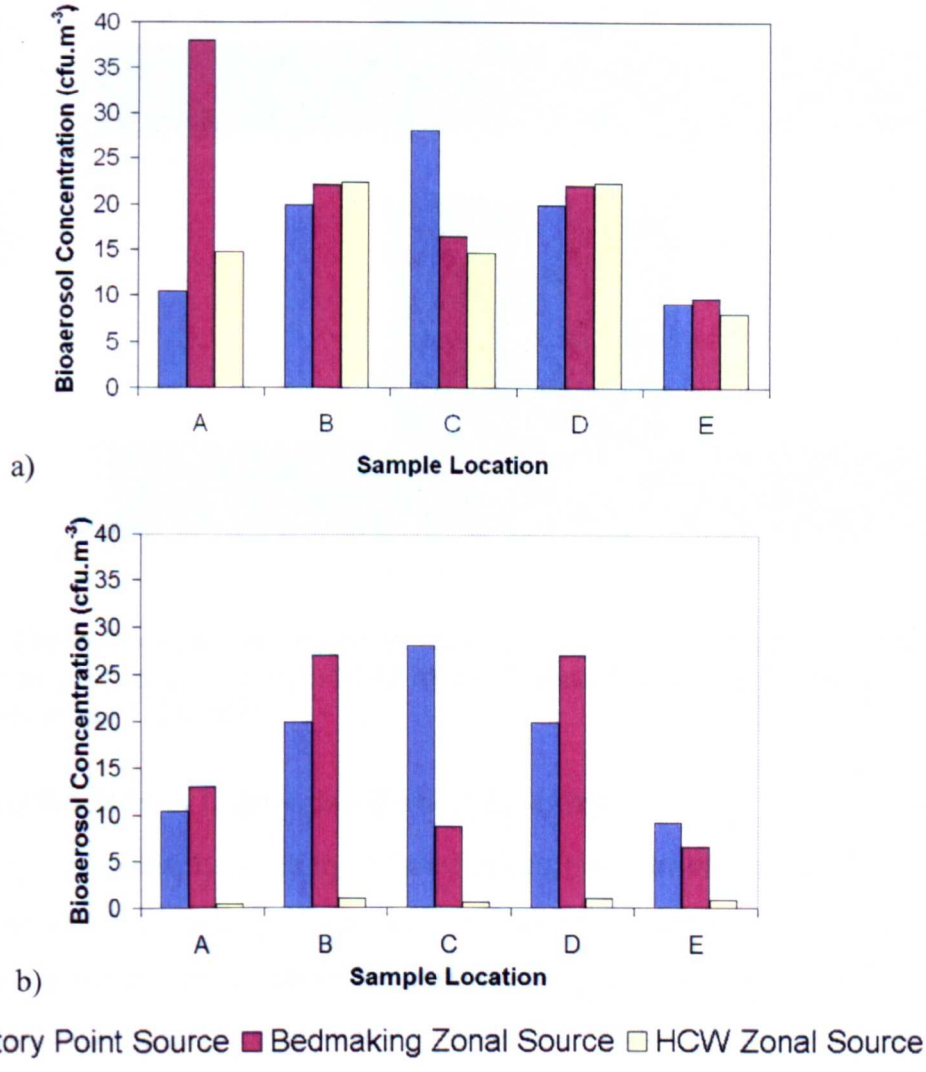

Figure 7-21: Bioaerosol concentration at 5 sample points as shown in Figure 7-19 for the type of source as indicated in the diagram in location a) bed 1, and b) bed 2.

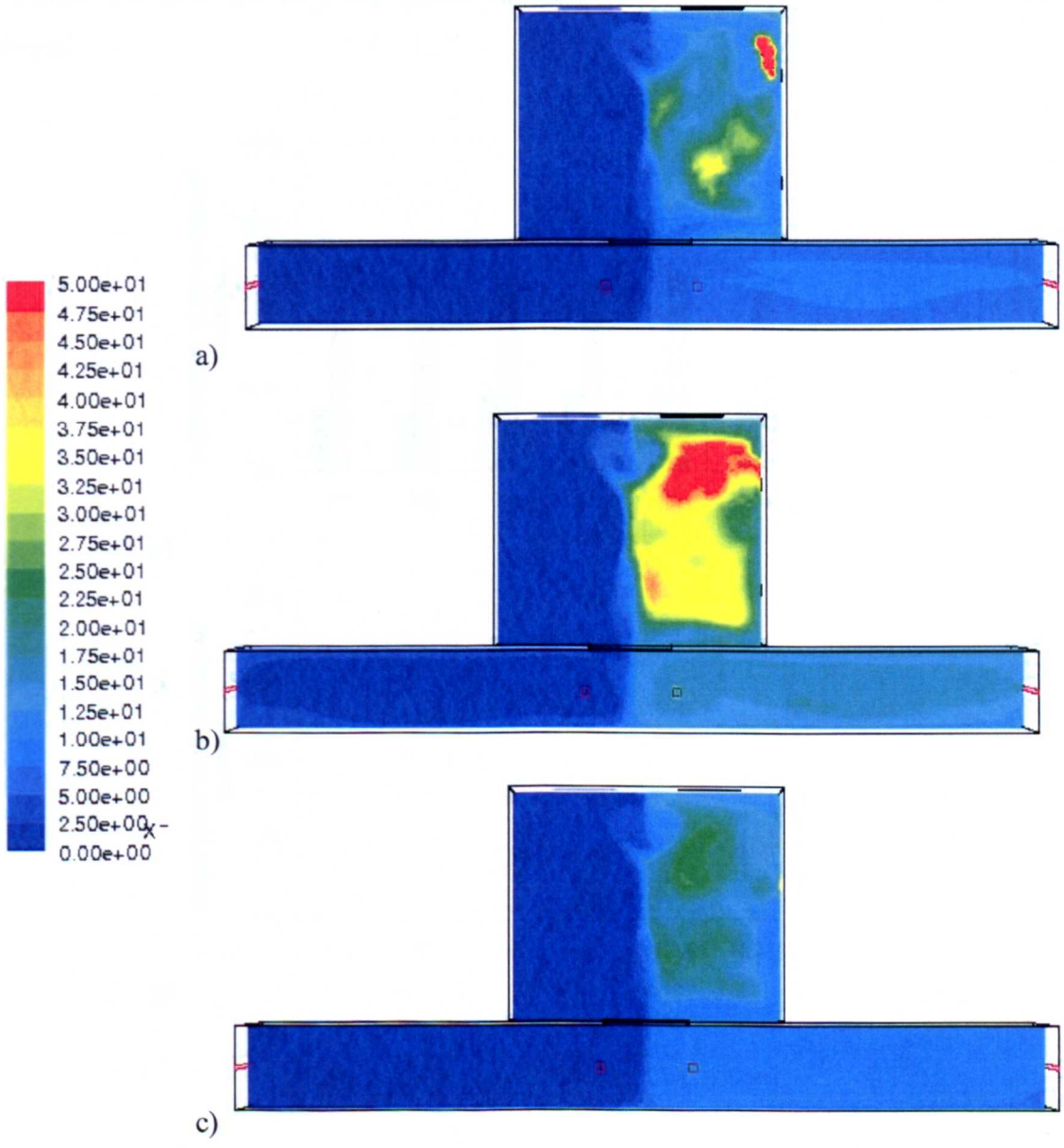

Figure 7-22: Contours of bioaerosol concentration (cfu.m^{-3}) on a plane at y=1.35m for three sources a) point source in bed 1(P1) b) zonal source over bed 1 (B1) c) zonal source adjacent to bed 1 (HCW1)

Relative Risks found from Lagrangian Particle Tracking

As in the previous models, Lagrangian particle tracking was carried out with 5, 14 and 20μm particles. The total number of particles removed from the bay is shown in Figure 7-23 for 5μm and 14μm particles. Removed from the bay includes all particles that pass out of the bay doorway, and is then split into those that deposit in the corridor or are removed by the mechanical extracts or the far doorways at the corridor ends. Only results for 5μm and 14μm particles are shown as very few particles of diameter 20μm

are removed from the bay, the greater diameter meaning they deposit closer to the source.

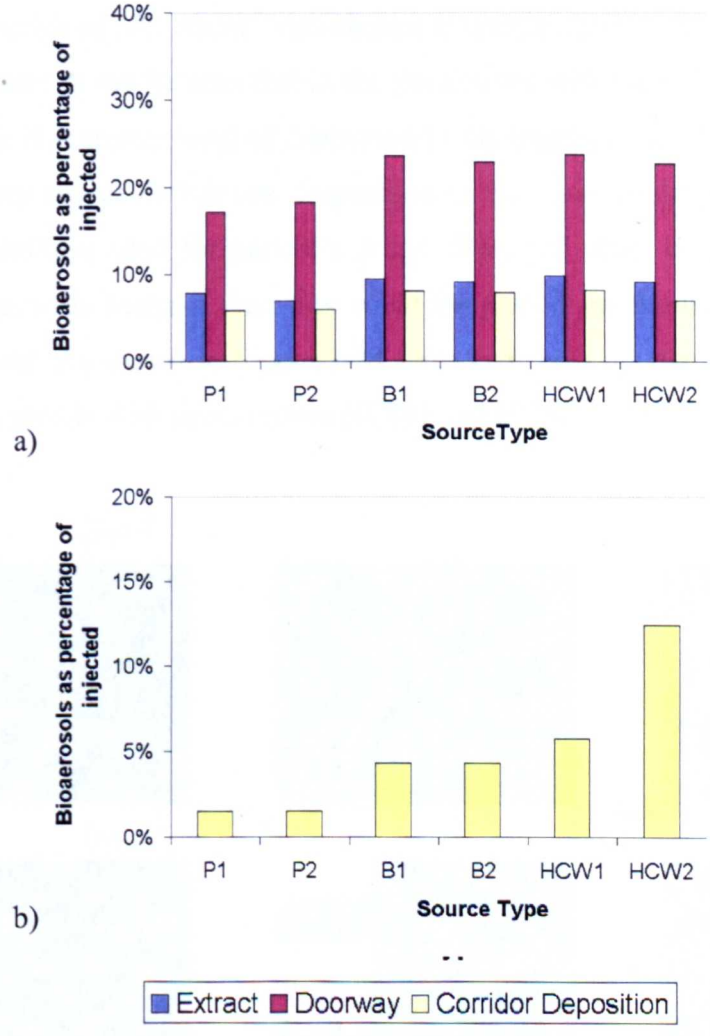

Figure 7-23: The number of particles removed from the bay for a) 5μm and b) 14μm diameter particles and whether deposited in the corridor, or extracted through the mechanical ventilation system or the doorways at the end of the corridor.

For the 5μm particles the different source specifications give similar results, although the removal ratio, compared to those injected, is higher for the zonal sources. For the 14μm diameter particles, most of those that leave the bay deposit onto surfaces in the corridor. The number that escape the bay has a greater dependency on source type, with a higher likelihood of escape with the activity sources than the respiratory source, and particularly with source HCW2.

Figure 7-24 illustrates the different deposition fractions on six floor zones and the four beds in the space. The maximum deposition plotted in each zone is 300 cfu.m^{-2}, although the values of deposition near the source location were much higher than this. The cut-off value of 300 cfu.m^{-2} was chosen to enable other variations of deposition to be much clearer. It can be seen that in the simulations with the bedmaking related zonal sources there is a greater level of deposition in the central aisle of the bay compared to the respiratory source definitions. Deposition in this zone could mean viable particles landing on trolleys used for patient's drugs, files, and other equipment. If these are contaminated with bacteria then this could be passed on through contact spread to another patient. As shown in Figure 7-24 (aiii) and (biii) the dispersion to this central zone is even greater with source zones HCW1 and HCW2.

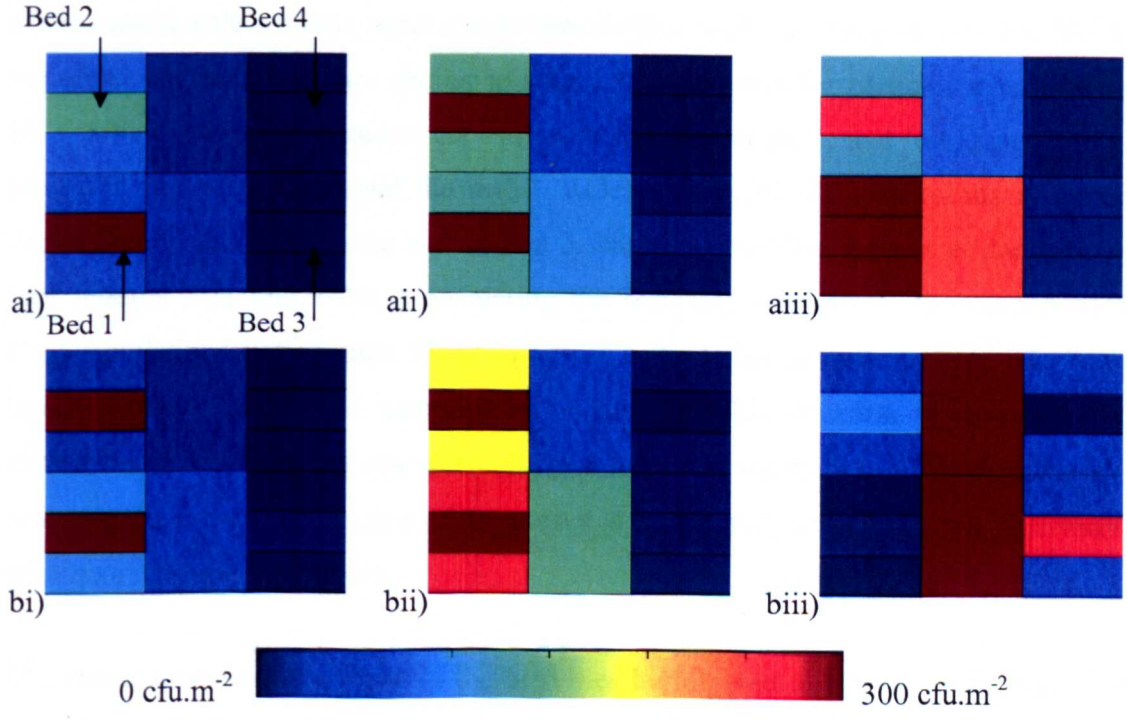

Figure 7-24: Deposition of 14μm particles on 6 floor zones and the beds. The key shows the number of particles deposited. a) Sources at bed 1, b) sources at bed 2. Source i) point (P), ii) bed (B), ii) adjacent to bed (HCW)

The length of time that particles remain suspended in the air of the bay or corridor seems to depend more on source type (either point or zonal) than injection position (either bed 1 or bed 2). 14μm particles released from a point source at either bed 1 or 2 results in particles remaining airborne for a maximum of 1759 or 2125 seconds respectively, whereas the maximum time suspended for the zonal sources are all longer

than the point source; 2240, 2710, 2790, or 2800 seconds for the two bedmaking and two HCW sources respectively. For particles that may be inhaled this results in a greater length of time that they may pose a risk to patients and HCWs in the bay.

7.3.2 Discussion

Depending on the type of source the highest bioaerosol concentration out of the five points sampled varies by location. CFD can be used to assess the location of highest and lowest risks. However it is important to define the source correctly as the concentration varies with different source definitions. In this case the respiratory sources result in higher concentrations at point C between the two beds, for sources at both beds. However for all the results from the zonal source models there is a higher concentration at the points in the central aisle. Particle tracking also demonstrates a greater deposition in the central aisle with the zonal source models than with the point sources. For HCW1 the scalar concentrations are similar to source B1. However for particles released from HCW1 there is a much greater deposition in the central aisle, and less deposition on patient 2 and the area around the bed 2. Release from HCW2 also results in greater deposition in the central aisle and on bed 3 than the other two sources at this location (see Figures 7-21 and 7-24). Considering the sampling position A, the concentration from simulations with source P1 is less than a third that with the source B1. When injecting from bed 2 and sampling at location C this situation is reversed with simulations using the point source resulting in higher concentrations. This demonstrates how important the specification of the source is to the analysis of risk from bioaerosols within an indoor environment.

The zones specified here relate to the activities highlighted in Chapter 4. However the activities indicated as producing the largest quantities of bioaerosols occur behind closed curtains. The presence of the curtains has not been included in the CFD models here as they are opened after the activity takes place. The curtains may affect the transport of the bioaerosols as permanent partitions have been shown to reduce the cross contamination of airborne bioaerosols (Noakes *et al.*, 2006). The temporary barrier that a curtain creates is more likely to have an effect on the large particles which deposit out of the air more quickly. For example in the case of HCW2 the 20μm diameter particles deposit out of the air in 8 minutes, some of which reach the central aisle. Having the curtains closed may prevent this from occurring.

7.4 Summary

The sensitivity study carried out here suggests that simulations with a zonal source model are not as sensitive to the definition of source zone size as simulations using point source models are to the location of the point source. However very thin zonal sources should be treated with care as these can lead to high concentrations at the source, or high values of deposition directly under the source. With the model developed here, any increase in the depth of the zonal source above 0.3m had little effect. The zonal source did not represent the maximum concentrations as occurred with a point source at the head of the bed. Therefore the zonal source should be used to represent activity based sources but a point source should be used to represent a respiratory pathogen release to avoid underestimating the peak risks.

In all cases simulations carried out using point sources gave very different dispersion patterns depending on the source location. It is therefore very important to consider the source positioning carefully and carry out sensitivity analysis when using CFD to examine the effects of different interventions in the airborne spread of infection.

Modelling the zonal source in a pressure driven multi-zone model performed well when considering the overall variation in bioaerosol concentrations in the bay but it does not adequately represent sufficient detail to quantify the risk between patients within a bay. It is therefore a useful tool for evaluating overall risks in an environment, but the local risk within a single space requires CFD modelling to make a realistic judgement.

The levels of risk predicted from a zonal source model differs from that of a respiratory point source. In the case of the four-bed bay simulated here, the activity sources produced higher values of concentration and deposition in the central aisle, and also resulted in particles remaining airborne for longer periods of time.

Chapter 8
Conclusions and Further Work

8.1 Conclusions

This thesis has introduced and validated a zonal source model that provides a reasonable representation of the production of bioaerosols from activity within a simple steady state CFD model. The technique avoids the more complicated and time demanding aspects of transient models to provide the equivalent of a time averaged simulation of spatially varying bioaerosol dispersion. Importantly, in its simplicity, it avoids giving the impression of accuracy that may occur with a transient model, when in fact a large number of assumptions are still necessary in its creation.

In order to define and develop the zonal source methodology a series of objectives were set in Chapter 1, including observational studies to evaluate the types of activities that should be defined by the model, experimental validation of the CFD bioaerosol transport models and numerical validation of the zonal source. The main conclusions drawn from this thesis are detailed below under each of these objectives.

8.1.1 Objective 1:

To assess the effect of typical hospital activities on the airborne concentrations of bioaerosols

A review of the current literature in Chapter 2 identified that certain activities could result in the generation of large quantities of bioaerosols in hospitals. The sampling and observational studies detailed in Chapter 4 considered the effect of typical activities on the bio-burden of hospital air in a respiratory ward. The main conclusions drawn from these studies are as follows:

1) Within a hospital ward the presence of hospital staff, in terms of number and time spent in the bay, is a reasonable marker for quantifying activity which is likely to produce particles > 5μm diameter and bioaerosols. However the total number of *people* in a bay is not as good an indicator because visitors may be present in large numbers for long periods of time but are mainly sedentary and have little effect on the particulate or bio-burden of the air.

2) Overall there was a general pattern on all study days with peaks in the production of bioaerosols and particles > 5μm in the morning. The value of these peaks varied and there were clear differences between busy and quiet days. However some non-daily activities such as ward cleaning, opening windows or specific activities from certain patients had a strong effect on these patterns.

3) It is possible to represent all the particle size ranges sampled in these studies (0.3-0.5μm, 0.5-1μm, 1-3μm, 3-5μm and >5μm) by considering only the behaviour in the size ranges 1-3μm and >5μm.

4) On most days the majority of bioaerosols appeared to be transported on particles > 5μm. However when a NIV was in use there appeared to be a greater number of smaller particles that correlated to the sampling of bioaerosols.

5) Although the presence of staff can be used as a general marker for activity it was found that certain activities were responsible for greater bioaerosol and particle production than others:

   a. General nursing activity that occurs in the morning period and behind curtains seems to contribute the most to the airborne micro-flora. These include patient washing, commode use and bedmaking.

   b. Activities such as cleaning and nebuliser use although producing a large number of particles of size >5μm and 0.3-0.5μm respectively, did not appear to generate viable bioaerosols.

   c. Although the curtains were contaminated with bacteria the movement of these did not seem to increase the airborne micro-flora.

As the studies were carried out on a single ward, generalising the results to other wards has to be approached with caution. However, with the exception of conclusion (4) relating to the use of NIV, the activities that were responsible for the highest production of particles and bioaerosols were generic nursing activities likely to be carried out on most types of hospital wards.

8.1.2 Objective 2:

To validate the use of CFD modelling techniques to study airborne dispersal and deposition of bioaerosols

The following conclusions are important as they are the first time CFD has been systematically validated against controlled experimental conditions to directly mimic the model to compare CFD models to bioaerosol transport. Although the use of a passive scalar has been well validated with tracer gases, this study extends that approach to considering the transport of bioaerosols and shows the method gives reasonable comparisons. Lagrangian particle tracking has been previously assessed against airborne concentrations of particles, but the work presented here is the first study to measure actual deposition of bioaerosols under controlled conditions for direct comparison with CFD simulations. This study found that when using the Lagrangian particle tracking

approach, the effect of turbulent dispersion, simulated here with the discrete random walk model, should be included as neglecting this leads to unrealistically low deposited fractions. Simulated deposition of bioaerosols is of the same order of magnitude as the experiments for the range tested (Table 5-3) however there is greater deposition near the inlet in the simulation. This is likely to be due to the higher velocities that are simulated because of the assumption of isotropic turbulence used in the DRW model. This will be discussed below in the section on Further Work.

8.1.3 Objective 3:

To develop and validate a zonal source model

Numerical validation of the zonal source model showed that it provided a good representation of the time averaged dispersal of a transient source (passive scalar transport) along with the total deposition, and extraction of particles (Lagrangian particle tracking) within a space. In comparison the use of a point source generally showed very poor correlation to the transient source. In certain flow regimes the deposition pattern from a point source may provide reasonable representation to a transient source, but in others it will not. Since the ability of a point source to represent this is not known unless comparative simulations are carried out, the zonal source will provide a more robust method for all airflow regimes.

8.1.4 Objective 4:

To assess the sensitivity of the zonal model and demonstrate its application within hospital environments

The observational and sampling study found that those activities that correlate with the highest sampled counts of particles and bioaerosols occur in zones in the immediate vicinity of the patients' bed. Therefore zones were applied over and directly adjacent to a patient's bed in CFD models of a typical side room and hospital ward. A sensitivity study was carried out to evaluate the sensitivity of the source definition as well as the application of the zonal source in a simple pressure driven zonal ventilation model. These studies enabled the following conclusions to be drawn:

1) Variation in the height and width of a zone covering a patient's bed had very little effect on the dispersion pattern in the side room model. The only cause for concern was when the zone is very thin (less than 2 cell widths) in which case high concentrations and rates of deposition may be predicted.

2) The point source, however, is highly sensitive to source location with the concentration at one sampling point reduced by 75% by moving the source location by only 50cm. Therefore when point source models are used great care must be taken to ensure the source is located in the correct position.

3) A comparison between simulations with the point sources and zonal source found that the point source can lead to greater concentrations in certain regions, and hence yield different risk factors depending on the source used. Therefore the source definition must be appropriate to the analysis; zonal sources may underestimate risk for respiratory diseases and ideally both a point and zonal source should be used to assess the risk from respiratory and activity sources respectively.

4) Although the zonal source is easily adapted to the pressure driven multi-zone model this does not model the flow within a bay in enough detail to accurately define the risk to other patients and health care workers. However the overall results for a multi-connected space are similar and the pressure driven model is a good method for the global evaluation of complex indoor environments.

8.2 Further Work

Particle modelling and validation

A key area that would benefit from further study is around the techniques for modelling bioaerosols as a discrete particle phase. As discussed in this thesis the release of particles from activities is generally associated with particles in the range 5-20μm. These cannot be realistically modelled as a passive scalar as their size and mass must be accounted for and therefore in this thesis are modelled using Lagrangian particle tracking. Experimental validation in this thesis found it necessary to include the effects of turbulent dispersion. However including this using the DRW model over estimation

of deposition near the airflow inlet was found in the test chamber model. Other authors have also found significant over estimation of particle deposition for smaller particles. Therefore in order to correctly model the trajectory and deposition of particles injected from a zonal source it is necessary to overcome this problem.

There is currently research into methods to improve these techniques, either through using complex turbulence models (Tian *et al.*, 2006) or through UDFs to reduce the over estimated velocities normal to the boundary (Lai and Chen, 2007). Both these methods will result in larger computational times due to the finer meshes required. Although it has been suggested that these methods show improved results they have only been compared numerically. There is little experimental validation of the deposited fraction of injected particles and although the airborne concentration has been validated to a greater extent this has not been carried out using bioaerosols. The experimental validation carried out in this thesis is the first controlled comparison between CFD modelling and bioaerosol dispersion and showed good correlations with the simulation. However only one range of particle sizes was considered in this experiment and so further validation should be carried out considering a number of distinct size ranges. For use with the zonal source it is particularly important to consider particles in the size region 5-20μm within a room air flow. Generating this size particle for experimental validation within the test chamber may possibly be achieved through the use polymer latex particles aerosolised from a liquid suspension (Mitchell, 1995a), although it would have to be established if these could carry micro-organisms. Deposition could be measured through increases in mass, growth of micro-organisms if the particles are aerosolised from a bacterial solution, or through the decrease in airborne counts measured with an optical particle counter.

Further to this work on deposition, the particles in this thesis are sized by their aerodynamic diameter, and the effect the shape has, other than changing the diameter definition, is not included. This may be simplifying the transport mechanism as in reality if they are generated through skin shedding, they are more likely to be flake like in appearance. This may have an effect on the particle trajectory and deposition properties and further research could be of interest to the deposition in indoor environments. Similarly, further studies on how air samplers such as the MicroBio and

Andersen sampler could be used to understand the range of geometric particle sizes and shapes sampled, as opposed to sizing based purely on the aerodynamic diameter.

Zonal Source Model

The definition of the zonal source would benefit from further development. The activity that creates this source is likely to produce momentum and increased turbulence at the source. A study by Brohus (2006) discussed in Chapter 3 showed how he developed a method of representing movement within a steady state model using a series of zones. A combination of his model with the zonal source models presented here could be developed to include the effect of the activity on the momentum and turbulence of the local air flow and the dispersion of bioaerosols for the specific activities highlighted in Chapter 4. Brohus used a method of trial and error; defining the CFD method by comparison to smoke visualisation during movement in order to get good qualitative analysis. As with the zonal source method developed in this thesis, this aims to improve the risk analysis by providing better patterns of dispersal. As such the use of the two methods should compliment each other, although further work would be needed to define suitable momentum for the hospital based activities.

Application of the zonal source model has only received a small amount of assessment in this thesis, however the model may have significant application for a variety of hospital situations, particularly if is can be combined with the momentum and turbulence models of Brohus. Knowledge of the time taken for typical particles to deposit and the distance travelled from the source is useful for many reasons. For example in Chapter 4 it was noted that the majority of bioaerosol producing activities occurred behind closed curtains, and that there was sometimes a large increase in particles and bioaerosols when the curtains opened. If the curtains contain the bioaerosols, CFD modelling could inform whether keeping the curtains closed for specific lengths of time after an activity would prevent deposition on neighbouring beds, and contain the viable particles near the source bed. This may then be compared with other control techniques such as using local air extracts, or air cleaning devices within the curtained region. Alternatively the question may be asked; if particles do deposit on many beds in the ward after an activity is there a recommended time after it occurs to carry out cleaning of surfaces in the ward, once the particles have deposited? There is growing interest in influence of electrostatics in hospital environments,

including the use of ionisers to clean air (Noakes *et al.*, 2007) which causes greater electrostatic deposition of particles. Therefore improvements to modelling deposition of particles will benefit this area of research and aid understanding of the effect of ionisers on contact spread due to contaminated surfaces.

Ward Based Assessment of Bioaerosols

The study presented in Chapter 4 showed very interesting results relating activities to bioaerosol and particle concentrations. This was only carried out on a respiratory ward and so it is necessary to carry out a similar study on a different type of ward in order to assess the similarities and differences in terms of activities performed and bioaerosols generated.

Further work needs be carried out to study those activities highlighted, such as bedmaking and washing, in more detail. For example carrying out a similar study in a side room where the production will only be from one patient and respective HCWs or through controlled experiments in the test chamber. The lack of use of non-invasive ventilators in this study meant no strong conclusions could be drawn and this would benefit from more detailed approach, including air sampling at the face mask in order to assess what the patient may be inhaling through the ventilator. Within these further studies the correlations between activity and bioaerosol generation may be made more robust through the use of Polymerase Chain Reaction (PCR) to identify the specific strain of bacteria sampled and those colonising the patient.

References

Andersen, A. A. (1958) New Sampler for the Collection, Sizing, and Enumeration of Viable Airborne Particles. *Journal of Bacteriology,* **76**(5), 471-484.

Archibald, L. K. & Hierholzer, W. J. (2004) Principles of Infectious Diseases Epidemiology. IN MAYHALL, C. G. (Ed.) *Hospital Epidemiology and Infection Control.* 3rd ed. Philadelphia, Lippincott Williams and Wilkins.

Arup (2001) VENT E+TA manual. London, Arup.

ASHRAE (1992) Standard 55-1992 Thermal Environmental conditions for human occupancy (ANSI Approved). ASHRAE.

Awbi, H. B. (1989) Application of Computational Fluid Dynamics in Room Ventilation. *Building and Environment,* **24**(1), 73-84.

Ayliffe, G. A. J., Collins, B. J., Lowbury, E. J. L., Babb, J. R. & Lilly, H. A. (1967) Ward Floors and Other Surfaces as Reservoirs of Hospital Infection. *Journal of Hygiene-Cambridge,* **65**(4), 515-536.

Baba, T., Takeuchi, F., Kuroda, M., Yuzawa, H., Aoki, K., Oguchi, A., Nagai, Y., Iwama, N., Asano, K., Naimi, T., Kuroda, H., Cui, L., Yamamoto, K. & Hiramatsu, K. (2002) Genome and virulence determinants of high virulence community- acquired MRSA. *Lancet,* **359**(9320), 1819-1827.

Banfield, K. R. & Kerr, K. G. (2005) Could hospital patients' hands constitute a missing link? *Journal of Hospital Infection,* **61**, 183-188.

Beggs, C. B. (2003) The airborne transmission of infection in hospital buildings: Fact or fiction? *Indoor and Built Environment,* **12**(1-2), 9-18.

Beggs, C. B., Kerr, K. G., Noakes, C. J., Hathway, E. A. & Sleigh, P. A. (2007) The Ventilation of Multi-Bed Hospital Wards: Review and Analysis. *American Journal of Infection Control* **36**(4), 250-259.

Beggs, C. B. & Sleigh, P. A. (2002) A quantitative method for evaluating the germicidal effect of upper room UV fields. *Journal of Aerosol Science,* **33**(12), 1681-1699.

Bethune, D. W., Blowers, R., Parker, M. & Pask, E. A. (1965) Dispersal of Staphylococcus aureus by patients and staff. *The Lancet*, 480-483.

BGI Collison Nebuliser (2007) Output distribution of the Collison Nebuliser. (Accessed Sept. 2007):Available on the world wide web: http://www.bgiusa.com /agc/output_distribution.htm

Bhalla, A., Pultz, J., Gries, D. M., Ray, A. M., Eckstein, R. N., Aron, D. C. & Donskey, C. J. (2004) Acquisition of Nosocomial Pathogens on hands after contact with Environmental Surfaces Near Hospitalised Patients. *Infection Control and Hospital Epidemiology*, **25**(2), 164-166.

Bjorn, E. & Nielsen, P. V. (2002) Dispersal of exhaled air and personal exposure in displacement ventilated rooms. *Indoor Air*, **12**(3), 147-164.

Blythe, D., Keenlyside, D., Dawson, S. J. & Galloway, A. (1998) Environmental Contamination due to Methicillin-Resistant Staphylococcus aureus (MRSA). *Journal of Hospital Infection*, **38**, 67-70.

Boswell, T. C. & Fox, P. C. (2006) Reduction in MRSA environmental contamination with a portable HEPA-filtration unit. *Journal of Hospital Infection*, **63**, 47-54.

Bouilly, J., Limam, K., Beghein, C. & Allard, F. (2005) Effect of ventilation strategies on particle decay rates indoors: An experimental and modelling study. *Atmospheric Environment*, **39**(27), 4885-4892.

Boyce, J. M., Potter-Bynou, G. & Chenevert, G. (1997) Environmental Contamination due to methicillin-resistant Staphylococcus aureus: possible infection control implications. . *Infection Control and Hospital Epidemiology*, **16**, 622-7.

Brachman, P. S. (1970) Airborne infection - airborne or not? In American Hospital Association (Ed.) *International Conference Nosocomial infection*

Britton, N. F. (2003) *Essential Mathematical Biology*, London, Springer.

Brohus, H., Balling, K. D. & Jeppesen, D. (2006) Influence of movements on contaminant transport in operating room. *Indoor Air*, **16**(5), 356-372.

Brouns, C. & Waters, B. (1991) A guide to Contaminant Removal Effectiveness. Warwick, University of Warwick Science Park.

Buchanan, C. R. & Dunn-Rankin, D. (1998) Transport of Surgically Produced Aerosols in an Operating Room. *American Industrial Hygiene Association Journal,* **59**(6), 393-402.

CDC (2005) Guidelines for Preventing the Transmission of Mycobacterium tuberculosis in Health-Care Settings, 2005. *Mobility and Mortality Weekly report,* **54**(RR17), 1-141.

Chambers, H. F. (2001) The Changing Epidemiology of Staphylococcus. *Emerging Infectious Diseases,* **7**(2), 178-182.

Chang, T. J., Hsieh, Y. F. & Kao, H. M. (2006) Numerical investigation of airflow pattern and particulate matter transport in naturally ventilated multi-room buildings. *Indoor Air,* **16**(2), 136-152.

Chang, T. J., Kao, H. M. & Hsieh, Y. F. (2007) Numerical Study of the Effect of Ventilation Pattern on Coarse, Fine, and Very Fine Particulate Matter Removal in Partitioned Indoor Environment. *Journal of Air and Waste Management Association,* **57,** 179-189.

Chao, C. Y. H. & Wan, M. P. (2006) A study of the dispersion of expiratory aerosols in unidirectional downward and ceiling-return type airflows using a multiphase approach. *Indoor Air,* **16,** 296-312.

Chau, O. K. Y., Liu, C. H. & Leung, M. K. H. (2006) CFD analysis of the performance of a local exhaust ventilation system in a hospital ward. *Indoor and Built Environment,* **15**(3), 257-271.

Chen, Q. (1995) Comparison of different k-e models for indoor air flow computations. *Numerical Heat Transfer, Part B,* **28**(3), 353-369.

Cheong, K. W. D. & Phua, S. Y. (2006) Development of ventilation design strategy for effective removal of pollutant in the isolation room of a hospital. *Building and Environment,* **41**(9), 1161-1170.

Chief Medical Officer (2002) Getting ahead of the curve: a strategy for combating infectious diseases (including other aspects of health protection). London, Department of Health,.

Chief Medical Officer (2003) Winning Ways. Working together to reduce Healthcare Associated Infection in England. London, Department of Health,.

Chow, T. T. & Yang, X. Y. (2003) Performance of ventilation system in a non-standard operating room. *Building and Environment,* **38**(12), 1401-1411.

Chow, T. T. & Yang, X. Y. (2004) Ventilation Performance in the Operating Theatre Against Airborne Infection: Review of Research Activities and Practical Guidance. *Journal of Hospital Infection,* **56**(2), 85-93.

Chung, K. & Hsu, S. (2001) Effect of ventilation pattern on room air and contaminant distribution. *Building and Environment,* **36,** 989-998.

CIBSE (2005) AM10 Natural Ventilation in Non-Domestic Buildings. London, Chartered Institute of Building Services Engineers.

CIBSE (2006) Guide A: Environmental Design. London, Chartered Institute of Building Services Engineers.

Clark, R. P. & Cox, R. N. (1973) Dispersal of Bacteria from the Human Body Surface. IN Hers, J.P. and Winkler, K.C. (Ed.) *International Symposium on Aerobiology.* Technical University at Enschede, The Netherlands, Oosthoek Publishing Company.

Cleyton, F. Y., Van de Mark, Y. S. & Van Toom, M. J. (1968) Effect of shower-bathing on dispersal of recenlty acquired transient skin flora. *The Lancet,* **291**(7547), 865.

Cole, E. C. & Cook, C. E. (1998) Characterization of infectious aerosols in health care facilities: An aid to effective engineering controls and preventive strategies. *American Journal of Infection Control,* **26**(4), 453-463.

Colquhoun, J. & Partridge, L. (2003) Computational Fluid Dynamics Applications in Hospital Ventilation Design. *Indoor and Built Environment,* **12**(1-2), 81-88.

Cotterill, S., Evans, R. & Fraise, A. P. (1996) An unusual source for an outbreak of methicillin resitant *Staphylococcus aureus* on an intensive therapy unit. *Journal of Hospital Infection,* **32,** 207-216.

Cox, C. S. (1987) *The Aerobiological Pathway of Micro-organisms,* Chichester, John Wiley and Sons.

Crook, B. (1995) Inertial Samplers: Biological perspectives. IN COX, C. S. & WATHES, C. M. (Eds.) *Bioaerosols Handbook.* New York, Lewis Publishers.

Daley, D. J. & Gani, J. (1999) *Epidemic Modelling: An introduction.* , Cambridge, Cambridge University Press.

Das, I., Lambert, P., Hill, D., Noy, M., Bion, J. & Elliott, T. (2002) Carbapenem-resistant Acinetobacter and role of curtains in an outbreak in intensive care units. *Journal of Hospital Infection,* **50**(50), 110-114.

Davies, R. R. & Noble, W. C. (1962) Dispersal of Bacteria on Desquamated Skin. *Lancet,* **2**(7269), 1295-1297.

DeAngelis, C. D. & Flanagin, A. (2005) Tuberculosis. A global Problem Requiring a Global Solution. *Journal of the American Medical Association,* **293**(22), 2793-2794.

Department of Health (2006) The Health Act 2006: Code of practice for the prevention and control of healthcare associated infections. London, Department of Health.

Department of Health (2007a) Saving Lives: reducing Infection, delivering clean and safe care. London, Department of Health

Department of Health (2007b) Hospital organisation, specialty mix and MRSA. London, Department of Health

Department of Health (2008a) Clean, safe care: reducing infections and saving lives London. Department of Health

Dietze, B., Rath, A., Wendt, C. & Martiny, H. (2001) Survival of MRSA on sterile goods packaging. *Journal of Hospital Infection,* **49**, 225-261.

Duguid, J. P. & Wallace, A. T. (1948) Air Infection with Dust Liberated from Clothing. *Lancet,* **252**(6535), 845-849.

Eichenwald, H. F., Kotsevalov, O. & Fasso, L. A. (1960) The Cloud Baby - an Example of Bacterial-Viral Interaction. *American Journal of Diseases of Children,* **100**(2), 161-173.

Elghobashi, S. (1994) On Predicting Particle-Laden Turbulent Flows. *Applied Scientific Research,* **52**, 309-329.

Etheridge, D. & Sandberg, M. (1996) Computational Fluid Dynamics and its Applications. *Building Ventilation. Theory and Measurement.* Chichester, John Wiley and Sons.

Farrington, M., Ling, J., Ling, T. & French, G. L. (1990) Outbreaks of infection with methicillin-resistant Staphylococcus aureus on neonatal and burns units of a new hospital. *Epidemiology and Infection,* **105**(2), 215-28.

Fendler, E. J., Ali, Y., Hammond, B. S., Lyons, M. K., Kelley, M. B. & Vowell, N. A. (2002) The impact of alcohol hand sanitizer use on infection rates in an extended care facility. *American Journal of Infection Control,* **30(4),** 226-233.

Ferziger, J. H. & Peric, M. (2002) *Computational Methods for Fluid Dynamics. 3rd Edition,* Berlin, Springer.

Fisk, W. (2008) Commentary on predictive models of control strategies involved in containing indoor airborne infections, *Indoor Air* **18**(1):72-73.

Fluent Inc (2001) *Gambit 2: Users Guide,* Lebanon, Fluent Incorporated.

Fluent Inc (2005) Fluent 6.2 Documentation. Lebanon, Fluent Incorporated.

French, G. L., Otter, J. A., Shannon, K. P., Adams, N. M. T., Watling, D. & Parks, M. J. (2004) Tackling contamination of the hospital environment by methicillin-resistant Staphylococcus aureus (MRSA):a comparison between conventional terminal cleaning and hydrogen peroxide vapour decontamination. *Journal of Hospital Infection,* **57,** 31-37.

Friberg, B., Friberg, S., Burman, L. G., Lundholm, R. & Ostensson, R. (1996) Inefficiency of upward displacement operating theatre ventilation. *Journal of Hospital Infection,* **33,** 263-272.

Gao, N. P. & Niu, H. L. (2006) Transient CFD simulation of the respiration process and inter-person exposure assessment. *Building and Environment,* **41**(9), 1214-1222.

Greene, V. W., Bond, R. G., Vesley, D. & Michaels.Gs (1962) Microbiological contamination of Hospital air. 1. Quantitative Studies. *Applied Microbiology,* **10**(6), 561-566.

Griffiths, W. D. & Stewart, I. W. (1999) Performance of bioaerosol samplers used by the UK biotechnology industry. *Journal of Aerosol Science,* **30**(8), 1029-1040.

Hambraeus, A. (1973) Transfer of Staphylococcus aureus via nurses uniforms. *Journal of Hygiene-Cambridge,* **71,** 799.

Hamburger, M. & Robertson, O. H. (1948) Expulsion of group a hemolytic streptococci in droplets and droplet nuclei by sneezing, coughing and talking. *The American Journal of Medicine,* **4**(5), 690-701.

Han, Zhuolin, Lautenbach, Ebbing, Fishman, Neil, Nachamkin & Irving (2007) Evaluation of mannitol salt agar, CHROMagar, Staph aureus and CHROMagar MRSA for detetion of

methicillin-resistant Staphylococcus aureus from nasal swab specimens. *Journal of Medical Microbioogy,* **56,** 43-46.

Harbarth, S., Sax, H. & Gastmeier, P. (2003) The preventable proportion of nosocomial infections:an overview of published reports. *Journal of Hospital Infection,* **54,** 258-266.

Hare, R. & Ridely, M. (1958) Further transmission of Staphylococcus aureus *British Medical Journal,* **1,** 69-73.

Hare, R. & Thomas, C. G. A. (1956) The Transmission of Staphylococcus Aureus. *British Medical Journal,* **2**(4997), 840-844.

Hartstein, A. I., Sebastian, T. J. & Strausbaugh, L. J. (2004) Methicillin -Resistant Staphylococcus aureus. In Mayhall, C. G. (Ed.) *Hospital Epidemiology and Infection Control.* 3rd ed. Philadelphia, Lippinvott Williams and Wilkins.

Health Protection Agency (2006) Mandatory Surveillance of Healthcare Associated Infections Report 2006. London, Health Protection Agency

Health Protection Agency (2008) Quarterly Reporting Results for Clostridium difficile and MRSA Bacteraemia: April 2008. London, Health Protection Agency. Available from www.hpa.org.uk/web/HPAweb&Page&HPAwebAutoListName/Page/1191942126541. Accessed 22nd May 2008.

Heidelberg, J. F., Shahamat, M., Levin, M., Rahman, I., Stelma, G., Grim, C. & Colwell, R. R. (1997) Effect of Aerosolization on Culturability and Viability of Gram-Negative Bacteria. *Applied and Environmental Microbiology,* **63**(9), 3585-3588.

Hill, J., Howell, A. & Blowers, R. (1974) Effect of clothing on the dispersal of Staphylococcus aureus by males and females. *Lancet,* **304**(7889), 1131-1133.

Hinds, W. C. (1982) *Aerosol Technology,* New York, John Wiley and Sons.

Hinton, P.R. (2004) *SPSS Explained,* Hove, Routeledge

Holmberg, S. & Li, Y. (1998) Modelling of the Indoor Environment - Particle Dispersion and Deposition. *Indoor Air,* **8,** 113-122.

Hota, B. (2004) Contamination, Disinfection, and Cross-Colonization: Are Hospital Surfaces Reservoirs for Nosocomial Infection? *Healthcare Epidemiology,* **39,** 1182-1189.

Huang, J. M., Chen, Q. Y., Ribot, B. & Rivoalen, H. (2004) Modelling contaminant exposure in a single-family house. *Indoor and Built Environment,* **13**(1), 5-19.

Joint Tuberculosis Committee of the British Thoracic Society (2000) Control and Prevention of Tuberculosis in the United Kingdom: Code of Practice 2000. *Thorax,* **55**(11), 887-901.

Kao, P. H. & Yang, R. J. (2006) Virus diffusion in isolation rooms. *Journal of Hospital Infection,* **62**(3), 338-345.

Khan, J. A., Feigley, C. E., Lee, E., Ahmed, M. R. & Tamanna, S. (2006) Effects of inlet and exhaust locations and emitted gas density on indoor air contaminant concentrations. *Building and Environment,* **41**(7), 851-863.

Kirkby, W. M. M. (1944) Extraction of a highly potent penicillin inactivator from penicillin resistant staphylococci. *Science,* **99**(2579), 452-3.

Kluytmans, J., vanBelkum, A. & Verbrugh, H. (1997) Nasal carriage of Staphylococcus aureus: Epidemiology, underlying mechanisms, and associated risks. *Clinical Microbiology Reviews,* **10**(3), 505-520.

Kumari, D. N. P., Haji, T. C., Keer, V., Hawkey, P. M., Duncanson, V. & Flower, E. (1998) Ventilation grilles as a potential source of methicillin- resistant Staphylococcus aureus causing an outbreak in an orthopaedic ward at a district general hospital. *Journal of Hospital Infection,* **39**(2), 127-133.

Lai, A. C. K. & Chen, F. (2006) Modeling particle deposition and distribution in a chamber with a two-equation Reynolds-averaged Navier-Stokes model. *Aerosol Science,* **37,** 1770-1780.

Lai, A. C. K. & Chen, F. Z. (2007) Comparison of new Eulerian model with a modified Lagrangian approach for particle distribution and deposition indoors. *Atmospheric Environment,* **41,** 5249-5256.

Larson, E. (1988) A causal link between handwashing and risk of infection – Examination of the evidence. *Infection Control and Hospital Epidemiology,* **9**(1), 28-36.

Leduc, S., Fredriksson, C. & Hermansson, R. (2006) Particle-tracking option in Fluent validated by simulation of a low pressure impactor. *Advanced Powder Technology,* **17**(1), 99-111.

Lee, E., Feigley, C. E. & Khan, J. (2002) An investigation of air inlet velocity in simulating the dispersion of indoor contaminants via computational fluid dynamics. *Annals of Occupational Hygiene,* **46**(8), 701-712.

Lee, N., Hui, D., Wu, A., Chan, P., Cameron, P., Joynt, G. M., Ahuja, A., Yung, M. Y., Lueng, C. B., To, K. F., Lui, S. F., Szeto, C. C., Chung, S. & Sung, J. J. Y. (2003) A Major Outbreak of Severe Acute Respiratory Syndrome in Hong Kong. *The New England Journal of Medicine,* **238**(20), 1986-1994.

Li, Y., Huang, X., Yu, I. T. S., Wong, T. W. & Qian, H. (2005) Role of air distribution in SARS transmission during the largest nosocomial outbreak in Hong Kong. *Indoor Air,* **15**(2), 83-95.

Lowy, F. D. (1998) Staphylococcus aureus infections. *The New England Journal of Medicine,* 520-532.

Lu, W. & Howarth, A. T. (1996) Numerical analysis of indoor aerosol particle deposition and distribution in two-zone ventilation system. *Building and Environment,* **31**(1), 41-50.

Lu, W., Howarth, A. T., Adam, N. & Riffet, S. (1996) Modelling and Measuremet of Airflow and Aerosol Particle Distribution in a Ventilated Two Zone Chamber. *Building and Environment,* **31**(5), 417-423.

Macher, J. M. (1989) Positive-Hole Correction of Multiple-Jet Impactors for Collecting Viable Microorganisms. *American Industrial Hygiene Association Journal,* **50**(11), 561-568.

Mackintosh, C. A., Lidwell, O. M., Towers, A. G. & Marples, R. R. (1978) The dimensions of skin fragments dispersed into the air during activity. *Journal of Hygiene-Cambridge,* **81,** 471-479.

Martinez, K. F., Rao, C. Y. & Burton, N. C. (2004) Exposure assessment and analysis for biological agents. *Grana,* **43**(4), 193-208.

Matsumoto, H. & Ohba, Y. (2004) The Influence of a Moving Object on Air Distribution in Displacement Ventilated Rooms. *Journal of Asian Architecture and Building Engineering* **3**(1), 71-75.

Mattsson, M. & Sandberg, M. (1996) Velocity Field Created by Moving Objects in Rooms. *ROOMVENT '96 5th International Conference on Air Distribution in Rooms.* Japan.

May, K. R. (1973) The collison nebulizer: Description, performance and application. *Journal of Aerosol Science,* **4**(3), 235-238.

May, K. R. & Pomeroy, N. R. (1973) Bacterial dispersion from the body surface. In Hers, J.P. and Winkler, K.C. (Eds.) *Airborne Transmission and Airborne Infection: 4th International Symposium on Aerobiology.* Technical University at Enschede, The Netherlands, Oosthoek Publishing Company.

Mazumdar, S. & Chen, Q. (2007) Impact of moving bodies on airflow and contaminant transport inside aircraft cabins. In Seppanen, O. & Sateri, J. (Eds.) *Roomvent 2007.* Helsinki, Finland.

Micallef, A., Caldwall, J. & Colls, J. J. (1998) The influence of Human Activity on the Vertical Distribution of Airborne Particle Concentration in Confined Environments: Preliminary Results. *Indoor Air,* **8,** 131-136.

Mitchell, J. P. (1995a) Aerosol Generation for Instrument calibration. In Cox, C. S. & Wathes, C. M. (Eds.) *Bioaerosols handbook.* New York, Lewis Publishers.

Mitchell, J. P. (1995b) Particle Size Analyzers: Practical Procedures and Laboratory Techniques. In Cox, C. S. & Wathes, C. M. (Eds.) *Bioaerosols Handbook.* New York, Lewis Publishers.

Mora, L., Gadgil, A. J. & Wurtz, E. (2003) Comparing Zonal and CFD model predictions of isothermal flow indoor airflows to experimental data. *Indoor Air,* **13,** 77-85.

Morawska, L. (2006) Droplet fate in indoor environments, or can we prevent the spread of infection? *Indoor Air,* **16,** 335-347.

Morris, G., Kokki, M. H., Anderson, K. & Richardson, M. D. (2000) Sampling of Aspergillus spores in air. *Journal of Hospital Infection,* **44**(2), 81-92.

Morsi, S. A. & Alexander, A. J. (1972) An investigation of particle trajectories in two-phase flow systems. *Journal of Fluid Mechanics,* **55**(2), 193-208.

Mortimer, E. A., Wolinsky, E., Gonzaga, A. J. & Rammelka.Ch (1966) Role of Airborne Transmission in Staphylococcal Infections. *British Medical Journal,* 1(5483), 319-322.

Nardell, E. A., Keegan, J., Cheney, S. A. & Etkind, S. C. (1991) Airborne Infection - Theoretical Limits of Protection Achievable by Building Ventilation. *American Review of Respiratory Disease,* **144**(2), 302-306.

National Audit Office (2000) The Management and Control of Hospital Acquired Infections in Acute NHS Trusts in England. London, National Audit Office.

Nazaroff, W. W. (2004) Indoor Particle Dynamics. *Indoor Air,* **14**(Suppl 7), 175-183.

Neely, N. & Maley, M. P. (2000) Survivial of Enterococci and Staphylococci on Hospital Fabrics and Plastics. *Journal of Clinical Microbiology,* **38**(4), 724-726.

Nettleman, M. D. (2003) Cost and Cost Benefit of Infection Control. In Wenzel, R. P. (Ed.) *Prevention and Control of Nosocomial Infections 4th Edition.* Philadelphia, Lippincott Williams and Wilkins.

NHS Estates (1989) Health Technical Memorandum 55: Windows. London, Department of Health.

NHS Estates (2005) HBN4 Supplement 1: Isolation facilities in acute settings. London, The Stationary Office.

Nicas, M. (1996) Estimating exposure intensity in an imperfectly mixed room. *American Industrial Hygiene Association Journal,* **57**(6), 542-550.

Nicas, M. (2000) Markov modeling of contaminant concentrations in indoor air. *Aihaj,* **61**(4), 484-491.

Nicas, M., Nazaroff, W. W. & Hubbared, A. (2005) Toward Understanding the Risk of Secondary Airborne Infection: Emission of Respirable Pathogens. *Journal of Occupational and Environmental Hygiene,* **2**, 143-154.

Noakes, C. J., Beggs, C. B. & Sleigh, P. A. (2004a) Modelling the performance of upper room ultraviolet germicidal irradiation devices in ventilated rooms: Comparison of analytical and CFD methods. *Indoor and Built Environment,* **13**(6), 477-488.

Noakes, C. J., Beggs, C. B., Sleigh, P. a., Fletcher, L. A. & Kerr, K. G. (2006a) Modelling the transmission of airborne infections in enclosed spaces. *Epidemiology and Infection,* **134**(5), 1082-1091.

Noakes, C. J., Fletcher, L. A., Beggs, C. B., Sleigh, P. A. & Kerr, K. G. (2004b) Development of a numerical model to simulate the biological inactivation of airborne microorganisms in the presence of ultraviolet light. *Journal of Aerosol Science,* **35**(4), 489-507.

Noakes, C. J., Sleigh, P. A. & Beggs, C. B. (2007) Modelling the air cleaning performance of negative air ionisers in ventilated rooms. In Seppanen, O. & Sateri, J. (Eds.) *Roomvent.* Helsinki Finland.

Noakes, C. J., Sleigh, P. A., Escombe, A. R. & Beggs, C. B. (2006b) Use of CFD analysis in modifying a TB ward in Lima, Peru. *Indoor and Built Environment,* **15**(1), 41-47.

Noakes, C. J., Sleigh, P. A., Fletcher, L. A. & Beggs, C. B. (2006c) Use of CFD Modelling to Optimise the Design of Upper-room UVGI Disinfection Systems for Ventilated Rooms. *Indoor and Built Environment,* **15**(4), 347-356.

Noble, W. C. (1962) Dispersal of Staphylococci in Hospital Wards. *Journal of Clinical Pathology,* **15**(6), 552-558.

Noble, W. C. (1975) Dispersal of Skin Microorganisms. *British Journal of Dermatology,* **93**(4), 477-485.

Noble, W. C. & Davies, R. R. (1965) Studies on Dispersal of Staphylococci. *Journal of Clinical Pathology,* **18**(1), 16-19.

Noble, W. C., Lidwell, O. M. & Kingston, D. (1963) The size distribution of airborne particles carrying micro-organisms. *Journal of Hygiene-Cambridge,* **61**, 385-391.

Pablos-Medez, A., Raviglione, M. C., Laszlo, A., Binkin, N., Rieder, H. L., Bustreo, F., Cohn, D. L., Lambregts-van Weezenbeek, C. S. B., Kim, S. J., Chaulet, P., Nunn, P. & The World Health Organisation - International Union against Tuberculosis and Lung Disease Working Group on Anti-Tuberculosis Drug Resistance Surveillance (1994-1998) Global Surveillance for antituberculosis-drug resistance, 1994-1997. *The New England Journal of Medicine,* **338**(23), 1641-1649.

Palmer, R. (1999) Bacterial contamination of curtains in clinical areas. *Nursing Standard,* **14**(2), 33-35.

Papinieni, R. & Rosenthal, F. S. (1997) The size distribution of droplets in the exhaled breath of healthy human subjects. *Journal of Aerosol Medicine,* **10**, 105-116.

Parker, M. T. (1972) Transmission in Hospitals. In Hers, J.P. and Winkler, K.C. (Eds.) *Airborne Transmission and Airborne Infection: 4th International Symposium on Aerobiology.* Technical University at Enschede, The Netherlands, Oosthoek Publishing Company.

Patanker, S. V. (1980) Numerical Heat Transfer and Fluid Flow. *Numerical Heat Transfer and Fluid Flow.* minnesota, Taylor and Francis.

Pittet, D., Allegranzi, B., Sax, H., Bertinato, L., Concia, E., Cookson, B., Fabry, J., Richet, H., Philip, P., Spencer, R. C., Ganter, B. W. K. & Lazzari, S. (2005) Considerations for a WHO European strategy on health-care-associated infection, surveillance, and control. *The Lancet Infectious Diseases,* **5**(4), 242-250.

Plowman, R., Graves, N., Griffin, M. A. S., Roberts, J. A., Swan, A. V., Cookson, B. & Taylor, L. (1999) The Socio-economic Burden of Hospital Acquired Infections., Public Health Laboratory Service, Health Protection Agency.

Plowman, R., Graves, N., Griffin, M. A. S., Roberts, J. A., Swan, A. V., Cookson, B. & Taylor, L. (2001) The rate and cost of hospital-acquired infections occurring in patients admitted to selected specialties of a district general hospital in England and the national burden imposed. *Journal of Hospital Infection,* **47**(3), 198-209.

Pratt, R. J., Pellowe, C. M., Wilson, J. A., Loveday, H. P., Harper, P. J., Jones, S. R. L. J., McDougall, C. & Wilcox, M. H. (2007) epic2: National Evidence-Based Guidelines for Preventing Healthcare-Associated Infections in NHS Hospitals in England. *Journal of Hospital Infection,* **65**(Supplement 1), S1-S59.

Prescott, L. M., Harley, J. P. & Klein, D. A. (2005) *Microbiology.* 6th ed. New York, McGraw Hill.

Rampling, A., Wiseman, S., Davis, L., Hyett, A. P., Wallbridge, A. N., Payne, G. C. & Cornaby, A. J. (2001) Evidence that hospital hygiene is important in the control of methicillin-resistant *Staphylococcus aureus*. *Journal of Hospital Infection,* **49**(109-116).

Ren, Z. G. & Stewart, J. (2005) Prediction of personal exposure to contaminant sources in industrial buildings using a sub-zonal model. *Environmental Modelling & Software,* **20**(5), 623-638.

Richmond-Bryant, J., Eisner, A. D., Brixey, L. A. & Wiener, R. W. (2006) Short-term dispersion of indoor aerosols: can it be assumed the room is well mixed? *Building and Environment,* **41**(2), 156-163.

Riley, E. C., Murphy, G. & Riley, R. L. (1978) Airborne Spread of Measles in a Suburban Elementary School. *American Journal of Epidemiology,* **107**(5), 421-432.

Riley, R. L., Shivpuri, D. N., Wittstadt, F., Ogrady, F., Sultan, L. U. & Mills, C. C. (1962) Infectiousness of Air from a Tuberculosis Ward - Ultraviolet Irradiation of Infected Air - Comparative Infectiousness of Different Patients. *American Review of Respiratory Disease,* **85**(4), 511-525.

Roberts, K., Hathway, A., Fletcher, L. A., Beggs, C. B., Elliott, M. W. & Sleigh, P. A. (2006) Bioaerosol production on a respiratory ward. *Indoor and Built Environment,* **15**(1), 35-40.

Rosebury, T. (1947) *Experimental Airborne Infection,* Baltimore, Williams and Wilkins Company.

Rui, Z., Guangbei, T. & jihong, L. (2008) Study on biological contaminant control srtategies under different ventilation models in a hospital operating room. *Building and Environment,* **43,** 793-803.

Rutala, W. A., Blythe Setzer Katz. E, Sherertz, R. J. & Sarubbi, F. A. (1983) Environmental Study of Methicillin Resistant *Staphylococcus aureus* Epidemic in a Burn Unit. *Journal of Clinical Microbiology,* 683-688.

Sciple, G. W., Riemensinder, D. K. & Schleyer, C. (1967) Recovery of Micro-organisms shed by humands into a sterilized environment. *Applied Microbiology,* **15**(6), 1388-1392.

Sekhar, S. C. & Willem, H. C. (2004) Impact of airflow profile on indoor air quality - a tropical study. *Building and Environment,* **39**(3), 255-266.

Sheretz, R. J., Reagan, D. R., Hampton, K. D., Robertson, K. L., Streed, S. A., Hoen, H. M., Thomas, R. & Gwaltney, J. M. (1996) A Cloud Adult: The Staphylococcus aureus Virus interaction revisited. *Annals of Internal Medicine,* **124**(6), 539-544.

Shih, Y.-C., Chiu, C.-C. & Wang, O. (2007) Dynamic airflow simulation within an isolation room. *Building and Environment,* **42**(9), 3194-3209.

Shiomori, T., Miyamoto, H., Makishima, K., Yoshida, M., Fujiyoshi, T., Udaka, T., Inaba, T. & Hiraki, N. (2002) Evaluation of bedmaking-related airborne and surface methicillin-resistant Staphylococcus aureus contamination. *Journal of Hospital Infection,* **50**(1), 30-35.

Shooter, R. A., Smith, M. A., Griffiths, J. D., Brown, M. E. A., Williams, R. E. O., Rippon, J. E. & Jevons, M. P. (1958) Spread of Staphylococci in a Surgical Ward. *British Medical Journal,* **1**(5071), 607-612.

Siegel, J. D., Rhinehart, E., Jackson, M., Chiarello, L. & Committee., Healthcare Infection Control Practices Advisory Committee. (2007) Guideline for Isolation Precautions:Preventing Transmission of Infection Agents in Healthcare Settings 2007 Atlanta, Georgia, USA, Centres for Disease Control and Prevention.

Sorensen, D. N. & Nielsen, P. V. (2003) Quality control of computational fluid dynamics in indoor environments. *Indoor Air,* **13**(1), 2-17.

Speers, R., Bernard, H., Ogrady, F. & Shooter, R. A. (1965) Increased Dispersal of Skin Bacteria into Air after Shower-Baths. *Lancet,* **1**(7383), 478-480.

Speers, R., Ogrady, F. W., Shooter, R. A., Bernard, H. R. & Cole, W. R. (1966) Increased Dispersal of Skin Bacteria into Air after Shower Baths - Effect of Hexachlorophene. *Lancet,* 1(7450), 1298-1299.

Srebic, J. & Chen, Q. (2002) Simplified Numerical Models for Complex Air Supply Diffusers. *HVAC&R Research,* **8**(3), 277-294.

Stockley, J. M., Constantine, C. E., Orr, K. E., The Association of Medical Microbiologists & Group, N. H. D. P. (2005) Building New Hospitals: a UK infection control perspective. *Journal of Hospital Infection,* **62,** 285-299.

Talon, D. (1999) The role of the hospital environment in the epidemiology of multi-resistant bacteria. *Journal of Hospital Infection,* **43**(1), 13-17).

Tang, J. W., Li, Y., Eames, I., P.K.S, C. & Ridgway, G. L. (2006) Factors involved in the aerosol transmission of infection and control of ventilation in healthcare premises. *Journal of Hospital Infection,* **64**(100-114).

Tenover, F. C. (2006) Mechanisms of antimicrobial resistance in bacteria. *American Journal of Infection Control,* **34**(5), S3-S10.

Tezduyar, T. E. (2006) Interface-tracking and interface-capturing techniques for finite element computation of moving boundaries and interfaces. *Computer Methods in Applied Mechanics and Engineering,* **195**(23-24), 2983-3000.

Tham, K. W. & Zuraimi, M. S. (2005) Size relationship between airborne viable bacteria and particles in a controlled indoor environment. *Indoor Air,* **15** (Suppl 9), 48-57.

Thatcher, T. L. & Layton, D. W. (1994) Deposition, Resuspension, and Penetration of Particles within a Residence. *Atmospheric Environment,* **29**(13), 1487-1497.

Thornton, T., Fletcher, L. A., Beggs, C. B., Elliott, M. W. & Kerr, K. G. (2004) Airborne Microflora in a Respiratory Ward. *American Society of Heating, Refrigeration and Air Conditioning Engineer. Indoor Air Quality Conference.* Tampa, Florida.

Tian, Z. F., Tu, J. Y., Yeoh, G. H. & Yuen, R. K. K. (2006) On the numerical study of contaminant particle concentration in indoor airflow. *Building and Environment,* **41,** 1504-1514.

Tinker, J. A. & Roberts, D. (1998) Indoor Air Quality and Infection Problems in Operating Theatres. *EPIC'98. 3rd International Conference on Energy Performance and Indoor Air Quality.* Lyon, France.

Versteeg, H. K. & Malalasekera, W. (1995) An Introduction to Computational Fluid Dynamics: The Finite Volume Method. *An Introduction to Computational Fluid Dynamics: The Finite Volume Method.* London, Prentice Hall.

Voss, A. (2004) Preventing the spread of MRSA - Common sense and observational studies are of benefit. *British Medical Journal,* **329**(7465), 521-521.

Wagenvoort, J. H. T., Davies, B. I., Westermann, E. J. A., Werink, T. J. & Toenbreker, H. M. J. (1993) MRSA from Air-Exhaust Channels. *Lancet,* **341**(8848), 840-841.

Walker, J. T., Hoffman, P., Bennett, A. M., Vos, M. C., Thomas, M. & Tomlinson, N. (2007) Hospital and Community acquired infection and the built environment - design and testing of infection control rooms. *Journal of Hospital Infection,* **65**(52), 43-49.

Walter, C. W. & Kundsin, R. B. (1973) Airborne Component of Wound Contamination and Infection. *Archives of Surgery,* **107**(4), 588-595.

Walter, C. W., Kundsin, R. B., Sholkret, M. A. & Day, M. M. (1958) The Spread of Staphylococci to the Environment. *Antibiotics Annual,* **6,** 952-957.

Wan, M. P., Chao, C. Y. H., Ng, Y. D., Sze To, G. N. & Yu, W. C. (2007) Dispersion of Expiratory Droplets in a General Hospital Ward with Ceiling Mixing Type Mechanical Ventilation System. *Aerosol Science and Technology,* **41**(3), 244-258.

Wang, L. & Chen, Q. (2007) Validation of a Coupled Multizone-CFD program for Building Airflow and Contaminant Transport Simulations. *HVAC&R Research,* **13**(2), 267-281.

Webster, R. G. (1998) Influenza: An emerging disease. *Emerging Infectious Diseases,* **4**(3), 436-441.

Weinstein, R. A. (1998) Nosocomial infection update. *Emerging Infectious Diseases,* **4**(3), 416-420.

Wells, W. (1955) *Airborne Contagion and Air Hygiene.* Massachusetts, Harvard University Press.

White, A. (1961) Relation between Quantitative Nasal Cultures and Dissemination of Staphylococci. *Journal of Laboratory and Clinical Medicine,* **58**(2), 273-277.

Williams, R. E. O. (1966) Epidemiology of Airborne Staphylococcal Infection. *Bacteriological Reviews,* **30**(3), 660-674.

Williams, R. E. O., Jevons, M. P., Shooter, R. A., Hunter, C. J. W., Girling, J. A., Griffiths, J. D. & Taylor, G. W. (1959) Nasal Staphylococci and Sepsis in Hospital Patients. *British Medical Journal,* **2**(OCT10), 658-662.

Williams, R. E. O., Lidwell, O. M., Noble, W. C., White, R. G., Thom, B. T., Shooter, R. A., Jevons, M. P. & Taylor, G. W. (1962) Isolation for Control of Staphylococcal Infection in Surgical Wards. *British Medical Journal,* (5300), 275-282.

Wong, T. W., Lee, C. K., Tam, W., Lau, J. T. F., Yu, T. S., Lui, S. F., Chan, P. K. S., Li, Y. G., Bresee, J. S., Sung, J. J. Y. & Parashar, U. D. (2004) Cluster of SARS among medical students exposed to single patient, Hong Kong. *Emerging Infectious Diseases,* **10**(2), 269-276.

Xie, X., Li, Y., Chwang, A. T. Y., Ho, P. L. & Seto, W. H. (2007a) How far droplets can move in indoor environments - revisiting the Wells evaporation - falling curve. *Indoor Air,* **17,** 211-225.

Xie, X., Sun, H. & Li, Y. (2007b) Number, Size and Total Mass of Respiratory Droplets of Healthy Individuals. In Seppanen, O. & Sateri, J. (Eds.) *Roomvent 2007.* Helsinki, Finland.

Yang, X. D., Srebric, J., Li, X. T. & He, G. Q. (2004) Performance of three air distribution systems in VOC removal from an area source. *Building and Environment,* **39**(11), 1289-1299.

Yu, I. T. S., Li, Y. G., Wong, T. W., Tam, W., Chan, A. T., Lee, J. H. W., Leung, D. Y. C. & Ho, T. (2004) Evidence of airborne transmission of the severe acute respiratory syndrome virus. *New England Journal of Medicine,* **350**(17), 1731-1739.

Zhang, Z. & Chen, Q. (2006) Experimental measurements and numerical simulations of particle transport and distribution in ventilated rooms. *Atmospheric Environment,* **40,** 3396-3408.

Zhang, Z., Chen, X., Sagnik, M., Zhang, T. & Chen, Q. (2007) Experimental and numerical investigation of airflow and contaminant transport in an airliner cabin mock-up. IN SEPPANEN, O. & SATERI, J. (Eds.) *Roomvent 2007.* Helsinki, Finland.

Zhao, B., Li, X. & Zhang, Z. (2004a) Numerical study of particle deposition in two differently ventilated rooms. *Indoor and Built Environment,* **13,** 433-451.

Zhao, B., Yang, C., Yang, X. & Liu, S. (2008) Particle dispersion and deposition in ventilated rooms: Testing and evaluation of different Eulerian and Lagrangian models. *Building and Environment,* **43,** 388-397.

Zhao, B., Zhang, Y., Li, X. T., Yang, X. D. & Huang, D. T. (2004b) Comparison of indoor aerosol particle concentration and deposition in different ventilated rooms by numerical method. *Building and Environment,* **39**(1), 1-8.

Zhu, S., Kato, S. & Yang, J. H. (2006) Study on transport characteristics of saliva droplets produced by coughing in a calm environment. *Building and Environment,* **41,** 1691-1702.

PAGE MISSING IN ORIGINAL

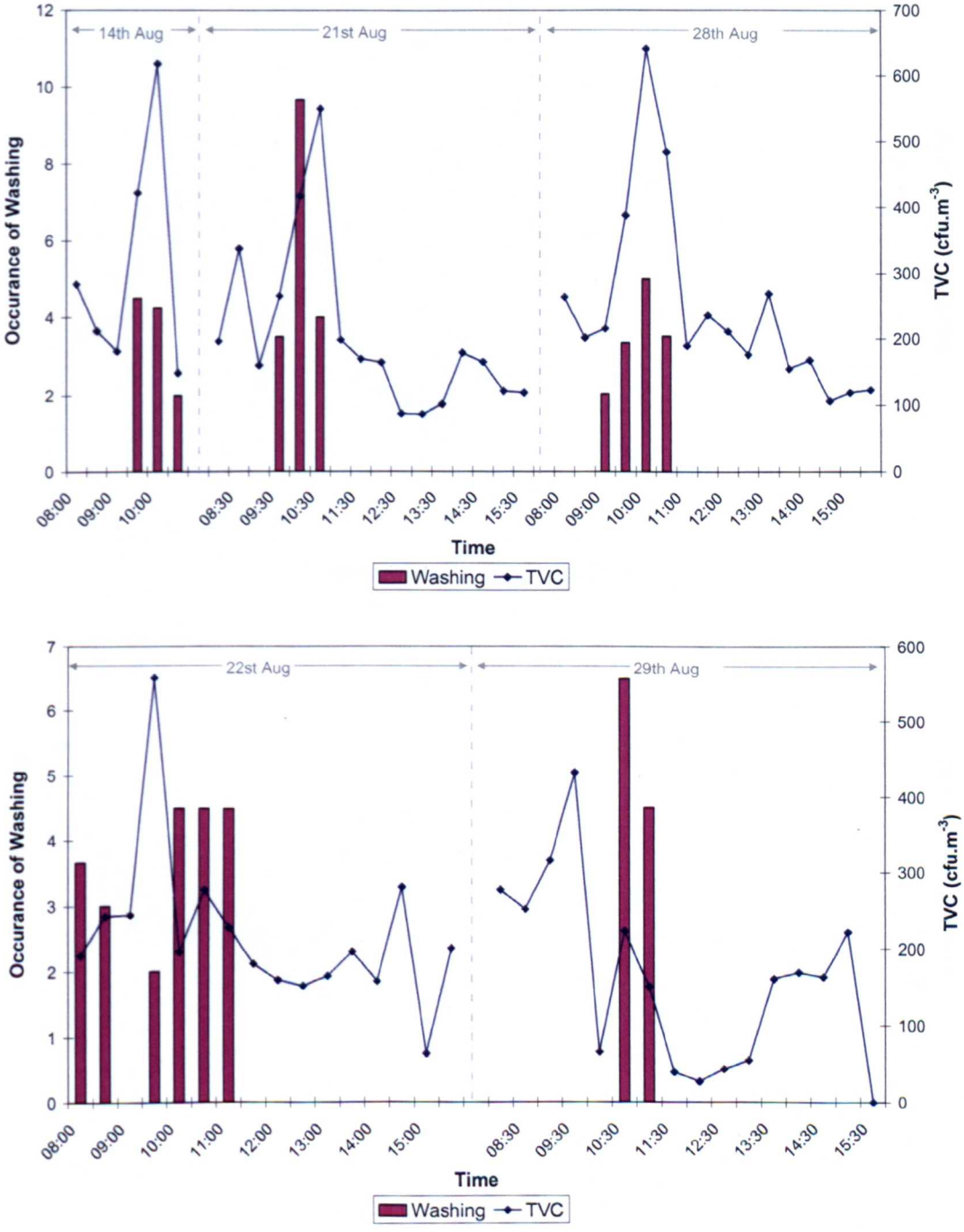

Figure A 1-2 Fluctuations of Washing and TVC on both the busy (top) and quiet (bottom) days of Study 2.

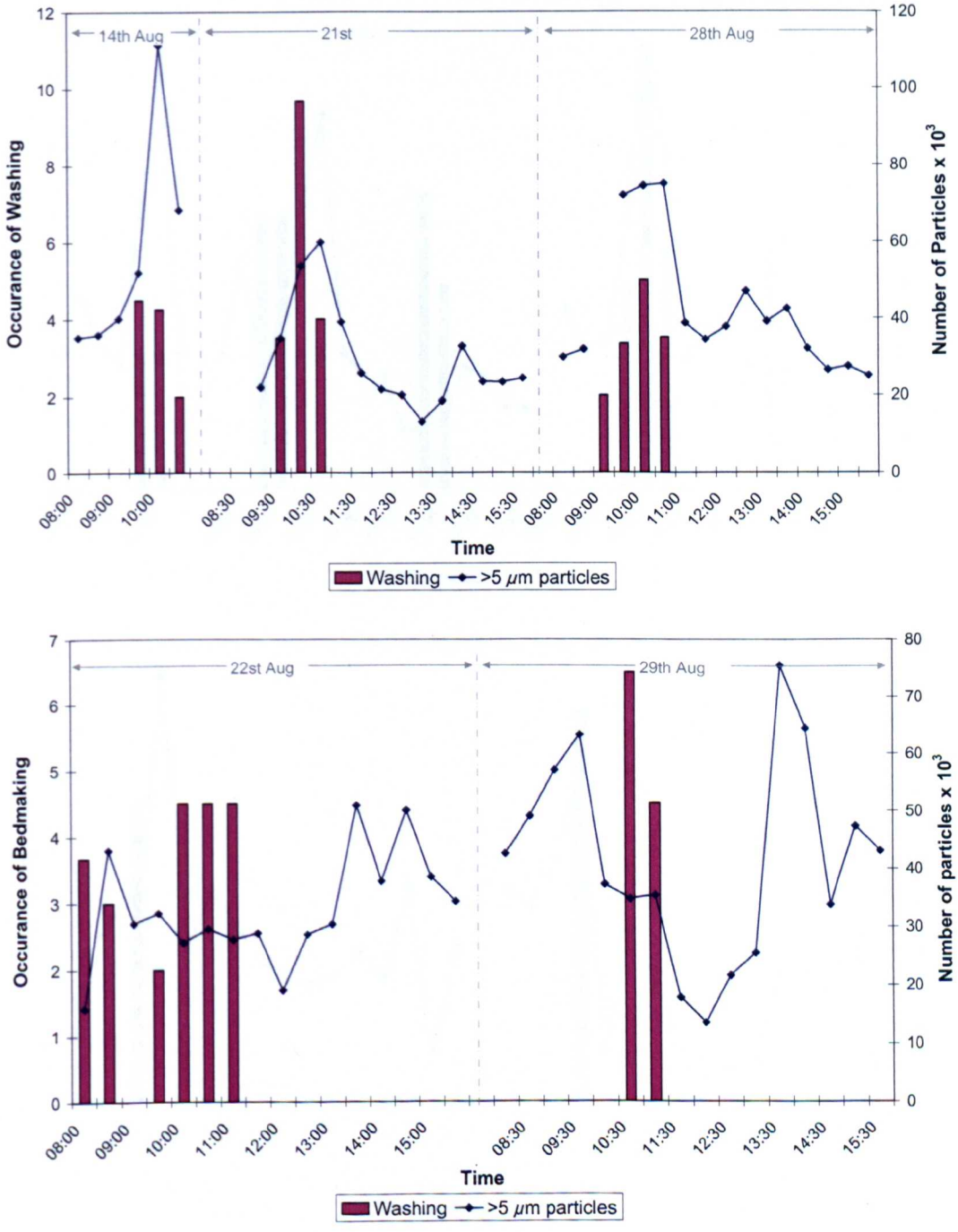

Figure A 1-3 Fluctuations of Washing and particles >5μm characteristic diameter on the busy (top) and quiet (bottom) days of Study 2.

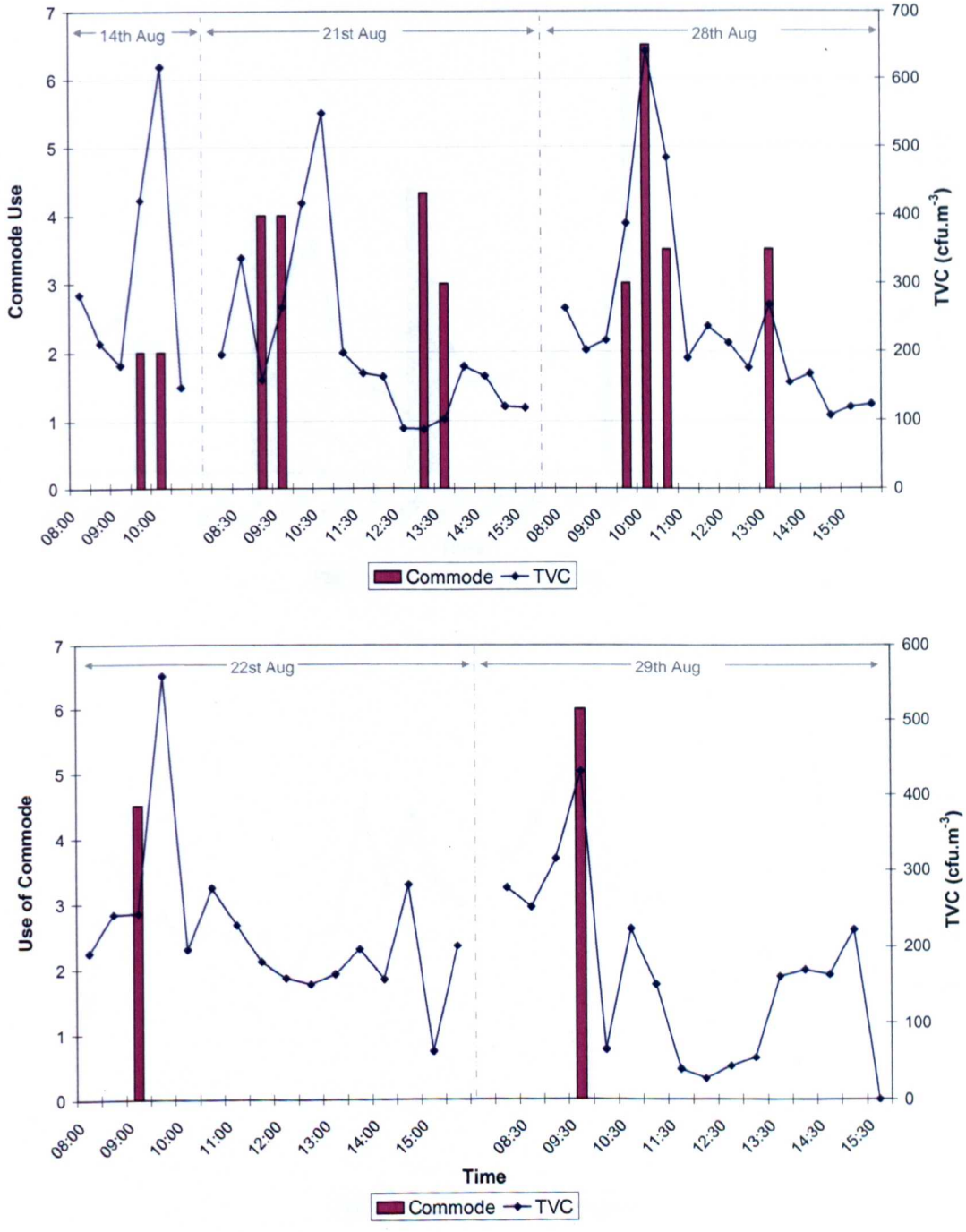

Figure A 1-4 Fluctuations in the use of the Commode and TVC on the busy (top) and quiet (bottom) days of Study 2.

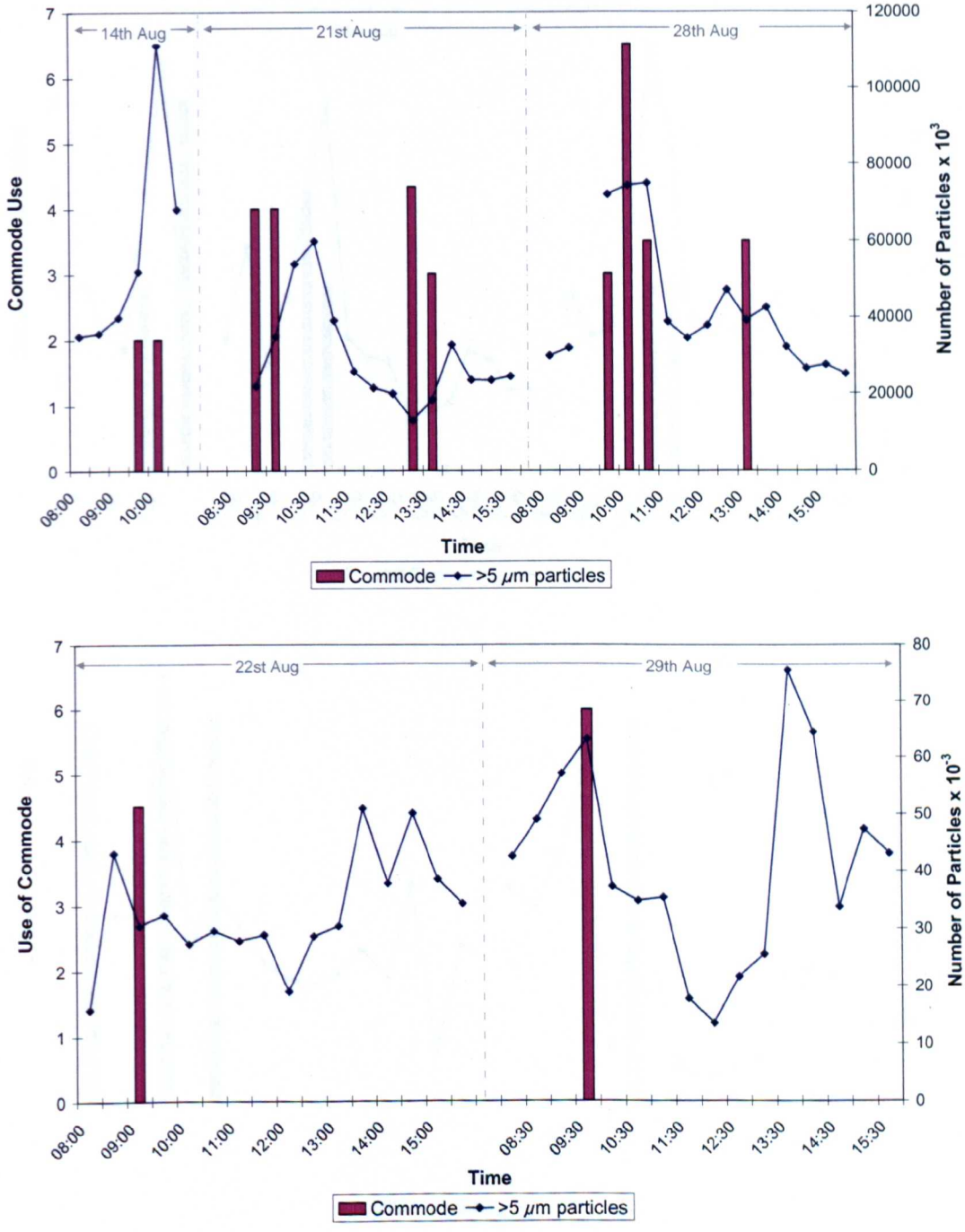

Figure A 1-5 Fluctuations of Commode use and particles > 5μm characteristic diameter on busy (top) and quiet (bottom) days of Study 2.

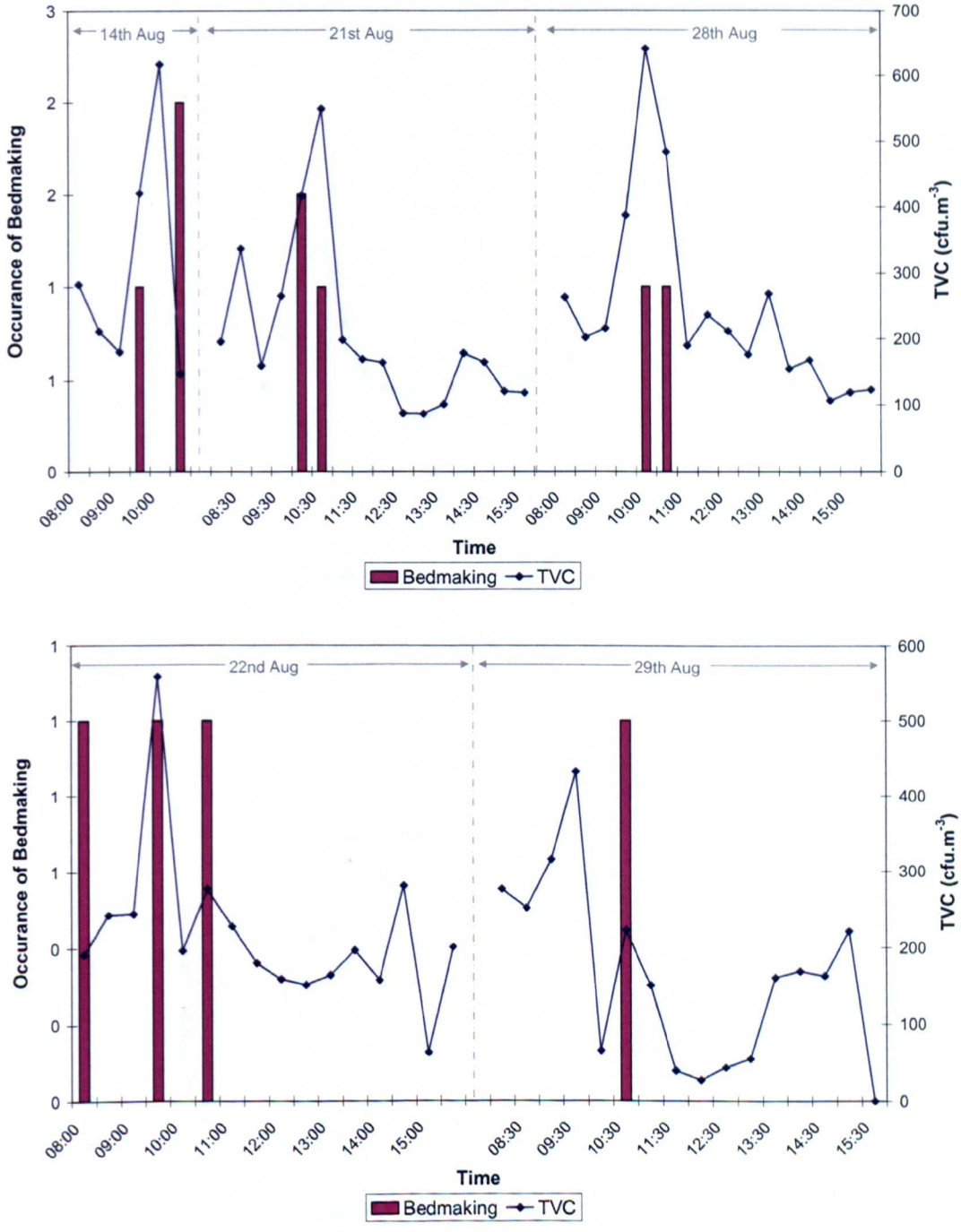

Figure A1-6 Fluctuations of Bedmaking and TVC on busy (top) and quiet (bottom) days of Study 2. On the 29th the window was open during bedmaking.

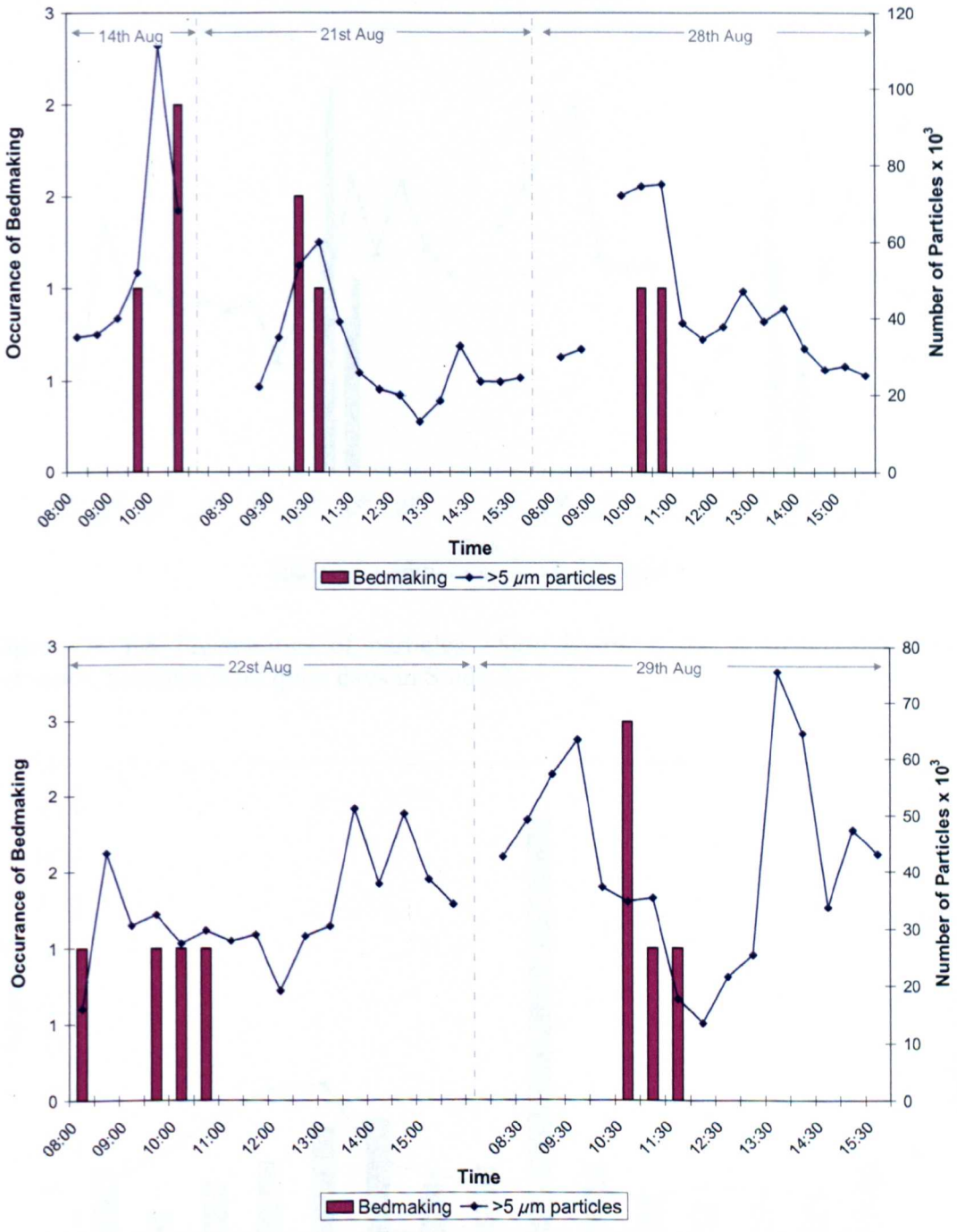

Figure A 1-7 Fluctuations of Bedmaking and > 5μm characteristic diameter on busy (top) and quiet (bottom) days of Study 2.

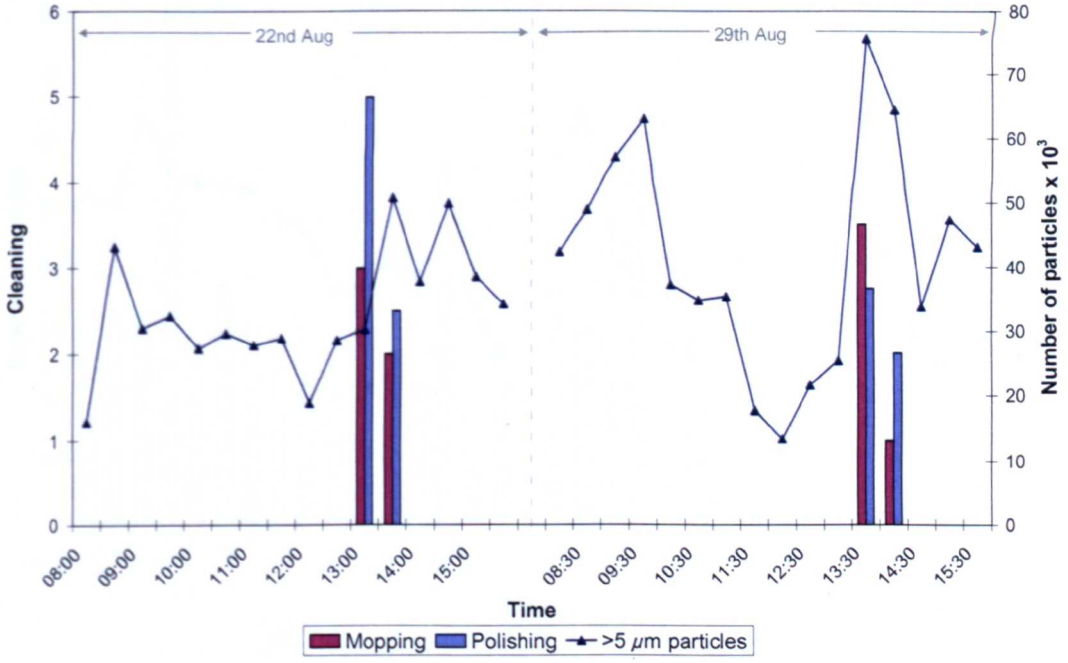

Figure A 1-8 Fluctuations of particles >5μm characteristic diameter and cleaning activities. Samples from quiet days in Study 2.

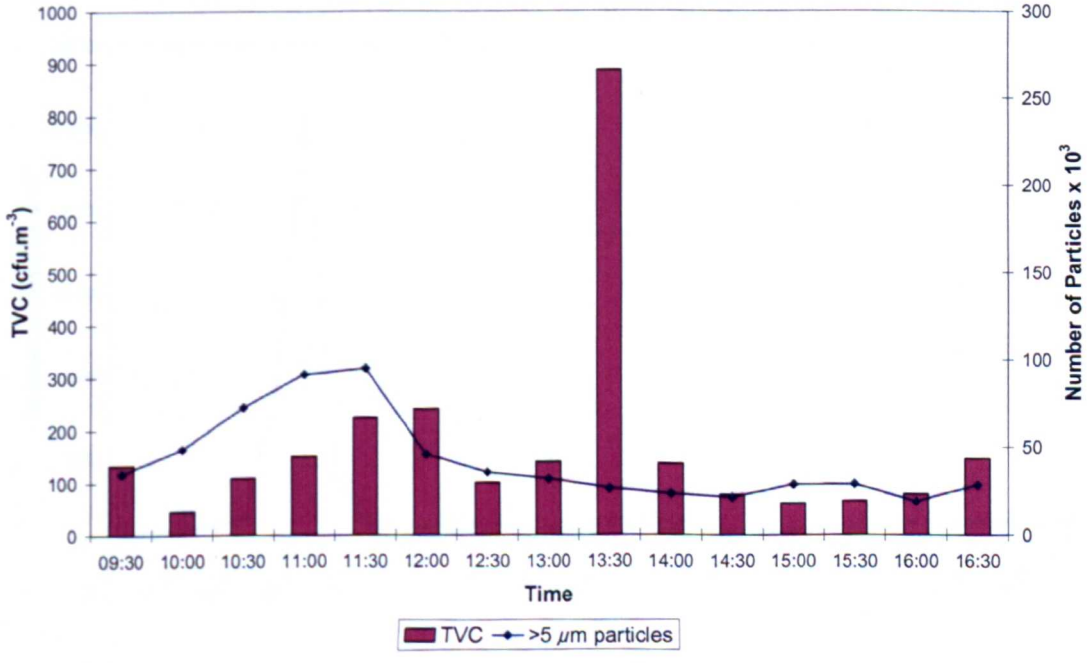

Figure A 1-9. Fluctuations of TVC and particles > 5μm characteristic diameter on Study 1 quiet day.

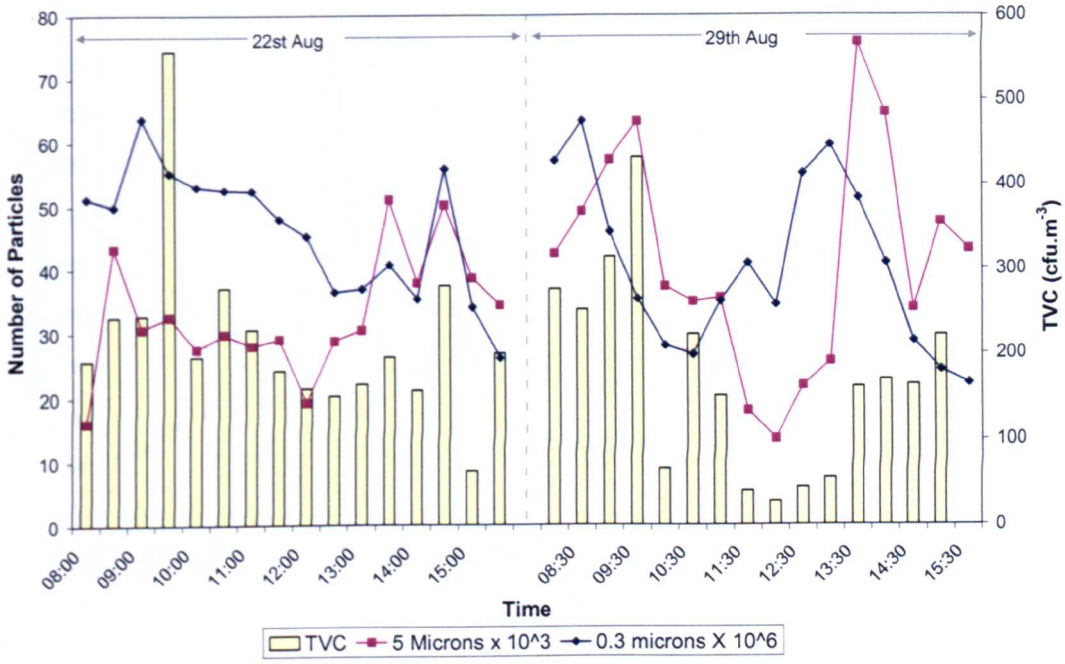

Figure A 1-10 Fluctuations of TVC and particles. Values of particles 0.3-0.5μm characteristic diameter are shown at 10^6 and >5μm particles are shown at 10^{-3} on the left y axis. For quiet days of Study 2.

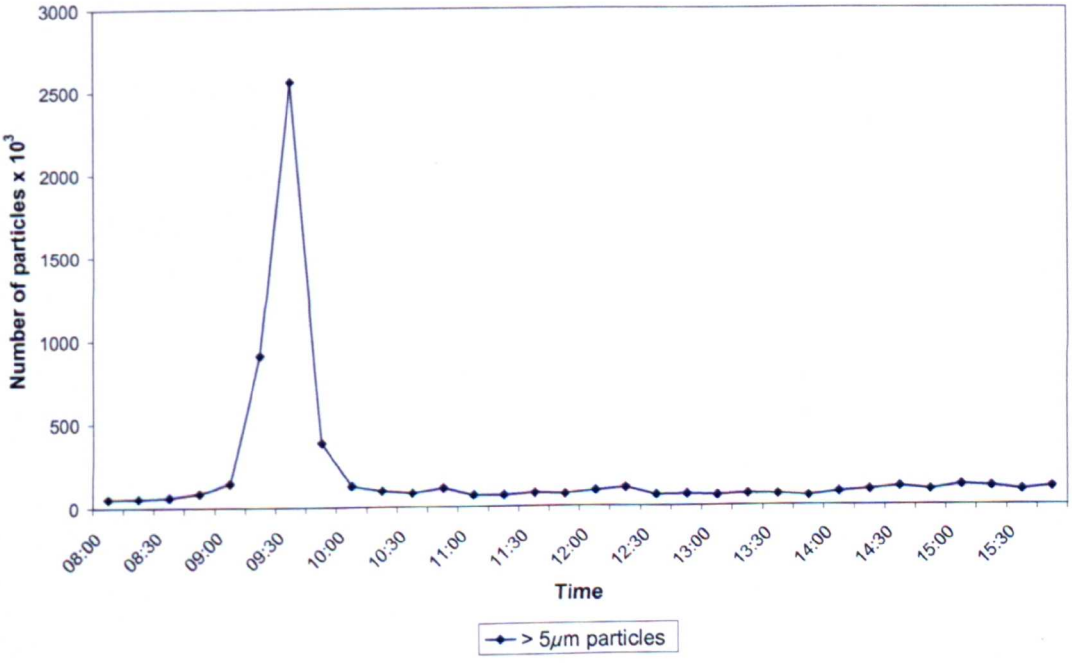

Figure A 1-11 Fluctuations of particles > 5μm characteristic diameter Study 2 7th August 2007

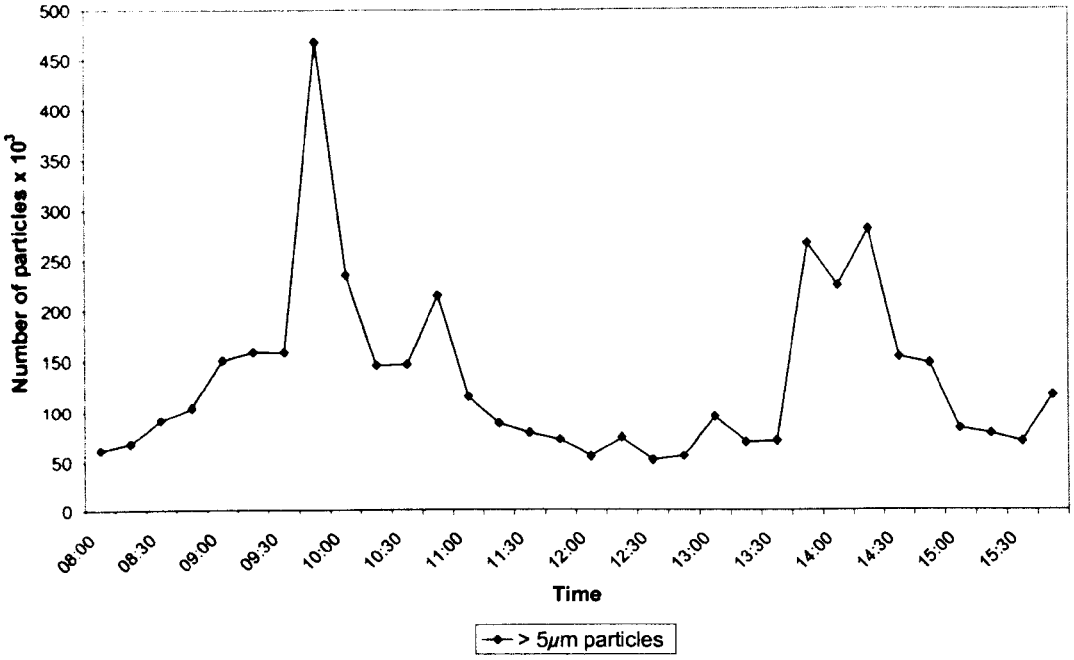

Figure A1-12 Fluctuations of particles > 5μm characteristic diameter Study 2 8th August 2007

Appendix 2: Related Publications

The following is a list of publications published or submitted. 1, 2, 4 and 5 in the list below are printed in full in the following section as these have been published and relate directly to work in Chapter 4, 5, 6 and 7 as specified at the beginning of this thesis.

1. Roberts, K., Hathway, A., Fletcher, L.A., Beggs, C.B., Elliot, M.W., Sleigh, P.A. (2006). "Bioaerosol production on a respiratory ward." Indoor and Built Environment **15**(1): 35-40.

2. Hathway, E.A., Sleigh, P.A. Noakes, C.J. (2007). "CFD Modelling of Transient Pathogen Release in Indoor Environments due to Human Activity". Proceedings of Roomvent. Helsinki. Finland.

3. Beggs, C.B., Kerr, K.G. Noakes, C.J., Hathway, E.A., Sleigh, P.A., (2008). "The Ventilation of Multi-Bed Hospital Wards: Review and Analysis" American Journal of Infection Control **36**(4):250-259.

4. Hathway, E.A., Sleigh, P.A., Noakes, C.J. "CFD Modelling of a Hospital Ward: Assessing risk from bacteria produced from respiratory and activity sources." Submitted to Indoor Air 2008 Conference, Copenhagen.

5. Hathway, E.A., Fletcher L.A., Noakes, C.J. Sleigh, P.A. "Bioaerosol production from routine activities within a hospital ward" Submitted to Indoor Air 2008 Conference. Copenhagen.

Bioaerosol production on a respiratory ward

K Roberts [1], A Hathway [1], LA Fletcher [1], CB Beggs [2], MW Elliott [3], PA Sleigh [1]

[1] *School of Civil Engineering, University of Leeds, Leeds*
[2] *School of Engineering, Design and Technology, University of Bradford, Bradford*
[3] *St James's University Hospital, Leeds*

Abstract
Although much hospital acquired infection is associated with person-to-person contact, there is increasing evidence that some nosocomial infections may be transmitted via the airborne route. However, the knowledge base concerning airborne microflora in hospitals is poor. In particular, there is a need for good quality data relating bioaerosol production to clinical activity in hospital wards. A short aerobiological survey was therefore undertaken by the authors on a respiratory ward at St James's University Hospital in Leeds in order to gain an understanding of the relationship between activity and bioaerosol production. This survey involved regular microbiological and particulate (0.3 – 5 μm) sampling of the ward air, together with an observational study of ward activity. Two identical four bedded ward bays were surveyed, one containing high dependency patients who regularly used non-invasive ventilators (NIVs), and the other containing patients who did not require mechanical ventilation. The survey found a correlation between activity and aerosol production.

1.0 Introduction

Nosocomial infection is a serious and widespread problem; with approximately 1 in 10 patients acquiring an infection during a hospital stay (1). While many of these infections are associated with person-to-person contact, there is growing evidence that some can be transmitted by the airborne route. Indeed, it has been estimated that this route of transmission accounts for 10-20% of all endemic nosocomial infections (2). However, the contribution made by airborne microorganisms towards the overall burden of nosocomial infection is unclear and much scepticism surrounds the issue (3, 4). Consequently, the importance of airborne microflora in hospitals has largely been ignored, and little has been done in this field since the 1960s (5, 6, 7), with the result the epidemiology associated with airborne infection remains ill understood.

Given the paucity of reliable data on airborne microflora in the clinical environment, a short aerobiological survey was undertaken in 2003 on a respiratory ward at St James's University Hospital, Leeds, in the United Kingdom (8). This study indicated that Gram-negative bacteria were widely dispersed in the ward air, and suggested that one possible dissemination source might be the non-invasive mechanical ventilators used on the ward. In order to investigate this further, a second short aerobiological study was carried out on the same ward in December 2004. The aim of this study was to gain an understanding of the relationship between ward activity and the production of aerosol particles. This paper presents the results of this study and discusses its findings.

2.0 The Study

The study was undertaken in a large respiratory ward at St James's University Hospital. Two identical four-bedded bays on the ward were studied, one containing high dependency (HD) patients who regularly used non-invasive ventilators (NIVs), and the other containing non-HD patients who did not use ventilators. The HD-bay was observed and surveyed on the 16th December and the non-HD-bay on the 17th December. The two study bays were identical to each other and as shown in Figure 1. Both bays were located off a long corridor, either side of a nurses station (see Figure 2). Both were naturally ventilated and were open to the corridor, which was mechanical ventilated. With the exception of one occasion, the windows in both bays were closed during the study period.

For both bays, ward activity was observed from 9.00 to 17.00, and the movements of patients, nurses, doctors, visitors, cleaners and other workers recorded. So as not to interfere with activity within the bays, observations were made from the corridor. Regular microbiological and particulate samples were taken from the air throughout the study period. The air sampling points were located near the window in each bay, as shown in Figure 1.

2.1 Microbiological and Particulate Air Sampling

The number and size distribution of airborne particulate matter on the wards was recorded using a Kanomax 3886 laser particle counter (Kanomax, Andover, NJ, USA). This was programmed to run continuously from 9.00 to 17.00 and recorded the particle count every five minutes for five size distributions, 0.3 - 0.5µm, 0.5 - 1µm, 1 - 3µm, 3 - 5µm and >5µm. The particle counter was placed on a metal trolley and positioned near the window at a height of 870 mm above the floor. Microbial air sampling was undertaken using a single stage Microbio MB2 impactor (FW Parrett Ltd, London, UK). Three 500 litre samples were collected every 30 minutes (nominally) throughout the study period. The microbial samples were collected on tryptone soy agar plates in the Microbio sampler. The samples were incubated overnight at 37°C and the total viable count (TVC) recorded. The Microbio sampler was placed on a tripod, 1100 mm above floor level, and located next to the laser particle counter.

Because of limited resources and the large amount of microbial data collected it was not possible to speciate the samples collected. However, cultures isolated from a few colonies were plated onto mannitol salt agar in order to select for the presence of *Staphylococcus aureus*. These were incubated overnight at 37°C.

3.0 Results

Figures 3 and 4 show logarithmic graphs of particulate counts recorded on the 16th and 17th December for the HD and non-HD bays, respectively. The data are presented for five particle sizes, 0.3 - 0.5 µm, 0.5 – 1 µm, 1 – 3 µm, 3 - 5 µm, and >5 µm. The occurrence and duration of key activities (e.g. bed making) are also indicated. From both graphs it can be seen that a cyclical pattern emerges, with peaks occurring at the start of both the morning and afternoon periods. Table 1 shows the correlation of 0.3 - 0.5 µm, 0.5 - 1 µm, 3 - 5 µm, and >5 µm particle size data with the 1 - 3 µm data for both the HD and non-HD bays. From this it is evident that for both bays there is a strong correlation between the 0.3 - 0.5 µm, 0.5 – 1 µm, 3 – 5 µm data and the 1 - 3µm data, whereas no correlation exists between the >5 µm data and the 1 – 3 µm data.

Bay	Particulate Size	Correlation with 1 - 3 µm data	Correlation
HD bay	0.3 - 0.5 µm	$R^2 = 0.771$	Strong
	0.5 - 1.0 µm	$R^2 = 0.958$	Very Strong
	3.0 - 5.0 µm	$R^2 = 0.884$	Very Strong
	>5 µm	$R^2 = 0.009$	None
Non-HD bay	0.3 - 0.5 µm	$R^2 = 0.728$	Strong
	0.5 - 1.0 µm	$R^2 = 0.956$	Very Strong
	3.0 - 5.0 µm	$R^2 = 0.877$	Very Strong
	>5 µm	$R^2 = 0.003$	None

Table 1 Correlation of data for various particulate sizes with the 1-3µm data for the HD and non-HD bays

The results of the microbial air sampling are presented in figures 5 and 6. Key events which to appear to have influenced bioaerosol production are marked on these graphs. Although, figures 5 and 6 show only the TVC, *Staphylococcus aureus* was cultured from the air on both the study days.

3.1 Observations

With regard to airborne particulate matter, both figures 3 and 4 show a similar cyclical pattern, with 'peaks' occurring for all particle sizes, except >5 µm, at the start of both the morning and afternoon periods. Interestingly, while there appears to be strong correlation between the data in the 0.3 - 5 µm range, there appears to be little correlation between this data and that for >5 µm. The behaviour of the data for the 1 - 3 µm particles on the 17th December is noteworthy – in the morning these data correlate with the >5 µm data, but in the afternoon they correlate more strongly with the <3 µm data. By contrast, the particulate data for the 16th December indicates a

close correlation between the 1 - 3 µm data and the <3 µm data. From figures 3 and 4 is can be seen that particulate counts were generally lower during periods of inactivity (e.g. late morning and mid-afternoon). This effect was particularly pronounced for the <3 µm particles. For example, during the afternoon on both study days (when the bays are relatively quiet), the <3 µm particle counts smoothly tailed off to a minimum value. This effect is not observed in the >5 µm data, which is much more noisy.

3.2 16th December

Many of the peaks observed in the particulate data correspond to activities observed on the ward. Key events which noticeably influenced particulate behaviour in the HD bay on the 16th December are listed in Table 2.

Time	Events	Outcome
9.10 – 9.30	Meal trolley; ward round (6 people); bed made for patient B	Peak in <5 µm particles
9.55 – 10.00	Use of NIV equipment by patient B	Sharp rise in <5 µm particles
10.17 – 10.35	Use of NIV equipment by patient B	Large peak in <5 µm particles
11.10 – 11.45	Floor mopping; beds made for patients B, C and D	Twin peek in >3 µm particles
12.35 – 12.45	Activity around patient C's bed	Small pear in >5 µm particles
12.55 – 13.10	Unclear (possibly associated with lunchtime activity)	Sharp rise in <5 µm particles
13.20	Visitor adjacent to particulate counter	Small rise in 1 – 5 µm particles
13.25 – 13.41	Use of nebulizer by patient C	Rise in <5 µm particles
13.25 – 14.00	Use of nebulizer by patient D	Rise in <5 µm particles
14.20 – 14.35	Beds A & C made and bed C disinfected ready for new patient; new patient admitted to bed C	Peak in <3 µm particles
15.50 – 16.05	Activity around Patient B's bed; curtains closed	Sharp rise in >5 µm particles

Table 2 Events associated with peaks in particulate production in the HD bay on 16th December.

If the particulate data shown in Figure 3 are compared with the corresponding microbiological data in Figure 5, it is evident that there is some correlation between the microbiological data and the >5 µm data. With reference to Figure 5, the peaks at events A, C, D, E, F and G all coincide with peaks in the >5 µm in Figure 3, as do the 'microbiological' peaks preceding event I and following event K.

3.3 17th December

Although the particulate graphs for the 16th and 17th December are similar in general appearance, it is noticeable that on 17th December the <3 µm particle counts start off high and then fall steadily, whereas on the 16th December they started low and rose to a peak. Key events which noticeably influenced particulate behaviour in the non-HD bay on the 17th December are listed in Table 3.

Time	Events	Outcome
9.20 – 9.55	Window open	Sharp dip in >0.5 μm particles
9.40 – 10.10	Use of nebulizers by patient B	Sharp rise in particles of all sizes (effect masked by closing window)
11.00	Patient C washes	Large peak in >3 μm particles
11.30	Bed making	Large peak in >3 μm particles
12.45 – 13.15	Use of nebulizer by patient D	Sharp rise in <5 μm particles
12.45 – 13.40	Use of nebulizer by patient C	Sharp rise in <5 μm particles
14.00 – 14.25	Use of nebulizer by patient D	Sharp rise in <5 μm particles
15.30	Visitor adjacent to particulate counter	Sharp peak in >3 μm particles

Table 3 Events associated with peaks in particulate production in the non-HD bay on 17th December.

If the particulate data shown in Figure 4 are compared with the corresponding microbiological data in Figure 6, it can be seen there is only a modest correlation between the data. With reference to Figure 6, the peaks at events B and C coincide with peaks in the >5 μm in Figure 4, while the large 'microbiological' peak at 13.35 hours occurred during a period of nebulization when the <5 μm particle count was very high.

4.0 Discussion

The study described in this paper is, to the authors' best knowledge, the first of its kind. Never before has an aerobiological survey in a hospital been correlated with ward activity. Although only a short study, it generated a large amount of useful data and shed light on the sources of aerosol production within the clinical environment. In particular, the study demonstrated that aerosol particles can easily be generated by a variety of everyday activities.

The particulate data for both the study days are consistent with the expected behaviour of aerosol particles suspended in a ventilated space. For example, on the 17th December after 14.25 (when patient D stopped using a nebulizer), the <5 μm data exhibit a classic exponential decay curve, which flattens out at about 15.30. A very similar picture is observed for the data collected on the 16th December. With respect to <5 μm data for the 17th December, the horizontal line exhibited after 15.30 indicates that steady state has been reached, and that the rate of aerosol production is equal to the rate of aerosol removal. Aerosol particles are generally removed by room ventilation. If the ventilation rate is increased, then the slope of the aerosol decay curve will become steeper. This is amply illustrated by the open window in the non-HD bay, which occurred on the morning of the 17th December. When the window was opened there was a sharp decrease in the particulate count for all particle sizes. The fact that the particulate count fell when the window was open indicates that the particles were generated within the room space and were not entering the ward from outside.

The fact that >5 μm particulate data is completely independent of the <3 μm data, indicates that the larger aerosol particles are emanating from different sources to the smaller particles. It is noticeable in both figures 3 and 4, that the >3 μm data (particularly the >5 μm data) is more 'noisy' than the <3 μm data. While individual fluctuations in the <3 μm data are generally much greater than those in the >3 μm data, the fluctuations in the >3 μm data are much more frequent. This suggests that aerosol generating events are much more numerous amongst the >3 μm particles compared with the smaller particles. Presumably, many of the >3 μm particles are skin squamae released into the air during activities such as bed making. Skin squamae are generally in the size range 4 - 25 μm and often carry staphylococci. Given that *Staphylococcus aureus* isolates where cultured from the air in both the study bays, this suggests that during the study skin squamae were disseminated through the air. The fact that the <3 μm data is much smoother than that for the larger particles, indicates that these smaller particles were generated

by fewer events. For example, in the afternoons of both the study days, the bulk of the additional <3 µm particles generated appear to have come from nebulizers used by the patients. When nebulizer use ceased the <3 µm particle count smoothly decayed over a period of several hours.

It is evident from tables 2 and 3 that heightened activity in the study bays is reflected in the >3 µm particle count. Bed making and curtain movement in particular appear to be associated with increased >3 µm particle production. This corroborates the findings of Greene et al. (5) who observed that the process of bed making caused a significant increase in the microbial bioburden. It also supports the findings of Das *et al.* (9) who suggested that contaminated bed curtains, when moved, could promote the airborne dissemination of microorganisms.

While the study has demonstrated that patient nebulizers can disseminate large quantities of small aerosol particles into the environment, the results of the study are much less conclusive with regard to NIVs. Although the use of NIVs clearly contributed to aerosol production in the HD bay before 11.00 on the 16th December, their use from 11.15 – 13.15 and from 14.15 – 16.45 (not shown in Figure 3) on the same day appears to have had little impact on overall particulate counts.

5.0 Conclusions

The study has demonstrated that aerosol particles (including bioaerosol particles) are frequently liberated within the clinical environment. It has also demonstrated that it is possible to link aerosol production with specific tasks, using the methodology described. The use of nebulizers appears to be associated with the production of <3 µm particles, whereas the movement of people and bed making is more likely to be associated with the production of >3 µm particles.

References

1. Mertens RAF. Methodologies and results of national surveillance. *Baillieres Clinical Infectious Diseases.* 3 (1996) 159 – 178
2. Brachman PS. Airborne infection – airborne or not? *Proceedings of the International Conference on Nosocomial Infection. American Hospital Association.* (1970) 189-192
3. Rhame FS. The inanimate environment. Chapter 20, *Hospital Infections.* Fourth Edition, Edited by JV Bennett, PS Brachman, Lippincott-Raven Publishers, 1998
4. Beggs CB. The airborne transmission of infection in hospital buildings: fact or fiction? *Indoor and Built Environment.* 12; pp. 1-10; (2003)
5. Greene VW, Bond RG, Michlaelsen MS. Air handling systems must be planned to reduce the spread of infection. *Modern Hospital*, August 1960
6. Greene VW, Vesley D, Bond RG, Michlaelsen MS. Microbiological studies of hospital air. I. Quantitative studies. *Applied Microbiology.* 10 (1962) 561
7. Greene VW, Vesley D, Bond RG, Michlaelsen MS. Microbiological studies of hospital air. II. Quantitative studies. *Applied Microbiology.* 10 (1962) 567
8. Thornton T, Fletcher LA, Beggs CB, Elliott MW, Kerr KG. Airborne microflora in a respiratory ward. *ASHRAE IAQ Conference*, Tampa, Florida, 15 – 17th March (2004)
9. Das I, Lambert P, Hill D, Noy M, Bion J, Elliott T. Carbapenem-resistant *Acinetobacter* and role of curtains in an outbreak in intensive care units. *Journal of Hospital Infection.* 2002; 50; 110-114

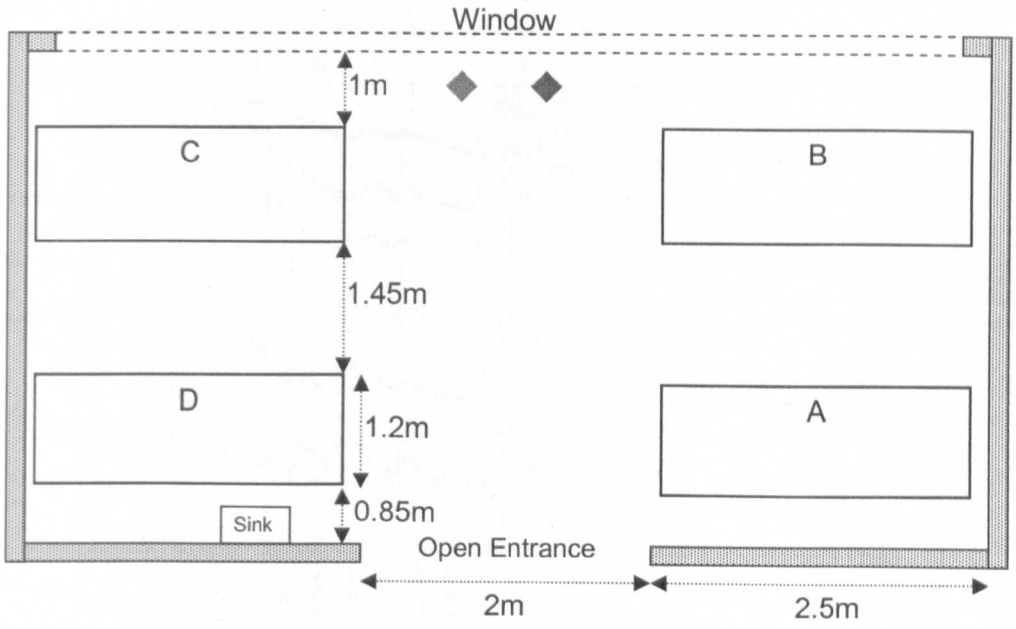

Figure 1 Plan of a four bedded study bay.

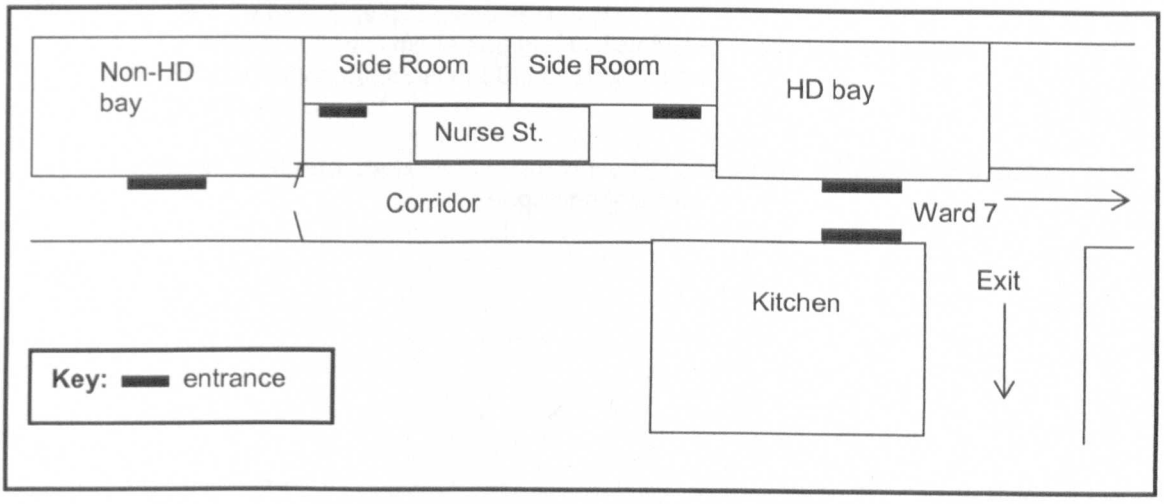

Figure 2 Floor plan of the respiratory ward showing the location of the study bays.

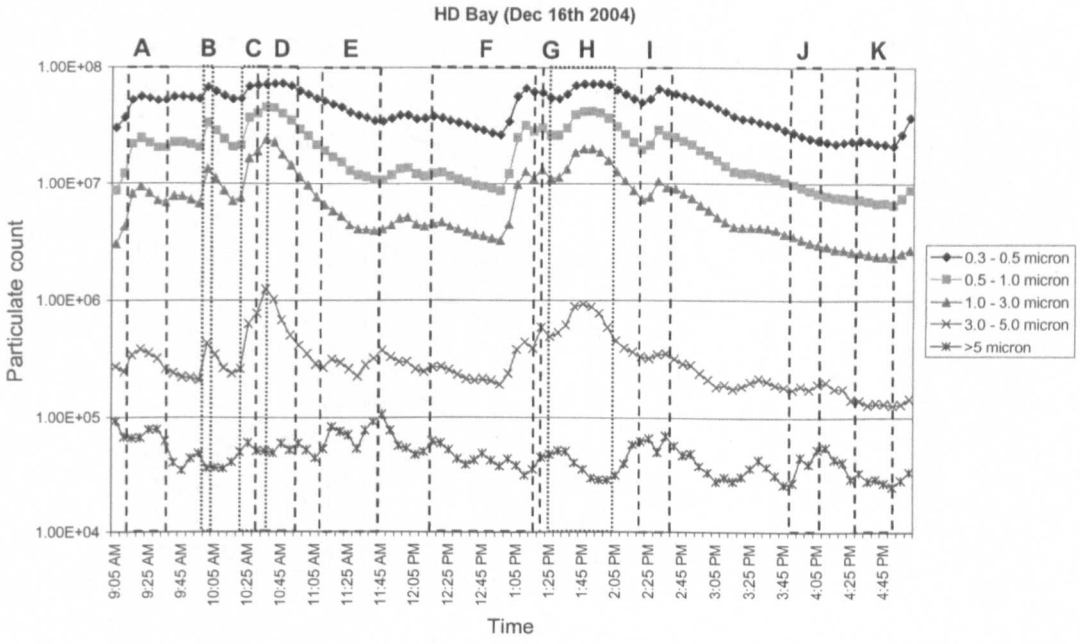

A = Breakfast, ward round and bed making (Bed B)
B = Patient B using NIV
C = Patient B using NIV
D = Bed making (Bed D) and cleaning
E = Furniture moved, floor mopping and bed making (Beds B, C & D)
F = Lunch time and drugs round
G = Visitor adjacent to particulate counter
H = Patients C and D using nebulizers
I = Beds A and C made and bed C disinfected ready for new patient
J = Activity around patient B, curtains closed
K = Evening meal

Figure 3 Airborne particulate count in the HD bay on the 16th December 2004 (logarithmic scale)

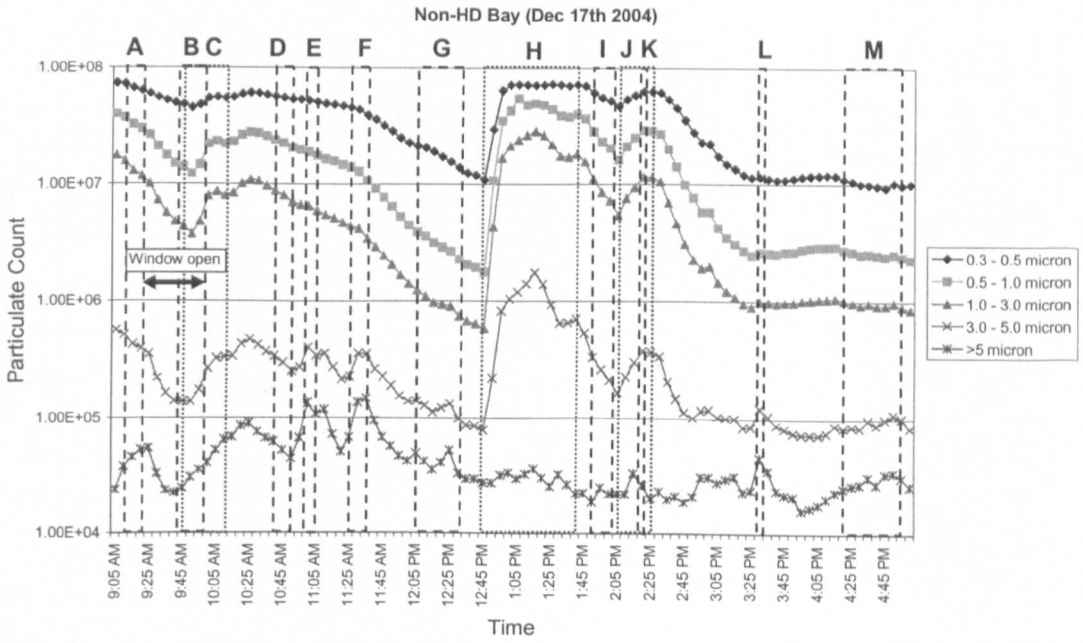

A = Breakfast and bed making
B = Ward round
C = Patient B using nebulizer
D = Floor mopping
E = Patient C washing
F = Bed making
G = Lunch time
H = Patients C and D using nebulizers
I = Activity at bed B
J = Patients using nebulizers
K = Tea trolley round
L = Visitor adjacent to particle counter
M = Evening meal

Figure 4 Airborne particulate count in the non-HD bay on the 17th December 2004 (logarithmic scale)

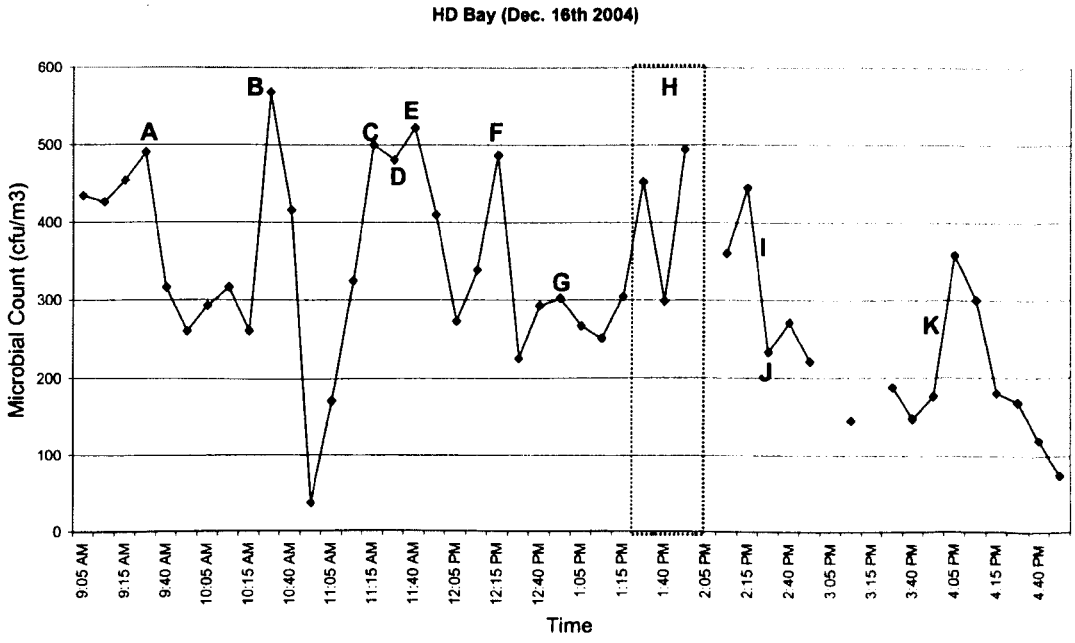

A = Bed making at bed B
B = Bed making at bed B
C = Bed making at bed C
D = Bed making at bed D
E = Bed making at bed B
F = Meal trays dispensed
G = Meal trays collected
H = Patients using nebulizers
I = Bed making at beds A and C
J = New patient in bed C and furniture moved
K = Activity around bed B

Figure 5 Airborne microbial count in the HD bay on the 16th December 2004

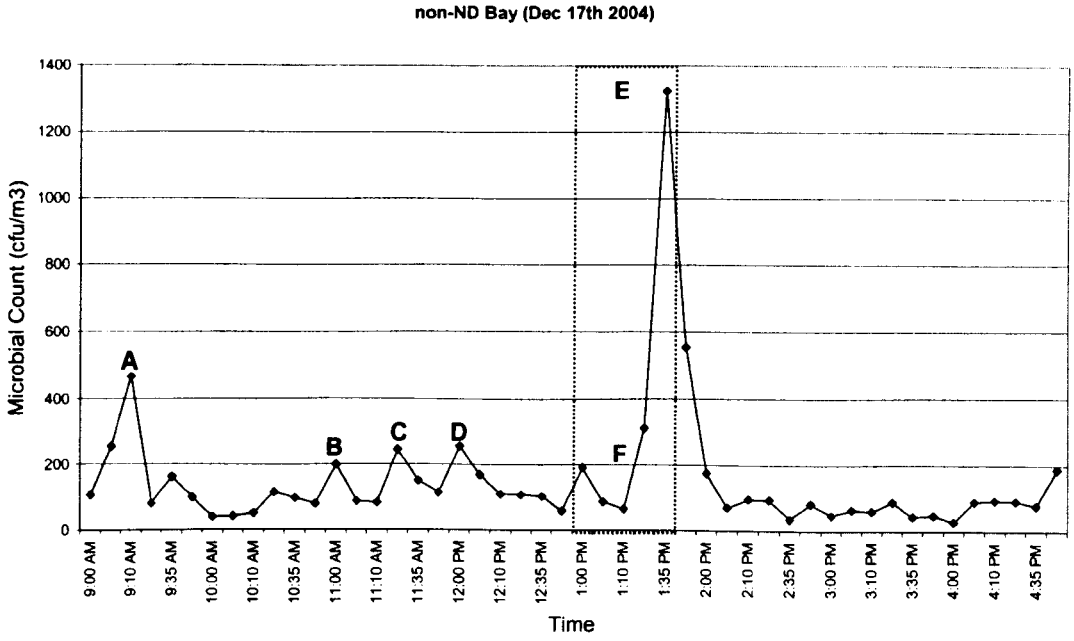

A = Breakfast and bed making
B = Patient C washing
C = Activity around bed B
D = Meal trolley outside entrance to bay
E = Patients C and D using nebulizers
F = Waste bins changed

Figure 6 Airborne microbial count in the non-HD bay on the 17th December 2004

CFD Modelling of Transient Pathogen Release in Indoor Environments due to Human Activity

E.A.Hathway, P.A.Sleigh, C.J.Noakes
Pathogen Control Engineering Research Group, School of Civil Engineering, University of Leeds, LS2 9JT, UK

Corresponding email: E.A.Hathway99@leeds.ac.uk

SUMMARY

Certain routine hospital activities have been identified as a potential source for the airborne dispersal of micro-organisms. With increasing use of CFD to model hospital situations a method of modelling this type of spread within a simple steady state model is required. Since this type of dispersal will vary with space and time a single point source would not provide adequate information to represent these sources. Instead a zonal bioaerosol source is introduced to represent the time average of the varying release from the activity. In this paper, data from experiments conducted in a bioaerosol test chamber are compared to CFD results. Numerical validation is also carried out comparing the zonal source to an equivalent transient source. The results indicate that the zonal source provides excellent comparison to the time averaged behaviour of a moving source, but greatly underestimates the maximum value at any one location.

INTRODUCTION

The dissemination of micro-organisms within indoor environments increases the potential for the rapid spread of disease. Many hospital patients are in some sense immuno-compromised and it is common that they are alongside patients who are suffering from infectious diseases. This close confinement provides a situation well suited to the dissemination and acquisition of infection[1].

There are several routes for the transfer of infection within the hospital environment, the most significant being that via hand contact between health-care workers and patients. However, infection through an airborne mechanism (if only partially) is also important. There are several mechanisms for micro-organisms to become airborne: being expelled by coughing and sneezing; through vomiting, diarrhoea, and through the natural shedding of skin particles. Certain routine activities in hospital wards can also cause a number of large particles, e.g. skin particles, to be dispersed into the environment. These particles may carry with them viable bacteria potentially capable of spreading disease. For instance it is well recognised that activities such as walking, undressing/dressing and bedmaking all disperse large numbers of bacteria into the air [2-6]. Within a busy hospital ward a significant level of activity occurs that could result in the dispersion of bacteria. Indeed our own studies have found that particles are frequently dispersed into the air within a respiratory ward and that activity may be responsible for the release of a large number of particles greater than 3μm [7]. In addition 70% of isolates sampled from the air in the respiratory ward were organisms that may form part of the normal skin flora[8].

Computational Fluid Dynamics is an increasingly popular tool for detailed modelling of the movement of air and this basic technique can be extended to analyse the spread of

contaminants transported by an air flow. However most attempts at simulating a hospital ward do not account for many of the transient influences, preferring to consider a 'freeze frame', representative situation. A number of published works using CFD to model bio-aerosol spread in hospitals have considered respiratory infections such as SARS [9-11]and Tuberculosis [12]. In all of these cases a directed point source is used to represent the dispersal of particles from a cough, which is appropriate where the patient is primarily bed bound. Some interesting recent work by Brohus *et al* [13] highlighted the need for considering the effect of movement on airflow patterns in an operating room situation. They found that movement could cause the transport of bioaerosols from the non-clean area of the operating room to the clean area and used a simple model that included distributed momentum sources and a turbulent kinetic energy source to simulate the influence of movement on the air flow. However, despite the obvious potential for pathogens to be released through general ward activity, the use of CFD to directly model the spread of particles in this manner has not been considered. As CFD is increasingly being used to model hospital situations, a method of easily modelling this airborne dispersal of infectious material may lead to a greater understanding of the spread of disease within the ward environment.

This study considers how to represent the dispersion of micro-organisms that are shed from the human skin during activity. Activity related dispersal may occur over a large area varying in position and rate with time as people move about the hospital, carrying out different tasks. A detailed transient model of this situation would not only use an unfeasible amount of CPU, but would provide misleadingly detailed information about a situation that would change continuously. This study aims to develop a representative method for modelling the dispersion from a bacteria source that varies in time and space, within a steady state model. The study introduces the concept of using a 'zonal' source that time averages the dispersion over the area in which the activity occurs. In order to assess the validity of this zonal representation, experiments are carried out in a bioaerosol test chamber under controlled environmental conditions, introducing bacteria across a zone. The dispersion pattern from this is compared to a CFD model using a zonal source. Numerical validation is then carried out using this model to assess the suitability of using a zonal source instead of a point source to represent the dispersion of bacteria from a transient source. Steady state models are developed to model the dispersion from the point and zonal source and the dispersion patterns from these are compared to a transient model of a bioaerosol point source that moves through the space.

METHODS

Experimental Methods

All experiments were carried out in a climatically controlled aerobiological test chamber at The University of Leeds. This is a hermetically sealed 32.25m^3 (3.35 x 4.26 x 2.26m) room with a controlled, hepa filtered ventilation system. Air is supplied to the room through an inlet at low level and extracted near the ceiling as shown in figure 1 (Inlet A/Outlet A).

Bioaerosol Source

A pure culture of *Serratia marcescens* suspended in distilled water was aerosolised using a six jet Collinson nebuliser (CN 25,BGI Inc, USA) and injected over a zone into

the space through 8 sets of 4 holes spaced 15cm apart around the edge of a 34mm diameter plastic pipe. Each set of holes is rotated by 45°.This is centred at a height of 1.15m and bioaerosols are emitted starting 0.42m from the wall over a space of 1.2m. As shown in figure 2. *Serratia marcescens* was used to create the bio-aerosols. This particular bacterium was chosen as it is easy to grow on nutrient agar, poses minimal risk and the colonies are pink, enabling any contamination from other sources to stand out.

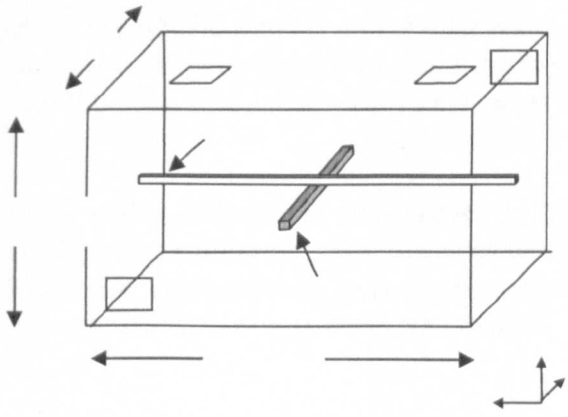

Figure 1: Schematic of the Room geometry

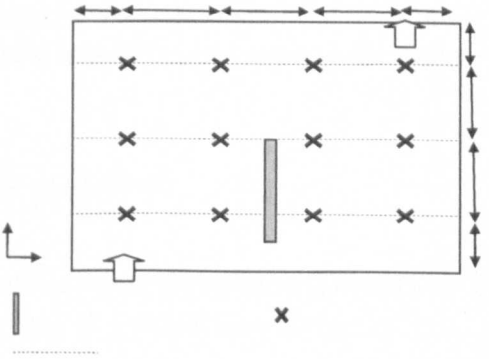

Figure 2: Plan of room showing bioaerosol source for experimental validation and sampling points.

During the experiments the ventilation rate was set at a constant rate and the nebuliser operated continuously to maintain a steady-state bioaerosol concentration in the chamber. Before any samples were taken the air flow and the nebuliser were allowed to run for 45 minutes to achieve this steady-state. Air samples were then taken from the test chamber through 5mm tubes pulling air out at 12 points spaced equally in the room as shown in figure 2. The sampling locations were at the same height as the bioaerosol inlet, 1.15m above floor level. An Anderson sampler was used to take the air samples, impacting the bacteria onto nutrient agar. Only levels 5 and 6 of the Anderson sampler were used, relating to bioaerosol sizes of smaller than 2μm. Samples were taken from each of the 12 points in the room, every 10 minutes, with 44 litres of air sampled in each case. This was then repeated 8 times with the order of sampling varied. After incubating overnight at 37°C the microbial colonies on the plates were counted and *positive hole correction* applied [14] to quantify the concentration in terms of colony forming units per cubic metre (cfu/m^3).

Description of CFD Model

Airflow Simulation

The CFD analysis of the test chamber was carried out using Fluent 6.1.22. Two 3D models were created of a 32.25m^2 (3.35 x 4.26 x 2.26 high) room with geometry as shown in figure 1 to simulate two different ventilation regimes. A tetrahedral grid was used containing approx 540,000 cells with refinement around the inlet, outlet and bacterial source. A grid refinement study was carried out prior to choosing this mesh. A standard k-ϵ turbulence model was used with enhanced wall treatment and a no slip condition was applied at the walls. The model was treated as isothermal as there were

no heat sources within the test chamber during the experiments and the incoming air temperature was controlled.

Velocity inlets were defined to simulate an air change rate of 6 AC/h for the two different ventilation regimes. Ventilation regime A used a low to high ventilation system as shown by Inlet A/Outlet A in figure 1. The angled louvers on the inlet were represented by describing the inlet velocity as a series of velocity profiles resulting in an average velocity of 0.04m.s^{-1}, 10mm in front of the inlet. The extract was modelled as a zero pressure boundary (with 0 Pa imposed).

In order to consider the effect of the zonal source with a different air flow pattern in the numerical validation, a second method, regime B, using ceiling mounted diffusers was defined. This is shown in figure 1 by Inlet B/Outlet B. Air enters the space with a speed of 0.59m.s^{-1}, at a downwards angle of 45°, from vertical slits 60mm deep. The extract was treated again as a zero pressure boundary.

Bioaerosol Distribution

For this study the bioaerosols were assumed to remain airborne for long periods of time which is suitable for small micro-organisms 2μm in diameter or less. With this assumption it is reasonable to use a passive scalar to model the bacterial sources. The movement of the bacteria within the space was therefore solved using the scalar transport equation:

$$\frac{\partial \phi}{\partial t} + div(\phi \mathbf{u}) - div(\Gamma grad\phi) = 0, \qquad (1)$$

Where ϕ is the concentration of micro-organisms per unit volume (quantity.m^{-3}); $\mathbf{u}$ is the velocity vector (u,v,w) of the air (m.s^{-1}); and Γ is the diffusivity (m^2.s^{-1}).

Natural decay of viable micro-organisms in the space is not considered in this case. The diffusivity of the bio-aerosols is set to 1x10^{-7}m^2.s^{-1}.

CFD Source definition for Experimental Validation

A zonal source was set up to represent the injection of bacteria over an entire zone 0.1 x 0.1 x 1.2 m long, located as shown in figure 2. A small volumetric momentum source was applied to represent the expulsion into the air that these particles will receive, for which 0.1 N.m^{-3} was added in all directions around the edge of the source. Sensitivity tests were carried out on adding this volumetric momentum source, and since it is over a thin area it does not affect the global room air flow.

CFD Source definition for Numerical Validation

In order to validate the zonal source model, dispersion from this and a point source were compared to an equivalent transient source moving through the space. These three different types of bioaerosol source are described below.

Transient Source: The scalar source is applied over a small cube 0.1m3 this moves through the space at 1.2x10-3 m.s-1. For case 1 (figure 1a) this moves in the z direction through 3m across the centre of the room, with the initial position at z = 0.42m. For case 2 the source moves in the x direction starting at x = 0.33m, for 3.93m. A slow speed was chosen in order to ensure there was large amount of dispersion during the time the

source is moving. A momentum source was added as detailed above. This model is used to find the time averaged scalar values across the space, the volume average scalar values and the maximum value in the space over the whole time.

Zonal Source: The zonal source was set up to inject the same overall scalar quantity into the space as the transient source injects per time step. This injection takes place over the entire zone that the transient source travels through. For case 1 the zonal source is 0.1 x 0.1 x 3.0m long and runs across the centre of the room in the z direction. For case 2 the zonal source is 0.1 x 0.1 x 3.6m running in the x direction centrally in the room. A momentum source is added at the edge of the whole zone as before.

Point Source: The point source is positioned in the centre of the room; and therefore the centre of the zonal source. The same quantity of scalar is again dispersed into the space over a volume of 0.1m3 with a small volumetric momentum source of 0.1N.m-3 defined at the edges.

Solution Process

Second order discretisation of the governing equations was used over the whole domain and solutions found using a segregated, implicit solver. The solution was considered to be converged when the residuals were less than 5×10^{-4} and the net imbalance of mass flow within the space was less than 0.1%.

The air flow was considered as steady state for all cases however the scalar transport equation was solved transiently to simulate the moving source. A first order implicit solution was carried out using a time step of 10s. This was chosen by running a series of models with times steps of 1s, 10s, 100s. The results with a time step of 10s were deemed to be of a suitable

accuracy when compared to a 1s time step, hence this was chosen for the final model.

RESULTS

Experimental Validation of Zonal Source

The experimental results showed a large amount of variation for each point. This variation is to be expected as turbulence factors in the room will affect the movement of the contaminant. The process of spraying micro-organisms into the room and sampling by impaction onto an agar plate is highly stressful and will lead to some organisms dying, which will also increase the variance of the results.

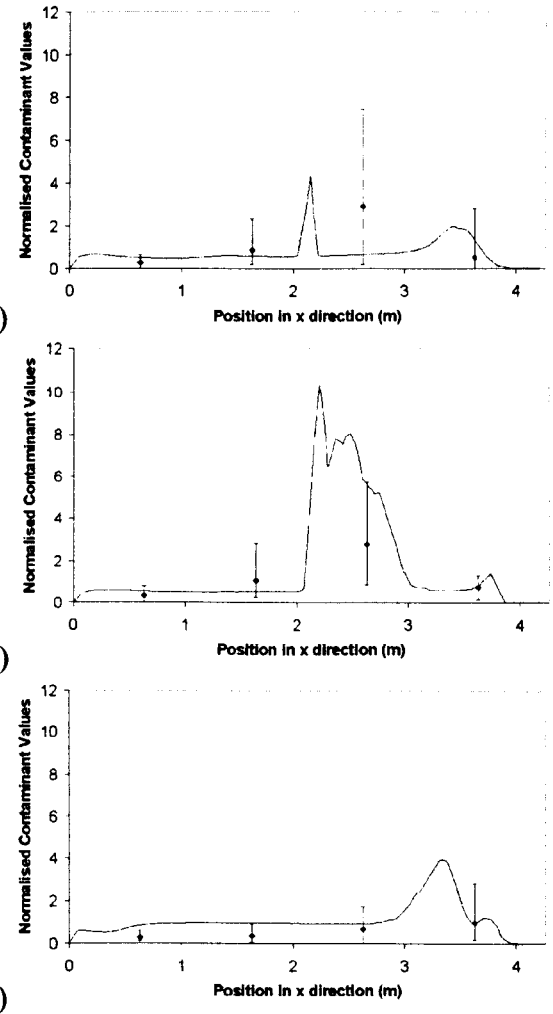

Figure 3: Experimental point values and error bars compared to CFD line values normalised about the average value on that plane. a) Line z = 0.67m 1b) Line z = 1.67m, c) Line z = 2.67m

In order to compare the experimental and CFD results for a zonal source, the computed bioaerosol concentration was plotted along three lines running in the x direction at the height of the experimental sampling plane. These lines are shown in figure 2. The experimental sample point values were averaged and normalised around the total average for the plane during one experimental run. These values were plotted on the same figures (figure 3), together with error bars to show the variance in the experiments. Figure 3 shows the general trend in the experiment is reflected in the CFD model. There are some differences in the results, particularly close to the source; this is likely to be due sampling a volume in the experiment but taking point values from the CFD results. All the points fall within the experimental error bars, indicating the maximum and minimum values sampled, or very close to them. Figures 4a and b show concentration contours on the horizontal sampling plane. The pull towards the inlet side of the source is visible in both the experimental and CFD results. Figure 4c shows clearly where there are higher build ups of bio-aerosols in 3 dimensions.

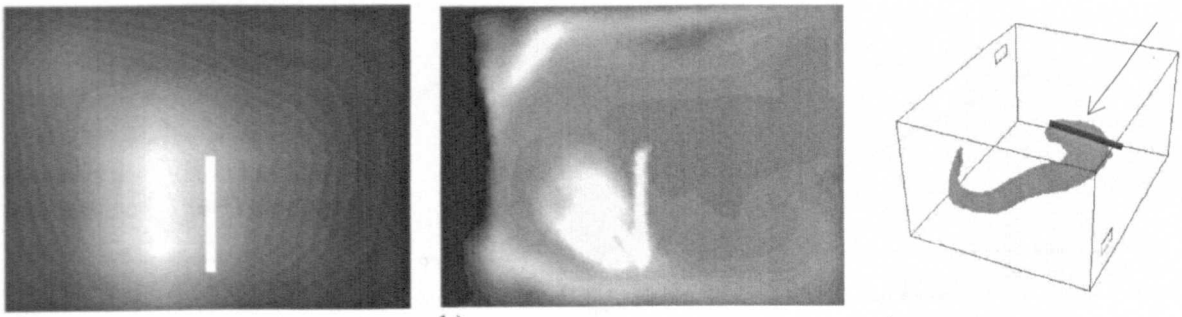

a) b) c)

Figure 4: Contours of bioaerosol values on plane y = 1.15m a) experimental results, b) CFD results. c) Plume showing 3D dispersal pattern from the zonal source in CFD.

Numerical Validation of Zonal Source

To numerically compare the dispersion patterns from the three sources; transient, zonal and point, plots of scalar concentration values were produced on x-z planes, y = 1.15m, the height
of the source, and y = 1.60m, representing the breathing height of a standing person. The scalar values at each cell were output in each case. In order to assess the ability of the zonal source in representing the time averaged behaviour of a transient source, scatter plots of the two results were created to show the correlation between them. This was also carried out to compare the transient source to the point source

For the two different ventilation regimes, orientation of sources and planes of results the graphs show clearly that the time averaged dispersion from the transient source is more closely represented by a zonal source than a central point source (figures 5-8). Statistical analysis showed that the correlation of the zonal source is consistently close to the time averaged with values of r^2 over 0.84 (table 1). When using the point source the correlation to the time averaged model improves as the sample plane is moved further from the source. For instance figure 6bii shows very good correlation using a point source. But this is not always the case, figure 8bi shows very poor correlation with the point source even on the plane at y = 1.60m. Depending on the position of the source and the ventilation regime the correlation for a point source varies greatly.

However, the zonal source greatly underestimates the maximum scalar value in the room. For ventilation regime A, case 1, the maximum value for the point source is much closer to the transient source than the zonal source (figure 9a). However comparing the maximum values in the room with the other regimes show even the results from the point source model give very low maximum values in the room relative to the transient source. In these cases the zonal model gives a maximum scalar value that is only 4-9% of the value for the transient source. This may be because, depending the source position, the scalar will get caught in areas of recirculation which leads to a large build up over time. The zonal source tends to over estimate the time average of the volume average in the space (figure 10) but is representative of the maximum volume average that occurs throughout the whole time period.

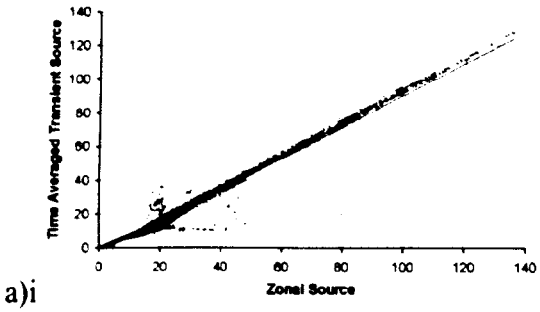

a)i

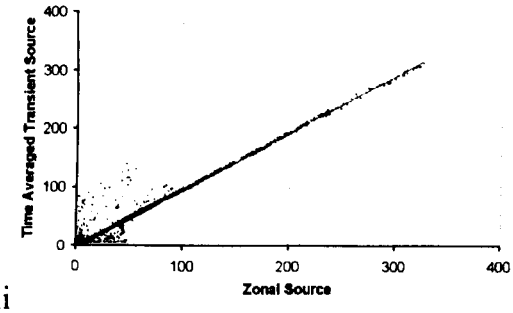

a)ii

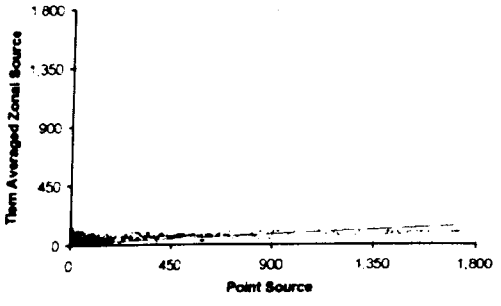

b)i

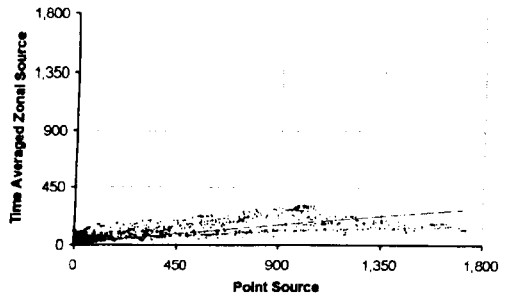

b)ii

Figure 5: Scalar concentration (x1000) at each cell. Ventilation Regime A. Sample plane y=1.15m. a) zonal source against the time averaged values from a transient source b) Point source against the time averaged values from a transient source i) Case 1 ii) Case 2.

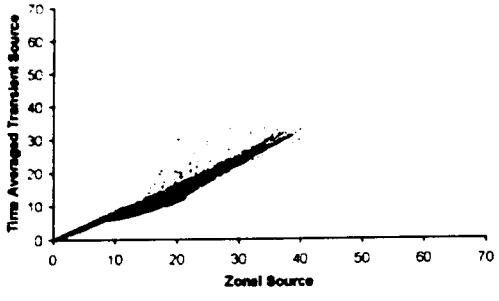

a)i

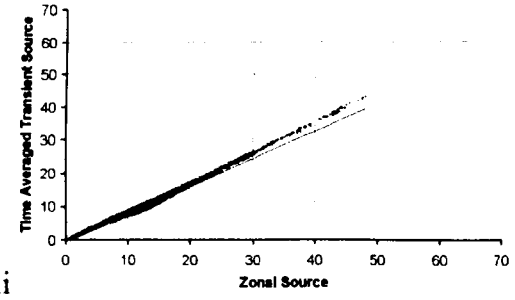

a)ii

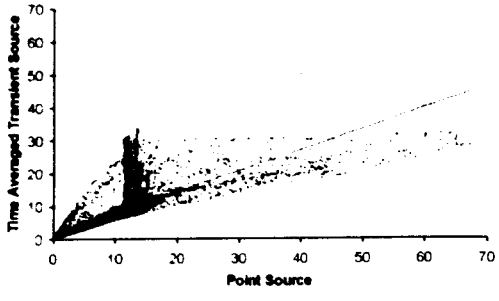

b)i

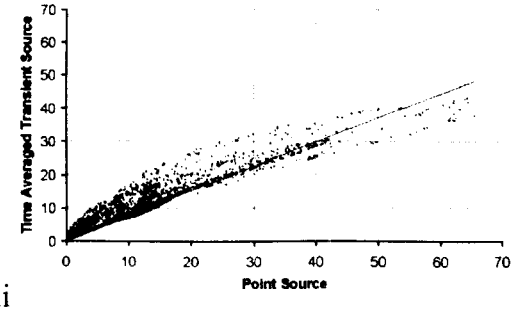

b)ii

Figure 6: Scalar concentration (x1000) at each cell. Ventilation Regime A. Sample plane y=1.60m. a) zonal source against the time averaged values from a transient source. b) Point source against the time averaged values from a transient source i) Case 1 ii) Case 2.

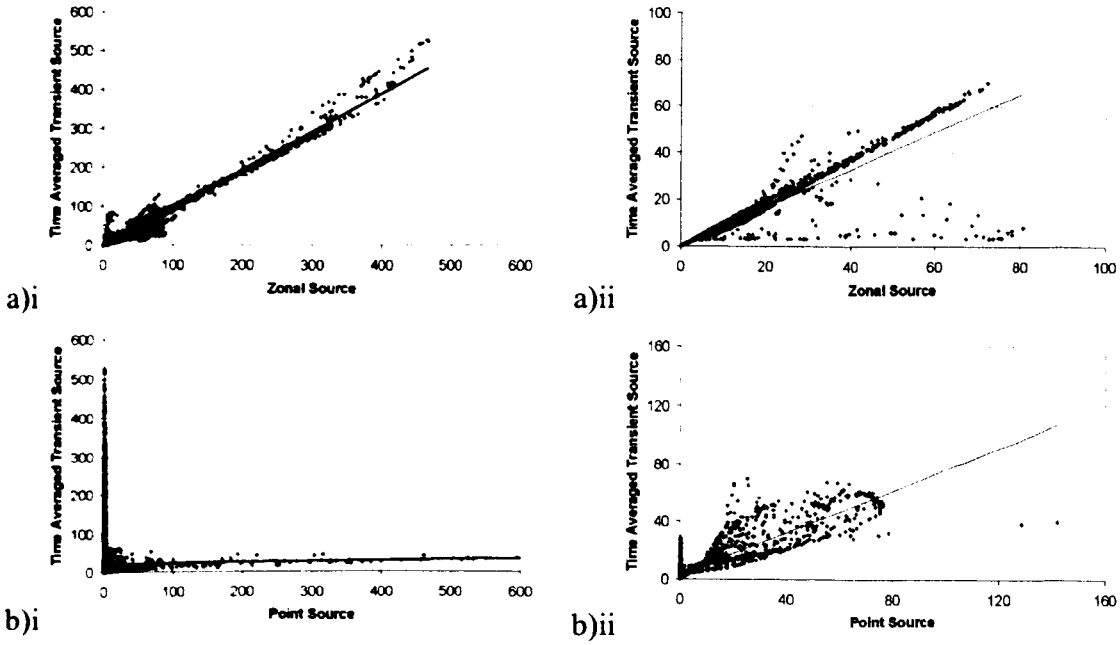

Figure 7: Scalar concentration (x1000) at each cell. Ventilation Regime B. Sample plane y=1.15m. a) zonal source against the time averaged values from a transient source. b) Point source against the time averaged values from a transient source. i) Case 1 ii) Case 2.

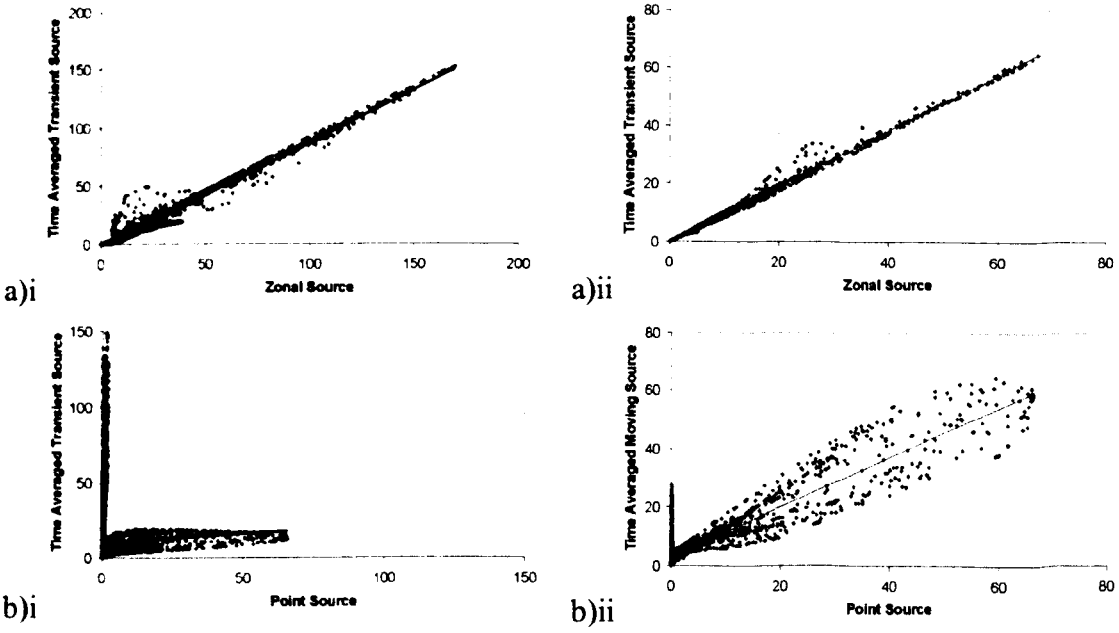

Figure 8: Scalar concentration (x1000) at each cell. Ventilation Regime B. Sample plane y=1.60m. a) zonal source against the time averaged values from a transient source b) Point source against the time averaged values from a transient source i) Case 1 ii) Case 2.

DISCUSSION

It has been identified that a simple method is necessary to use CFD to model the dispersal of bio-aerosols from general activities within a hospital ward. The results presented here show that a steady state model using a zonal source will adequately represent a source of bio-aerosols that varies in position with time. The zonal model is

easy to set up and is simpler and less computational expensive to run than a time dependant simulation of a moving source. The dispersal pattern from the zonal source represents well the average behaviour of a moving source; whereas the ability of a point source to do the same is generally poor and varies greatly on the position of the source and the ventilation regime. In order to predict the average dispersal pattern of bioaerosols in hospital wards from activities the use of a zonal source will therefore be more suited. The zonal source may be applicable for modelling situations such as bedmaking, or general nursing activities around a bed, where the bacteria will be dispersed over the entire zone of the bed.

Although this method gives a reasonable representation of the position of the maximum value of contamination in the space it will greatly underestimate the magnitude of this maximum. In order to find this maximum value it is necessary that the dispersion pattern is known, a point source will only give a reasonably acceptable value if it is positioned in the *correct* place. It may be possible to scale up the value acquired from the zonal source but further work is needed in order to assess the value for this scaling.

Since the concept of the zonal source is to represent the activity from people further work will be carried out including a source of heat with the scalar. The skin particles the zonal source is intending to represent may be larger than 5μm, and so future work will be carried out using a lagrangian approach, including the effect of the size and mass of the particles.

Table 1: r^2 values showing the correlation between the time average moving source and a point or zonal source.

		Fig No.	Zonal Source	Point Source
Regime A Case 1	Y=1.15	4ai/4bi	0.9842	0.1877
	Y=1.60	5ai/5bi	0.9554	0.5412
Regime A Case 2	Y=1.15	4aii/4bii	0.9819	0.5052
	Y=1.60	5aii/5bii	0.9787	0.9035
Regime B Case 1	Y=1.15	6ai/6bi	0.9771	0.0004
	Y=1.60	7ai/7bi	0.9794	0.0018
Regime B Case 2	Y=1.15	6aii/6bii	0.8493	0.766
	Y=1.60	7aii/7bii	0.9955	0.8374

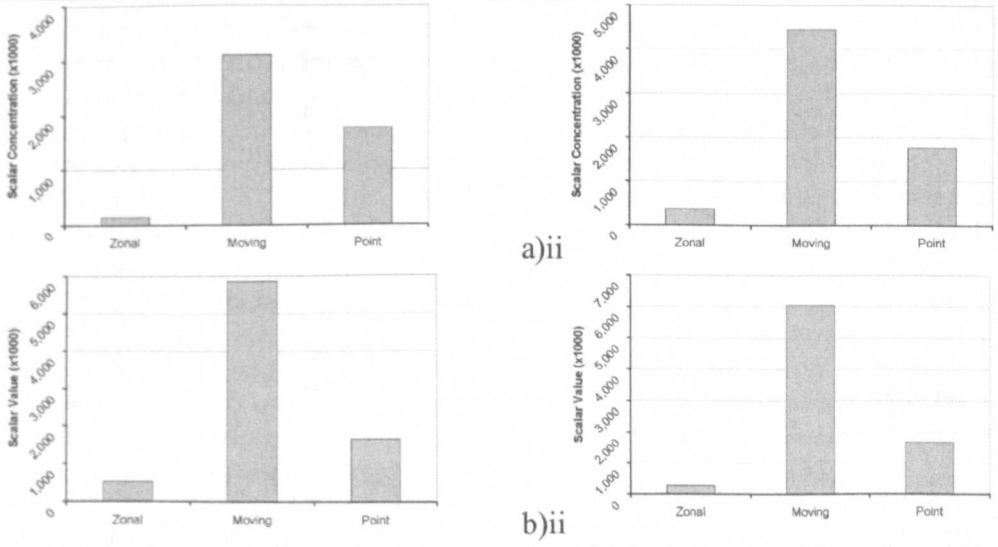

Figure 9: Maximum Scalar values at any point within the room. a)Ventilation Regime A. b)Ventilation Regime B i) Case 1 ii) Case 2.

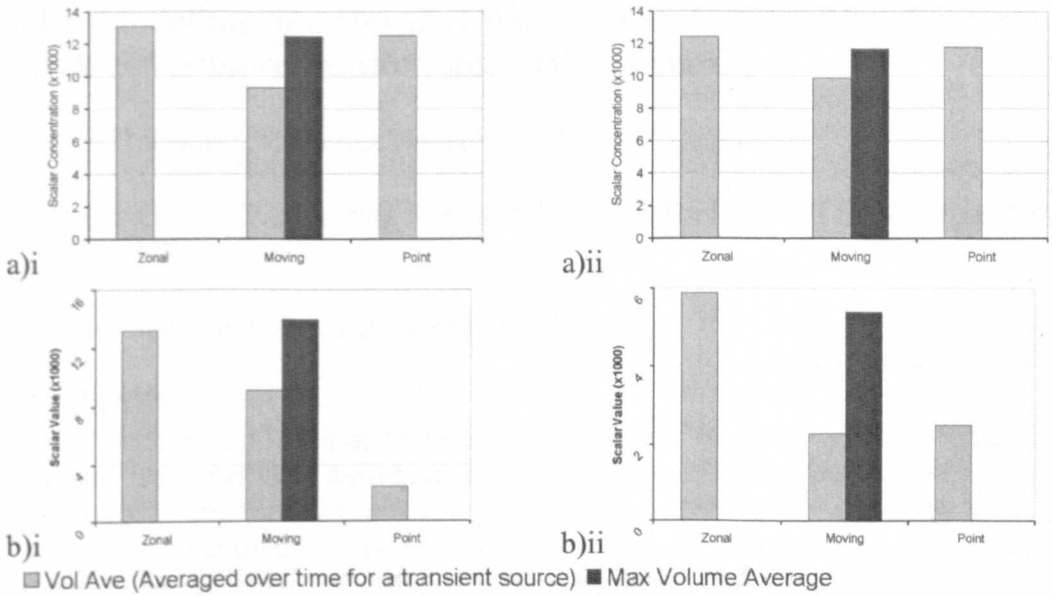

Figure 10: Volume Averaged Scalar values within the room. a)Ventilation Regime A. b)Ventilation Regime B i) Case 1 ii) Case 2.

REFERENCES

1. Parker, M T. *Transmission in Hospitals*. in *International Symposium on Aerobiology (4th)*. 1972. Technical University at Enschede, The Netherlands: Utrecht Oosthoeck.
2. Speers, R, Bernard, H, Ogrady, F, and Shooter, R A, *Increased Dispersal of Skin Bacteria into Air after Shower-Baths.* Lancet, 1965. **1**(7383): p. 478-480.
3. Noble, W C, *Dispersal of Skin Microorganisms.* British Journal of Dermatology, 1975. **93**(4): p. 477-485.
4. Duguid, J P and Wallace, A T, *Air Infection with Dust Liberated from Clothing.* Lancet, 1948. **255**(NOV27): p. 845-849.
5. May, K R and Pomeroy, N R. *Bacterial dispersion from the body surface*. in *Airborne Transmission and Airborne Infection: 4th International Symposium on Aerobiology*. 1973. Technical University at Enschede, The Netherlands: Oosthoek.
6. Hare, R and Thomas, C G A, *The Transmission of Staphylococcus Aureus.* British Medical Journal, 1956. **2**(OCT13): p. 840-844.
7. Roberts, K, Hathway, A, Fletcher, L A, et al., *Bioaerosol production on a respiratory ward.* Indoor and Built Environment, 2006. **15**(1): p. 35-40.
8. Thornton, T, Fletcher, L A, Beggs, C B, et al. *Airborne Microflora in a Respiratory Ward*. in *American Society of Heating, Refrigeration and Air Conditioning Engineer. Indoor Air Quality Conference*. 2004. Tampa, Florida.
9. Wong, T W, Lee, C K, Tam, W, et al, *Cluster of SARS among medical students exposed to single patient, Hong Kong.* Emerging Infectious Diseases, 2004. **10**(2): p. 269-276.
10. Li, Y, Huang, X, Yu, I T S, et al., *Role of air distribution in SARS transmission during the largest nosocomial outbreak in Hong Kong.* Indoor Air, 2005. **15**(2): p. 83-95.
11. Chau, O K Y, Liu, C H, and Leung, M K H, *CFD analysis of the performance of a local exhaust ventilation system in a hospital ward.* Indoor and Built Environment, 2006. **15**(3): p. 257-271.
12. Noakes, C J, Sleigh, P A, Escombe, A R, and Beggs, C B, *Use of CFD analysis in modifying a TB ward in Lima, Peru.* Indoor and Built Environment, 2006.**15**(1): p.41-47
13. Brohus, H, Balling, K D, and Jeppesen, D, *Influence of movements on contaminant transport in operating room.* Indoor Air, 2006. **16**(5): p. 356-372.
14. Macher, J M, *Positive-Hole Correction of Multiple-Jet Impactors for Collecting Viable Microorganisms.* American Industrial Hygiene Association Journal, 1989. **50**(11): p. 561-568.

CFD Modelling of a Hospital Ward: Assessing risk from bacteria produced from respiratory and activity sources

Abigail Hathway*, Catherine Noakes and Andrew Sleigh

Pathogen Control Engineering Research Group, School of Civil Engineering, University of Leeds, UK

*Corresponding email: A.Hathway@Sheffield.ac.uk

SUMMARY

It has been identified that potentially pathogenic bacteria, such as MRSA can be released from the skin during routine activities within hospital wards, such as bed-making, washing patients, dressing and walking. CFD is often used to study airflow patterns and ventilation regimes within hospitals, however such models tend not to consider these types of dispersal mechanisms and concentrate on respiratory transmission, using a point source at the mouth position. A zonal source is demonstrated to represent this release from activity within CFD simulations using both passive scalar and Lagrangian particle tracking. Sensitivity studies are carried out for point and zonal sources. The point source was found to not adequately represent the release of bacteria from a zone and therefore the zonal source is recommended to be used in conjunction with this type of source in order to simulate both respiratory and activity sources of bacteria.

KEYWORDS

Bio-aerosol, CFD, Hospitals, Source definition, Health-care Associated Infection.

INTRODUCTION

Health-care Associated Infection (HAI) is a world wide concern with 2 -3 million people in Europe infected annually (Pittet *et al*, 2005). Although the most significant route for the transfer of infection is via contact spread there is evidence that the airborne route may also have importance (Brachman, 1970). Infection resulting from airborne transfer of bacteria is not only caused by inhalation of infectious particles, but may also be due to contamination of surfaces by these particles. This contamination may then lead to further infection through transport on health care workers (HCWs) or patient's hands.

Computational Fluid Dynamics (CFD) is a useful tool to understand the dynamics of infectious particles through the air. It has been used successfully to study the effect of different ventilation regimes, and layouts of wards and isolation rooms (Zhao *et al*, 2004; Noakes *et al*, 2006; Chang *et al*, 2007). This can extend to modelling other engineering infection control interventions such as the effect of UV-C irradiation (Noakes *et al*, 2004).

Modelling the transport of infectious particles in indoor environments tends to focus on respiratory diseases such as SARS and TB and for this reason the source of bio-aerosols is usually taken as being at the head of the patients bed. However this is not the only release mechanism of bacteria that is important for hospital acquired infection. Bacteria such as *Staphylococcus aureus*, including MRSA are known to colonise the skin and can become released into the air on skin flakes due to friction during activity. Noble

(1962) found that a patient colonised with *Staphylococci* could rapidly contaminate their environment, and more recently Shiormori *et al* (2002) concluded that the process of bed-making resulted in airborne counts up to 26 times that in the resting period. Within a respiratory ward it has been shown that airborne bacteria sampled over the course of a day fluctuated with activity (Roberts *et al,* 2006). This type of release from activities such as bed-making will not occur at a single point, as can be assumed when a cough is the release mechanism.

There is currently growing interest in simulating movement directly within CFD models (Shih *et al,* 2007; Mazumdar and Chen, 2007). Despite the complexity of these models they still only provide limited results for one particular occasion, whereas in reality the activities will be enacted differently on every occasion, resulting in different dispersal mechanisms. By modelling the motion directly there is the risk of giving the user, or clients, an incorrect sense of certainty about the results. However it is possible to identify the spatial zones over which an activity occurs, and for this reason the concept of the zonal source was introduced. The zonal source aims to *represent* a time-averaged release from activity within a steady state model. This applies a time averaged concentration for the release which in reality varies in time and space over the entire zone the activity occurs in. A previous validation study (Hathway *et al,* 2007) showed the time-averaged concentration distribution from a moving source was well represented by a zonal source. However the results from the moving source could differ greatly from the point source depending on the ventilation regime.

This paper aims to demonstrate the application of a zonal source bio-aerosol release model within a hospital side room and compare the risks to patients and staff from a zonal release with a point source. The zonal source will be tested for sensitivity to size and risks from this source compared to that with a point source. A sensitivity study on the location specification of the point source was also carried out to enable a comparison with the possible errors from the zonal source application.

METHODS

Numerical simulations of the air flow pattern and bio-aerosol transport are carried out using the commercial package Fluent 6.2. The simulated side room is mechanically ventilated in accordance with the NHS estates recommendations (2005) with a pressure difference at the extract of –10Pa and a ventilation rate through the room corresponding to 10 ac/h. The air enters the room from a four-way ceiling diffuser as shown in figure 1, at an angle of 10 degrees to the ceiling. The injected air has a temperature of 20°C. This is then extracted through a ceiling mounted grille as shown in the figure. Within the room is a patient, bed, table and sink. The patient is given a heat flux of $60W.m^{-2}$ and the lights $50W.m^{-2}$. Turbulence is modelled using the standard k-ϵ model with enhanced wall functions. All the walls are adiabatic and set to the no slip condition.

The computational grid is comprised of approximately 600,000 cells using a tet/hybrid automatic meshing scheme. A boundary layer was applied to all walls, resulting in a maximum node distance of 0.01m from the wall. The grid was refined at the inlet and outlet. The airflow was assumed converged when the residuals had dropped by three orders of magnitude and the mass flux within the space was less than 0.1%. The solution for the bio-aerosol sources were run using the converged airflow solutions in order to save time, with the same criteria applied.

Bio-aerosol Source

The bio-aerosols were initially assumed to be small enough to stay airborne for long periods of time, and were therefore modelled using a passive scalar. This was extended to a study using Lagrangian particle tracking to more realistically simulate larger particles that are released from skin.

In the passive scalar study the transport of bio-aerosols (ϕ) was solved using equation 1.

$$\frac{\partial \phi}{\partial t} + div(\phi \mathbf{u}) - div(\Gamma grad\phi) = 0 \qquad (1)$$

Here **u** is the velocity vector (u,v,w) of the air ($m.s^{-1}$); and Γ is the diffusivity ($m^2.s^{-1}$). In order to study the sensitivity of a point source location nine injections are defined across the bed as shown in Figure 1. Each of these is represented by a cube of volume $10cm^3$ with a source concentration of 500 cfu. The sensitivity of the zonal source to size and location is studied by considering six sources with a plan geometry that ranges between the area of the whole bed to an area just covering the patient. The location and geometry of these sources are given in table 1. For all the bio-aerosol sources a momentum source of $1N.m^3$ is applied in the positive y direction to simulate an upward release.

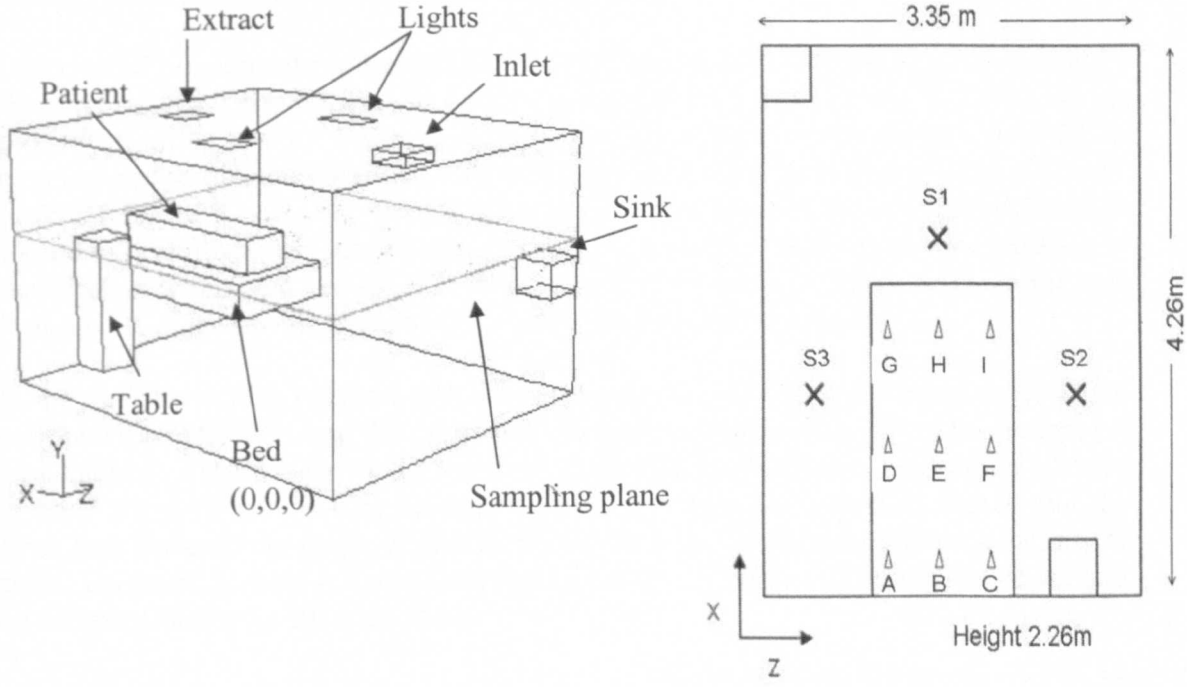

Figure 1: a) Schematic of the side room. b) Position of sampling points (x) and point source locations (Δ)

Lagrangian particle tracking was used to model particulate release across the same six zonal sources, and point injections were carried out at the centre of the scalar point sources. The velocity of the particles (u_p) was solved using equation 2.

$$\frac{\partial u_p}{\partial t} = F_D(u - u_p) + \frac{g_x(\rho_p - \rho)}{\rho_p} \qquad (2)$$

Here $F_D(u-u_p)$ is the drag force per unit of particle, ρ density and g the gravitational acceleration. The subscript p refers to particles, whereas the unsubscripted terms refer to the bulk air. Turbulent dispersion was modelled using the stochastic discrete random

walk (DRW) approach. Three diameters of particles were considered; 5, 14 and 20 microns each with a density of 1000 $kg.m^{-3}$. Ten thousand particles of each diameter were injected and tracked for 50,000 steps. A particle was considered trapped when it hit a surface and escaped when it hit the extract.

Table 1:Geometry of the Zonal Sources showing x,y,z coordinates at max and min positions

	x		y		z	
	min	**max**	**min**	**max**	**min**	**max**
z(u)1	2.46	4.23	1.3	1.4	1.425	1.925
z(u)2				1.7		
z(u)3				2.0		
z(l)4	2.26	4.26	1.0	1.4	1.175	2.275
z(l)5				1.7		
z(l)6				2.0		

RESULTS

Figure 2 shows the velocity vectors for the airflow across the central x and z planes in the room. The air speed across the patient is less than $0.25 m.s^{-1}$ as required by ASHRAE to provide adequate comfort, and avoid drafts. Figure 2b shows clearly two areas of recirculation down each side of the room.

Contours of bio-aerosol concentration from the passive scalar simulations are shown for three representative point sources and the six zonal sources in Figure 3. These are all plotted on a plane at y= 1.35m, just above the top surface of the patient. In order to compare the results the volume of the room with a concentration greater than 5 $cfu.m^{-3}$ is found for each case and shown in Figure 4. To compare the risk posed by each source to health care workers standing in specific locations the average concentration at three points around the bed (S1, S2, S3 in figure 1) are given in figure 5. The error bars indicate the range of values depending on the source position or size.

In the particle tracking results a distinction is made between the lower zonal sources that surround the patient (l), and the upper sources that are immediately above the patient (u) (see Table 1). Figure 6 shows the number of particles extracted as a percentage of those injected for each source. The average value is given for each type of source and the error bars indicate the range of results for the different individual source locations or sizes. The same process is carried out for the results in figure 7 showing the deposition on different surfaces within the room.

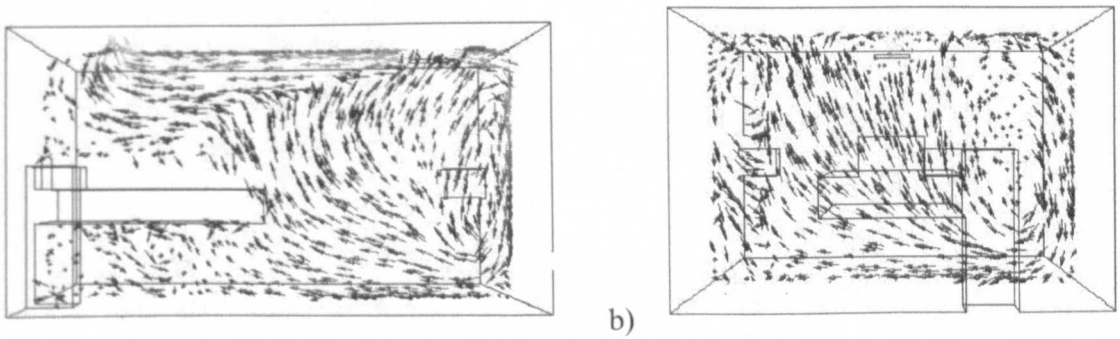

Figure 2: Vectors of velocity on the planes z=1.65 (a) and x=2.13 (b).

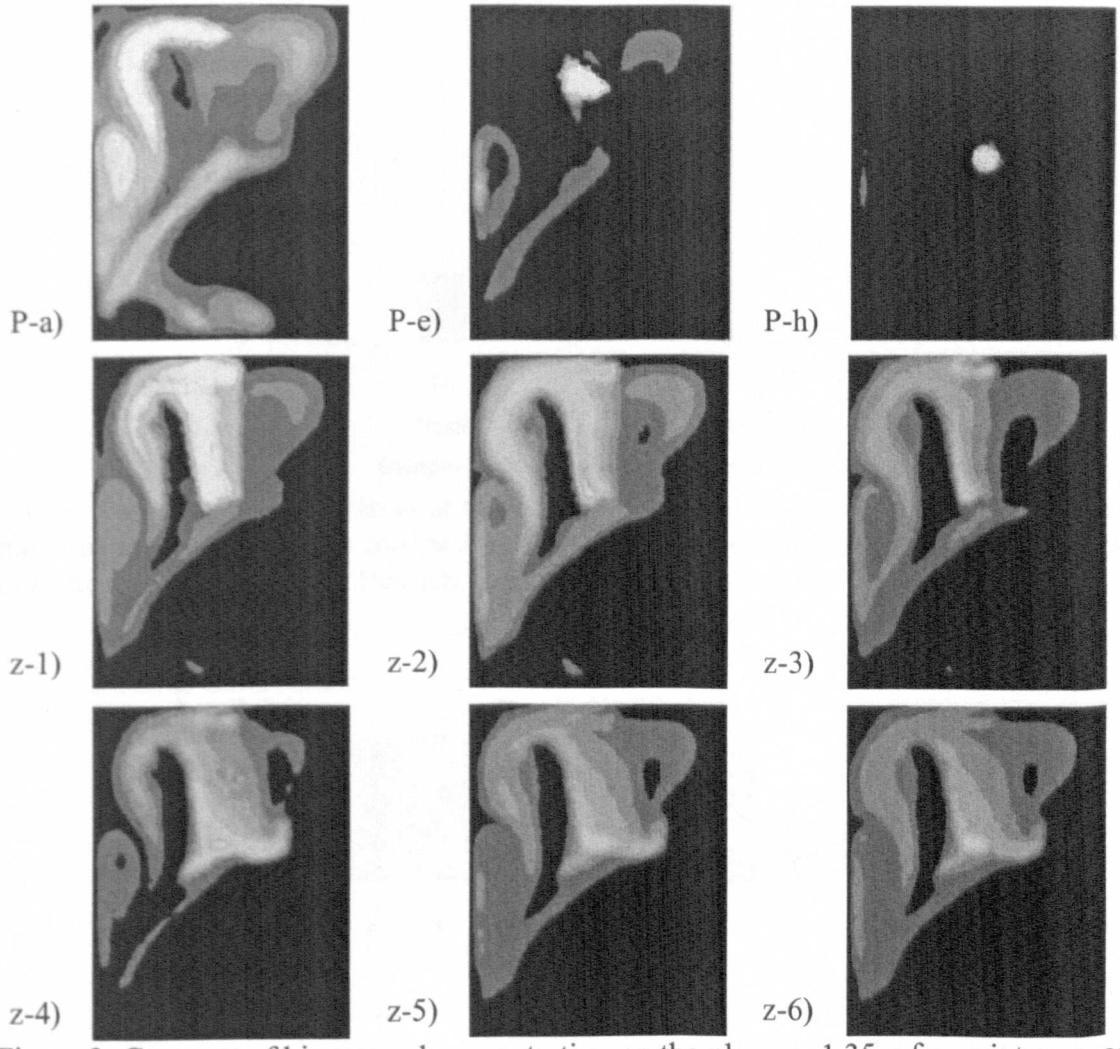

Figure 3: Contours of bio-aerosol concentration on the plane y=1.35m for point sources (P) as shown in figure 1, and zonal sources (z) described in table 1. The colours are equivalent for each plot.

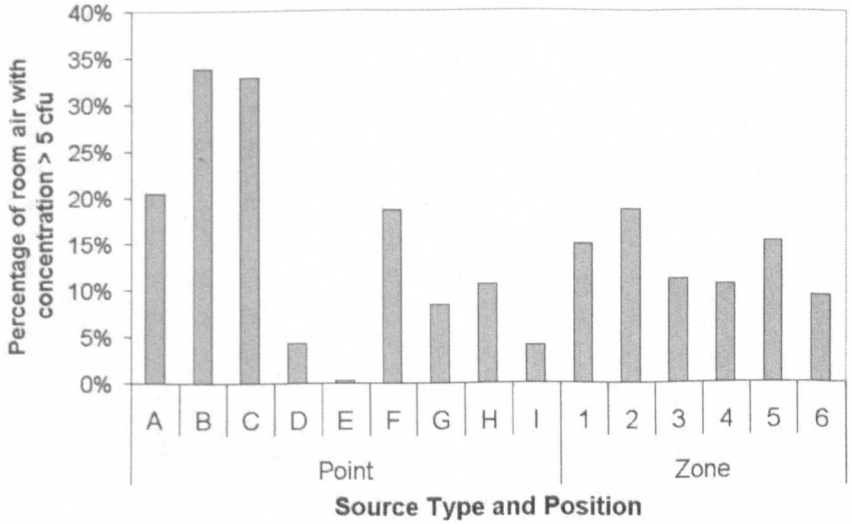

Figure 4: The percentage by volume of the room air with a scalar concentration > 5cfu.m^{-3}

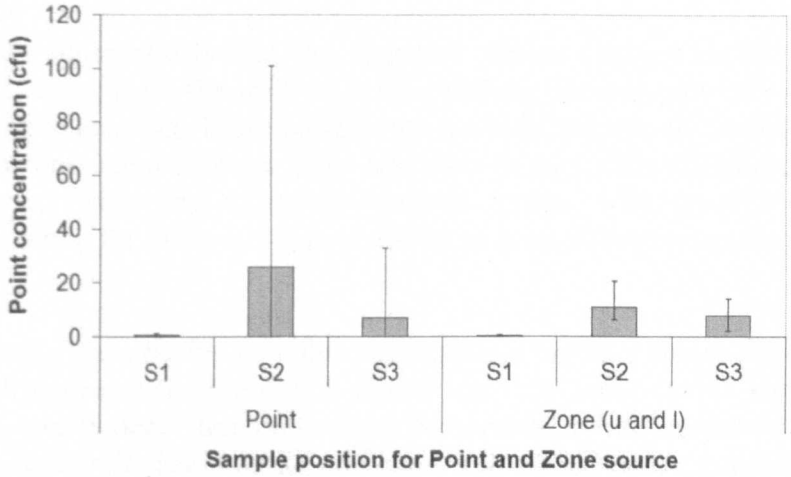

Figure 5: Average concentration at three HCW locations (shown in figure 1) based on mean of all 9 point source results and all 6 zonal source simulations. The error bars indicate the range of values for each type of source.

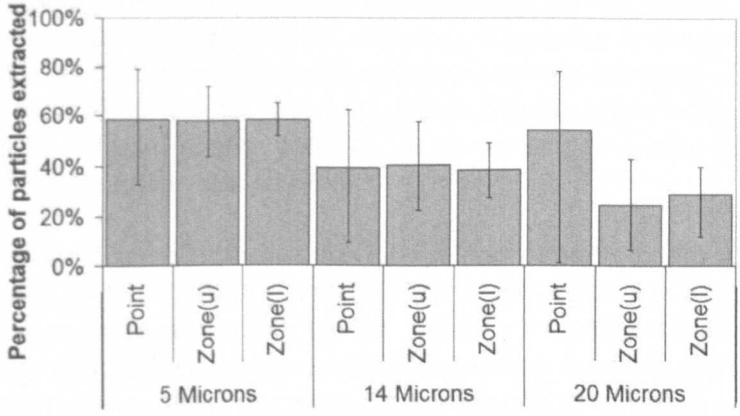

Figure 6: The average number of particles extracted from the space as a percentage of those injected, based on mean of 9 point source, 3 (u) zonal source and 3 (l) zonal source simulations. The error bars show the range of values found for the different types of source.

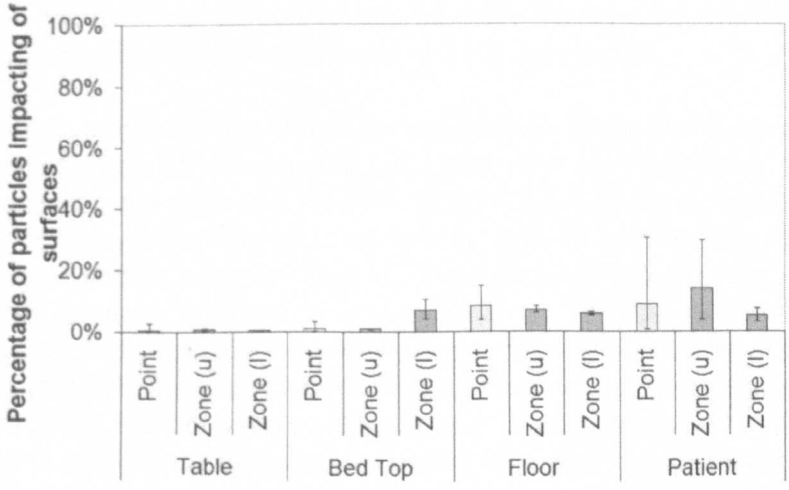

Figure 7: The average percentage of 5μm particles impacting on surfaces within the room, based on mean of 9 point source, 3 (u) zonal source and 3 (l) zonal source simulations. The range of values for each type of source is shown by the error bars.

DISCUSSION

Figure 2 shows quite clearly that the dispersal pattern changes as the point source location moves away from the wall, with the resulting contour plot very dependant on the original source location. These patterns are quite different to those that occur due to release from a zonal source. In the latter case there is very little difference between the dispersal patterns when the source dimensions change, with greatest difference in concentration, when the source is thin resulting in a much higher concentration at the source.

Comparing these concentration patterns quantitatively, figure 4 shows the percentage of the room with concentrations above 5 cfu.m^3. For the point source simulations this volume varies greatly depending on location with the largest differences between points B and E despite them being only 64 cm apart. The zonal source simulations result in percentage values between the extremes of the point source simulations, with only a small variation with size of the source. The results shown in Figure 5 aim to quantify the potential risk to a HCW located at three positions around the bed. The results show immediately how the risk at a particular location depends very much on the nature and location of the source. In particular the variation at position B for point sources is very large, as depending on the position of the point source the bio-aerosols are immediately extracted, or recirculate around the room. These results show how important it is to locate a point bio-aerosol source correctly as incorrect positioning can give very false results when calculating the risk to HCWs.

These findings are also reflected in the Lagrangian particle tracking results (figures 5 and 6). Although particle tracking is more susceptible to the size of a zone, particularly for the upper zone (u) results which have a smaller plan area. The depth of the zone for these models greatly influences the level of deposition on the patient and the bed. Lai and Chen (2006) showed how the incorrect assumption of isotropic turbulence in the k-ϵ model can result in over deposition and when a large number of particles are injected close to a surface, as with the thin sources, this effect may have a greater effect. They also showed that Lagrangian particle tracking is more sensitive to the grid size than the simulation of the bulk air flow. For this reason over deposition with thin sources may be reduced by a finer grid. However since the zone thickness does not otherwise have a great effect on the dispersal pattern it may be more appropriate to consider a thicker zone so less particles are injected in the area close to the surface.

As discussed in the introduction, the release of bacteria from activity can significantly affect the concentration of bio-aerosols and these may be pathogenic. It is therefore important to consider the type and location of activity when simulating hospital wards. To model the release of bacteria from an activity such as bed-making, dispersion will occur in varying amounts over the length of the bed. From the results shown here it is clear that a point source at the head of the bed could give misleading results, but equally a point source located at another position on the bed would also be incorrect. When using CFD to research the effect of airflows on the risk of transmission of infection, incorrectly assuming a point source release could lead to erroneous results. Therefore when using CFD simulations to study bio-aerosol transport it is important to understand the types of sources that may exist in the space and the purpose of any interventions. It may then be necessary to consider both respiratory and activity based bio-aerosol sources, and to achieve this by using a combination of point and zonal sources to build a realistic simulation of the risks in a space.

CONCLUSIONS

When using CFD simulations for research or design of hospital isolation or side rooms it is important to consider the type of infection that a bio-aerosol transport model is intending to represent. Pathogens that contaminate the skin, and can therefore be released from the skin due to friction during activity will have different dispersion characteristics to respiratory aerosols. It is therefore important to consider the pathogen source when researching the design of ventilation and engineering infection control interventions in side rooms, isolation rooms and hospital wards. The dispersion patterns from point and zonal sources are different and it may be necessary to use both to represent the release from respiratory and activity based sources of infection. The results of this study also highlight the importance of specifying a realistic location for the source of a pathogen and understanding the limitations in the model created by making this choice.

ACKNOWLEDGEMENT

The author would like to thank the EPSRC for their financial support in this work.

REFERENCES

Brachman, 1970 Airborne Infection – Airborne or not? *International conference of nosocomial infection*

Caul, E. O. (1994). "Small Round Structured Viruses - Airborne Transmission and Hospital Control." *Lancet* 343(8908): 1240-1242.

Chang, T. J., H. M. Kao, et al. (2007). "Numerical Study of the Effect of Ventilation Pattern on Coarse, Fine, and Very Fine Particulate Matter Removal in Partitioned Indoor Environment." *Journal of Air and Waste Management Association* 57: 179-189.

Hathway, A., P. A. Sleigh, et al. (2007). CFD Modelling of Transient Pathogen Release in Indoor Environments due to Human Activity. *Roomvent* Helsinki Finland.

Lai, A. C. K. and F. Chen (2006). "Modeling particle deposition and distribution in a chamber with a two-equation Reynolds-averaged Navier-Stokes model." *Aerosol Science* 37: 1770-1780.

Mazumdar, S. and Q. Chen (2007). Impact of moving bodies on airflow and contaminant transport inside aircraft cabins. *Roomvent 2007*, Helsinki, Finland.

NHS Estates (2005). HBN4 Supplement 1: Isolation facilities in acute settings. N. Estates. London, The Stationary Office

Noakes, C. J., L. A. Fletcher, et al. (2004). "Development of a numerical model to simulate the biological inactivation of airborne microorganisms in the presence of ultraviolet light." *Journal of Aerosol Science* 35(4): 489-507.

Noakes, C. J., P. A. Sleigh, et al. (2006). "Use of CFD analysis in modifying a TB ward in Lima, Peru." *Indoor and Built Environment* 15(1): 41-47.

Noble, W. C. (1962). "Dispersal of Staphylococci in Hospital Wards." *Journal of Clinical Pathology* 15(6): 552.

Pittet, D., B. Allegranzi, et al. (2005). "Considerations for a WHO European strategy on health-care-associated infection, surveillance, and control." *The Lancet Infectious Diseases* 5(4): 242-250.

Roberts, K., A. Hathway, et al. (2006). "Bioaerosol production on a respiratory ward." *Indoor and Built Environment* 15(1): 35-40.

Shih, Y.-C., C.-C. Chiu, et al. (2007). "Dynamic airflow simulation within an isolation room." *Building and Environment* 42(9): 3194-3209.

Shiomori, T., H. Miyamoto, et al. (2002). "Evaluation of bedmaking-related airborne and surface methicillin-resistant Staphylococcus aureus contamination." *Journal of Hospital Infection* 50(1): 30-35.

Bioaerosol production from routine activities within a hospital ward

Abigail Hathway[1*], Louise Fletcher[1], Cath Noakes[1], Andrew Sleigh[1], Mark Elliot[2], Ian Clifton[2]

[1]Pathogen Control Engineering, School of Civil Engineering, University of Leeds
[2]St James's University Hospital, Leeds

[*]*Corresponding email: A.Hathway@Sheffield.ac.uk*

Keywords: Hospital acquired infection, Bio-aerosols, Skin squame, Staphylococcus aureus

1 Introduction

The ability of a human to shed bacteria, including the pathogen *Staphylococcus aureus* on skin particles during activities has been well documented by many authors (e.g. Davies and Noble, 1962). The majority of these studies consider only specific activities, often in controlled conditions and for short time periods. To understand how these releases may impact on infection control it is necessary to understand how the bio-aerosol concentration fluctuates with activities on a typical day in a hospital ward. For this reason the authors carried out a scoping study in 2004 on a respiratory ward and found large variation with bio-aerosol concentrations over the day (Roberts *et al.* 2006). The current work builds on this previous study and aims to establish whether the activity of staff on a ward can be statistically correlated to bio-aerosol concentrations. Fluctuations on multiple days are compared in order to identify typical patterns of release.

2 Methods

The study was carried out over seven days on a 4 bed bay of a respiratory ward between 8am and 4pm. The air was sampled to determine a total viable count of bacteria using a Micro-bio MB2 sampler. Particles in five size ranges; 0.3-0.5μm, 0.5-1μm, 1-3μm, 3-5μm and >5μm, were sampled using a Kanomax laser particle counter. The particles were summed over 15 minute periods. Within this same period the number of hospital staff within the bay were summed and multiplied by the number of minutes present. Bio-aerosols were sampled for 5 minutes at the end of each 15 minute period.

3 Results

The results presented here consider the three days on which ward cleaning was not carried out. Figure 1 shows the number of hospital staff in the bay with the total viable count of sampled airborne bacteria over 2.5 sampling days. The statistical analysis used Spearmans Rho correlation test since the data was not normally distributed. There is a statistical similarity between the activity and bio-aerosols ($r=0.522$; $p<0.01$; $n=38$) shown clearly in Figure 1 with peaks of both in the morning, tailing off into the afternoon. The fluctuation of bio-aerosols was found to be similar to that of particles sized >5μm ($r=0.77$; $p<0.01$; $n=35$). The two full days show a statistically similar pattern of bio-aerosol fluctuation ($r=0.52$; $p<0.05$; $n=16$).

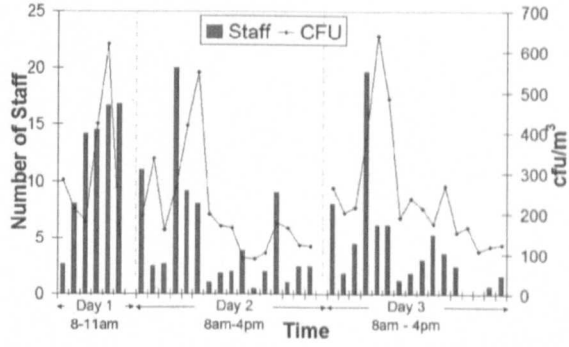

Figure 1: Fluctuation of number of staff in the bay and the quantity of sampled bio-aerosols.

4 Conclusions

There are high peaks of bio-aerosols and particles > 5μm during the morning when there is more activity, quantified here by the number of staff in the bay. This is demonstrated on all the days observed.

5 References

Davies R.R., Noble W.C. 1962. Dispersal of Bacteria on Desquamated Skin. *Lancet* **2**(7269): 1295.

Roberts, K, Hathway A. et al 2006. Bioaerosol production on a respiratory ward. *Indoor and Built Environment* **15**(1): 35-4